Controls of anaerobic oxidation of methane in ocean margin sediments

Dissertation

zur Erlangung des Doktorgrades
der Naturwissenschaften

-Dr. rer nat.-

dem Fachbereich Biologie/Chemie der Universität Bremen
vorgelegt von

Nina Jeannette Knab

Bremen
Januar 2007

Die vorliegende Arbeit wurde in der Zeit von November 2002 bis Dezember 2006 am Max-Planck Institut für Marine Mikrobiologie in Bremen durchgeführt.

1. Gutachter: Prof. Dr. Bo Barker Jørgensen
2. Gutachter: Priv. Doz. Dr. Jens Harder

Weitere Prüfer:
Prof. Dr. Rudolf Amann
Dr. Marcus Elvert

Tag des Promotionskolloquiums: 6. Februar 2007

Cover picture: Seismic profile of methane in marine sediment
(Jørn Bo Jensen/ GEUS Denmark; METROL 2004)

Danksagung

An dieser Stelle möchte ich allen danken, die zum Fortgang und Gelingen dieser Arbeit beigetragen haben:

Vielen Dank an Prof. Dr. Bo Barker Jørgensen für die Betreuung meiner Doktorarbeit und die Ermöglichung so vieler interessanter Erlebnisse. Danke für die Diskussionen, Erklärungen und Unterstützung beim Schreiben der Manuskripte.

Ich möchte Dr. Jens Harder danken für die Übernahme des zweiten Gutachten, sowie den Mitgliedern des Prüfungskomitees, Prof. Dr. Rudolf Amann, Dr. Marcus Elvert, Susanne Hinck und Antje Voßmeyer.

Ein besonderer Dank geht an Tim Ferdelman für seine Hilfsbereitschaft während meiner Arbeit und für die anregenden und motivierenden Diskussionen.

Ich danke allen Mitarbeitern im METROL Projekt, besonders Christian Borowski für die Organisation der Ausfahrten, Henrik Fossing, Andy Dale und Barry Cragg für die gute Zusammenarbeit, sowie Antje Boetius, John Parkes, Rich Pancost, Ed Hornibrook, Troels Laier, Joern Bo Jensen und Philippe Van Cappellen für die schöne und interessante Zeit in dem Projekt.

Vielen Dank an Imke Busse, Kirsten Imhof und Tomas Wilkop für die technische Unterstützung im Labor und bei *Henry*-Ausfahrten, sowie an Tanja Quotrup von NERI / Dänemark für die tolle Zusammenarbeit in Silkeborg und bei den *Gunnar-Thorson* Ausfahrten.

Danke an alle Mitarbeiter des MPIs, besonders der Arbeitsgruppe Biogeochemie, die mir durch ihre Erfahrungen und Diskussionen sehr viel geholfen haben und durch eine nette Arbeitsatmosphäre die Zeit am MPI verschönert haben, insbesondere an Tina Treude, Niko Finke, Natascha Riedinger, Karsten Lettmann, Jochen Nüster, Verona Vandieken, Helge Niemann, Tina Lösekann und Heiko Löbner.

Vielen Dank für die gute Atmosphäre in unserem Büro an meine zeitlängsten Bürokollegen Elsabe Julies, Robert Hamersley und Alberto Rhobador, und ganz besonders an Jutta Niggemann und Beth! Orcutt für die permanente Bereitschaft zum Gedankenaustausch und für die vielen anregenden Gesprächen.

Nicht zuletzt möchte ich meinen Freunden und meiner Familie für ihre Unterstützung und Vertrauen danken, ganz besonders meinem Bruder Christoph für seine bedingungslose Hilfsbereitschaft.

Table of Contents

Summary

For a long time it was suspected that methane could only be oxidized under aerobic conditions until 30 years ago it was discovered that marine microbes can also oxidize methane anaerobically in marine sediments of the oceans, using sulfate as electron acceptor. The ocean sediments contain vast amounts of methane, but the sediment horizon in which anaerobic oxidation of methane and sulfate reduction occur acts as a barrier for upwards diffusing methane and is responsible for the oceans modest role in methane release. Even though multiple studies have investigated this process since, the controls on the effectiveness of the methane barrier are poorly understood. The purpose of this thesis was to add to the growing database of information about the role this process plays in diffusion dominated systems and to understand the factors that regulate AOM rates. In this work AOM and sulfate reduction rates (SRR) were determined in sediment cores from different sites on the European continental margin and were compared to the concentration profiles of methane and sulfate as well as of the products of the coupled AOM-SRR process, sulfide and bicarbonate. This data was complemented by organic carbon content and concentrations of volatile fatty acids, as well as rates of methane production and at some sites with biomarker or stable isotope data.

The data from two of the locations that were visited on research cruises as part of the EU-project METROL (**Met**hane fluxes in ocean margin sediments: microbiological and geochemical cont**rol**) are presented in this thesis, as examples for AOM-systems in organic-rich diffusive marine sediments: the Skagerrak, where the methane and sulfate profiles formed a well defined narrow sulfate methane transition zone (SMTZ) with moderate rates of AOM and sulfate reduction, and secondly the Black Sea, where methanotrophic archaea only turn over methane with very sluggish rates and the SMTZ stretched over a broad horizon.

The results from the Skagerrak show that the methane barrier of the SMTZ is usually very efficiently retaining methane and that the rates in diffusion dominated systems are in the range of 0-10 nmol cm^{-3} d^{-1}, which is extremely lower than at sites with advective transport and seepage. Advective transport and high methane fluxes, as they occur in a pockmark, lead to a more shallow SMTZ and high AOM rates that also accomplish complete methane turnover.

AOM rates are generally higher the closer they are located to the sediment surface but the depth of the SMTZ is not directly indicative for AOM activity between different sites. Rates from a SMTZ in 100 cm in the Skagerrak were higher than those in a very shallow SMTZ from the western Baltic In contrast to earlier assumptions, methane generation from bicarbonate was not excluded from the sulfate zone but methanogenesis rates were significantly lower than AOM or sulfate reduction rates. The biomarker pattern that was found in the SMTZ of the Skagerrak resembled the pattern observed for other AOM locations, indicating that the microorganisms mediating this process in the Skagerrak are similar to the community at those locations.
The methane and sulfate profiles of the Black Sea were unique in that the SMTZ was located entirely inside the formerly limnic sediments and methane disappeared at the limnic-marine boundary. The characteristic tailing of methane in the upper SMTZ was observed at two of the three sampling sites, whereas a concise SMTZ was found in the third gravity core. AOM rates at the bottom of the SMTZ were in the same range as at the other continental margins investigated by METROL but low methane concentrations were only depleted very reluctantly. It is not clear yet what causes the sluggish rates and the upwards tailing of methane above the major zone of AOM activity but this feature might be associated with the limnic history of the sediment. Evidence for this assumption was provided by the only core with a distinct SMTZ, where this zone was located closely underneath the limnic-marine transition and the limnic sediments were covered by a thick layer of marine deposits.

The data acquired from field measurements created the basis to determine the controls on AOM with a reactive transport model, which investigated the sensitivity of AOM rates towards variability in different parameters. Furthermore, it was also applied to calculate the energetic and kinetic constrains of the process that are defined by the *in situ* concentrations. The result revealed that the energy yield of the combined AOM-SRR is favorable as soon as methane and sulfate are present simultaneously, and that the energy yield is rather constant throughout the SMTZ. The observation that the major AOM activity occurred at the bottom of this zone is the consequence of the highest kinetic drive in this horizon. The good coherence of the depth of AOM activity in the cores with the thermodynamic-kinetic regulation demonstrated the important role, especially of the kinetic drive, for AOM regulation.

Zusammenfassung

Lange Zeit wurde angenommen, dass Methan nur unter aeroben Bedingungen zur Energiegewinnung oxidiert werden könnte. Doch vor etwa 30 Jahren entdeckte man, dass Mikroorganismen in marinen Sedimenten Methan auch anaerob oxidieren können, indem sie Sulfat als Elektronenakzeptor benutzen. Obwohl im Meeresboden Methan in sehr großen Mengen vorkommt, stellt der Ozean aufgrund dieser anaeroben Methanoxidation (AOM) keine bedeutende Quelle für atmosphärisches Methan dar, denn die Sedimentschicht, in der dieser Prozeß stattfindet, die Sulfat-Methan Transition Zone (SMTZ), wirkt wie eine Barriere für das zur Sedimentoberfläche diffundierende Methan. Die Verbreitung und Bedeutung von AOM wurde seit seiner Entdeckung durch zahlreiche Studien an unterschiedlichen marinen Sedimenten untersucht, doch die Funktionsweise dieses Prozesses und auch die Faktoren, welche die Wirksamkeit der SMTZ als Methan-Barriere beeinflussen, sind noch weitgehend unbekannt. Um die Regulation der mikrobiellen AOM Raten besser zu verstehen und um den bereits bestehenden Datensatz zu erweitern, wurden sowohl die Konzentrationen der Substrate Methan und Sulfat und der Produkte Sulfid und Bicarbonat, als auch AOM- und Sulfatreduktionsraten (SRR) in Sedimentbohrkernen von verschiedenen Standorten entlang der europäischen Küsten gemessen. Diese wurden ergänzt durch Methanproduktionsraten aus Bicarbonat und Acetat sowie deren Substratkonzentrationen und auch durch zusätzliche Informationen über die Herkunft des Methans durch seine Kohlenstoffisotopie, oder über die an dem Prozeß beteiligten Mirkoorganismen durch Untersuchung der im Sediment vorhandenen Lipide.

Die Arbeit wurde im Rahmen des EU-Projekts METROL (Methanflüsse in marinen Küstensedimenten: Mikrobielle und geochemische Regulation) durchgeführt und konzentrierte sich auf AOM in diffusiven Sedimenten, mit hohem Gehalt an organischem Material. Stellvertretend für die in diesem Projekt untersuchten Gebiete werden die Ergebnisse von zwei Standorten vorgestellt: Das Skagerrak, wo die Methan- und Sulfatprofile eine klar definierte, schmale SMTZ bilden und das Schwarze Meer, wo die Methanumsetzung nur sehr langsam vonstatten geht und die SMTZ sich über eine breite Sedimentschicht erstreckt.
Die Daten aus dem Skagerrak zeigen, dass die SMTZ eine sehr wirksame Methan-Barriere darstellt und das in diese Zone diffundierende Methan vollständig umsetzt. AOM Raten lagen in

diesen Sedimenten zwischen 0-10 nmol cm^{-3} d^{-1} und sind damit bedeutend niedriger, als an Standorten, an denen Methan durch advektive Prozesse transportiert wird. Je höher der nach oben gerichtete Methanfluß in einem Sediment ist, desto dichter unter der Sedimentoberfläche befindet sich die SMTZ und desto höher sind die AOM Raten. Dadurch konnte selbst der hohe Methanfluß in einem Kern aus einem Pockmark vollständig oxidiert werden, obwohl an dieser Stelle advektiver Transport stattfand. Im Gegensatz zu der Annahme, dass Methanogenese mit Substraten, die auch für SRR genutzt werden können nicht stattfindet, solange Sulfat vorhanden ist, wurde Bicarbonat-Methanogenese in der SMTZ gemessen, in der Schicht direkt über den AOM- und Sulfatreduktionsraten. Diese Methanproduktionsraten waren jedoch deutlich niedriger als die maximalen AOM Raten. Die identifizierten Biomarker-Lipide in der SMTZ der Sedimente aus dem Skagerrak entsprachen dem Muster, das auch schon an anderen AOM-Standorten gefunden worden war, was darauf hindeutet, dass die an dem Prozeß beteiligten Mikroorganismen ähnlich sind.
Die Methan- und Sulfatprofile im Schwarzen Meer unterschieden sich von anderen Gebieten, indem sich die SMTZ innerhalb des ehemals limnischen Sediments befand und das Methan erst am Übergang zu den marinen Ablagerungen vollständig oxidiert war. An zwei der drei untersuchten Stationen war die SMTZ durch langsame Methanoxidation über 1 m breit, während die dritte Station eine ähnlich eng begrenzte SMTZ aufwies, wie die Sedimentkerne aus anderen diffusiven Küstengebieten. Wodurch die langsame Methanoxidation und das lineare Profil des nach oben diffundierenden Methans verursacht wird, ist noch nicht geklärt, aber die Daten weisen darauf hin, dass es mit der limnischen Vergangenheit des Sediments im Schwarzen Meer zusammenhängen könnte. In dem einzigen Kern mit einer eng umrissenen SMTZ fanden die AOM Raten nicht tief in den limnischen Sedimenten statt, und die Mächtigkeit der marinen Ablagerungen war deutlich größer als an den beiden Standorten mit erweiterter SMTZ.

Die erhobenen Daten bildeten die Grundlage, um mathematische Modelle zu entwickeln, mit denen die Regulierung der AOM Raten und der Einfluß verschiedener Parameter untersucht werden kann. Aus den *in situ* Konzentrationsprofilen der Substrate und Produkte des gekoppelten AOM-SRR Prozesses wurden außerdem die energetischen und kinetischen Bedingungen in der SMTZ berechnet, und mit der Verteilung der AOM Raten verglichen. Aus den errechneten ΔG Werten kann man ersehen, dass der Prozeß in jedem Falle energetisch

günstig ist, sobald sowohl Methan als auch Sulfat zur Verfügung stehen, und dass die freie Energie sich über die Breite der SMTZ fast gar nicht mit den Konzentrationen ändert. Am unteren Ende der SMTZ gibt es eine Schicht, in der die Kinetik für den Ablauf des Prozesses am günstigsten ist, und dies ist auch genau die Tiefe, in der die AOM Raten hauptsächlich stattfinden. Dadurch wurde gezeigt, dass das Auftreten der AOM Raten durch die energetischen und kinetischen Bedingungen reguliert wird und aus diesem Grunde die Raten meist am unteren Ende der SMTZ stattfinden.

Chapter 1

General introduction

1.1. HISTORY OF ANAEROBIC OXIDATION OF METHANE

The oxidation of methane in the presence of oxygen is an important reaction for energy generation, in natural environments as well as in human society. In marine sediments methane is also oxidized under anaerobic conditions, which was first postulated by Martens and Berner (1974), who observed from the methane concentration profiles that methane was consumed on its way from deeper sources to the sediment surface, and was only accumulating in the sediment below the depth of sulfate depletion. Barnes and Goldberg (1976) proposed that methane oxidation is linked to sulfate reduction as the electron accepting process, according to the equation:

$$CH_4 + SO_4^{2-} \rightarrow HCO_3^- \quad HS^- + H_2O \qquad (1)$$

The process itself was first demonstrated with tracer experiments under laboratory conditions by Zehnder and Brock (1979), even though no net oxidation of methane could be observed. The occurrence of anaerobic oxidation of methane (AOM) in the environment was first verified by Reeburgh (1980) and Iversen and Blackburn (1981), who also confirmed that sulfate reduction is likely to act as electron accepting process. Additional evidence for the microbial oxidation of methane came from the observation of an enrichment of the ^{13}C- isotope in the methane pool (Alperin, 1988; Oremland and Des Marais, 1983; Reeburgh, 1980; Whiticar, 1999), from the visualization of the microbial communities mediating the process (Boetius et al., 2000; Orphan et al., 2001b; Orphan et al., 2002) as well as from the identification of characteristic biomarkers of the organisms involved (Elvert et al., 2003; Hinrichs et al., 2000; Pancost et al., 2000).

Multiple studies have investigated the geochemistry and microbiology of anaerobic methane oxidation in recent years, but the detailed functioning of the process, its regulation and magnitude are still not fully understood.

1.2. CONTINENTAL SHELFS AND EARLY DIAGENESIS

The continental shelf at the ocean margins is an area of high primary production and high turnover rates of nutrients (Berger et al., 1989) (Figure 1). Even though they constitute only 7.5 % of the ocean area, they comprise about 80 % of the total organic carbon accumulation in the ocean (Ver et al., 1999; Wollast, 1991).

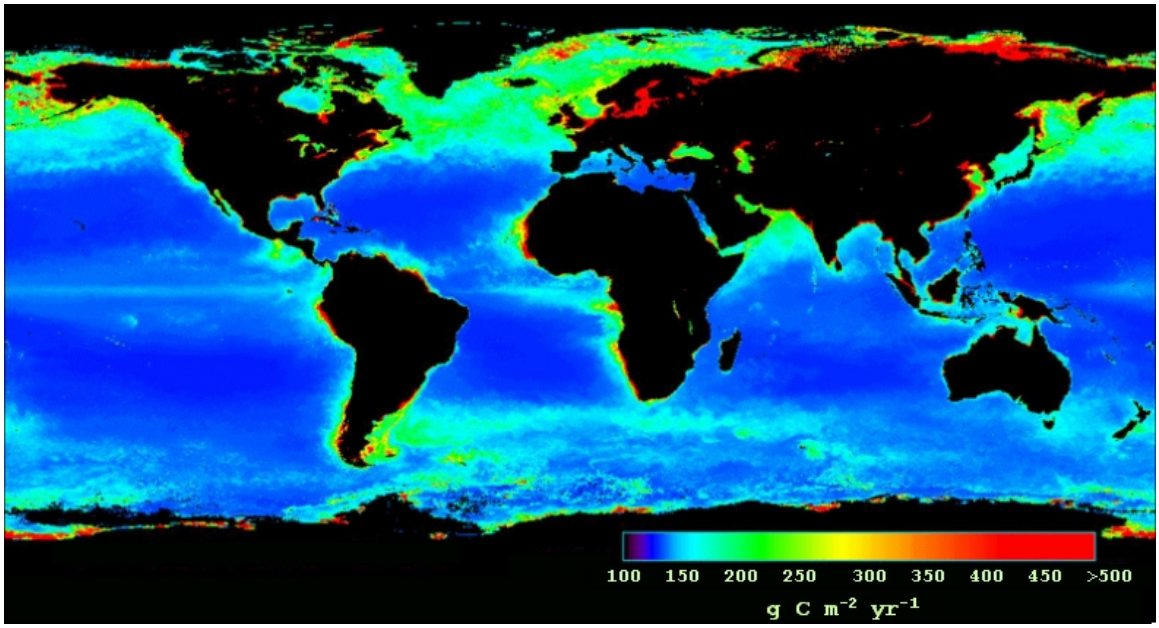

Figure 1: Annual ocean primary productivity 1999 (Image by SeaWiFS, NASA)

The shallow nutrient-rich waters as well as the land-mass effect promote algal and phytoplankton growth (Strickland, 1965) and foster photosynthesis to reach an annual average primary production of ~ 140 gC m^{-2} yr^{-1} and lead to a high recycling rate of organic matter (Field et al., 1998). The shelf sediments are therefore characterized by a high influx of organic matter of up to ~ 60 cm per 1000 years, which is degraded by microorganisms to CO_2 and methane (Figure 2).

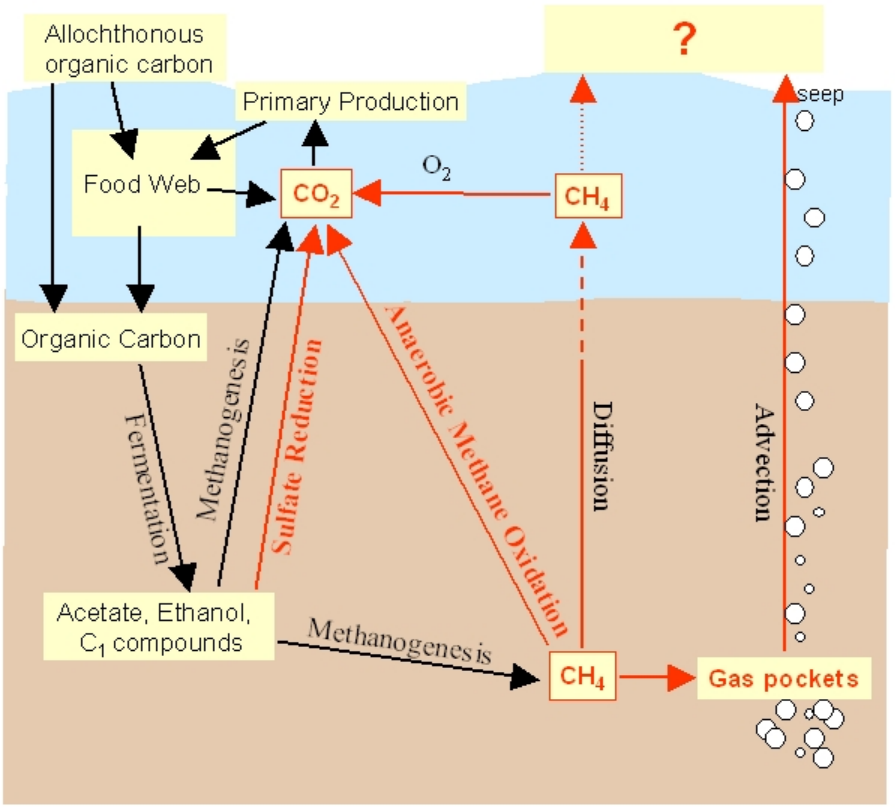

Figure 2: Pathways of the carbon cycle in the oceans, with methane and bicarbonate as the main products of organic carbon degradation.

This remineralization takes place through aerobic degradation in the oxic zone at the sediment surface followed by a sequence of anaerobic redox reactions (Champ et al., 1979; Froehlich et al., 1979; Reeburgh, 1983) (Figure 3a). Thereby, the order of the terminal electron accepting processes is determined by the free energy yield of the mineralization reactions (Claypool and Kaplan, 1974; Froehlich et al., 1979) and the reduction of one electron acceptor can be inhibited in the presence of more electrochemically positive electron acceptors (Cord-Ruwisch et al., 1988; Hoehler et al., 1998; Lovley and Goodwin, 1988). This leads to a typical zonation of the redox processes that are mediated by microorganisms in anoxic marine sediments (Figure 3b). The terminal electron acceptors O_2 and SO_4^{2-} are transported from the seawater above the sediment surface through the pore water by molecular diffusion, whereas Fe^{3+} and Mn^{4+} occur as metal oxides in the upper sediment layers and NO_3^- is mainly produced in the shallow sediments.

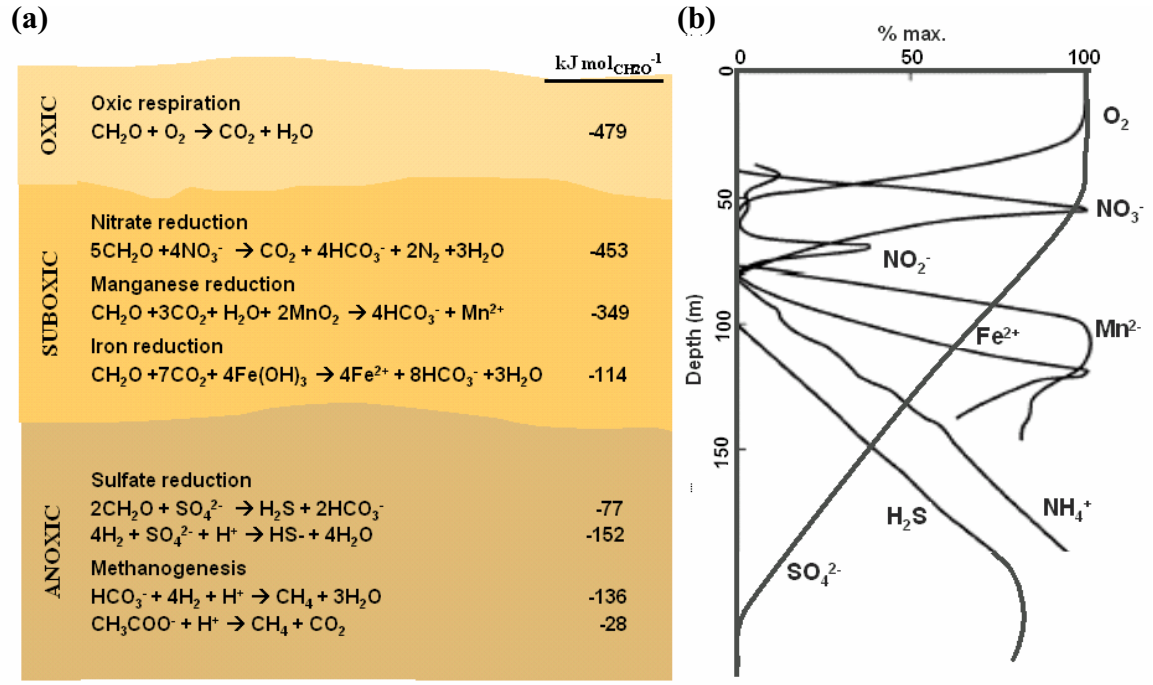

Figure 3: (a) Sequence of organic matter mineralization processes mediated by microorganisms in marine sediments. The order of terminal electron accepting processes is determined by their decreasing energy yield. (b) This sequence of reactions leads to a typical distribution of electron acceptors and reduced products in the sediment (modified after Nealson, 1997).

Because of the high organic matter input on the continental shelf, oxygen concentrations are rapidly depleted. Nitrate and Mn^{4+} are mostly of minor importance as electron acceptors and both usually occur in very low concentrations (< 100 µM for NO_3^- (Canfield et al., 1993b; Kostka et al., 1999; Sharp, 1983) and < 10 µmol cm^{-3} for Mn^{4+} (Aller, 1994; Rysgaard et al., 1998; Thamdrup and Canfield, 1996; Thamdrup et al., 1994; Thamdrup et al., 2000)) in the upper sediment layers. Therefore, the quantitatively most important anaerobic pathway for remineralization of organic carbon in ocean margin sediments is sulfate reduction, which can account for up to 25-50 % of organic matter mineralization (Canfield et al., 1993a; Christensen, 1989; Jørgensen, 1982; Reeburgh, 1983).

1.3. SULFATE REDUCTION

More than 90 % of the oceanic sulfate reduction takes place in the sediments of the continental shelfs (Jørgensen, 1982). Concurrent studies of oxygen uptake have revealed that sulfate reduction is responsible for the remineralization of up to 50 % of the organic matter deposited in coastal sediments (Jørgensen, 1982; Kasten and Jørgensen, 2000; Martens and Klump, 1984) and is therefore an important link between the sulfur cycle and the carbon cycle. This high influence on the carbon mineralization rate is possible because sulfate reduction requires eight electrons per SO_4^{2-} reduced, and because the sulfate concentrations in marine bottom water that is diffusing into the pore water of the sediment, are in the range of 28 mM (varying with salinity), which is more than 50 x higher than the concentrations of the other electron acceptors (D'Hondt et al., 2002). The main pathway of sulfate reduction is dissimilatory (i.e. used as electron acceptor for energy generation only). Assimilatory sulfate reduction might occur, but is not significant for sulfate reduction rates in sediments.

Two modes of sulfate reduction can be distinguished by the substrate that is used as electron donor: a) sulfate reduction that uses fermentation products from organic carbon degradation pathways like H_2 (2), or volatile fatty acids (3) and b) methane related sulfate reduction (1), where methane is oxidized to bicarbonate.

$$4\,H_2 + SO_4^{2-} + H^+ \rightarrow HS^- + 4\,H_2O \qquad (2)$$

$$2\,CH_2O + SO_4^{2-} \rightarrow H_2S + 2\,HCO_3^- \qquad (3)$$

In sediments with high input of organic matter, sulfate reduction with fermentation products as substrates occurs close to the sediment surface, because other electron acceptors, except CO_2, are exhausted rapidly. Sulfate reduction rates (SRR) depend on the amount and degradability of organic matter as well as on burial rates and bioturbation (Jørgensen et al., 1990) and the magnitude of SRR is an indicator of the activity of organic carbon turnover of the site (Henrichs and Reeburgh, 1993).

Methane related sulfate reduction can overlap with sulfate reduction based on fermentation products but usually it forms a second deep sulfate reduction peak that is distinct from the sulfate reduction peak at the sediment surface, and it mostly utilizes much lower sulfate concentrations.

The organisms that mediate methane related sulfate reduction belong to the *Desulfosarcina-Desulfococcus* branch of the Deltaproteobacteria (Boetius et al., 2000; Ince et al., 2006; Knittel et al., 2005; Orphan et al., 2001a), and they are also among the most abundant groups of sulfate reducing bacteria (SRB) in the zone of sulfate reduction with fermentation products as substrates at the sediment surface (Ince et al., 2006; Musat et al., 2006; Mußmann et al., 2005). Since SRB have been detected even below the zone of measurable sulfate concentrations in sediments from the Black Sea (Leloup et al., 2006), low rates of sulfate reduction might occur much deeper than previously thought.

1.4. METHANOGENESIS

Methanogenesis is the major source of methane in the ocean. Because it is the least exergonic of the diagenetic redox-processes, it takes place in a methanogenic zone below the sulfate zone. Multiple groups of strictly anaerobic archaea are distributed over several lineages of the archaeal phylogenetic tree, like *Methanobacteriales, Methanococcales, Methanomicrobiales, Methanosarcinales,* and *Methanopyrales* (Madigan et al., 2000). These organisms mediate methane production by transforming various fermentation substrates like bicarbonate (4), volatile fatty acids (5), methanol (6) or methylamine to the final product methane (Daniels et al., 1984; Heyer, 1990; Zehnder, 1988) via a 2-electron reduction by methyl-coenzyme M reductase (MCR) (Deppenmeier, 2004; McBride and Wolfe, 1971), a highly conserved enzyme (Lehmacher and Klenk, 1994; Nölling et al., 1996; Sørensen et al., 2001; Springer et al., 1995) that appears to be unique to methanogens (Thauer, 1998).

$$CO_2 + 4\,H_2 \rightarrow CH_4 + 2\,H_2O \quad (4)$$

$$CH_3COO^- + H^+ \rightarrow CH_4 + CO_2 \quad (5)$$

$$CH_3OH + H_2 \rightarrow CH_4 + H_2O \quad (6)$$

Methanogens are the only organisms known to produce methane as an endproduct, and methanogenesis is their only way of energy generation (Thauer, 1998). Most of the methane in nature is produced from acetoclastic methanogenesis (Deppenmeier et al., 1996; Ferry, 1999) in

a modified reverse acetyl-CoA-pathway, where the electrons for methane production derive from the oxidation of the carbonyl-group to CO_2 (Deppenmeier et al., 1996; Ferry, 1999) (Figure 4).

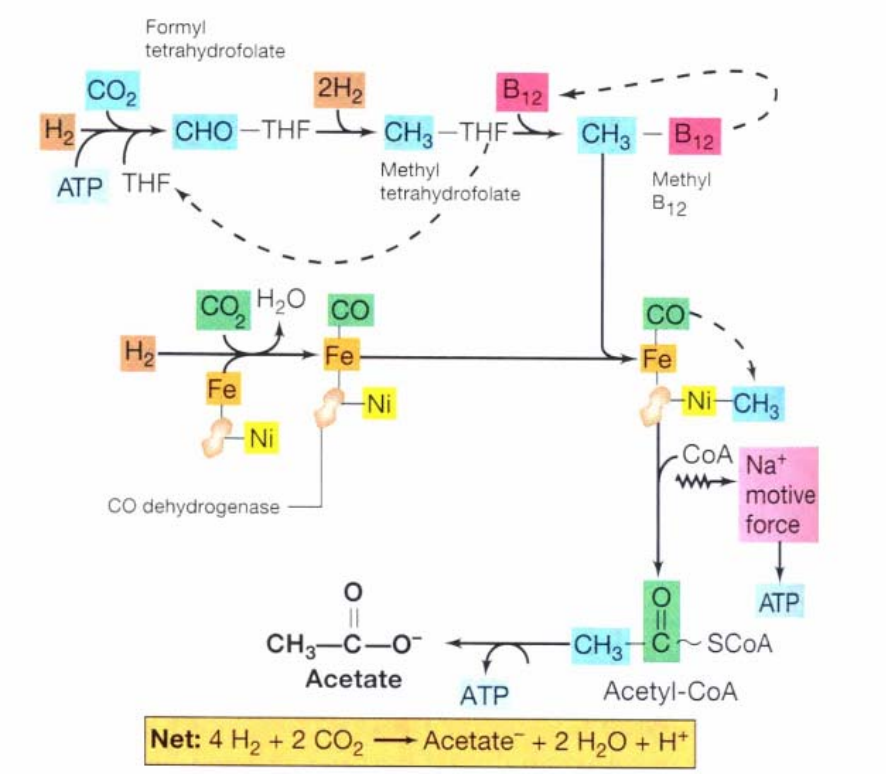

Figure 4: Reactions of the acetyl-CoA pathway, in which two CO_2 are used to form acetate (modified after Madigan et al., 2000). A similar CO-dehydrogenase-based pathway is used by acetoclastic methanogens, producing CO_2 and CH_4 from acetate, with different coenzymes (CoM) involved in the conversion of the methyl group to CH_4.

In contrast to this, bicarbonate-based methanogenesis depends on H_2 to provide electrons for CO_2-reduction. All enzymatic reactions in the methanogenic pathway are reversible with the exception of the final, MCR-catalyzed reduction of the methyl-group to methane, which is mediated by the cofactor F430, that provides the electrons from a hydrogenase (Deppenmeier et al., 1996; Diekert et al., 1981; Ellefson et al., 1982; Gunsalus and Wolfe, 1978).

Both acetate and H_2 are substrates that are also utilized by sulfate reducing bacteria, which are supposed to outcompete methanogens, because they appear to have a greater affinity (lower K_m) for several common substrates like hydrogen, and maintain concentrations at such a low level that these cannot be used by methanogens (Capone and Kiene, 1988; Claypool and Kaplan, 1974; Hoehler et al., 1998; Lovley and Goodwin, 1988; Lovley and Klug, 1982; Sansone and

Martens, 1982). Observations of methanogenesis occurring in the sulfate zone are usually attributed to non-competitive substrates, such as methylamines (Ferdelman et al., 1997b; Lovley and Klug, 1983; Oremland and Polcin, 1982; Raskin et al., 1996). Because of this competition for substrates, the methanogenic zone is located below the depth of sulfate depletion and bicarbonate methanogenesis is the predominant mode of methanogenesis in marine environments. In limnic systems with low sulfate concentrations, where low sulfate reduction rates do not exhaust volatile fatty acids, acetoclastic methanogenesis is the main pathway of methane production (Whiticar, 1999). Recently, a new pathway for methanogenic archaea was proposed (Ferry and House, 2006; Rother and Metcalf, 2004) using CO to produce acetate, formate and methane. It is, however, not yet known if this process is quantitatively important for methane generation.

The methane produced by bicarbonate or acetate methanogenesis in the sediment accumulates from the integrated activity over large depths below the sulfate zone, and because methanogenesis activity has been detected in very deep sediment layers (Horsfield et al., 2006; Newberry et al., 2004; Parkes et al., 2000) it might be an energy generating process that supports life in the deep biosphere (Judd, 2004).

1.5. METHANE

Methane is the most basic organic molecule and by far the most unreactive hydrocarbon due to its four apolar C-H bondages in a tetraedric molecule structure. It occurs as the main component of natural gas (75 %) and has the ability to form clathrate-hydrates under certain pressure and temperature conditions (Buffet, 2000; Crabtree, 1995; Kvenvolden, 1993). Before 2.7 billion years ago, methane was a prominent component of the early atmosphere. After the increase of oxygen levels through photosynthesis methane concentrations decreased to ~ 0.8 ppmv (Chang et al., 1983). Due to human activities, such as large scale-cattle farming and rice cultivation, methane concentration in the atmosphere increased again to 1.7 ppmv in recent years (Cicerone, 1988; Crutzen, 1991) (Figure 5).

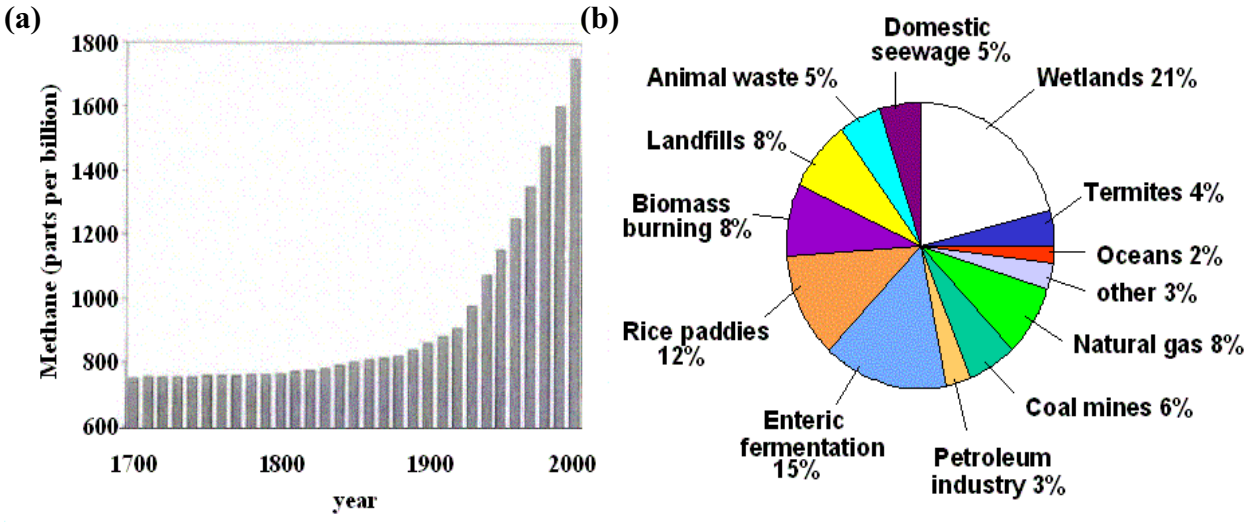

Figure 5: (a) Increase of methane concentrations in the atmosphere in the last 300 years (Reay, 2003). (b) Wetlands, rice paddies, and cattle farming are the most important methane sources. The oceans contain large amounts of methane but only very small amounts reach the atmosphere (Houghton et al., 1996).

Today, methane is considered to significantly influence global climate changes because it affects the Earth's radiative and chemical balance (Kvenvolden and Rogers, 2005) and accounts for 20 % of the trapping of infrared radiation in the atmosphere (Mackenzie, 1998). Its absorbance characteristics make it a 26x more effective green house gas than CO_2 (Lelieveld et al., 1993). Although low in concentration, it is the most abundant organic compound in the atmosphere, where it has a lifetime of ~ 7.9 years (Lelieveld et al., 1998). The chemical reaction with oxygen radicals in the hydrosphere (Lelieveld et al., 1998; Levy, 1971) as well as the aerobic oxidation to CO_2 are the major sinks for atmospheric methane.

The ocean as source of atmospheric methane is estimated to contribute ~20 Tg yr^{-1} (Judd, 2004). In marine systems, methane accumulates in shallow gas reservoirs below the sediment surface that are widespread in most areas of methane generation (Fleischer et al., 2001; Judd, 2004). The solubility of methane in water increases with pressure according to Henry's Law and depends on temperature and salinity (Yamamoto et al., 1976) so that these accumulations can consist of methane dissolved in pore water, free gas, or gas hydrates, which constitute the largest methane reservoir on earth and correspond to three times the entire terrestrial biomass (Kvenvolden,

1993). The marine methane occurrences are not only relevant as a green-house gas, especially because they mainly consist of fossil methane (Judd, 2003; Judd, 2004; Judd et al., 2002) but they also constitute an important energy source. Furthermore, methane accumulations can pose a risk for the stability of continental slopes (Best et al., 2006) and in particular gas hydrates can destabilize the seabed and cause underwater landslides (Kvenvolden, 1999).

The methane reservoirs in the ocean are to a large extend of microbial origin (Claypool and Kvenvolden, 1983). Methanogenesis is estimated to convert about 10 % of the total organic carbon in sediments to methane (Clayton, 1992) and is responsible for 80 % of the methane in the ocean, whereas 20 % is fossil methane, produced through geochemical processes from the thermocatalytic decomposition of organic matter (Breas et al., 2001; Kvenvolden and Rogers, 2005; Schoell, 1988; Sorokin et al., 2001).

The origin of the methane can be distinguished by their carbon and hydrogen isotopic signature and the proportions of other hydrocarbon contents (Whiticar, 1999) (Figure 6). If microbial mechanisms are involved in the production of methane, the isotopic carbon composition of the methane pool is lighter (about -110 ‰) compared to methane that originates from inorganic sources, because microbes discriminate against the heavier ^{13}C-isotope (Whiticar, 1999).

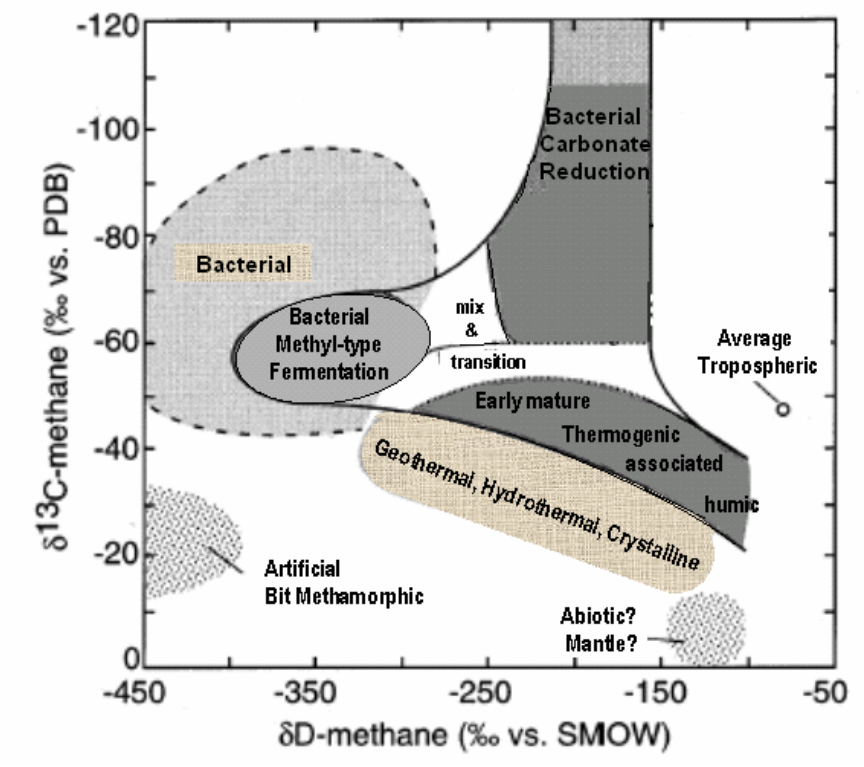

Figure 6: The stable isotope signature ($\delta^{13}C$-CH_4 and δD_{CH4}) of methane can be used to distinguish between thermogenic methane from geological sources or biogenic methane from different methanogenic pathways. (Modified after Whiticar, 1999.)

Despite the extensive production and occurrence of methane in marine environments, the role of the ocean as a methane source to the atmosphere is moderate, because aerobic oxidation of methane (Hanson and Hanson, 1996) and anaerobic oxidation of methane (AOM) act as a sink for marine methane. It was estimated that ~ 80 % of the uprising methane is consumed (Reeburgh, 1996) before it reaches the atmosphere, and that anaerobic methane oxidation in diffusive systems accounts for the turnover of ~300 Tg yr^{-1} (Hinrichs and Boetius, 2002).

1.6. ANAEROBIC OXIDATION OF METHANE (AOM)

Early investigations of anaerobic oxidation of methane (AOM) estimated that it has a similar quantitative importance as aerobic methane oxidation in marine systems (Barnes and Goldberg, 1976; Martens and Berner, 1974; Reeburgh, 1976). Pore water profiles of methane concentration from marine sediment show that methane diffusing upwards from deeper parts of the sediment reaches a zone where it is rapidly depleted (Figure 7).

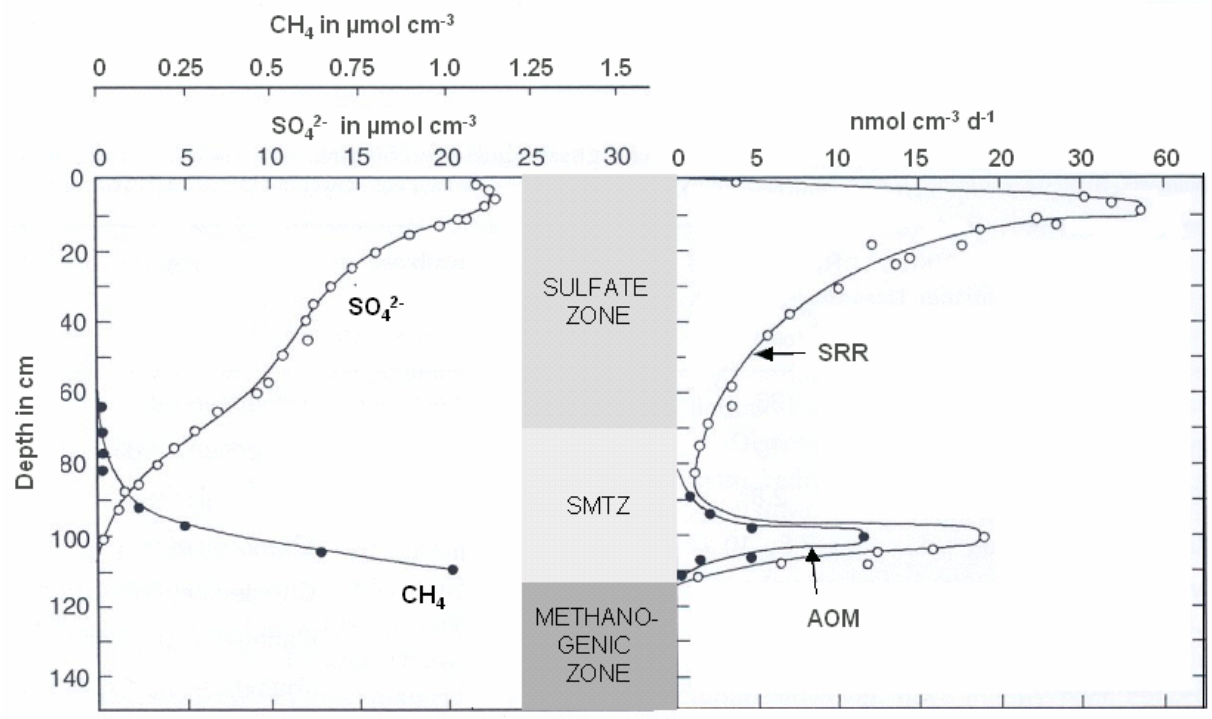

Figure 7: Typical depth profiles of methane and sulfate concentrations in anoxic marine sediments (modified after Iversen and Jørgensen, 1985). AOM rates and SRR occur in the same depth in the sulfate methane transition zone. The methanogenic zone starts below the depth of sulfate depletion.

In the same zone the sulfate concentration of the pore water that diffuses from the bottom water downwards into the sediment is declining, so that the two overlapping profiles form the sulfate-methane transition zone (SMTZ). In this zone, where methane and sulfate are present simultaneously and where concentrations of both molecules are generally low, AOM rates and sulfate reduction rates occur, and it acts as a barrier for methane from marine sediments.

The mechanism of AOM is so far poorly understood. The coupling of AOM to sulfate reduction has been validated by inhibition experiments of both processes (Alperin and Reeburgh, 1985; Hansen et al., 1998) and by rate measurements, which showed that both rates occur in the same sediment horizon (Iversen and Jørgensen, 1985) and at a 1:1 stoichiometry under laboratory conditions (Nauhaus et al., 2002). Stable isotope analyses have indicated that an intermediate must be shuffled between the AOM-mediating cells and SRB, because the sulfate reducers are depleted in $\delta^{13}C$, which can only be explained by the uptake of light AOM products (Orphan et al., 2001b). But the coupling between AOM and SRR has also been confirmed by identification of methanotrophic archaea ANME-1, ANME-2 or ANME-3 in AOM sediments that are related to the group of *Methanosarcinales* (Boetius et al., 2000; Knittel et al., 2005; Knittel et al., 2002; Lösekann, 2006; Niemann et al., 2006) and are associated with sulfate reducting bacteria. In addition to structured consortia of AMNE and SRB, other community structures have been observed in different environments, like densely populated microbial mats or small chains of ANME-1 cells (Figure 8).

However, it is not clear if there are always two cells involved in AOM and sulfate reduction, or if there could also be a single cell mediating the entire redox-reaction. So far there is no evidence that any of the intermediates like H_2, acetate, formate, methanol, and methylamines that have been proposed to function as link between the methanotrophs and the sulfate reducing bacteria is shuffled between these cells (Nauhaus et al., 2002; Nauhaus et al., 2005; Sørensen and Finster, 2001).

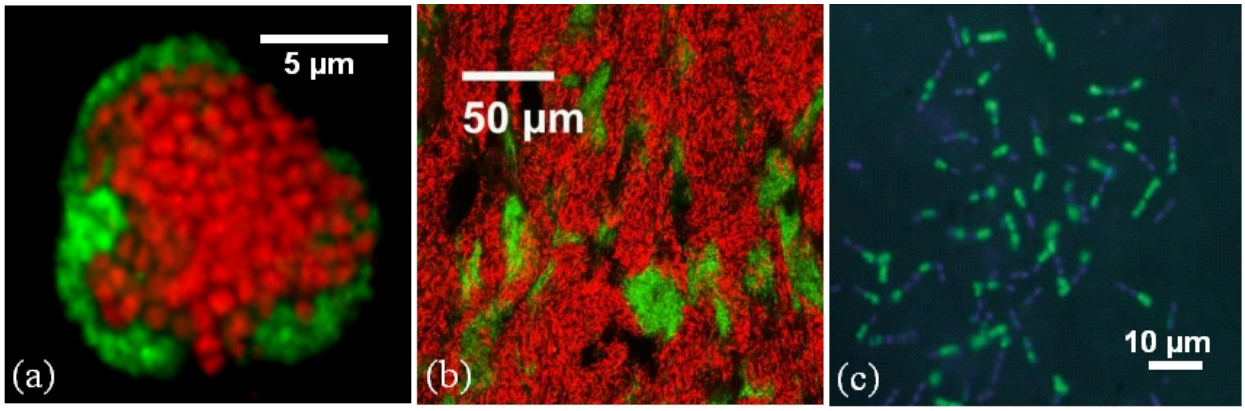

Figure 8: Methanotrophic archaea of the AMNE group (red) can be associated with sulfate reducing bacteria (green in (a) and (b)) in consortia (a) or microbial mats (b), but they can also occur as single cells (green in (c)).

Although bacteria using any other electron acceptor than sulfate could in theory also mediate AOM (Hoehler et al., 1994) this had not been observed in marine sediments. The first evidence that AOM can indeed be coupled to other electron acceptors was recently reported from the identification of a consortium that links anaerobic methane oxidation with denitrification in a freshwater sediment (Raghoebarsing et al., 2006; Thauer and Shima, 2006), but this seems to be limited to few environments with very high nitrate concentrations.

One possibility for the mechanism of AOM would be that it represents the reversed pathway of bicarbonate methanogenesis (Hallam et al., 2004; Hoehler et al., 1994; Krüger et al., 2003; Shima and Thauer, 2005; Valentine et al., 2000) (Figure 9). Methanogenic archaea have homologs of the genes for all three subunits of methyl-coenzyme M reductase (MCR), suggesting that MCR or a similar enzyme might also be responsible for AOM (Hallam et al., 2003). In addition, an alternative co-factor F430 was discovered in microbial mats that mediate anaerobic methane oxidation in the Black Sea (Krüger et al., 2003), and it was proposed that this co-factor might enable the reversibility of the MCR-reaction, which would also be energetically possible under physiologic conditions (Shima and Thauer, 2005). Nevertheless, there is also evidence that the pathway for AOM might be similar but altered from reversed methanogenesis, because one enzyme of the methanogenic pathway from bicarbonate, converting methylene-H_4MPT to methyl-H_4MPT (Figure 9, (5.)), is missing in ANME-1 cells (Hallam et al., 2004).

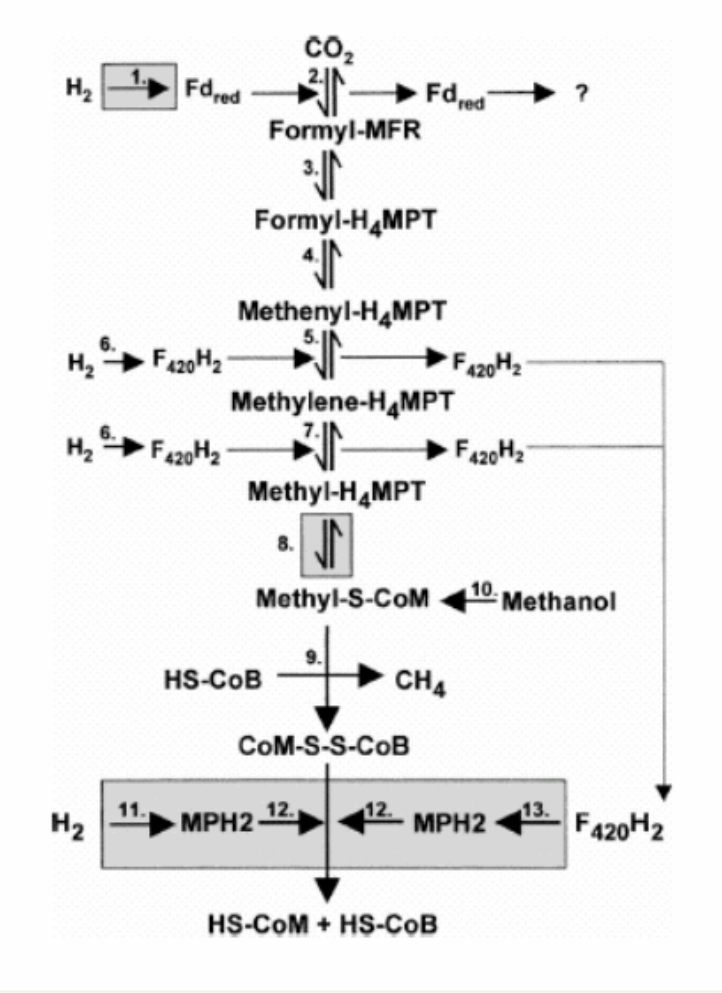

Figure 9: Pathway of methanogenesis from H_2 + CO_2. The conversion from CO_2 to Methyl-S-CoM (methyl-mercaptoethanesulfonate) is carried out by enzymatic reactions that are all reversible. The only non-reversible step is the energy-generating reduction of Methyl-S-CoM by *MCR* (9.). (from Deppenmeier et al., 1996.)

Apart from this, other biochemical mechanisms would also be possible, since methanogenic archaea and sulfate reducing bacteria both posses all the enzymes of the acetyl-CoA pathway, and all the enzymes of the methanogenic pathway have also been found in sulfate reducers (Vorholt et al., 1995). Since all efforts to isolate anaerobe methane oxidizers in pure culture have failed so far, the functioning of the pathway remains speculative.

Beyond pursuing an understanding of how methane cycling occurs in contemporary settings, there is evidence that AOM and methanogenesis were important pathways throughout Earth's history. At several locations rock-like structures of authigenic carbonate were found that are derived from precipitation of bicarbonate produced by AOM, which was verified by stable isotope analysis (Dando and Hovland, 1992; Wallmann et al., 1997). Such carbonate structures have been discovered in various locations, e.g. in the Black Sea (Michaelis et al., 2002), in the

Kattegat (Jensen et al., 1992; Jørgensen, 1989), and in Bulgaria (de Boever et al., 2006). Moreover, the important role of the variable acetyl-CoA pathway and the sole usage of C_1-compounds as energy- and carbon source make AOM and methanogenesis interesting models for ancient metabolisms. Because bicarbonate methanogenesis is by far the most common metabolic process in thermophiles, which represent the deepest branches on the phylogenetic trees of both the archaeal and bacterial domains (Amend and Shock, 2001), metabolisms like AOM and methanogenesis might be among the most original metabolism of life on Earth. More information on these mechanisms and their regulation, especially in connection to sulfate reduction, which also played an important role in the Earths´ geochemical evolution (Anbar and Knoll, 2002; Canfield et al., 2000) is needed to obtain a better understanding of early Earth.

1.7. AOM IN DIFFERENT MARINE SYSTEMS

AOM is widespread in marine sediments and can occur at sites where methane is spread by diffusion as well as at seep sites, where free gas or methane rich fluids are transported by advection from deeper reservoirs or gas hydrates. Sediments that contain enough organic matter for methane generation are mainly fine grained and impermeable (Judd, 2004), and the migration of methane towards the surface may be impeded by impervious strata, leading to the formation of accumulations, including commercial gas reservoirs (Judd, 2003). Seepage occurs only at sites where a passage of the gas or fluid is possible and seeps are therefore most commonly associated with faults, breached antiforms and salt diapirs (Judd, 2003). Because of the high methane fluxes at such seep sites, they are hot spots of AOM, and rates are much higher than in purely diffusive sediments.

The highest AOM rates have so far been observed in the sediments overlying gas hydrates at Hydrate Ridge (Treude et al., 2003) and these activities were even higher than the rates in dens microbial mats from methane seeps in the Black Sea (Treude, 2005) and at cold seeps of Gulf of Mexico (Joye et al., 2004). In contrast to the high availability of methane as substrate for AOM through active transport at seep sites, the diffusion of methane is very slow and leads to much lower AOM rates (Devol and Anderson, 1984; Iversen and Blackburn, 1981; Iversen and Jørgensen, 1985; Reeburgh, 1980). The diffusive transport in marine sediments is determined by

Fick´s law of diffusion, and therefore reactive transport models can be applied to predict AOM rates and to investigate the controls on AOM activity.

1.8. CONTROLLING PARAMETERS ON AOM

The factors that control AOM and how they affect AOM rates are so far largely unknown. It would be expected that a high input of organic matter to the sediment surface leading to increased SRR, causes a faster depletion of sulfate in the sediment, which would result in a shallow SMTZ. However, the sulfate profiles in steady state systems decrease linearly with depth and do not seem to be influenced by the rate of fermentation products related sulfate reduction and the amount of organic matter input (Fossing et al., 2000). The sulfate flux and the depth of the SMTZ is supposed to be controlled only by the methane flux from below (Borowski and Paull, 1996; Borowski et al., 1999). If the methane flux is high, the SMTZ is located close to the sediment surface and rates are usually higher than in sediments with a low methane flux and a deeper SMTZ. Therefore, the concentrations of methane and sulfate are supposed to play a major role in regulating AOM activity. It was demonstrated on enrichments from Hydrate Ridge that SRR and AOM rates strongly depend on methane concentrations (Nauhaus et al., 2002), and also an increase in sulfate concentrations seemed to be stimulating SRR and AOM rates similarly in *in vitro* experiments (Löbner, 2003).

The *in situ* concentrations can influence microbial turnover rates kinetically as well as thermodynamically, which is expressed in the rate model for microbial respiration developed by Jin and Bethke (2003) and Van Cappellen et al. (2004):

$$R = B \cdot v_{max} \cdot F_K \cdot F_T$$

where the rate R is determined by the biomass of the microbial population, B, the maximum rate, v_{max} , the kinetic drive, F_K, and the thermodynamic driving force, F_T. The kinetic drive is based on a Michaelis-Menten rate expression, which was originally derived for enzyme-catalyzed reactions and the kinetic effect of the electron donating and accepting reactions (Jin and Bethke, 2002):

$$F_K = v_{max} \left(\frac{[D]^{\alpha}}{K_D + [D]^{\alpha}} + \frac{[A]^{\beta}}{K_A + [A]^{\beta}} \right)$$

where D and A are the electron donor and acceptor raised by their stoichiometric coefficients α and β, and K is the half saturation constant for D or A. At high concentrations the rate approaches a maximum, but at low concentrations the reaction is kinetically inhibited and only proceeds slowly.

Furthermore, it is only favorable for an organism to mediate the turnover of substrates if the energy yield of the reaction is negative and sufficient to drive the synthesis of ATP. The free energy yield of a reaction, ΔG, is determined with the Gibbs-Helmholtz equation from the free energy under standard conditions, $\Delta G°$, corrected for the temperature, T, the gas constant, R, and the concentrations of substrates, C_S, and products, C_P, of the reaction raised to their stoichiometric coefficients, a and b:

$$\Delta G = \Delta G° + R \cdot T \cdot \ln \left(\frac{\prod C_P^{\,a}}{\prod C_S^{\,b}} \right)$$

The influence that the concentrations of the reactants have on the energy yield becomes more important the closer the reaction is to equilibrium, and for low energy yields they determine if the reaction is favorable for the organism under the conditions prevailing in the sediment or not. It was proposed that the energy yield acts as a threshold for microbial activity and in addition inhibits rates at low substrate concentrations (Jin and Bethke, 2003; Jin and Bethke, 2005; Van Cappellen et al., 2004):

$$F_T = 1 - e^{\left(\frac{\Delta G + m\Delta G_{ATP}}{\chi \cdot R \cdot T} \right)}$$

where ΔG is the energy yield of the reaction and χ is the stoichiometry constant. The threshold $m\Delta G_{ATP}$, where ΔG_{ATP} is the energy needed to produce one ATP molecule, and m is the number of ATP synthesized would be determined by the biological energy quantum, i.e. the lowest energy that organisms can conserve for ATP synthesis (Hoehler, 2004). This amount is supposed to be the energy required for the translocation of a proton across the cellular membrane, for which ~ 20 kJ would be required (Schink, 1997). Some microorganisms can, however, mediate reactions with much lower energy yields (Jackson and McInerney, 2002) so that this value, which is based on growing *E. coli* cultures, is probably overestimated.

The coupled reaction of AOM and SRR has a very low energy yield under standard conditions, and the rates occur in the SMTZ, where substrate concentrations are changing significantly. Therefore kinetic and thermodynamic constraints might play an important role in regulating SRR and AOM rates.

1.9. OBJECTIVES OF RESEARCH

The work of this thesis was conducted as part of the EU-project METROL (Methane fluxes in ocean margin sediments: microbiological and geochemical control), which used an integrated approach of geophysical, geochemical and microbiological methods to investigate the processes responsible for the formation and oxidation of methane and the controls of the SMTZ as a methane barrier in selected European margin sediments.
This thesis mostly focused on the geochemistry of the pore water and the analysis of microbial rates involved in methane dynamics, with the purpose to acquire a dataset that can be correlated to seismic measurements and molecular investigations of the microbial community, and that can be used for predictive models on the processes involved in methane production and consumption.

The main objectives of this work were:

- Quantification of methane budgets and fluxes in diffusive sediments
- Evaluation of the effectiveness of the SMTZ as a methane barrier
- Identification of the factors that control AOM and methane related SRR
- Quantification of the magnitude of AOM and SRR in different diffusive sediments
- Determination of the role of methanogenesis in these sediments and its implication for AOM and SRR
- Investigation of thermodynamic and kinetic regulation of AOM

To investigate these questions the following study sites were visited (Figure 10):

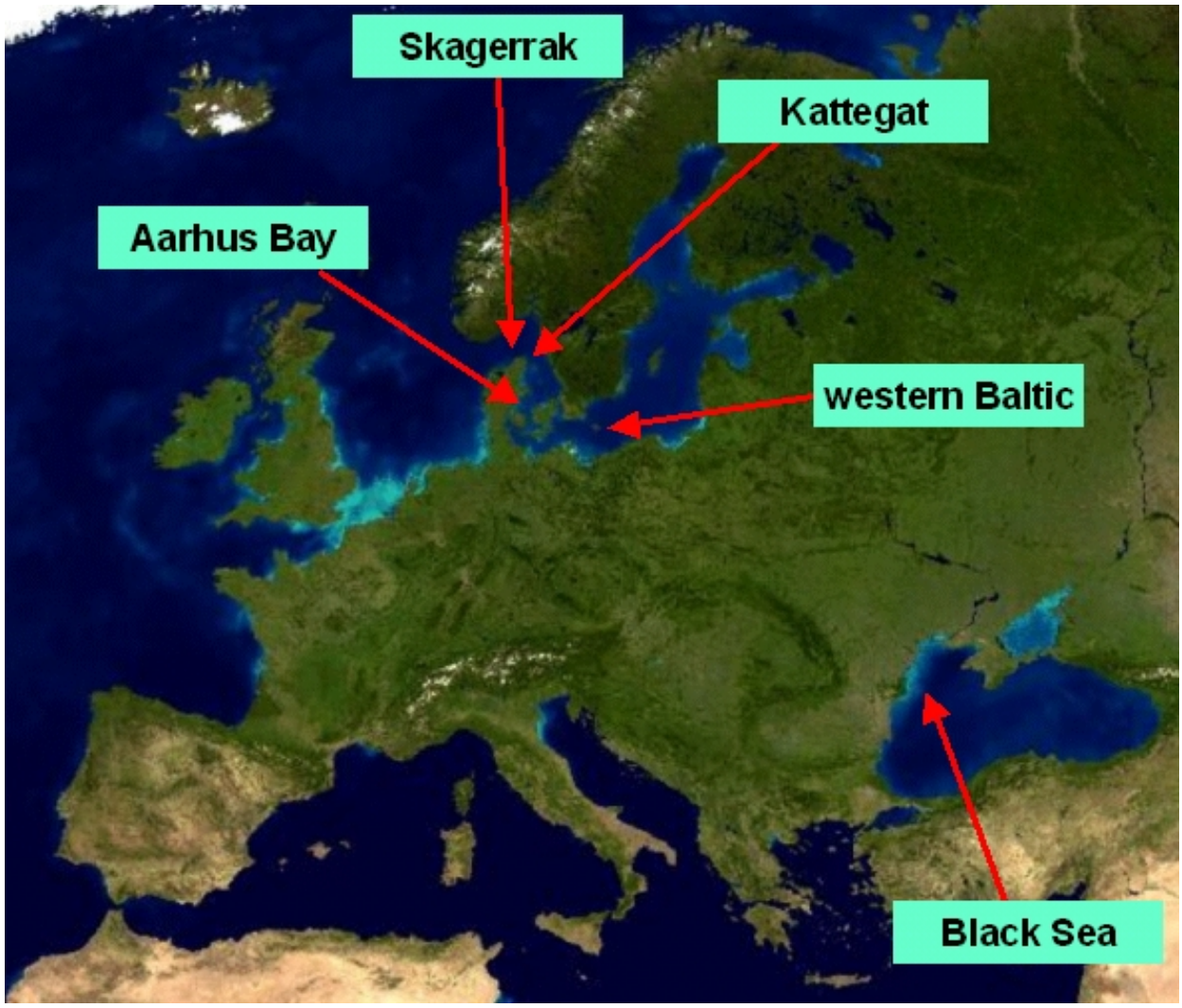

Figure 10: Map of study sites in the METROL project that were investigated for this thesis.

Aarhus Bay is a half-sheltered shallow bay at the eastern coast of Denmark that is covered by fine grained Holocene deposits. The depth of the methane gas front is gradually rising from > 4 m to < 0.5 m below the sediment surface. This site was visited five times during the project to study the influence of seasonal variability on the SMTZ and to correlate pore water profiles with seismic data.

The Skagerrak forms the western part of the North Sea - Baltic Sea transition, and is exposed to high sedimentation rates. Therefore the sediments contain large amounts of organic matter which leads to enhanced methane production. Pockmarks with incomplete methane retention occur in close vicinity of sites with a deep SMTZ, where methane is efficiently oxidized. The sediments of the Skagerrak were investigated to determine the effectiveness of the methane barrier, and how the methane and sulfate profiles are distributed in a pockmark.

The Kattegat is located at the transition of the North Sea and the Baltic Sea, northeast of Denmark. The Holocene sediments contains large areas of shallow gas accumulation in addition to methane plumes in glacial and interglacial deposits (Laier et al., 1992). The aim of the research at this site was to understand the impact of the depositional history of the sediment on the SMTZ and on methane production and consumption.

The *Western Baltic Sea* contains areas with thick organic-rich Holocene deposits and biogenic methane production. The influence of these Holocene deposits on methane distribution and the regulation of the SMTZ was studied in this area. In addition it was examined how the depth of the gas bubble front is related to pore water profiles and rates of AOM, SRR, and methanogenesis.

In the *Black Sea* electron acceptors like oxygen, nitrate and metal ions are depleted in the anoxic water column and the underlying sediments, and it therefore serves a model system to study direct carbon remineralization through sulfate reduction and methanogenesis. Sediments from different sites in the western Black Sea were analyzed to better understand the occurrence of very sluggish AOM rates and SRR that were observed in earlier studies (Jørgensen et al., 2001).

1. 10. REFERENCES

Aller R. C. (1994) The sediment Mn cycle in Long Island Sound: Its role as intermediate oxidant and the influence of bioturbation, O_2 and C_{org} flux on diagenic reaction balance. *Journal of Marine Research* **52**, 259-295.

Alperin M. J. (1988) The carbon cycle in an anoxic marine sediment: Concentrations, rates, isotope ratios, and diagenic models. PhD thesis, University of Alaska.

Alperin M. J. and Reeburgh W. S. (1985) Inhibition experiments on anaerobic methane oxidation. *Applied and Environmental Microbiology* **50**(4), 940-945.

Amend J. P., Shock E. L. (2001) Energetics of overall metabolic reactions of thermophilic and hyperthermophilic archaea and bacteria. *FEMS Microbiology Reviews* **25**(2), 175-243.

Anbar A. D. and Knoll A. H. (2002) Proterozoic ocean chemistry and evolution: A bioinorganic bridge? *Science* **297**(5584), 1137-1142.

Barnes R. O. and Goldberg E. D. (1976) Methane production and consumption in anoxic marine sediments. *Geology* **4**(5), 297-300.

Berger W. H., Smetacek V. S., and Wefer G. (1989) Ocean productivity and paleoproductivity: An overview. In *Productivity of the Ocean: Present and Past.* (ed. W. H. Berger, V. S. Smetacek, and G. Wefer), pp. 1.34. J. Wiley & Sons.

Best A. I., Richardson M. D., Boudreau B. P., Judd A. G., Leifer I., Lyons A. P., Martens C. S., Orange D. L., and Wheeler S. J. (2006) Shallow seabed methane gas could pose coastal hazard. *EOS Transactions, American Geophysical Union* **87**(22), 213-220.

Boetius A., Ravenschlag K., Schubert C. J., Rickert D., Widdel F., Gieseke A., Amann R., Jørgensen B. B., Witte U., and Pfannkuche O. (2000) A marine microbial consortium apparently mediating anaerobic oxidation of methane. *Nature* **407**(6804), 623-626.

Borowski W. S. and Paull C. K. (1996) Marine pore-water sulfate profiles indicate *in situ* methane flux from underlying gas hydrates. *Geology* **24**(7), 655-658.

Borowski W. S., Paull C. K., and Ussler III W. (1999) Global and local variations of interstitial sulfate gradients in deep-water, continental margin sediments: Sensitivity to underlying methane and gas hydrates. *Marine Geology* **159**, 131-154.

Breas O., Guillou C., Reniero F., and Wada E. (2001) The global methane cycle: isotopes and mixing ratios, sources and sinks. *Isotopes and Environmental Health Studies* **37**, 257-379.

Buffet B. A. (2000) Clathrate hydrates. *Annual Review of Earth and Planetary Sciences* **28**, 477-507.

Canfield D. E., Jørgensen B. B., Fossing H., Glud R., Gundersen J., Ramsing N. B., Thamdrup B., Hansen J. W., Nielsen L. P., and Hall P. O. J. (1993a) Pathways of organic-carbon oxidation in three continental-margin sediments. *Marine Geology* **113**(1-2), 27-40.

Canfield D. E., Kisten S. H., and Thamdrup B. (2000) The Archaean sulfur cycle and the early history of atmospheric oxygen. *Science* **288**, 658-661.

Canfield D. E., Thamdrup B., and Hansen J. W. (1993b) The anaerobic degradation of organic matter in Danish coastal sediments: Iron reduction, manganese reduction, and sulfate reduction. *Geochimica Et Cosmochimica Acta* **57**, 3867-3883.

Capone D. G. and Kiene R. P. (1988) Comparison of microbial dynamics in marine and freshwater sediments. *Limnology & Oceanography* **33**(4), 725-749.

Champ D. R., Gulens J., and Jackson R. E. (1979) Oxidation-reduction sequences in ground water flow systems. *Canadian Journal of Earth Sciences* **16**, 12-23.

Chang S., Des Marais D. J., Mac R., Miller S. L., and Strathearn G. E. (1983) Prebiotic organic synthesis and origin of life. In *Earth´s Earliest Biosphere - its Origin and Evolution* (ed. J. W. Schopf), pp. 99-139. Princeton University Press.

Christensen J. P. (1989) Sulfate reduction and carbon oxidation rates in continental-shelf sediments, an examination of offshelf carbon transport. *Continental Shelf Research* **9**(3), 223-246.

Cicerone R. J. (1988) Methane linked to warming. *Nature* **334**(21 July), 198.

Claypool G. E. and Kaplan I. R. (1974) The origin and distribution of methane in marine sediments. In *Natural Gases in Marine Sediments* (ed. I. R. Kaplan), pp. 99-139. Plenum Press.

Claypool G. E. and Kvenvolden K. A. (1983) Methane and other hydrocarbon gases in marine sediment. *Annual Review of Earth and Planetary Sciences* **11**, 299-327.

Clayton C. J. (1992) Source volumetrics of biogenic gas generation. In *Bacterial Gas* (ed. R. Vially), pp. 191-204. Editions Technip.

Conrad R. (1996) Soil microorganisms as controllers of atmospheric trace gases (H_2, CO, CH_4, OCS, N_2O and NO). *Microbiological Reviews* **60**, 609-640.

Cord-Ruwisch R., Seitz H.-J., and Condar R. (1988) The capacity of hydrogenotrophic anaerobic bacteria to compete for traces of hydrogen depends on the redox potential of the terminal electron acceptor. *Archives of Microbiology* **149**, 350-357.

Crabtree R. H. (1995) Aspects of methane chemistry. *Chemical Reviews* **95**, 987-1007.

Crutzen P. J. (1991) Methane's sinks and sources. *Nature* **350**, 380-381.

Dando P. R. and Hovland M. (1992) Environmental effects of submarine seeping natural-gas. *Continental Shelf Research* **12**(10), 1197-&.

Daniels L., Sparling R., and Sprott G. D. (1984) The bioenergetics of methanogenesis. *Biochimica Et Biophysica Acta* **768**, 113-163.

de Boever E., Swennen R., and Dimitrov L. (2006) Lower Eocene carbonate cemented chimneys (Varna, NE Bulgaria): Formation and the (a)biological mediation of chimney growth. *Sedimentary Geology* **185**(3-4), 159-173.

Deppenmeier U. (2004) The membrane-bound electron transport system of *Methanosarcina* species. *Journal of Bioenergetics and Biomembranes* **36**(1), 55-64.

Deppenmeier U., Müller V., and Gottschalk G. (1996) Pathways of energy conservation in methanogenic archaea. *Archives of Microbiology* **165**, 149-163.

Devol A. H. and Anderson J. J. (1984) A model for coupled sulfate reduction and methane oxidation in the sediments of Saanich Inlet. *Geochimica Et Cosmochimica Acta* **48**, 993-1004.

D'Hondt S., Jørgensen B. B., Blake R., Dickens G., Hindrichs K., Holm N., Mitterer R., and Spivack A. (2002) Microbial activity in deeply buried marine sediments. *Geochimica Et Cosmochimica Acta* **66**(15A), A163-A163.

Diekert G., Konheiser U., Piechulla K., and Thauer R. K. (1981) Nickel requirement and factor F_{430} content of methanogenic bacteria. *Journal of Bacteriology* **148**(2), 459-464.

Ellefson W. L., Whitman W. B., and Wolfe R. S. (1982) Nickel-containing factor F_{430}: Chromophore of the methylreductase of *Methanobacterium*. *Proceedings of the National Academy of Sciences of the United States of America* **79**, 3707-3710.

Elvert M., Boetius A., Knittel K., and Jørgensen B. B. (2003) Characterization of specific membrane fatty acids as chemotaxonomic markers for sulfate-reducing bacteria involved in anaerobic oxidation of methane. *Geomicrobiology Journal* **20**(4), 403-419.

Ferdelman T. G., Lee C., Pantoja S., Herder, J., Bebout B. M., and Fossing H. (1997) Sulfate reduction and methanogenesis in a *Thioploca*-dominated sediment off the coast of Chile. *Geochimica et Cosmochimica Acta* **61**(15), 3056-3079.

Ferry J. G. (1999) Enzymology of one-carbon metabolism in methanogenic pathways. *FEMS Microbiology Reviews* **23**, 13-37.

Ferry J. G. and House C. H. (2006) The stepwise evolution of early life driven by energy conservation. *Molecular Biology and Evolution* **23**(6), 1286-1292.

Field C. B., Behrenfeld M. J., Randerson J. T., Falkowski P. (1998) Primary production of the biosphere: Integrating terrestrial and oceanic components. *Science* **281**, 237-240.

Fleischer P., Orsi T. H., Richardson M. D., and Anderson A. L. (2001) Distribution of free gas in marine sediments: A global overview. *Geo-Marine Letters* **21**, 103-122.

Fossing H., Ferdelman T. G., and Berg P. (2000) Sulfate reduction and methane oxidation in continental margin sediments influenced by irrigation (south-east Atlantic off Namibia). *Geochimica Et Cosmochimica Acta* **64**(5), 897-910.

Froehlich P. N., Klinkhammer G. P., Bender M. L., Luedtke N. A., Heath G. R., Cullen D., Dauphin P., Hammond D., Hartman B., and Maynard V. (1979) Early oxidation of organic matter in pelagic sediments of the eastern equatorial Atlantic: suboxic diagenesis. *Geochimica Et Cosmochimica Acta* **43**, 1075-1088.

Gunsalus R. P. and Wolfe R. S. (1978) Chromophoric factors F_{342} and F_{430} of *Methanobacterium thermoautotrophicum*. *FEMS Microbiology Letters* **3**(4), 191-193.

Hallam S. J., Girguis P. R., Preston C. M., Richardson P. M., and DeLong E. F. (2003) Identification of methyl coenzyme M reductase A (mcrA) genes associated with methane-oxidizing archaea. *Applied and Environmental Microbiology* **69**(9), 5483-5491.

Hallam S. J., Putnam N., Preston C. M., Detter J. C., Rokhsar D., Richardson P. M., and DeLong E. F. (2004) Reverse methanogenesis: Testing the hypothesis with environmental genomics. *Science* **305**(5689), 1457-1462.

Hansen L. B., Finster K., Fossing H., and Iversen N. (1998) Anaerobic methane oxidation in sulfate depleted sediments: Effects of sulfate and molybdate additions. *Aquatic Microbial Ecology* **14**(2), 195-204.

Hanson R. S. and Hanson T. E. (1996) Methanotrophic bacteria. *Microbiological Reviews* **60**(2), 439-471.

Henrichs S. M., Reeburgh W. S. (1987) Anaerobic mineralization of marine sediment organic matter: Rates and the role of anaerobic processes in the ocean carbon economy. *Geomicrobiology Journal* **5**, 191-237.

Heyer J. (1990) *Der Kreislauf des Methans*. Akademie-Verlag.

Hinrichs K. U. and Boetius A. (2002) The anaerobic oxidation of methane: New insights in microbial ecology and biogeochemistry. In *Ocean Margin Systems* (ed. G. Wefer) Springer-Verlag Berlin, Heidelberg, 457-477.

Hinrichs K. U., Summons R. E., Orphan V., Sylva S. P., and Hayes J. M. (2000) Molecular and isotopic analysis of anaerobic methane-oxidizing communities in marine sediments. *Organic Geochemistry* **31**(12), 1685-1701.

Hoehler T. M. (2004) Biological energy requirements as quantitative boundary conditions for life in the subsurface. *Geobiology* **2**, 205-215.

Hoehler T. M., Alperin M. J., Albert D. B., and Martens C. S. (1994) Field and laboratory studies of methane oxidation in an anoxic marine sediment - evidence for a methanogen-sulfate reducer consortium. *Global Biogeochemical Cycles* **8**(4), 451-463.

Hoehler T. M., Alperin M. J., Albert D. B., and Martens C. S. (1998) Thermodynamic control on hydrogen concentrations in anoxic sediments. *Geochimica Et Cosmochimica Acta* **62**(10), 1745-1756.

Horsfield B., Schenk H. J., Ondrak R., Diekmann. V., Kallmeyer J., Mangelsdorf K., di Primio R., Wilkes H., Parkes R. J., Fry J., and Cragg B. (2006) Living microbial ecosystems within the active zone of catagenesis: Implications for feeding the deep biosphere. *Earth and Planetary Science Letters* **246**, 55-69.

Houghton J. T., Meira Filho L. G., Callander B. A., Harris N., Kattenberg A. Maskel K. (1996) *Climate change 1995: The science of climate change*. Cambridge University Press for the Inter-government Panel on Climate Change, Cambridge

Ince B. K., Usenti I., Eyigor A., Oz N. A., Kolukirik M., and Ince O. (2006) Analysis of methanogenic archaeal and sulphate reducing bacterial populations in deep sediments of the Black Sea. *Geomicrobiology Journal* **23**(5), 285-292.

Iversen N. and Blackburn T. H. (1981) Seasonal rates of methane oxidation in anoxic marine sediments. *Applied and Environmental Microbiology* **41**(6), 1295-1300.

Iversen N. and Jørgensen B. B. (1985) Anaerobic methane oxidation rates at the sulfate methane transition in marine sediments from Kattegat and Skagerrak (Denmark). *Limnology and Oceanography* **30**(5), 944-955.

Jackson B. E. and McInerney M. J. (2002) Anaerobic microbial metabolism can proceed close to thermodynamic limits. *Nature* **415**, 454-456.

Jensen P., Aagaard I., Burke R. A., Dando P. R., Jørgensen N. O., Kuijpers A., Laier T., Ohara S. C. M., and Schmaljohann R. (1992) Bubbling reefs in the Kattegat - submarine landscapes of carbonate-cemented rocks support a diverse ecosystem at methane seeps. *Marine Ecology-Progress Series* **83**(2-3), 103-112.

Jin Q. and Bethke C. M. (2002) Kinetics of electron transfer through the respiratory chain. *Biophysical Journal* **83**, 1797-1808.

Jin Q. and Bethke C. M. (2003) A new rate law describing microbial respiration. *Applied and Environmental Microbiology* **69**(4), 2340-2348.

Jin Q. and Bethke C. M. (2005) Predicting the rate of microbial respiration in geochemical environments. *Geochimica Et Cosmochimica Acta* **69**(5), 1133-1143.

Jørgensen N. O. (1989) Holocene methane-derived dolomite cemented sandstone pillars from Kattegat, Denmark. *Marine Geology* **88**, 71-81.

Jørgensen B. B. (1982) Mineralization of organic matter in the sea bed - the role of sulfate reduction. *Nature* **296**(5858), 643-645.

Jørgensen B. B., Bang M., and Blackburn T. H. (1990) Anaerobic mineralization in marine sediments from the Baltic Sea - North Sea transition. *Marine Ecology-Progress Series* **59**, 39-54.

Jørgensen B. B., Weber A., and Zopfi J. (2001) Sulfate reduction and anaerobic methane oxidation in Black Sea sediments. *Deep-Sea Research I* **48**(9), 2097-2120.

Joye S. B., Boetius A., Orcutt B. N., Montoya J. P., Schulz H. N., Erickson M. J., and Lugo S. K. (2004) The anaerobic oxidation of methane and sulfate reduction in sediments from Gulf of Mexico cold seeps. *Chemical Geology* **205**(3-4), 219-238.

Judd A. G. (2003) The global importance and context of methane escape from the seabed. *Geo-Marine Letters* **23**, 147-154.

Judd A. G. (2004) Natural seabed gas seeps as sources of atmospheric methane. *Environmental Geology* **46**, 988-996.

Judd A. G., Hovland M., Dimitrov L. I., Gil S. G., and Jukes V. (2002) The geological methane budget at continental margins and its influence on climate change. *Geofluids* **2**(2), 109-126.

Kasten S. and Jørgensen B. B. (2000) Sulfate reduction in marine sediments. In *Marine Geochemistry* (ed. H. D. Schulz and M. Zabel), pp. 263-282. Springer.

Knittel K., Lösekann T., Boetius A., Kort R., and Amann R. (2005) Diversity and distribution of methanotrophic archaea at cold seeps. *Applied and Environmental Microbiology* **71**(1), 467-479.

Knittel K., Lösekann T., Boetius A., Nadalig T., and Amann R. (2002) Diversity of microorganisms mediating anaerobic oxidation of methane. *Geochimica Et Cosmochimica Acta* **66**(15A), A407-A407.

Kostka J. E., Thamdrup B., Glud R. N., and Canfield D. E. (1999) Rates and pathways of carbon oxidation in permanently cold Arctic sediments. *Marine Ecology Progress Series* **180**, 7-21.

Krüger M., Meyerdierks A., Glöckner F. O., Amann R., Widdel F., Kube M., Reinhardt R., Kahnt R., Bocher R., Thauer R. K., and Shima S. (2003) A conspicuous nickel protein in microbial mats that oxidize methane anaerobically. *Nature* **426**(6968), 878-881.

Kvenvolden K. A. (1993) Gas hydrates - Geological perspective and global change. *Geophysical Reviews* **31**, 173-183.

Kvenvolden K. A. (1999) Potential effects of gas hydrate on human welfare. *Proceedings of the National Academy of Sciences of the United States of America* **96**, 3420-3426.

Kvenvolden K. A. and Rogers B. W. (2005) Gaia´s breath - global methane exhalations. *Arine and Petroleum Geology* **22**, 579-590.

Laier T., Jørgensen N. O., Buchardt B., Cederberg T., and Kuijpers A. (1992) Accumulation and seepages of biogenic gas in northern Denmark. *Continental Shelf Research* **12**(10), 1173-&.

Lehmacher A. and Klenk H. P. (1994) Characterization and phylogeny of MCRII, a gene-cluster encoding an isoenzyme of methyl-M reductase from hyperthermophilic *Methanothermus fervidus*. *Molecular & General Genetics* **243**, 198-206.

Lelieveld J., Crutzen P. J., and Brühl C. (1993) Climate effects of atmospheric methane. *Chemosphere* **26**, 739-768.

Lelieveld J., Crutzen P. J., and Dentener F. J. (1998) Changing concentrations, lifetime and climate forcing of atmospheric methane. *Tellus Series B - Chemical and Physical Meterology* **50**(2), 128-150.

Leloup J., Loy A., Knab N. J., Borowski C., Wagner M., and Jørgensen B. B. (2006) Diversity and abundance of sulfate-reducing microorganisms in the sulfate and methane zones of a marine sediment, Black Sea. *Environmental Microbiology* doi:10.1111/j.1462-2920.2006.01122.x.

Levy H. (1971) Normal atmosphere - large radical and formaldehyde concentrations predicted. *Science* **173**(3992), 141&.

Löbner H. (2003) Der regulatorische Einfluss der Sulfat- und Methankonzentration auf die anaerobe Methanoxidation in marinen Sedimenten. Diplomarbeit, Universität Bremen.

Lösekann T. (2006) Molecular characterization of methanotrophic and chemoautotrophic communities at cold seeps. PhD thesis, Universität Bremen.

Lovley D. R. and Goodwin S. (1988) Hydrogen concentrations as an indicator of the predominant terminal electron-accepting reactions in aquatic solutions. *Geochimica Et Cosmochimica Acta* **52**, 2993-3003.

Lovley D. R. and Klug M. J. (1982) Kinetic analysis of competition between sulfate reducers and methanogens for hydrogen in sediments. *Applied Environmental Microbiology* **43**, 1373-1379.

Lovley D. R. and Klug M. J. (1983) Sulfate reducers can outcompete methanogens at freshwater sulfate concentrations. *Applied Environmental Microbiology* **45**, 187-192.

Mackenzie F. T. (1998) *Our changing planet: An introduction to Earth System Science and Global Environmental Change*. Prentice Hall.

Madigan M. T., Martinko J. M., and Parker J. (2000) *Brock - Biology of Microorganisms*. Prentice-Hall.

Martens C. S. and Berner R. A. (1974) Methane production in the interstitial waters of sulfate-depleted marine sediments. *Science* **185**(4157), 1167-1169.

Martens C. S. and Klump J. V. (1984) Biogeochemical cycling in an organic-rich coastal marine basin-4. An organic carbon budget for sediments dominated by sulfate reduction and methanogenesis. *Geochimica Et Cosmochimica Acta* **48**, 1987-2004.

McBride B. C. and Wolfe R. S. (1971) A new coenzyme of methyl transfer, coenzyme M. *Biochemistry* **10**(12), 2317-2324.

Michaelis W., Seifert R., Nauhaus K., Treude T., Thiel V., Blumenberg M., Knittel K., Gieseke A., Peterknecht K., Pape T., Boetius A., Amann R., Jørgensen B. B., Widdel F., Peckmann J. R., Pimenov N. V., and Gulin M. B. (2002) Microbial reefs in the Black Sea fueled by anaerobic oxidation of methane. *Science* **297**(5583), 1013-1015.

Musat N., Werner U., Knittel K., Kolb S., Dodenhof T., van Beusekom E. E., de Beer D., Dubilier N., and Amann R. (2006) Microbial community structure of sandy intertidal sediments in the North Sea, Sylt-Rømø Basin, Wadden Sea. *Systematic and Applied Microbiology* **29**, 333-348.

Mußmann M., Ishii K., Rabus R., and Amann R. (2005) Diversity and vertical distribution of cultured and uncultured *Deltaproteobacteria* in an intertidal mud flat of the Wadden Sea. *Environmental Microbiology* **7**(3), 405-418.

Nauhaus K., Boetius A., Krüger M., and Widdel F. (2002) *In vitro* demonstration of anaerobic oxidation of methane coupled to sulphate reduction in sediment from a marine gas hydrate area. *Environmental Microbiology* **4**(5), 296-305.

Nauhaus K., Treude T., Boetius A., and Krüger M. (2005) Environmental regulation of the anaerobic oxidation of methane: a comparison of ANME-I and ANME-II communities. *Environmental Microbiology* **7**(1), 98-106.

Nealson K. H. (1997) Sediment bacteria: Who´s there, what are they doing, and what´s new? *Annual Review of Earth and Planetary Sciences* 25, 403-434.

Newberry C. J., Webster G., Cragg B., A., Parkes R. J., Weightman A. J., and Fry J. C. (2004) Diversity of prokaryotes and methanogenesis in deep subsurface sediments from the

Nankai Trough, Ocean Drilling Profgram Leg 190. *Environmental Microbiology* **6**(3), 274-287.

Niemann H., Lösekann T., de Beer D., Elvert M., Nadalig T., Knittel K., Amann R., Sauter E. J., Schlüter M., Klages M., Foucher J. P., and Boetius A. (2006) Novel microbial communities of the Haakon Mosby mud volcano and their role as a methane sink. *Nature* **443**, 854-858.

Nölling J., Elfner A., Palmer J. R., Steigerwald V. J., Pihl T. D., Lake J. A., and Reeve J. N. (1996) Phylogeny of *Methanopyrus kandleri* based on methyl coenzyme M reductase operons. *International Journal of Systematic Bacteriology* **46**(1170-1173).

Orcutt B., Boetius A., Elvert M., Samarkin V., Joye S. B. (2005) Molecular biogeochemistry of sulfate reduction, methanogenesis and the anaerobic oxidation of methane at Gulf of Mexico cold seeps. *Geochimica Et Cosmochimika Acta* **69** (17), 4267-4281.

Oremland R. S. and Des Marais D. J. (1983) Distribution, abundance and carbon isotopic composition of hydrocarbons in Big-Soda Lake, Nevada - an alkaline, meromictic lake. *Geochimica Et Cosmochimica Acta* **47**(12), 2107-2114.

Oremland R. S. and Polcin S. (1982) Methanogenesis and sulfate reduction: Competitive and noncompetitive substrates in estuarine sediments. *Applied and Environmental Microbiology* **44**(6), 1270-1276.

Orphan V. J., Hinrichs K. U., Ussler W., Paull C. K., Taylor L. T., Sylva S. P., Hayes J. M., and Delong E. F. (2001a) Comparative analysis of methane-oxidizing archaea and sulfate-reducing bacteria in anoxic marine sediments. *Applied and Environmental Microbiology* **67**(4), 1922-1934.

Orphan V. J., House C. H., Hinrichs K. U., McKeegan K. D., and DeLong E. F. (2001b) Methane-consuming archaea revealed by directly coupled isotopic and phylogenetic analysis. *Science* **293**(5529), 484-487.

Orphan V. J., House C. H., Hinrichs K. U., McKeegan K. D., and DeLong E. F. (2002) Multiple archaeal groups mediate methane oxidation in anoxic cold seep sediments. *Proceedings of the National Academy of Sciences of the United States of America* **99**(11), 7663-7668.

Pancost R. D., Sinninghe Damste J. S., de Lint S., van der Maarel M. J. E. C., Gottschal J. C., and Party t. M. S. S. (2000) Biomarker evidence for widespread anaerobic methane

oxidation in Mediterranean sediments by a consortium of methanogenic archaea and bacteria. *Applied and Environmental Microbiology* **66**(3), 1126-1132.

Parkes R. J., Cragg B., A., and Wellsbury P. (2000) Recent studies on bacterial populations and processes in subseafloor sediments: A review. *Hydrogeology Journal* **8**, 11-28.

Raghoebarsing A. A., Pol A., van der Schoonen K. T., Smolders A. J. P., Ettwig K. F., Rijpstra I. C., Schouten S., Sinninghe Damste J. S., Op den Camp H. J. M., and Strous M. (2006) A microbial consortium couples anaerobic methane oxidation to denitrification. *Nature* **440**, 918-921.

Raskin L., Rittmann B., and Stahl D. A. (1996) Competition and coexistence of sulfate-reducing and methanogenic populations in anaerobic biofilms. *Applied and Environmental Microbiology* **62**(10), 3847-3857.

Reay D. S. (2003) Sinking methane. *Biologist* **50**(1), 15-19.

Reeburgh W. S. (1976) Methane consumption in Cariaco Trench waters and sediments. *Earth and Planetary Science Letters* **28**, 337-344.

Reeburgh W. S. (1980) Anaerobic methane oxidation: Rate depth distributions in Skan Bay sediments. *Earth and Planetary Science Letters* **47**, 345-352.

Reeburgh W. S. (1983) Rates of biogeochemical processes in anoxic sediments. *Annual Review of Earth and Planetary Sciences* **11**(269-298).

Reeburgh W. S. (1996) "Soft spots" in the global methane budget. In *8th International Symposium on Microbial Growth on C_1 Compounds* (ed. M. E. Lidstrom and F. R. Tabita), pp. 334-342. Kluwer Academic Publishers.

Rother M. and Metcalf W. W. (2004) Anaerobic growth of *Methanosarcina acetivorans* C2A on carbon monoxide: An unusual way of life for a methanogenic archaeon. *Proceedings of the National Academy of Sciences of the United States of America* **101**, 16929-16934.

Rysgaard S., Thamdrup B., Risgaard-Petersen N., Fossing H., Berg P., Christensen P. B., and Dalsgaard T. (1998) Seasonal carbon and nutrient mineralization in a high-Arctic coastal marine sediment, Young Sound, Northeast Greenland. *Marine Ecology Progress Series* **175**, 261-276.

Sansone F. J. and Martens C. S. (1982) Volatile fatty acid cycling in organic-rich marine sediments. *Geochimica Et Cosmochimica Acta* **46**, 1575-1589.

Schink B. (1997) Energetics of syntropic cooperation in methanogenic degradation. *Microbiology and Molecular Biology Reviews* **61**(2), 262-280.

Schoell M. (1988) Multiple origins of methane in the Earth. *Chemical Geology* **71**, 1-10.

Sharp J. H. (1983) The distribution of inorganic nitrogen in the sea. In *Nitrogen in the Marine Environment* (ed. E. J. Carpenter and D. G. Capone), pp. 1-35. Academic Press.

Shima S. and Thauer R. (2005) Methyl-coenzyme M reductase and the anaerobic oxidation of methane in methanotrophic Archaea. *Current Opinion in Microbiology* **8**, 643-648.

Sørensen K. B., Finster K., and Ramsing, N. B. (2001) Thermodynamic and kinetic requirements in anaerobic methane oxidizing consortia exclude hydrogen, acetate, and methanol as possible electron shuttles. *Microbial Ecology* **42**, 1-10.

Sorokin O. G., Lein A. Y., and Balanyuk I. E. (2001) Thermodynamics of oceanic hydrothermal systems and abiogenic methane generation. *Oceanology* **41**, 861-909.

Springer E., Sachs M. S., Woese C. R., and Boone D. R. (1995) Partial gene sequences for the α-subunit of methyl-coenzyme M reductase (MCRI) as a phylogenetic tool for the family *Methanosarcinaceae*. *International Journal of Systematic Bacteriology* **275**, 554-559.

Strickland J. D. H. (1965) Phytoplankton and marine primary production. *Annual Review of Microbiology* **19**, 127-162.

Thamdrup B. and Canfield D. E. (1996) Pathways of carbon oxidation in continental margin sediments off Chile. *Limnology & Oceanography* **41**(1629-1650).

Thamdrup B., Fossing H., and Jørgensen B. B. (1994) Manganese, iron, and sulfur cycling in a coastal marine sediment, Aarhus Bay, Denmark. *Geochimica Et Cosmochimica Acta* **58**(23), 5115-5129.

Thamdrup B., Rossello-Mora R. A., and Amann R. (2000) Microbial manganese and sulfate reduction in Black Sea sediments. *Applied and Environmental Microbiology* **66**(7), 2888-2897.

Thauer R. (1998) Biochemistry of methanogenesis: A tribute to Marory Stephenson. *Microbiology* **144**, 2377-2406.

Thauer R. and Shima S. (2006) Methane and microbes. *Nature* **440**, 878-879.

Treude T., Knittel K., Blumenberg M., Seifert R., and Boetius A. (2005) Subsurface microbial methanotrophic mats in the Black Sea. *Applied and Environmental Microbiology* **71**(10), 6375-6378.

Treude T., Boetius A., Knittel K., Wallmann K., and Jørgensen B. B. (2003) Anaerobic oxidation of methane above gas hydrates at Hydrate Ridge, NE Pacific Ocean. *Marine Ecology-Progress Series* **264**, 1-14.

Valentine D. L., Blanton D. C., and Reeburgh W. S. (2000) Hydrogen production by methanogens under low-hydrogen conditions. *Archives of Microbiology* **174**(6), 415-421.

Van Cappellen P., Dale A., Pallud Y., Van Lith S., Bonneville S., Hyacinthe C., Thullner M., Laverman A., and Regnier P. (2004) Incorporating geomicrobial processes in subsurface reactive transport models. *Saturated & Unsaturated Zone*, 339-348.

Ver L. M. B., Mackenzie F. T., and Lerman A. (1999) Carbon cycle in the coastal zone: Effects of global perpetuations and change in the past three centuries. *Chemical Geology* **159**, 283-304.

Vorholt J., Kunow J., Stetter K. O., and Thauer R. K. (1995) Enzymes and coenzymes of the carbon monoxide dehydrogenase pathway for autotrophic CO_2 fixation in *Archaeoglobus lithotrophicus* and the lack of carbon monoxyde dehydogenase in the heterotrophic *A. profundus*. *Archives of Microbiology* **163**, 112-118.

Wallmann K., Linke P., Suess E., Bohrmann G., Sahling H., Schlüter, M.,, Dählmann A., Lammers S., Greinert J., and von Mirbach N. (1997) Quantifying fluid flow, solute mixing, and biogeochemical turnover at cold vents of the eastern Aleutian subduction zone. *Geochimica Et Cosmochimica Acta* **61**, 5209-5219.

Whiticar M. J. (1999) Carbon and hydrogen isotope systematics of bacterial formation and oxidation of methane. *Chemical Geology* **161**, 291-314.

Wollast R. (1991) The coastal organic carbon cycle: Fluxes, sources, and sinks. In *Ocean Margin Processes in Global Change.* (ed. R. F. C. Mantoura, J. M. Martin, and R. Wollast), pp. 365-381. John Wiley & Sons.

Yamamoto S., Alcauskas J., B., and Crozier T. E. (1976) Solubility of methane in distilled water and seawater. *Journal of Chemical and Engineering Data* **21**(1), 78-80.

Zehnder A. J. B. and Brock T. D. (1979) Methane formation and methane oxidation by methanogenic bacteria. *Journal of Bacteriology* **137**(1), 420-432.

Zehnder A. J. B. (1988) Geochemistry and biogeochemistry of anaerobic habitats. In *Biology of anaerobic microorganisms* (ed. A. J. B. Zehnder), pp1-18. Wiley & Sons.

Zehnder A. J. B., Stumm W. (1988) *Geochemistry and biogeochemistry of anaerobic habitats* (ed. A. J. B. Zehnder). John Wiley and Sons.

Overview of Manuscripts

The manuscripts that are presented in this thesis describe methane dynamics and regulation of AOM at two exemplarily diffusive systems: the Skagerrak representing sites with a distinct SMTZ and effective methane turnover, whereas Black Sea sediments are characterized by a broad SMTZ and low AOM rates.

The thesis comprises four manuscripts, presented here as chapters:

CHAPTER 2:

Anaerobic oxidation of methane (AOM) in marine sediments from the Skagerrak (Denmark): I. Geochemical and microbiological analyses

Nina J. Knab, Barry A. Cragg, Richard D. Pancost, Christian Borowski, R. John Parkes, and Bo B. Jørgensen

The sampling on board of the RV Heincke 181 cruise to the Skagerrak was performed by B. Cragg, F. Brock and me, with the help of J. Kallmeyer and M. Nickel. Pore water concentrations of methane and sulfate as well as AOM and SRR rate measurements were analyzed and evaluated by me, whereas volatile fatty acids and methanogenesis rates were determined by B. Cragg. The biomarker data and its description and interpretation in the manuscript was contributed by R. Pancost, and the total cell number counted by B. Cragg. The manuscript was written by me, with support and input from R. Pancost and B. Jørgensen.

CHAPTER 3:

Anaerobic oxidation of methane (AOM) in marine sediments from the Skagerrak (Denmark): II. Further insights with a reactive-transport model

Andrew W. Dale, Pierre Regnier, Nina J. Knab, Bo B. Jørgensen, Phillippe Van Cappellen

A. Dale was responsible for constructing the biogeochemical reaction network and its incorporation into the reaction-transport model (RTM). The data that was used for the modelling was acquired by me. A. Dale was responsible for interpreting the model data and writing the manuscript with input from P. Regnier and P. van Cappellen.

CHAPTER 4:

Thermodynamic and kinetic control on anaerobic oxidation of methane in marine sediments

Nina J. Knab, Andrew W. Dale, Karsten Lettmann, Henrik Fossing, and Bo B. Jørgensen

The manuscript includes data from the research cruises RV Heincke 181 to the Skagerrak, Gunnar Thorson 2004 to the western Baltic, and Poseidon 317/3 to the Black Sea. Pore water analyses were done by me, except SO_4^{2-} and CH_4 from 365MUC, performed by H. Fossing. AOM rates for all cores were determined by me. The energy yield and kinetic drive were calculated together by me and A. Dale, using a curve fitting program for measured profiles developed by K. Lettmann. The manuscript was written by me, with support and input from A. Dale and K. Lettmann, and with editorial input from B. Jørgensen.

CHAPTER 5:

Regulation of anaerobic methane oxidation in sediments of the Black Sea

Nina J. Knab, Barry A. Cragg, Ed Hornibrook, Lars Holmkvist, Christian Borowski, John R. Parkes, and Bo B. Jørgensen

The samples were obtained during RV Poseidon cruise 317/3 by the entire shipboard party. With the exception of volatile fatty acid concentrations, which were analyzed by B. Cragg, all pore water concentrations were measured and evaluated by me, as well as AOM and SRR rates. Methanogenesis rates and AODC counts were conducted by B. Cragg, stable isotope values were determined by E. Hornibrook, and dissolved as well as solid iron concentrations were contributed by L. Holmkvist. The manuscript was written by me, with support and input from B. Jørgensen.

Manuscripts not included in this thesis (Abstracts)

Diversity and abundance of sulfate-reducing microorganisms in the sulfate and methane zones of a marine sediment, Black Sea

Julie Leloup, Alexander Loy, Nina J. Knab, Christian Borowski, Michael Wagner, and Bo B. Jørgensen

The Black Sea, with its highly sulfidic water column, is the largest anoxic basin in the world. Within its sediments, the mineralization of organic matter occurs essentially through sulfate reduction and methanogenesis. In this study, the sulfate-reducing community was investigated in order to understand how these microorganisms are distributed relative to the chemical zonation: In the upper sulfate zone, at the sulfate-methane transition zone, and deeply within the methane zone. Total bacteria were quantified by real-time PCR of 16S rRNA genes whereas sulfate-reducing microorganisms (SRM) were quantified by targeting their metabolic key gene, the dissimilatory (b) sulfide reductase (*dsrA*). Sulfate reducing microorganisms were predominant in the sulfate zone but occurred also in the methane zone, relative proportion was maximal around the sulfate-methane transition, c. 30%, and equally high in the sulfate and methane zones, 5-10%. The *dsrAB* clone library from the sulfate-methane transition zone, showed mostly sequences affiliated with the *Desulfobacteraceae*. While, the *dsrAB* clone libraries from the upper, sulfate-rich zone and the deep, sulfate-poor zone were dominated by similar, novel deeply branching sequences which might represent Gram-positive spore-forming sulfate- and/or sulfide-reducing microorganisms. We thus hypothesize that terminal carbon mineralization in surface sediments of the Black Sea is largely due to sulfate reduction activity of previously hidden SRM. Although these novel SRM were also abundant in sulfate-poor, methanogenic areas of the Black Sea sediment, their activities and possibly very versatile metabolic capabilities remain subject of further study.

(Published in *Environmental Microbiology* (2006) doi:10.1111/j.1462-2920.2006.01122.x)

Biogeochemistry and biodiversity of methane cycling in subsurface marine sediments (Skagerrak, Denmark).

R. John Parkes, Natasha Banning, Fiona Brock, Gordon Webster, John C. Fry, Ed Hornibrook, Richard D. Pancost, S. Kelly, Nina Knab, Andrew J. Weightman and Barry A Cragg

An integrated biogeochemical, molecular genetic and lipid biomarker study was conducted on a 4 m long sediment core from the Skagerrak (Denmark) to study methane cycling in diffusively controlled sediment. These sediments had rapid sulphate reduction, resulting in sulphate removal by 0.7 m, methane formation below and a sharp sulphate-methane-transition zone (SMTZ); all characteristics of a diffusively controlled sediment. ^{14}C-radiotracer measurements demonstrated the presence of H_2/CO_2 & acetate methanogenesis and anaerobic oxidation of CH_4 (AOM). Maximum rates of AOM occurred at the SMTZ (~3 nmol/cm^3/d at 0.75 m) but also continued at greater depths at much lower rates. Maximum rates of both H_2/CO_2 & acetate methanogenesis occurred below the SMTZ but H_2/CO_2 rates were x10 those of acetate methanogenesis, and this was consistent with the presence of ^{13}C-depleted CH_4 (*ca.* δ^{13}C -80‰). Depth integrated rates of AOM (1.73 mmol/m^2/d) were similar to the total rates of methanogenesis (1.70 mmol/m^2/d) indicating that AOM provides an effective barrier to CH_4 release. A 16S rRNA gene clone library from 1.39 m combined with methanogen (T-RFLP), bacterial (DGGE) and lipid biomarker depth profiles showed the presence of ANME (-2a dominant & -3), *Methanomicrobiales*, *Methanosaeta* related *Archaea* with depth distributions which matched their expected activities. Some of the distributions of the *Gammaproteobacteria*, *Deltaproteobacteria* (including sequences loosely related to the *Desulfosarcina*/*Desulfoccocus* AOM associated sulphate-reducing bacteria, SRB), *Alphaproteobacteria*, *Spirochaete, Chloroflexi*, JS1 and OP8 related bacterial sequences were similar to those of the archaeal groups present. Below the SMTZ to ~ 1.7 m CH_4 became progressively more ^{13}C depleted (δ^{13}C -82‰) indicating a zone of CH_4 recycling which was consistent with the presence of ^{13}C depleted archaeol (δ^{13}C -55‰). Pore water acetate concentrations decreased in this zone (to ~ 7 µM) suggesting that acetate was probably not an important intermediate in CH_4 cycling. Non-isoprenoidal ether lipids increased below the SMTZ but distributions were more associated with JS1 and OP8 related sequences rather than SRB. At this site methane production and consumption are spatially separated and seem to be conducted by different groups of *Archaea*.

Also AOM is coupled to sulphate reduction unlike recent reports from some seep and gassy sediment sites.

(Accepted by *Environmental Microbiology)*

Chapter 2

Anaerobic oxidation of methane (AOM) in marine sediments from the Skagerrak (Denmark): I. Geochemical and microbiological analyses

Nina J. Knab[1], Barry A. Cragg[2], Richard D. Pancost[3], Christian Borowski[1], John Parkes[2], Bo B. Jørgensen[1]

Manuscript in preparation

[1] Max-Planck Institute for Marine Microbiology, Celsiusstr. 1, 28359 Bremen, Germany

[2] School of Earth, Ocean and Planetary Sciences, Cardiff University, Main Building, Park Place, Cardiff, Wales, CF10 3YE, U.K.

[3]School of Chemistry, University of Bristol, Cantocks Close, Bristol, England, BS8 1TS, U.K.

ABSTRACT

The organic rich sediments of the Skagerrak contain high amounts of shallow gas of mostly biogenic origin that is transported to the sediment surface by diffusion. The sulfate methane transition zone (SMTZ) where anaerobic oxidation of methane (AOM) and sulfate reduction occur functions as a methane barrier for this upwards diffusing methane.

To investigate the regulation of AOM and sulfate reduction rates (SRR) and the controls on the effectiveness of methane retention pore water concentrations and microbial rates of AOM, sulfate reduction and methanogenesis were analyzed from three gravity cores along the slope of the Norwegian Trench in the Skagerrak. SRR occurred in two distinct peaks, at the sediment surface and the SMTZ, the latter often exceeding the AOM rates that occurred at the bottom of the SMTZ. Highest rates of both AOM and SRR were observed in a core from a pockmark, where advective transport was involved and caused high methane and sulfate fluxes. But even at this site with a shallow SMTZ the entire flux of methane was oxidized below the sediment surface. Production of methane through bicarbonate methanogenesis occurred in the sulfate zone as well as in the methanogenic zone below the SMTZ, but methane oxidation compensated its production. AOM, SRR and methanogenesis seem to be closely associated and strongly depending on sulfate concentrations, which are in return being regulated by the methane flux. The identification of lipid biomarkers typically associated with AOM-environments was coherent with the geochemical profiles and indicated that the AOM community in the Skagerrak is similar to those at other AOM sites.

INTRODUCTION

Marine shelf systems are major sites of production and accumulation of organic carbon in the ocean, part of which is degraded subsequently to biogenic methane (Canfield, 1994) and therefore shallow gas accumulations are widely distributed (Judd et al., 2002). Anaerobic oxidation of methane (AOM) is an important microbial process in marine sediments and functions as a barrier for biogenic methane diffusing upwards. Intensive research on AOM in recent years has focused on rate measurements, geochemical analyses, and microbial community analyses (Valentine, 2002) in order to determine the significance of AOM in the ocean (Judd, 2004) and to understand the microbial mechanism of the reaction and its regulation (Alperin and Reeburgh, 1985; Hansen et al., 1998; Krüger et al., 2003; Nauhaus et al., 2002; Nauhaus et al., 2005).

Sediments of continental margins with high organic matter input are characterized by a zone of sulfate reduction in the surface sediment where fermentation products are used as substrates for sulfate reduction. A second sub-surface peak of sulfate reduction rates (SRR) based on methane as electron donor occurs where methane is diffusing up from deeper sources and meets the sulfate that is diffusing down into the sediment from the bottom water. Where methane and sulfate are both present they form a sulfate-methane transition zone (SMTZ). In this zone AOM is mediated by methanotrophic archaea of the ANME group in cooperation with sulfate reducing bacteria (SRB). The presence and distribution of these organisms in the sediment can be traced by biomarkers like non-isoprenoidal diether lipids that are characteristic of SRB (Pancost et al., 2001), whereas archaeal lipids like achaeol or hydroxyarchaeol indicate cells of the ANME group (Elvert et al., 2000; Hinrichs et al., 2000; Pancost et al., 2000). Below the SMTZ, in the methanogenic zone where sulfate is depleted, bicarbonate and acetate are used as substrates for methanogenesis.

Most sites where AOM coupled to sulfate reduction as an electron acceptor has been investigated are characterized by advective transport, e.g. sediments containing gas hydrates (Orcutt et al., 2004; Treude et al., 2003), mud volcanoes (Alain et al., 2006; Niemann, 2005), cold seeps (Joye et al., 2004; Orcutt et al., 2005; Orphan et al., 2002), or carbonate chimneys of microbial mats (Michaelis et al., 2002; Treude et al., 2005a). At these sites methane fluxes and therefore rates of AOM and sulfate reduction are usually very high and occur close to the sediment surface. The

regulation of methane turnover is not always the same in these different environments, which is reflected in differences in the microbial community at these locations (Knittel et al., 2005). The vast majority of methane-bearing sediments on the continental shelf are not such highly active methane seep systems but instead are dominated by diffusion and little is known about the regulation mechanism of AOM in these systems.

Most studies of AOM in diffusion-dominated systems have been based on concentration profiles and flux calculations (Fossing et al., 2000; Hensen et al., 2003; Niewöhner et al., 1998). Where rate measurements have been conducted in diffusive systems (Devol and Anderson, 1984; Iversen and Jørgensen, 1985; Reeburgh, 1980; Thomsen et al., 2001; Treude et al., 2005b) these rates have been considerably lower than at most active seep sites (Suess et al., 1999; Valentine, 2002). Flux calculations from methane concentration profiles are useful to estimate overall AOM activities of a site but tracer determined rates are needed to investigate the regulation and interaction of different rates and the depth in which they occur. Datasets of combined concentration and rate measurements from sites, where transport can be predicted by Fick´s law of diffusion and advective transport does not interfere with profiles, are important to develop models that predict AOM activity at different sites and investigate the influence of different geochemical conditions on AOM rates (Dale et al., 2006).

Methane concentrations and methane fluxes are supposed to be among the major factors influencing AOM rates (Nauhaus et al., 2002; Borowski et al., 1999) and it is therefore important to understand the role of methane production in relation to methane oxidation. Besides its influence on methane fluxes methanogenesis also competes for substrates with sulfate reduction (Lovley and Klug, 1982) and AOM is proposed to be a reversed reaction of bicarbonate methanogenesis (Hallam et al., 2003; Hoehler et al., 1994).

The goal of this work was to explore the efficiency of AOM as a methane barrier in the diffusive sediments of the Skagerrak and to investigate how the process of AOM is influenced by and interacts with other microbial processes such as sulfate reduction and bicarbonate- and acetate-methanogenesis. Since the organic matter input in the Skagerrak is relatively high and most of the shallow gas has been found to be of biogenic origin (Schmaljohann et al., 1990), it is an interesting site to investigate such interactions and AOM regulation in an area where purely diffusive sediment occur in close proximity with gas seeps and pockmarks displaying complete or incomplete methane retention.

METHODS

Study site

The Skagerrak is a marine basin that functions as a natural trap for particulate material (Anton et al., 1993; van Weering et al., 1993), reflected in the high organic content of the sediment (de Haas et al., 1997). Electron acceptors like oxygen, FeIII, and MnIV are almost depleted within the top 10 cm of the surface sediment (Canfield et al., 1993). Shallow gas accumulations have been extensively mapped by seismic studies (Hempel et al., 1994; Hovland, 1991) which revealed a wide field of shallow gas-containing sediment in the southern and eastern Skagerrak.

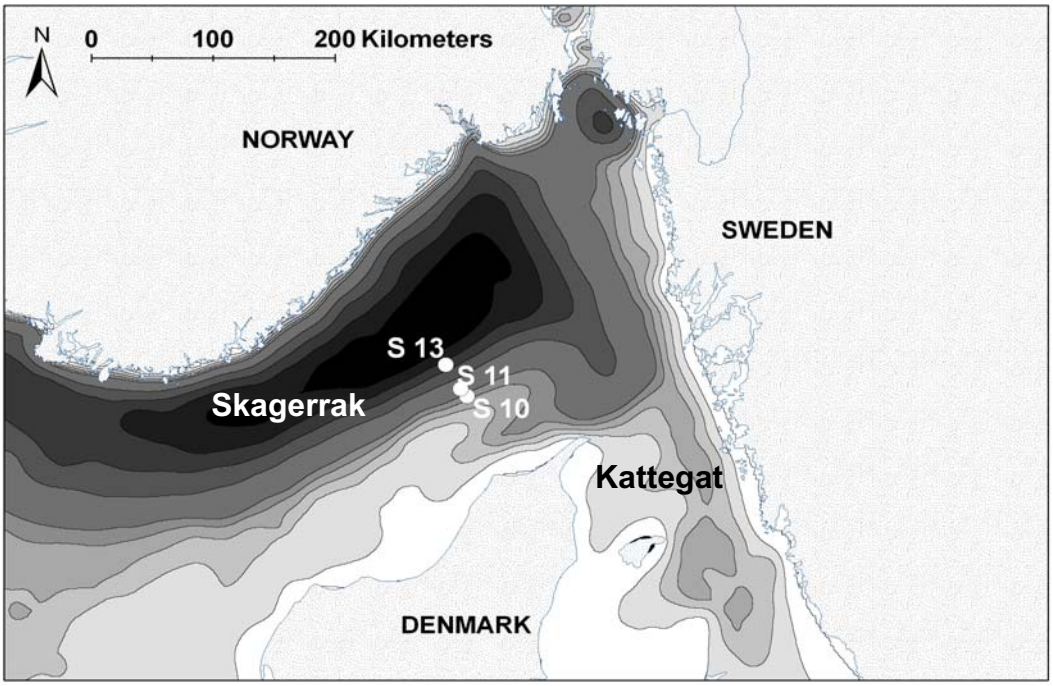

Figure 1: Map of the Skagerrak and location of the sampling sites of the gravity cores along the slope of the Norwegian Trench.

Gravity cores (Table 1) were sampled on a transect across the southern slope of the Norwegian Trench (Figure 1) starting at the top of the slope at 86 m water depth. The upper part of the slope, where S11 is located, is characterized by a field of elongated pockmarks parallel to the slope (Boe et al., 1998; Hempel et al., 1994). S13 was sampled on the lower part of the slope with increased organic carbon content. The stations were named in reference to earlier sediment stations S1-S9 of Canfield et al. (1993).

Station No.	Core ID	Latidude	Longitude	Water depth [m]	Surface sediment loss [cm]	C_{org} at surface [mmol g^{-1}]	Temperature of bottom water [°C]
S10	807GC	57°55.2453'	9°45.33555'	86	n.d.	0.20	8.7
S11	816GC	57°57.1217'	9°42.43051'	147	10	0.41	9.8
S13	789GC	58°3.25332'	9°36.00546'	391	10	1.54	4.5

Table 1: Overview of sampling stations

Sample collection

At each station two parallel gravity cores (GC) of 3 to 5.5 m length were obtained. The gravity cores were cut into 1-m sections on deck immediately after retrieving them capped and stored vertically at the respective *in situ* temperature of the SMTZ (6-10°C). The 1-m sections of one of the parallel cores were subsampled immediately with subcores at 5-10 cm depth intervals, starting from the top of the section, for concentration and process rate measurements. All rate measurements for AOM, sulfate reduction and methanogenesis were taken in close proximity in the core to ensure direct comparability. The second GC was sampled for microbiological analyses, including biomarkers and acridine orange direct counts (AODC). Sulfate and methane profiles from both cores were used to align the depth of the parallel cores from each station. At each station a Rumohr Lot (RL) or Multicorer (MUC) was deployed to sample the surface sediment that was lost or disturbed by gravity coring.

Concentration measurements

To determine **methane** concentrations a rough profile was first generated from samples taken at 1-m intersections immediately after the core was on deck. Subsequently, the core sections were subsampled at 10-cm intervals outside and 5-cm intervals inside the SMTZ. For all methane samples 3 cm^3 of sediment was transferred with a cut-off syringe into a glass vial with 6 ml sodium hydroxide (2.5 % w/v). After shaking for gas equilibrium methane concentrations were determined in the headspace using a gas chromatograph (5890A, Hewlett Packard) equipped with a packed stainless steel Porapak-Q column (6 ft., 0.125 in., 80/100 mesh, Agilent Technology) and a flame ionization detector. Helium was used as a carrier gas at a flow rate of 30 ml min^{-1}. The column temperature was 40°C.

For **sulfate** concentration measurements, pore water was squeezed from 2-cm sections of the subcores under nitrogen pressure (Pore water squeezer, KC Denmark) and 1 ml pore water was directly transferred into 0.25 ml $ZnCl_2$ (2 % w/v). This step was carried out as fast as possible to keep contact with oxygen at a minimum. The sample was analyzed by non-suppressed anion exchange chromatography (Waters 510 HPLC Pump; Waters IC-Pak 50 x 4.6 mm anion exchange column; Waters 430 Conductivity detector). Isophtalic acid (1 mM, pH 4.6) in methanol (10 % v/v) was used as eluant.

Total Carbon (TC) concentrations were measured from 500 µg freeze dried samples, analyzed by combustion gas chromatography (Carlo Erba NA-1500 CNS analyser). The **organic carbon (C_{org})** content was determined of the same sample acidified with 3 ml HCl (10 % v/v), and analyzed again by combustion gas chromatography.

Samples for **density** and **porosity** were taken in 10 ml cut-off syringes and 8 cm^3 were weighed. The density was determined from the wet weight per cm^3, and the water content was determined from the weight loss after drying at 60°C until constant weight was achieved.

Volatile fatty acid (VFA) concentrations in the pore water were measured, without any further sample preparation/dilution, on a Dionex® ICS-2000 Ion Chromatography System equipped with a Dionex® AS50 autosampler, Dionex® Anion Self-Regenerating Suppressor (ASRS®-ULTRA II 4-mm) and a conductivity detector. Concentrations in µM were calculated in relation to a standard curve. Samples were stored frozen, thawn immediately before analyses and transferred to the autosampler operating at 4 °C.

Diffusive fluxes of methane and sulfate were calculated from the linear concentration gradients into the SMTZ and the respective diffusion coefficients according to Fick´s first law of diffusion:

$$J = -\Phi \cdot D_s \frac{dC}{dz}$$

where J is the diffusive flux [mmol m^{-2} d^{-1}], Φ is the porosity [ml cm^{-3}], D_s is the diffusion coefficient in the sediment [cm^2 d^{-1}], and *d*C is the change of methane or sulfate concentration [µmol cm^{-3}] over the depth interval *dz*. At 10°C *in situ* temperature $D(CH_4) = 1.06 \cdot 10^{-5}$ cm^2 s^{-2} and $D(SO_4^{2-}) = 0.68 \cdot 10^{-5}$ cm^2 s^{-2} (Schulz, 2000) were used, and corrected for porosity of the sediment according to Iversen and Jørgensen (1993):

$$D_s = \frac{D}{1 + n(1-\Phi)}$$

with n = 2 for $\Phi < 0.7$ ml/cm^3 and n =3 for $\Phi > 0.7$ ml/cm^3.

Microbial process rates

Anaerobic oxidation of methane (AOM) was measured experimentally in 3 parallel samples at 5-cm depth intervals inside and 10-cm intervals outside the SMTZ. Values reported in the text represent the average of the 3 parallel samples. Dissolved ^{14}C-methane tracer (activity 1.35 kBq / sample) was injected into glass coring tubes containing 5 cm^3 sediment and sealed without headspace or gas enclosure. The tubes were incubated for 10 to 24 h at *in situ* temperature and the incubation was stopped by transferring the samples into a glass vial with 25 ml sodium hydroxide (2.5 % w/v), suspending the sediment completely. Zero-time controls were stopped immediately after tracer addition. AOM rates were determined according to (Treude et al., 2003), from the ratio of the injected ^{14}C-methane and the resulting ^{14}C-bicarbonate, in relation to the methane concentration measured in the AOM sample.

Samples for measurement of **sulfate reduction rates (SRR)** were injected with ^{35}S-sulfate tracer (500 kBq / 5 cm^3 sediment) and incubated as described for AOM. The incubation was stopped by transferring the samples into 50 ml plastic centrifuge vials containing 20 ml zinc acetate (20 % w/v). The total amount of ^{35}S-labelled reduced inorganic sulfur (TRIS) was separated using the single step cold distillation method (Kallmeyer et al., 2004). SRR was calculated from the ratio of ^{35}S-TRIS and the ^{35}S-sulfate injected in relation to the total sulfate pool of the pore water, as described by Fossing and Jørgensen (1989). As with AOM, SRR were measured in three

parallels at 5-10 cm depth intervals, and values described in the text refer to the average of the parallel samples.

The detection limit was determined as when the produced ^{35}S-TRIS of the samples exceeded the mean value for the blancs, where the reaction was stopped directly after tracer injection, plus three times their standard deviation (Ferdelman et al., 1999).

Acetate and Bicarbonate Methanogenesis were measured by injecting ^{14}C-acetate (activity 20 kBq) or ^{14}C-bicarbonate (activity 38 kBq) into 10-cm long subcores at 2-cm depth intervals. After incubation for 6 to 24 hours at *in situ* temperatures the incubations were stopped by transferring 2 cm slices of the subcores to glass vials (30 ml) containing 7 ml of 1 M NaOH. In the laboratory, the vial headspace was flushed (carrier gas 95 % N_2: 5 % O_2 at 70 ml/min for 20 min.) through a CO_2-trap (Supelco, UK) and then over copper oxide at 800°C in a furnace (Carbolite, UK) to oxidize any produced $^{14}CH_4$ to $^{14}CO_2$. The $^{14}CO_2$ was trapped in a series of three scintillation vials each containing 10 ml of Optiphase HiSafe-3 plus β-phenylethylamine (93:7), and the radioactivity was measured in a scintillation counter (Perkin Elmer, UK). Rates were estimated from the calculated label turnover times and the pore water concentrations of the substrate (acetate from VFA analysis, and dissolved CO_2 from DIC analysis).

Microbiology methods

Acridine orange direct counts (AODC) were used to determine the total number of microorganisms from 1 cm^3 of sediment preserved in a serum vial (previously furnaced at 450°C) containing 9 ml formaldehyde (2 % v/v in artificial seawater, filter sterilized 0.2 µm). Three replicate sub-samples (5-25 µl) were stained for 3 min with 50 µl acridine orange (0.1 % w/v) in 10 ml formaldehyde (2 % v/v in artificial seawater, filter sterilized 0.1µm) and vacuum filtered through a black polycarbonate membrane (0.22 µm). Paraffin oil mounted membranes were viewed under incident UV illumination with a Zeiss Axioskop epiflourescence microscope at X1000. Both unattached cells and cells attached to particles were counted and the number of attached cells was doubled to account for cells hidden from view (Goulder, 1977). Dividing and divided cells were separately counted to provide an index of the growth potential of the populations.

For **biomarker** analyses, samples (>100 ml) of frozen sediment were taken from the second gravity core at each site, freeze-dried, and extracted for 24 h with a Soxhlet apparatus using a dichlormethane (DCM)/methanol mixture (2:1 v/v). Elemental sulfur was removed from the total lipid extracts by activated copper. Aliquots of the total lipid extracts were separated into three operationally defined fractions (Kim and Salem, 1990) using pre-washed 500 mg amino-propyl (55 µm, 70 Å) columns (Phenomenex, USA). A sequence of isopropanol/DCM (2:1 v/v), 2% acetic acid in diethyl ether and methanol was used to elude the neutral lipid (hydrocarbons such as PMI, alcohols, ketones), as well as the free fatty acid (without glycerol group) and polar fractions (including both archaeal and bacterial phospholipids) respectively. The neutral fraction was further separated into apolar and neutral polar fractions using an alumina column and hexane/DCM (9:1 v/v) and DCM/methanol (1:2 v/v) to elude the two fractions, respectively. Free fatty acids were released from the phospholipid fractions by alkaline hydrolysis, and both free fatty acids and phospholipid fatty acids were methylated to fatty acid methyl esters by refluxing with BF_3 (14 % in methanol). Alcohols in the neutral polar, free fatty acid, and phospholipid fractions were converted to their trimethylsilyl derivatives using N,O-bis(trimethylsilyl)triflouroacetamide and pyridine. All fractions were screened initially by gas chromatography using a Carlo-Erba HRGC 5400 mega series with a flame ionization detector and a Chrompack fused silica capillary column (50 m length, 0.32 mm internal diameter) with a non-polar CP-Sil 5 CB stationary phase (dimethylpolysiloxane equivalent, film thickness 0.12 µm). Compounds were identified on a Thermoquest Finnigan Trace gas chromatograph interfaced to a Thermoquest Finnigan Trace mass spectrometer operating with electron ionization at 70 eV and scanning an *m/z* range of 50 to 850.

RESULTS

Biogeochemistry

The biogeochemical profiles and rate measurements at station S10 (807GC) are presented in Figure 2. The concave profile of upwards diffusing methane overlaps with the linear regression of sulfate concentrations from the sediment surface in a SMTZ centered at ~ 130 cm depth, which is typical for diffusive methane-bearing sediments. In this zone methane is completely oxidized in a depth of 100 cm. The methane values below 170 cm are the result of degassing and do not represent actual concentrations in this depth. Sulfate is depleted at a depth of 150 cm, but below this horizon, a remaining sulfate background concentration of ~ 1 mM was detected. The amount of total carbon at the sediment surface was below 1 mmol g^{-1}, half of which consisted of organic carbon. Direct AOM radiotracer measurements confirm the SMTZ as the zone of microbial methane turnover with the major peak in AOM rates (1.6 nmol cm^{-3} d^{-1}, as average of three parallel samples) at 130 cm depth in a very restricted horizon of only ~ 10 cm thickness. This AOM activity completely oxidizes the methane flux of 0.14 mmol m^{-2} d^{-1} that diffuses up into the SMTZ. Parallel radiotracer measurements of SRR show that a prominent peak of sulfate reduction based on fermentation products with an average of 16.3 nmol cm^{-3} d^{-1} occurs at or just below the sediment surface where organic matter degradation is taking place, but these rates do not continue into the SMTZ. There is a second, distinct SRR peak of 24.7 nmol cm^{-3} d^{-1} at 135 cm depth mediated by AOM. This deep SRR peak was even higher than the surface sulfate reduction activity and also much higher than the AOM rate. In this zone of sulfate reduction and AOM activity, bicarbonate-methanogenesis rates showed a local minimum of 0.26 nmol cm^{-3} d^{-1}. Higher rates of 0.6 nmol cm^{-3} d^{-1} were measured in the major methanogenesis zone below the SMTZ, where sulfate was depleted. Surprisingly, the highest bicarbonate-methanogenesis rates (0.72 nmol cm^{-3} d^{-1}) were observed right above the SMTZ even though sulfate was still present at > 5 mM at this depth and SRR could potentially take place, but was below detection. Even though acetate was abundant in the entire core, reaching up to 90 µM in the SMTZ, acetate-methanogenesis (max. 0.05 nmol cm^{-3} d^{-1}) was not detected in the sulfate zone, but strictly limited to below the SMTZ. Lactate and formate were also abundant in this core, but at much lower concentrations than acetate.

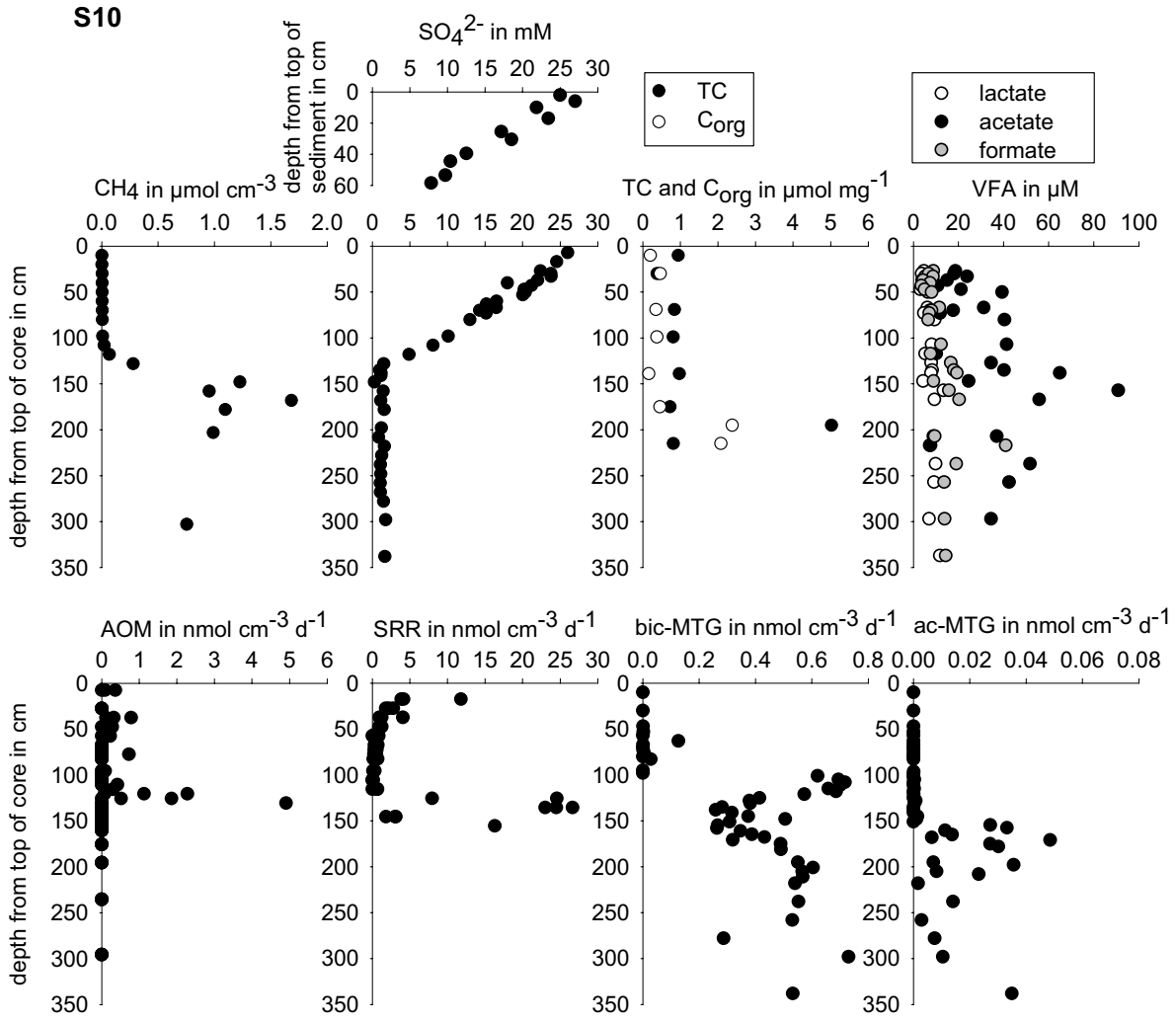

Figure 2: Distribution of concentrations (top) and rate measurements (bottom) at station S10. AOM and SRR are represented by three parallel samples. Methanogenesis rates are presented for the substrates bicarbonate (bic-MTG) and acetate (ac-MTG).

Station S11 (Figure 3) was located in a pockmark on the upper slope, where pockmarks are most abundant. The sulfate concentration of 29 mM at the sediment surface was the same as at station S10, but the linear decline was much steeper, with a high sulfate flux of 0.50 mmol m^{-2} d^{-1} into the SMTZ. Sulfate was already depleted at a depth of ~ 55 cm leading to a shallow SMTZ at 25-50 cm depth. There seemed to be a low peak of sulfate again between 200 and 250 cm, which might be due to lateral pore water input. Despite the shallow depth of the SMTZ, all of the methane was oxidized (18 nmol cm^{-3} d^{-1} mean max. AOM rate) before it reaches the sediment

surface. No methane was observed at 250 cm, but it was increasing to ~ 1 µmol cm^{-3} at 170 cm depth. This increase and the variability of the profile between 50 cm and 175 cm could be due to methanogenesis, lateral pore water transport, or a combination of both. It would also be possible that the methane concentration reached a maximum higher than 1 mM at a depth of ~ 125 cm, and that the scattered profile might be caused by outgassing at this horizon.

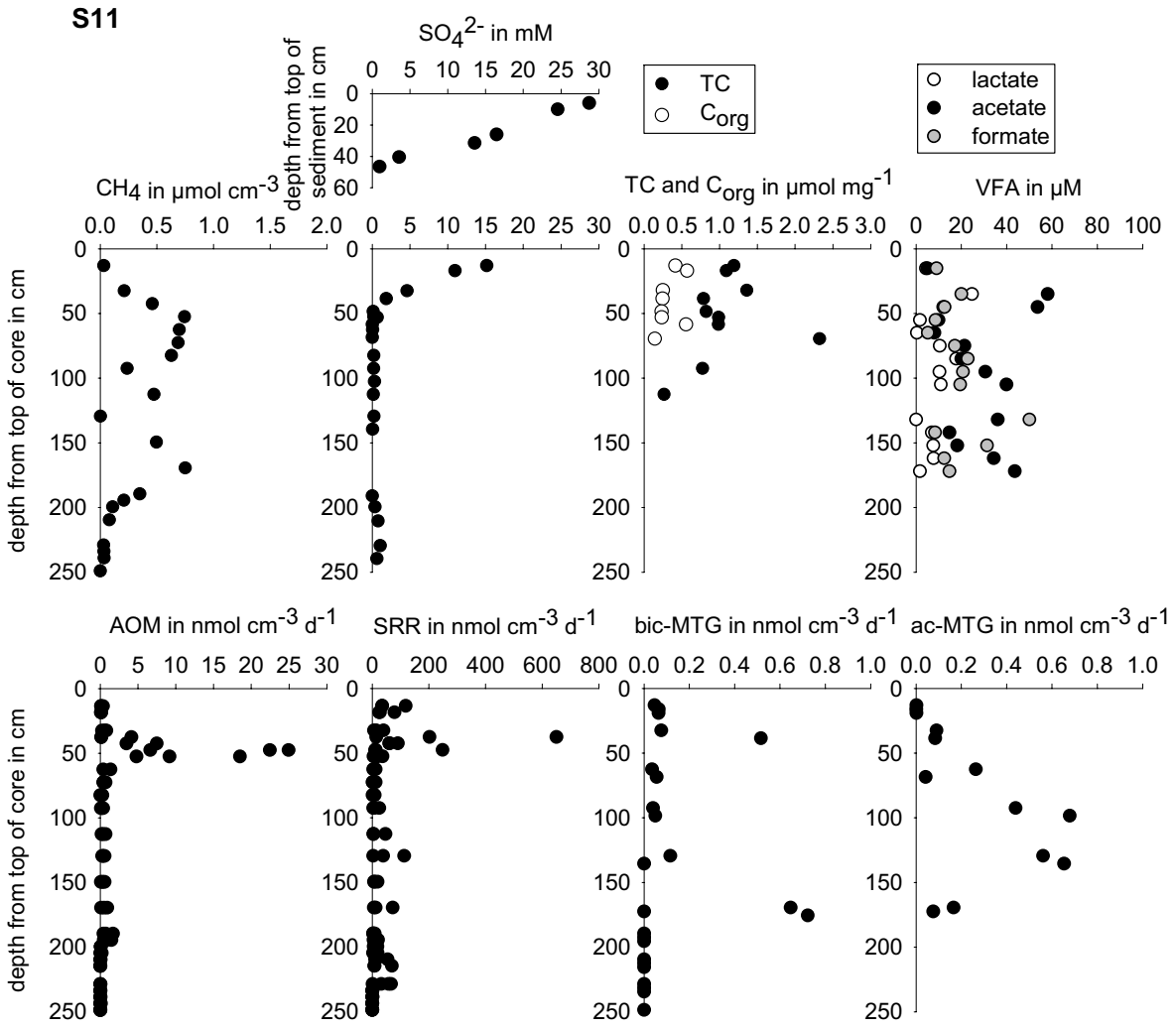

Figure 3: Distribution of concentrations (top) and rate measurements (bottom) at station S11 as described for Figure 2.

The highest SRR was observed in the SMTZ at 37 cm depth, but with a very high activity of 289 nmol cm^{-3} d^{-1} it was about 16-fold higher than the maximum AOM activity (Table 2), which was located at 47 cm, 10 cm deeper than the SRR. The lack of measurable SRR in the top 25 cm

confirms the loss of sediment from the top. Even though the SMTZ in this core is very close to the sediment surface, sulfate reduction based on fermentation products and AOM-mediated sulfate reduction show no overlapping peaks. Bicarbonate-methanogenesis activity (0.72 nmol cm^{-3} d^{-1}) was detected at 175 cm, as well as a rate of 0.50 nmol cm^{-3} d^{-1} that occurred in the upper part of the SMTZ. At 70-100 cm bicarbonate-methanogenesis was only taking place at background rates (< 0.05 nmol cm^{-3} d^{-1}). Instead, acetate-methanogenesis is highest in this horizon (max. 0.78 nmol cm^{-3} d^{-1}) and rates are an order of magnitude higher than acetate-methanogenesis at the other two sites. It is occurring in addition to bicarbonate-methanogenesis and it might be the major source of methane production below the SMTZ at this site, supporting the possibility of a maximum methane concentration at the depth of ~ 125 cm, where acetate-methanogenesis rates are highest.

Station	AOM maximum peak rate [nmol cm^{-3} d^{-1}]	SRR maximum peak rate [nmol cm^{-3} d^{-1}]	Rates ratio SRR:AOM	CH_4 flux to SMTZ [mmol m^{-2} d^{-1}]	SO_4^{2-} flux to SMTZ [mmol m^{-2} d^{-1}]	Flux ratio SO_4^{2-} : CH_4
S10	1.6	24.7	15.44	0.143	0.235	1.64
S11	18.0	289	16.06	0.126	0.501	(3.98)
S13	1.8	1.9	1.06	0.219	0.231	1.05

Table 2: Rates of AOM and SRR and fluxes at the three sample sites in the Skagerrak

Station S13 (Figure 4) was sampled half way down the slope at 391 m water depth, where the organic carbon content (1.5 mmol g^{-1} sed.) was much higher than at station S10 (0.2 mmol g^{-1} sed.) and S11 (0.4 mmol g^{-1} sed.). The sulfate profile resembles that at station S10 with a comparable sulfate flux into the SMTZ of 0.23 mmol m^{-2} d^{-1} (Table 2) but a more shallow location of the SMTZ at 84-120 cm. Because of the high input of organic matter SRR was high at the surface of the core, with an integrated activity in the top 100 cm of > 4.2 mmol m^{-2} d^{-1}. This total activity might be underestimated because the top sediment layer (10 cm) was lost during coring. Since the SRR based on fermentation products extended down into the SMTZ, overlapping with methane-based sulfate reduction, the deeper sulfate reduction peak related to AOM cannot be distinguished and must be much lower (max. 2 nmol cm^{-3} d^{-1}) than at S10. Furthermore the methane-based SRR does not seem to occur at a distinct depth zone, which was reflected also in the AOM rates that reached a maximum of 1.8 nmol cm^{-3} d^{-1} (as average of three parallel measurements) at 91 cm depth.

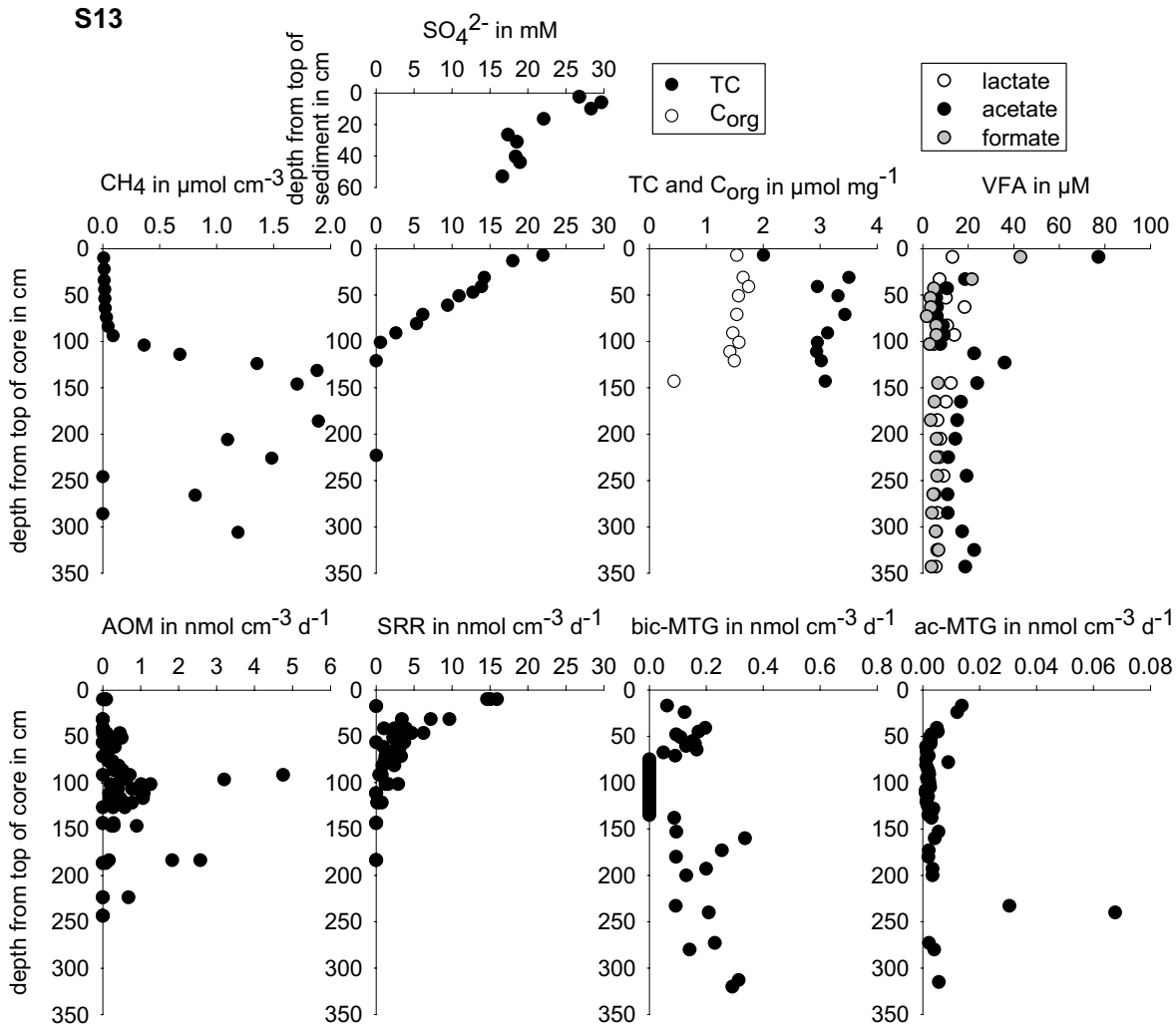

Figure 4: Distribution of concentrations (top) and rate measurements (bottom) at station S13 as described for Figure 2.

In the depth of AOM activity bicarbonate methanogenesis was not detected but it occurred in the sulfate reducing zone above the SMTZ (0.20 nmol cm^{-3} d^{-1}) as well as in the methanogenic zone below sulfate depletion (max. 0.34 pmol cm^{-3} d^{-1}). The shallower methanogenesis activity occurred in a horizon where sulfate reduction activity was present at 2-8 nmol cm^{-3} d^{-1}, and consisted of both bicarbonate methanogenesis (90 %) and acetate methanogenesis (10 %). In this zone of co-occurring sulfate reduction and methanogenesis above the SMTZ, acetate concentrations were relatively stable at 6 µM, whereas the acetate level directly below the SMTZ was around 14 µM. In accordance to S10 and S11 a peak in acetate concentration was also

observed in the SMTZ at station S13, and this was even more pronounced than at station S10. But the difference in VFA levels above and below the SMTZ was most distinct at S13, and this trend was also reflected in lactate and formate concentrations.

Microbial community

The microbial community was studied using acridine orange direct counts and biomarker analyses (Figure 5). At the surface, where microbial activity and cell abundances are highest, direct cell counts revealed abundances between 1.6 x 10^9 cells cm^{-3} at S11 and 1.3 x 10^9 cells cm^{-3} at S10 and S13. These numbers decreased steeper with depth at S10 than at the other two stations, which is consistent with the low surface SRR at this site. The increased organic matter content at S13 and high surface SRR was reflected in a high cell number being maintained to a depth of 60 cm. At site S11, the cell numbers were higher than at the other two sites, and this was coherent with the generally higher microbial rates in this core. At all three stations no increase in cell abundances were observed in the SMTZ, but the number of cells differed with highest amounts at station S11 (9.1 x 10^8 cells cm^{-3}) and lowest numbers at S10 (1.3 x 10^8 cells cm^{-3}). Below the zone of highest AOM and sulfate reduction rates cell numbers decreased in all tree cores, but still more than 10^8 cells cm^{-3} were remaining at > 300 m depth (data not shown) at all locations.

Additional FISH as well as CARD-FISH analyses for archaea and eubacteria revealed very few cells but the staining was only faint and cell density on the filters very low. Single archaea cells could be detected occasionally, but they were not in the vicinity of sulfate reducing bacteria cells and could not be stained with ANME-1 or ANME-2 probes.

The microbial community was also examined by biomarker analyses. The dominant lipid biomarkers at all sites were derived from phytoplankton (data not shown), including *n*-alkane-1,15-diols derived from eustigmatophytes (Volkman et al., 1999) and long chain alkenones derived from haptophytes (Marlowe et al., 1984). Terrestrial sources are also significant, reflected by high abundances of even-carbon number *n*-alkanols and odd-carbon

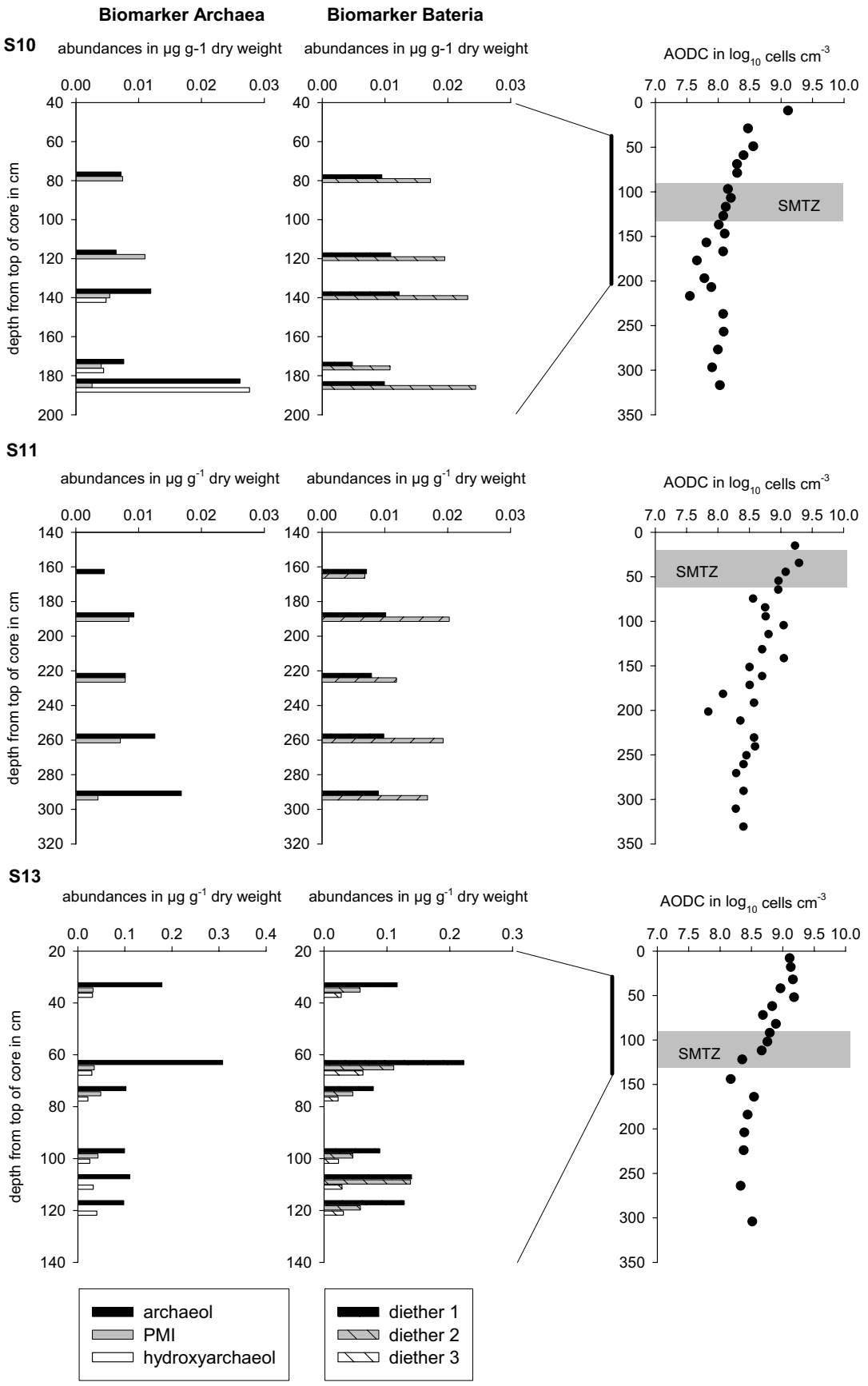
Biomarker Archaea
Biomarker Bateria
S10
S11
S13
abundances in µg g-1 dry weight
abundances in µg g-1 dry weight
AODC in log10 cells cm-3
depth from top of core in cm
SMTZ
archaeol
PMI
hydroxyarchaeol
diether 1
diether 2
diether 3

Figure 5: Biomarker distribution and total cell counts of S10, S11, and S13. The three bacterial biomarkers presented are series-1 non-isoprenoidal C-15 diglykol glycerol diethers supposed to derive from SRB as described by Pancost et al. (2001). The biomarkers and total cell count were determined in two parallel gravity cores from the same site. At S11 the location of the SMTZ in the two cores is not comparable because of the lateral heterogeneity in the pockmark.

number *n*-alkanes derived from higher plants (Eglinton and Hamilton, 1967). Despite the predominance of allochthonous inputs, sedimentary microbial biomarkers were detected at all three sites. The detection of the diethers archaeol and hydroxyarchaeol as well as pentamethylicosane (PMI) indicates the presence of archaea, whereas the occurrence of non-isoprenoidal diethers can be associated with bacteria, presumably SRB (Pancost et al., 2001). The abundances of these archaeal and bacterial biomarkers as well as the biomarkers from phytoplankton were much higher than in nearby Kattegat sediments (data not shown), which is consistent with the higher organic carbon content and evidence for higher productivity. Archaeal and SRB biomarker abundances in the Skagerrak sediments changed with depth with notable increases near the SMTZ (Figure 5). The lack of exact correspondence between the biomarkers and the SMTZ is probably due to the fact that the measurements were performed on a second gravity cores from the same station, where the SMTZ was located slightly deeper in the sediment. At S10 the highest abundance of biomarkers occurred between 120 and 185 cm only slightly below the SMTZ, with archaeal and bacterial lipids occurring in almost the same abundances. Due to the heterogeneity of the sediment in the pockmark the SMTZ in the second core at S11 was located much deeper (data not shown) than in core 816GC, and the highest abundances of biomarkers from archaea and bacteria were therefore found in concurrence with this deeper SMTZ from 180 to 300 cm depth.

Archaeol was by far the predominant archaeal biomarker at S13, the highest abundance coinciding with the peak in SRB biomarker abundance. Since both archaeol and non-isoprenoidal diethers were detected in the phospholipid fraction at the SMTZ, these must have been released from presumably intact polar lipids during saponification and, therefore, reflect living biomass. The abundances of all phospholipid fatty acids decreased with depth (data not shown), consistent with decreasing biomass of prokaryotes and the lower heterotrophic activity as organic matter becomes more recalcitrant.

DISCUSSION

In the majority of continental margin sediments methane transport takes place by molecular diffusion and the upwards methane flux is entirely oxidized by AOM. Methane release into the bottom water from marine sediments is limited to seep sites with advective transport, as shown by previous studies (Treude et al., 2005a). This was confirmed by the efficient turnover at S10 and S13 in the sediments from the Skagerrak. Even in core 816GC, where the methane flux in the Pockmark is high due to advective transport, the SMTZ acted as an efficient barrier to prevent methane release. Maximum AOM rates at S10 and S13 were in the range of 5 nmol cm^{-3} d^{-1}, which is comparable to rates measured in similar systems on the upper marine shelf (Hinrichs and Boetius, 2002) and also in the same range as those of the upwelling system off Chile (Treude et al., 2005b). But these rates are extremely low compared to AOM activities at cold seep sites, like the Gulf of Mexico (up to 500 nmol cm^{-3} d^{-1}; Joye et al., 2004) or Hydrate Ridge (~ 3000 nmol cm^{-3} d^{-1}; Treude et al., 2003) that are characterized by a very high methane flux.

Since the methane flux plays a major role in determining AOM rates, it is necessary to understand how methane and sulfate fluxes are regulated and the location and width of the SMTZ determined. Sulfate depletion is usually controlled by the quantity and quality of organic matter supply by deposition (Berner, 1978; Canfield, 1991; Toth and Lerman, 1977). But it has been observed in sediments above gas hydrates that the sulfate flux is steeper than at non-hydrate sites and it was thus proposed that the upward methane flux is responsible to control the sulfate flux and the sulfate penetration depth (Borowski and Paull, 1996; Borowski et al., 1999). This was further supported by the linear gradient of the sulfate profiles, which does not seem to be significantly influenced by higher SRR at the surface sediment (Niewöhner et al., 1998). In our cores from the Skagerrak, however, the difference of methane fluxes between S10 (0.14 mmol m^{-2} d^{-1}) and S13 (0.22 mmol m^{-2} d^{-1}) did not alter the sulfate flux, which was ~ 0.23 mmol m^{-2} d^{-1} at both sites (Table 2).

A significant difference between the two stations was the amount of organic matter in the sediment. The higher organic carbon content at S13 stimulated higher integrated surface SRR (> 4.16 mmol m^{-2} d^{-1} at S13 compared to 2.70 mmol m^{-2} d^{-1} at S10), which made up > 63 % of the

total SRR in this core, and would even be higher considering that 10 cm surface sediment was lost. In comparison to this domination of SRR based on fermentation products at S13, the fraction of methane related SRR at S10 of the total sulfate reduction was much higher. This indicates that even in diffusive systems with moderate methane fluxes AOM can be a very important electron donor for sulfate reduction, sometimes maybe even as important as the sulfate reduction driven by organic matter as electron donor. In addition, it is also interesting to notice that at S10 the peaks of surface SRR and methane related SRR were clearly separated by a horizon with very low SRR. It is not clear what the reason for these low rates in this zone is. Sulfate concentrations at 100 cm depth were ~ 10 mM and are only supposed to limit SRR at concentrations < 30 µM (Lovley and Klug, 1986) but the restriction of sulfate reducing activity could be related to a depletion of readily degradable organic matter in this depth. The low SRR coincided with an increase of acetate concentration between 50 cm and 120 cm, which reached ~ 100 µM in the SMTZ, where SRR is coupled to methane as electron donor. This increase in acetate concentrations in the SMTZ was also observed at S11 and S13.

Instead of SRR bicarbonate-methanogenesis activity was detected in this horizon between 50 and 120 cm. It is usually excluded from the sulfate zone where sulfate reduction dominates organic matter degradation (Crill and Martens, 1986; Martens and Berner, 1974; Whiticar, 2002) as well as competition for hydrogen as substrate (Capone and Kiene, 1988; Claypool and Kaplan, 1974; Hoehler et al., 1998; Lovley and Goodwin, 1988; Sansone and Martens, 1982). Previous reports that methanogenesis occurs in the sulfate zone were attributed to non-competitive substrates like methylamines zone (Ferdelman et al., 1997; Lovley and Klug, 1983; Oremland and Polcin, 1982). But at S10 the restriction of SRR seems to enable bicarbonate methanogenesis in this zone. At S13 bicarbonate methanogenesis also occurred above the SMTZ and at this site despite the presence of SRR. One possibility might be that this is related to the higher organic carbon content of the sediment (Capone and Kiene, 1988) at this station.

At both S10 and S13 bicarbonate methanogenesis rates that were present above and below the SMTZ decreased to a minimum in the zone of AOM activity. This pattern with AOM occurring exactly in the zone of low methanogenesis seems to indicate, that either SRR that drives AOM inhibits bicarbonate-methanogenesis as soon as methane is available as a substrate, or that the environmental conditions are more favorable for the reverse reaction of bicarbonate

methanogenesis, due to a higher thermodynamic yield of the AOM reaction under the methane-, sulfate-, or hydrogen concentrations in the SMTZ.

The regulation of sulfate reduction versus methanogenesis is also reflected in the concentration profiles of the volatile fatty acids. The acetate concentrations appear to be maintained and regulated at two distinct levels in the sulfate reducing and the methanogenic zone, which is most evident from the acetate profile at station S13, but is also reflected in the VFA data of S10. This pattern of lower VFA concentrations in the sulfate zone, and a higher level in the methanogenic zone possibly reflects the greater affinity of sulfate reducing bacteria for these substrates compared to methanogenic archaea (Lovley and Klug, 1986; Schönheit et al., 1982). Consistent with this, acetate-methanogenesis was mainly restricted to the methanogenesis zone below the SMTZ, and rates were far lower than SRR.

Pockmark

Although pockmarks might not necessarily be associated with methane seepage it is mostly the case in the Skagerrak (Hovland and Judd, 1988). The presence of sulfate, even though in very low concentrations, at the bottom of core 816GC at S11 and the absence of methane at the same depth is an indication that lateral advective transport may take place in the sediment of this pockmark. The observation is consistent with the hypothesis of Hübscher and Borowski (2006), that methane-free fluids of freshwater origin are advecting to the sediment surface. These authors suggest that accumulation of organic matter in the crater of the pockmark could be the source of methane, which might be a possible explanation for the acetate-methanogenesis values at ~ 100 cm depth, that are one order of magnitude higher than at the two other sites and in the same range as bicarbonate methanogenesis. If advective transport processes and lateral pore water intrusion are involved at S11, the diffusive fluxes of sulfate and methane are not directly coupled any more, which is consistent with the sulfate flux at S11 (0.50 mmol m^{-2} d^{-1}) being much higher than the methane flux (0.13 mmol m^{-2} d^{-1}). The difference of the fluxes is even more pronounced in AOM and SRR, with SRR exceeding more than 10 x the rate of AOM, and both rates are an order of magnitude higher than at the two other sites.

Microbiology

The depth distribution of the alternating redox processes shows no significant effect on cell numbers that could be correlated to any of the microbial activities but decrease uniformly with depth. The average activity rate for methane oxidizing cells was recently proposed to be in the range of ~ 0.2 fmol $cell^{-1}$ d^{-1} for sediments from Tommeliten / North Sea, which was consistent with findings from Hydrate Ridge and *in vitro* experiments of different AOM sites (Niemann et al., 2005). Assuming a similar cell-specific rate for the Skagerrak sediments the density of methanotrophs should be at least ~ 1.5 x 10^7 cells cm^{-3} sediment (~10^8 cells cm^{-3} at S11) to achieve the AOM rates observed. The total cell counts confirm this assumption and indicate for all cores a cell abundance that is almost ten times higher than that required to explain the observed rates at maximum activity. This means that the cell specific AOM rate is in the same range as at Tommeliten and Hydrate Ridge, if methanotrophic archaea constitute about 10 % of the counted cells, which is a realistic fraction also observed at Tommeliten (Niemann et al., 2005). It supports the hypothesis of these authors that the cell specific rate is similar in different environments and that cell abundance determines the total activity of the population.

The distribution of archaeal and bacterial lipids in the Skagerrak sediments resembles the observations commonly reported from cold seep sediments and is consistent with an AOM community (Bouloubassi et al., 2006; Hinrichs et al., 2000; Pancost et al., 2001; Pancost and Sinninghe Damste, 2003; Pancost et al., 2005; Zhang et al., 2003). In addition, the increase in biomarker abundances at the SMTZ indicates that the source organisms are involved with AOM and the presence of presumably labile ether lipids in the phospholipid fraction indicates that this is an active microbial population. Like AOM rates, archaeol and hydroxyarchaeol (archaea) and non-isoprenoidal diethers (SRB) are several orders of magnitude less abundant than at cold seeps.

Because of the low numbers of archaeal cells the identification of the organisms with CARD-FISH did not reveal a clear signal with fluorescent probes. The rectangular shape and isolated alignment in short chains observed with DAPI staining indicate that cells of the ANME-1 group might be responsible for AOM at these sites. The presence of consortia typical for organisms of the ANME-2 group, as were found in Eckernförde Bay (Treude et al., 2005a), have not been observed in the cores presented here, but might still be present (Parkes et al., 2007). Biomarker signals from both groups, archaea and sulfate reducing bacteria are present in the SMTZ, which

would rather imply the presence of a community of methanotrophs with bacterial sulfate reducers. But this signal could also be attributed to AOM independent sulfate reduction taking place in the SMTZ.

Discrepancy between AOM rates and SRR

In the upper part of the sediment the linear sulfate profile that is typically observed at steady state conditions (Hensen et al., 2003) does not show any net SRR, despite the high sulfate reduction activity in this zone, and therefore measured rates are more meaningful than fluxes in the top of the core. The linear sulfate gradient is determined by the sulfate flux, which represents the activity in the whole SMTZ and can be used to model sulfate turnover rates in this zone. Yet, tracer measurements have the advantage of directly demonstrating the reaction and to differentiate depth intervals at higher resolution. The rate measurements of AOM and SRR in all three cores from the Skagerrak revealed that the rates are not distributed equally over the SMTZ but that the main activity of these reactions always occurred at the bottom of this zone, which indicates a stronger influence of the methane flux on the location of AOM activity than the sulfate flux. Direct rate measurements, however, also comprise the variability of heterogeneous sediments, evident in replicate measurements on parallel samples, and often yield a higher activity than the rates calculated from concentration profiles.

The ratios of the sulfate and methane fluxes are very different in the three cores analyzed. At S11, fluid flow through the pockmark influences the system and fluxes are no longer based on diffusion. In this core the comparison of directly measured rates indicate a ratio of SRR:AOM of ~ 16. Such offsets of SRR and AOM are often observed in advective environments (Joye et al., 2004; Orcutt et al., 2004; Treude et al., 2003) but display a balanced stoichiometry when rates are determined under diffusive laboratory conditions (Nauhaus et al., 2002). Station S10 and S13 are purely diffusive and are expected to display a ratio of 1:1, which was coherent with the calculated fluxes at S13. But at S10 the sulfate flux was 1.6-fold higher than the methane flux. This offset was even more pronounced for the tracer measurements, because SRR was much higher than indicated by the sulfate flux. The tendency of higher SRR than AOM rates in the SMTZ has been reported for most tracer measurement studies (Bussmann et al., 1999; Devol and Anderson, 1984; Hansen et al., 1998; Iversen and Blackburn, 1981; Iversen and Jørgensen, 1985; Joye et al., 2004; Thomsen et al., 2001). In our study, this cannot be attributed to problems of

sample alignments when Multicorer cores were used and heterogeneity of the sediment (Treude et al., 2003), because the variation of the three parallel samples did not reflect such a heterogeneity on a centimeter scale as to explain the differences in rates. It has also been proposed that the methane loss during coring is responsible for an underestimation of *in situ* methane concentrations (Abegg and Anderson, 1997; Niewöhner et al., 1998) and this can potentially lead to an underestimation of methane fluxes and AOM. Such a loss is mainly observed at high methane concentrations and depends on the time between coring and taking individual samples (Abegg and Anderson, 1997). However, the methane concentration in the STMZ of the Skagerrak cores was well below saturation concentration at atmospheric pressure and is unlikely to have gassed out to such an extent as to create a 15 times lower AOM rate. Moreover, rough profiles sampled right after retrieval of the core at the top of each core section showed no significant loss of methane in the SMTZ but only in the bottom part of the core, where concentrations where higher than saturation at atmospheric pressure. Another possibility is that methanogenesis rates taking place in the AOM zone could counterbalance AOM rates. At station S10 methanogenesis was present in the SMTZ, but rates were only ~ 10 % of the AOM rates, so that this does not seem to be a likely explanation for either the difference between measured rates and calculated methane fluxes (Iversen and Jørgensen, 1985) or the low AOM rates compared to SRR.

Instead of AOM being underestimated, there might also be an overestimation of AOM-related SRR. Since AOM rates are in the same range at S10 as at S13, but SRR are much higher in the SMTZ of S10, additional sulfate reduction seems to be the most likely explanation for these high values. Sulfate reduction based on fermentation products often continues into the SMTZ and overlaps with the AOM derived sulfate reduction peak. This can be excluded at site S10 because both peaks can be clearly separated, and SRR almost completely ceases above the SRR peak of the SMTZ. Iversen and Jørgensen (1985) suggested that SRR from a Kattegat core were too high because the sulfate concentration was overestimated. Sulfate values in the SMTZ of the Skagerrak cores are very low, and can partly be under the detection limit of 0.2 mM. Control measurements of low sulfate concentrations to determine the detection limit did not indicate an overestimation of sulfate or a measurement background concentration, but the accuracy of the very low sulfate measurements is crucial for SRR calculations and scattering can lead to an overestimation of SRR in this zone. Additional sulfate reduction could also be mediated by the

presence of substrates other than methane. This would explain why the peaks of AOM and SRR are not exactly occurring in the same horizon. High molecular weight hydrocarbons that are reported to lead to increased SRR in Gulf of Cadiz AOM zones (Niemann, 2005) are not present in the Skagerrak sediments and can therefore not enhance additional SRR. However, in all three cores of the Skagerrak acetate was abundant in the SMTZ. This acetate could be utilized as a substrate for sulfate reduction in addition to methane. If this were the case, the flux of acetate into the SMTZ would need to be in the same range as the surplus sulfate flux into this zone, but it is far too low (~ 0.002 mmol m^{-2} d^{-1} at station S13) to explain the high SRR. Thus, it still remains unclear what the additional substrates for sulfate reduction could be in the SMTZ.

REFERENCES

Abegg F. and Anderson A. L. (1997) The acoustic turbid layer in muddy sediments of Eckernfoerde Bay, western Baltic: Methane concentration, saturation and bubble characteristics. *Marine Geology* **137**, 137-147.

Alain K., Holler T., Musat F., Elvert M., Treude T., and Krüger M. (2006) Microbial investigation of methane- and hydrocarbon-discharging mud volcanoes in the Carpathian Mountains, Romania. *Environmental Microbiology* **8**(4), 574-590.

Alperin M. J. and Reeburgh W. S. (1985) Inhibition experiments on anaerobic methane oxidation. *Applied and Environmental Microbiology* **50**(4), 940-945.

Anton K. K., Liebzeit G., Rudolph C., and Wirth H. (1993) Origin, distribution and accumulation of organic carbon in the Skagerrak. *Marine Geology* **111**, 287-297.

Berner R. A. (1978) Sulfate reduction and the rate of deposition of marine sediments. *Earth and Planetary Science Letters* **37**, 492-498.

Boe R., Rise L., and Ottesen D. (1998) Elongate depressions on the southern slope of the Norwegian Trench (Skagerrak): Morphology and evolution. *Marine Geology* **146**(1-4), 191-203.

Borowski W. S. and Paull C. K. (1996) Marine pore-water sulfate profiles indicate *in situ* methane flux from underlying gas hydrates. *Geology* **24**(7), 655-658.

Borowski W. S., Paull C. K., and Ussler III W. (1999) Global and local variations of interstitial sulfate gradients in deep-water, continental margin sediments: Sensitivity to underlying methane and gas hydrates. *Marine Geology* **159**, 131-154.

Bouloubassi I., Aloisi G., Pancost R. D., Hopmans E. C., Pierre C., and Sinninghe Damste J. S. (2006) Archaeal and bacterial lipids in authigenic carbonate crusts from eastern Mediterranean mud volcanoes. *Organic Geochemistry* **37**(4), 484-500.

Bussmann I., Dando P. R., Niven S. J., and Suess E. (1999) Groundwater seepage in the marine environment: role for mass flux and bacterial activity. *Marine Ecology-Progress Series* **178**, 169-177.

Canfield D. E. (1991) Sulfate reduction in deep-see sediments. *American Journal of Science* **291**, 177-188.

Canfield D. E. (1994) Factors influencing organic carbon preservation in marine sediments. *Chemical Geology* **114**, 315-329.

Canfield D. E., Jørgensen B. B., Fossing H., Glud R., Gundersen J., Ramsing N. B., Thamdrup B., Hansen J. W., Nielsen L. P., and Hall P. O. J. (1993) Pathways of organic-carbon oxidation in three continental-margin sediments. *Marine Geology* **113**(1-2), 27-40.

Capone D. G. and Kiene R. P. (1988) Comparison of microbial dynamics in marine and freshwater sediments. *Limnology & Oceanography* **33**(4), 725-749.

Claypool G. E. and Kaplan I. R. (1974) The origin and distribution of methane in marine sediments. In *Natural Gases in Marine Sediments* (ed. I. R. Kaplan), pp. 99-139. Plenum Press.

Crill P. M. and Martens C. S. (1986) Methane production from bicarbonate and acetate in an anoxic marine sediment. *Geochimica Et Cosmochimica Acta* **50**, 2089-2097.

Dale A. W., Regnier P., and van Cappellen P. (2006) Bioenergetic controls on anaerobic oxidation of methane (AOM) in coastal marine sediments: A theoretical analysis. *American Journal of Science* **306**(4), 246-294.

de Haas H., Boer W., and van Weering T. C. E. (1997) Recent sedimentation and organic carbon burial in a shelf sea: The North Sea. *Marine Geology* **144**(1-3), 131-146.

Devol A. H. and Anderson J. J. (1984) A model for coupled sulfate reduction and methane oxidation in the sediments of Saanich Inlet. *Geochimica Et Cosmochimica Acta* **48**, 993-1004.

Eglinton G. and Hamilton R. J. (1967) Leaf epicuticular waxes. *Science* **156**(3780), 1322-1335.

Elvert M., Suess E., Greinert J., and Whiticar M. J. (2000) Archaea mediating anaerobic methane oxidation in deep-sea sediments at cold seeps of the eastern Aleutian subduction zone. *Organic Geochemistry* **31**, 1175-1187.

Ferdelman T. G., Fossing H., Neumann K., and Schulz H. D. (1999) Sulfate reduction in surface sediments of the southeast Atlantic continental margin between 15 degrees 38'S and 27 degrees 57'S (Angola and Namibia). *Limnology and Oceanography* **44**(3), 650-661.

Ferdelman T. G., Glud R. N., and Fossing H. (1997) Measurement of sulfate reduction in marine sediment slurries using O-18-labeled sulfate. *Abstracts of Papers of the American Chemical Society* **214**, 82-GEOC.

Fossing H., Ferdelman T. G., and Berg P. (2000) Sulfate reduction and methane oxidation in continental margin sediments influenced by irrigation (South-East Atlantic off Namibia). *Geochimica Et Cosmochimica Acta* **64**(5), 897-910.

Fossing H. and Jørgensen B. B. (1989) Measurement of bacterial sulfate reduction in sediments - evaluation of a single-step chromium reduction method. *Biogeochemistry* **8**(3), 205-222.

Goulder R. (1977) Attached and free bacteria in an estuary with abundant suspended solids. *Journal of Applied Bacteriology* **43**(3), 399-405.

Hallam S. J., Girguis P. R., Preston C. M., Richardson P. M., and DeLong E. F. (2003) Identification of methyl coenzyme M reductase A (mcrA) genes associated with methane-oxidizing archaea. *Applied and Environmental Microbiology* **69**(9), 5483-5491.

Hansen L. B., Finster K., Fossing H., and Iversen N. (1998) Anaerobic methane oxidation in sulfate depleted sediments: Effects of sulfate and molybdate additions. *Aquatic Microbial Ecology* **14**(2), 195-204.

Hempel P., Spieß V., and Schreiber R. (1994) Expulsion of shallow gas in the Skagerrak - evidence from sub-bottom profiling, seismic, hydroacoustical and geochemical data. *Estuarine, Coastal and Shelf Science* **38**, 583-601.

Hensen C., Zabel M., Pfeiffer K., Schwenk T., Kasten S., Riedinger N., Schulz H., and Boetius A. (2003) Control of sulfate pore-water profiles by sedimentary events and the significance of anaerobic oxidation of methane for the burial of sulfur in marine sediments. *Geochimica Et Cosmochimica Acta* **64**(14), 2631-2647.

Hinrichs K. U. and Boetius A. (2002) The anaerobic oxidation of methane: New insights in microbial ecology and biogeochemistry. *Ocean Margin Systems* (ed. G. Wefer), pp. 457-477. Springer-Verlag Berlin Heidelberg

Hinrichs K. U., Summons R. E., Orphan V., Sylva S. P., and Hayes J. M. (2000) Molecular and isotopic analysis of anaerobic methane-oxidizing communities in marine sediments. *Organic Geochemistry* **31**(12), 1685-1701.

Hoehler T. M., Alperin M. J., Albert D. B., and Martens C. S. (1994) Field and laboratory studies of methane oxidation in an anoxic marine sediment - evidence for a methanogen-sulfate reducer consortium. *Global Biogeochemical Cycles* **8**(4), 451-463.

Hoehler T. M., Alperin M. J., Albert D. B., and Martens C. S. (1998) Thermodynamic control on hydrogen concentrations in anoxic sediments. *Geochimica Et Cosmochimica Acta* **62**(10), 1745-1756.

Hovland M. (1991) Large pockmarks, gas-charged sediments and possible clay diapirs in the Skagerrak. *Marine and Petroleum Geology* **8**(3), 311-316.

Hovland M. and Judd A. G. (1988) *Seabed Pockmarks and Seepages*. Graham and Trotman Inc.

Hübscher C. and Borowski C. (2006) Seismic evidence for fluid escape from Mesozoic cuesta type topography in the Skagerrak. *Marine and Petroleum Geology* **23**, 17-28.

Iversen N. and Blackburn T. H. (1981) Seasonal rates of methane oxidation in anoxic marine-sediments. *Applied and Environmental Microbiology* **41**(6), 1295-1300.

Iversen N. and Jørgensen B. B. (1985) Anaerobic methane oxidation rates at the sulfate methane transition in marine-sediments from Kattegat and Skagerrak (Denmark). *Limnology and Oceanography* **30**(5), 944-955.

Iversen N. and Jørgensen B. B. (1993) Diffusion-coefficients of sulfate and methane in marine-sediments - influence of porosity. *Geochimica Et Cosmochimica Acta* **57**(3), 571-578.

Joye S. B., Boetius A., Orcutt B. N., Montoya J. P., Schulz H. N., Erickson M. J., and Lugo S. K. (2004) The anaerobic oxidation of methane and sulfate reduction in sediments from Gulf of Mexico cold seeps. *Chemical Geology* **205**(3-4), 219-238.

Judd A. G. (2004) Natural seabed gas seeps as sources of atmospheric methane. *Environmental Geology* **46**, 988-996.

Judd A. G., Hovland M., Dimitrov L. I., Gil S. G., and Jukes V. (2002) The geological methane budget at Continental Margins and its influence on climate change. *Geofluids* **2**(2), 109-126.

Kallmeyer J., Ferdelman T. G., Weber A., Fossing H., and Jørgensen B. B. (2004) A cold chromium distillation procedure for radiolabelled sulfide applied to sulfate reduction measurements. *Limnology & Oceanography: Methods* **2**, 171-180.

Kim H. Y. and Salem N. (1990) Separation of lipid classes by solid-phase extraction. *Journal of Lipid Research* **31**(12), 2285-2289.

Knittel K., Lösekann T., Boetius A., Kort R., and Amann R. (2005) Diversity and distribution of methanotrophic archaea at cold seeps. *Applied and Environmental Microbiology* **71**(1), 467-479.

Krüger M., Meyerdierks A., Glöckner F. O., Amann R., Widdel F., Kube M., Reinhardt R., Kahnt R., Böcher R., Thauer R. K., and Shima S. (2003) A conspicuous nickel protein in microbial mats that oxidize methane anaerobically. *Nature* **426**(6968), 878-881.

Lovley D. R. and Klug M. J. (1982) Kinetic analysis of competition between sulfate reducers and methanogens for hydrogen in sediments. *Applied Environmental Microbiology* **43**, 1373-1379.

Lovley D. R. and Goodwin S. (1988) Hydrogen concentrations as an indicator of the predominant terminal electron-accepting reactions in aquatic solutions. *Geochimica Et Cosmochimica Acta* **52**, 2993-3003.

Lovley D. R. and Klug M. J. (1983) Sulfate reducers can outcompete methanogens at freshwater sulfate concentrations. *Applied Environmental Microbiology* **45**, 187-192.

Lovley D. R. and Klug M. J. (1986) Model for the distribution of sulfate reduction and methanogenesis in fresh-water sediments. *Geochimica Et Cosmochimica Acta* **50**(1), 11-18.

Marlowe I. T., Brassell S. C., Eglinton G., and Green J. C. (1984) Long chain unsaturated ketones and esters in living algae and marine sediments. *Organic Geochemistry* **6**, 135-141.

Martens C. S. and Berner R. A. (1974) Methane production in the interstitial waters of sulfate-depleted marine sediments. *Science* **185**(4157), 1167-1169.

Michaelis W., Seifert R., Nauhaus K., Treude T., Thiel V., Blumenberg M., Knittel K., Gieseke A., Peterknecht K., Pape T., Boetius A., Amann R., Jørgensen B. B., Widdel F., Peckmann J. R., Pimenov N. V., and Gulin M. B. (2002) Microbial reefs in the Black Sea fueled by anaerobic oxidation of methane. *Science* **297**(5583), 1013-1015.

Nauhaus K., Boetius A., Krüger M., and Widdel F. (2002) *In vitro* demonstration of anaerobic oxidation of methane coupled to sulphate reduction in sediment from a marine gas hydrate area. *Environmental Microbiology* **4**(5), 296-305.

Nauhaus K., Treude T., Boetius A., and Krüger M. (2005) Environmental regulation of the anaerobic oxidation of methane: A comparison of ANME-I and ANME-II communities. *Environmental Microbiology* **7**(1), 98-106.

Niemann H. (2005) Rates and signatures of methane turnover in sediments of continental margins. PhD thesis, Max-Planck Institute for Marine Microbiology.

Niemann H., Elvert M., Hovland M., Orcutt B., Judd A. G., Suck I., Gutt J., Joye S., Damm E., and Finster K. (2005) Methane emission and consumption at a North Sea gas seep (Tommeliten area). *Biogeosciences* **2**, 335-351.

Niewöhner C., Hensen C., Kasten S., Zabel M., and Schulz H. D. (1998) Deep sulfate reduction completely mediated by anaerobic methane oxidation in sediments of the upwelling area off Namibia. *Geochimica et Cosmochimica Acta* **62**(3), 455-464.

Orcutt B., Boetius A., Elvert M., Samarkin V., and Joye S. B. (2005) Molecular biogeochemistry of sulfate reduction, methanogenesis and the anaerobic oxidation of methane at Gulf of Mexico cold seeps. *Geochimica Et Cosmochimica Acta* **69**(23), 5633-5633.

Orcutt B. N., Boetius A., Lugo S. K., MacDonald I. R., Samarkin V. A., and Joye S. B. (2004) Life at the edge of methane ice: Microbial cycling of carbon and sulfur in Gulf of Mexico gas hydrates. *Chemical Geology* **205**(3-4), 239-251.

Oremland R. S. and Polcin S. (1982) Methanogenesis and sulfate reduction: Competitive and noncompetitive substrates in estuarine sediments. *Applied and Environmental Microbiology* **44**(6), 1270-1276.

Orphan V. J., House C. H., Hinrichs K. U., McKeegan K. D., and DeLong E. F. (2002) Multiple archaeal groups mediate methane oxidation in anoxic cold seep sediments. *Proceedings of the National Academy of Sciences of the United States of America* **99**(11), 7663-7668.

Pancost R. D., Bouloubassi I., Aloisi G., Sinninghe Damste J. S., and party t. M. s. (2001) Tree series of non-isoprenoidal dialkyl glycerol diethers in cold seep carbonate crusts. *Organic Geochemistry* **31**, 695-707.

Pancost R. D. and Sinninghe Damste J. S. (2003) Carbon isotopic composition of prokaryotic lipids as tracers of carbon cycling in diverse settings. *Chemical Geology* **195**(1-4), 29-58.

Pancost R. D., Pressley S., Coleman J. M., Benning L. G., and Mountain B. W. (2005) Lipid biomolecules in silica sinters: Indicators of microbial biodiversity. *Environmental Microbiology* **7**(1), 66-77.

Pancost R. D., Sinninghe Damste J. S., de Lint S., van der Maarel M. J. E. C., Gottschal J. C., and Party t. M. S. S. (2000) Biomarker evidence for widespread anaerobic methane oxidation in Mediterranean sediments by a consortium of methanogenic archaea and bacteria. *Applied and Environmental Microbiology* **66**(3), 1126-1132.

Parkes R. J., Cragg B., A., Banning N., Brock F., Webster G., Fry J., Pancost R. D., Kelly S., Knab N. J., Jørgensen B. B, Rinna J., and Weightman A. J. (in press) Biogeochemistry and biodiversity of methane cycling in subsurface marine sediments. *Environmental Microbiology*.

Reeburgh W. S. (1980) Anaerobic methane oxidation: Rate depth distributions in Skan Bay sediments. *Earth and Planetary Science Letters* **47**, 345-352.

Sansone F. J. and Martens C. S. (1982) Volatile fatty acid cycling in organic-rich marine sediments. *Geochimica Et Cosmochimica Acta* **46**, 1575-1589.

Schmaljohann R., Faber E., Whiticar M. J., and Dando P. R. (1990) Coexistence of methane-based and sulfur-based endosymbioses between bacteria and invertebrates at a site in the Skagerrak. *Marine Ecology-Progress Series* **61**(1-2), 119-124.

Schönheit P., Kristjansson J. K., and Thauer R. K. (1982) Kinetic mechanism for the ability of sulfate reducers to outcompete methanogens for acetate. *Archives of Microbiology* **132**, 285-288.

Schulz H. D. and Zabel M. (2000) *Marine Geochemistry*. Springer Verlag.

Suess E., Torres M. E., Bohrmann G., Collier R. W., Greinert J., Linke P., Rehder G., Trehu A., Wallmann K., Winckler G., and Zuleger E. (1999) Gas hydrate destabilization: enhanced dewatering, benthic material turnover and large methane plumes at the Cascadia convergent margin. *Earth and Planetary Science Letters* **170**, 1-15.

Thomsen T. R., Finster K., and Ramsing N. B. (2001) Biogeochemical and molecular signatures of anaerobic methane oxidation in a marine sediment. *Applied and Environmental Microbiology* **67**(4), 1646-1656.

Toth D. J. and Lerman A. (1977) Organic matter reactivity and sedimentation rates in the oceans. *American Journal of Science* **277**, 465-485.

Treude T., Boetius A., Knittel K., Wallmann K., and Jørgensen B. B. (2003) Anaerobic oxidation of methane above gas hydrates at Hydrate Ridge, NE Pacific Ocean. *Marine Ecology-Progress Series* **264**, 1-14.

Treude T., Krüger M., Boetius A., and Jørgensen B. B. (2005a) Environmental control on anaerobic oxidation of methane in the gassy sediments of Eckernfoerde Bay (German Baltic). *Limnology and Oceanography* **50**(6), 1771-1786.

Treude T., Niggemann J., Kallmeyer J., Wintersteller P., Schubert C. J., Boetius A., and Jørgensen B. B. (2005b) Anaerobic oxidation of methane and sulfate reduction along the Chilean continental margin. *Geochimica Et Cosmochimica Acta* **69**(11), 2767-2779.

Valentine D. L. (2002) Biogeochemistry and microbial ecology of methane oxidation in anoxic environments: A review. *Antonie Van Leeuwenhoek* **81**(1-4), 271-282.

van Weering T. C. E., Rumohr J., and Liebzeit G. (1993) Holocene sedimentation in the Skagerrak: A review. *Marine Geology* **111**, 379-391.

Volkman J. K., Barret S. M., and Blackburn S. I. (1999) Eustigmatophyte microalgae are potential sources of C29 sterols, C22-C28 n-alcohols and C28-C32 n-alkyl diols in freshwater environment. *Organic Geochemistry* **30**(5), 307-318.

Whiticar M. J. (2002) Diagenetic relationship of methanogenesis, nutrients, acoustic turbidity, pockmarks and freshwater seepages in Eckernförde Bay. *Marine Geology* **182**, 29-53.

Zhang C. L., Pancost R. D., Sassen R., Qian Y., and Macko S. A. (2003) Archaeal lipid biomarkers and isotopic evidence of anaerobic methane oxidation associated with gas hydrates in the Gulf of Mexico. *Organic Geochemistry* **34**(6), 827-836.

Chapter 3

Anaerobic oxidation of methane (AOM) in marine sediments from the Skagerrak (Denmark): II. Further insights with a reaction-transport model

Andrew W. Dale[1] , Pierre Regnier[1], Nina J. Knab[2], Bo B. Jørgensen[2],
Philippe Van Cappellen[1]

Manuscript in preparation

[1]Department of Earth Sciences - Geochemistry, Utrecht University, P.O. Box 80021, 3508 TA Utrecht, Netherlands

[2]Max Planck Institute of Marine Microbiology, Department of Biogeochemistry, Celsiusstrasse 1, 28359 Bremen, Germany

ABSTRACT

A steady-state reaction-transport model has been applied to sediments retrieved by gravity core from two stations (S10 and S13) in the Skagerrak to determine the main kinetic and thermodynamic controls on anaerobic oxidation of methane (AOM). The model was based on an extended biomass-implicit reaction network for organic carbon degradation, and included extracellular hydrolysis of particulate organic carbon to glucose, fermentation of glucose to acetate and hydrogen, sulfate reduction, methanogenesis, AOM, acetogenesis and acetotrophy. Catabolic reaction rates were quantified with an extension of the Michaelis-Menten rate expression that ensures thermodynamic consistency of the low in situ catabolic energy yields. Lower rates of fermentation at S10 led to a prominent model-predicted AOM peak of 2.2 nmol cm^{-3} d^{-1} in the sulfate-methane transition zone (SMTZ). The fraction of total sulfate reduction (SRR) due to AOM in the SMTZ was very high at this site (76.1 %). In contrast, AOM accounted for only 36.0 % of SRR in the SMTZ at S13 because of higher fermentative rates of hydrogen and acetate production which diverts available sulfate away from AOM. Consequently, the maximum AOM rate was lower (1.0 nmol cm^{-3} d^{-1}). Whole-core integrated AOM rates derived from the model were higher at S10 (25.0 nmol cm^{-2} d^{-1}) than S13 (9.1 nmol cm^{-2} d^{-1}), even though total sulfate input was 34 % lower at S10. At both sites, methane was not entirely consumed in the SMTZ, but exhibited diffusive tailing up to the top of the core. The tailing was due to bioenergetic limitation of AOM into the sulfate-reduction zone because the methane concentration was too low to engender favorable thermodynamic drive. AOM was also bioenergetically inhibited below the SMTZ because of high hydrogen concentrations (~3-6 nM). The model showed that pore water concentrations do not give a good representation of the minimum catabolic energy needed to support life (ΔG_{BQ}) because of the highly-coupled nature of the reaction network. Best model fits were obtained with a ΔG_{BQ} of 1.3-1.4 kJ e-mol^{-1} for AOM, which is within the range reported in the literature.

INTRODUCTION

There is growing interest in understanding how the functioning of microbial communities in subsurface marine sediments is characterized by the low supply of energy substrates required for microbial metabolism. The driving force for microbial growth is the catabolic Gibbs energy yield derived from the transfer of electrons from an electron donor substrate to a terminal electron acceptor (TEA). The principal TEAs are used sequentially in an order which generally reflects the Gibbs energy harvested by the microorganisms, that is, O_2 is used first, followed by NO_3^-, Mn(IV), Fe(III), SO_4^{2-}, and finally CO_2. This sequential consumption leads to the commonly observed vertical spatial zonation of redox conditions in marine sediments (Froelich et al., 1979). The electron donor substrates are usually produced by the decomposition of particulate organic carbon (POC) deposited on the sea floor. POC typically shows a decreasing reactivity with time and depth time due to preferential degradation of the more labile fractions (Berner, 1980; Westrich and Berner, 1984; Middelburg, 1985; Boudreau and Ruddick, 1991). Diagenetic reaction-transport models (RTMs) which describe the fate of chemical and biological species by coupling the rates of transport and biogeochemical reactions have been routinely employed to constrain the major terminal metabolic processes occurring in marine sedimentary environments (Van Cappellen and Wang, 1996; Steefel and Van Cappellen, 1998; Berg et al., 2003; Jourabchi et al., 2005; Thullner et al., 2005).

Microbial organic matter degradation in marine sediments can be described as a series of reactions through which POC is respired to CO_2 via the production of a series of high (HMW) and low molecular weight (LMW) dissolved organic carbon (DOC) compounds (Burdige and Gardner, 1998; Burdige, 2000). Essentially, POC is first degraded to HMW-DOC via extracellular hydrolysis and oxidative cleavage. Subsequently, most (>90 %) of the HMW-DOC is rapidly transformed to reactive monomeric LMW-DOC, which is fermented to volatile fatty acids and hydrogen, while the remainder accumulates in the pore water as poorly-reactive polymeric LMW-DOC. RTM modelling of this multi-step pathway represents a formidable challenge because the processes affecting DOC in marine sediments are only just beginning to be understood (Alperin et al., 1994; Arnosti and Holmer, 1999; Burdige et al., 2000; Hee et al., 2001; Komada et al., 2004; Jensen et al., 2005).

In this paper we implement a similar carbon degradation scheme into a RTM framework, building on the batch model for anaerobic carbon transformation of Dale et al. (2006). The current model does not represent the microbial dynamics explicitly and assumes steady-state conditions. It is calibrated using data from two gravity cores sampled in the Skagerrak (Denmark) at stations S10 and S13 (Knab et al., Chapter 2). The approach is similar to that of Burdige (2000), Komada et al. (2004) and Thullner et al. (2005) in that it provides a relatively detailed description of the organic carbon degradation pathways, especially the extracellular hydrolysis of POC to monomeric LMW-DOC. LMW-DOC is assumed to be glucose, which is a common carbohydrate in Skagerrak sediments (Jensen et al., 2005). The polymeric LMW-DOC pool is not considered. The model differs from previous contributions in that it simulates the catabolism of the compounds produced by LMW-DOC fermentation via TEA reduction. Two ubiquitous carbohydrate fermentation products included in the model are the volatile fatty acid acetate (Ac) and hydrogen (H_2) – (Arnosti et al., 2005). These reactive intermediates then provide the reducing power for a series of terminal metabolic pathways: hydrogenotrophic and acetotrophic sulfate reduction, methanogenesis, acetogenesis and acetotrophy. In view of the low Gibbs energy yields for these reactions under in situ conditions, reaction rates are calculated using a modified Michaelis-Menten rate expression that ensures thermodynamic consistency (Jin and Bethke, 2002).

The model is chiefly used to investigate the interplay between LMW-DOC fermentation and anaerobic oxidation of methane (AOM) in sediments from the Skagerrak. AOM is the process by which CH_4 diffusing upwards in an anoxic sediment is oxidized by SO_4^{2-} (Barnes and Goldberg, 1976; Alperin and Reeburgh, 1985), within a restricted depth interval of enhanced microbial activity known as the sulfate-methane transition zone (SMTZ). To date, the majority of AOM models in marine sediments use first- or second-order rate expressions for the net reaction between CH_4 and SO_4^{2-} (e.g. Van Cappellen and Wang, 1996; ; Haese et al., 2003; Luff et al., 2003; Wallmann et al., 2006). However, indirect experimental observations suggest that methane oxidation is not directly coupled to sulfate reduction, but is first oxidized to a reactive intermediate which is then consumed by the sulfate reducing bacteria in a syntrophic association (Hoehler et al., 1994; Boetius et al., 2000). The actual reactive intermediate is still a subject of debate, although a growing body of evidence suggests that H_2 is a likely candidate (Hoehler et al., 1994; Shima and Thauer, 2005; Krüger et al., 2003; Hallam et al., 2005). Thus,

hydrogenotrophic sulfate reduction can be fueled by either H_2 produced by fermentation or H_2 produced by AOM. Given that AOM appears to be strongly dependent on the in situ H_2 concentration (Hoehler et al., 1994; Dale et al., 2006) the rate of fermentation is thus expected to impact heavily on the efficiency of AOM. A suite of data collected as part of the EU-project METROL (http://www.metrol.org) and described in the companion paper (Knab et al., Chapter 1) is used to constrain the methane turnover rates and calibrate the RTM.

METHODS

Sample collection and chemical analyses

The sediment was sampled with a gravity corer (GC) during cruise HE191 with RV Heincke in summer 2003. The cores were cut into 1-m sections after retrieval, and the temperature was measured at the top of each section. The sections were subsampled immediately for pore water concentration and microbial rate measurements.

For **methane** concentrations 3 cm^3 sediment was sealed in glass tubes containing 6 mM NaOH (2.5 % w/v). The methane concentration of the headspace was analyzed by gas chromatography (5890A, Hewlett Packard), with Helium as a carrier gas, using a packed stainless steel Porapak-Q column (6 ft., 0.125 in., 80/100 mesh, Agilent Technology) at 40 °C, and a flame ionization detector.

Sulfate concentrations were measured on pore water squeezed under nitrogen pressure and fixed in $ZnCl_2$ (2 % w/v). The sulfate concentrations were determined by non-suppressed anion exchange chromatography (Waters 510 HPLC Pump; Waters IC-Pak 50 x 4.6 mm anion exchange column; Waters 430 Conductivity detector) using isophtalic acid (1 mM, pH 4.6) in methanol (10 % v/v) as eluant.

Samples for **anaerobic methane oxidation rates (AOM)** were obtained headspace free in glass tubes, and injected with ^{14}C-CH_4 (1.35 kBq). After incubation for 10-24h at in situ temperature,

the samples were transferred into glass vials containing 25 ml NaOH (2.5 % w/v), and analyzed for AOM as described by Treude et al. (2003), by measuring the methane concentration of the headspace in the vials, the total $^{14}C\text{-}CH_4$ by combustion and the produced $^{14}C\text{-}CO_2$ in the sediment by acidification of the sample with HCl (6M).

Sulfate reduction rates (SRR) were determined on sediment sampled in headspace-free glass vials, and injected with $^{35}S\text{-}\ SO_4^{2-}$ (500 kBq). The samples were incubated in the same way as described for AOM, and the reaction was stopped in vials containing 20 ml ZnAc (20 % w/v). The samples were analyzed for SRR by cold distillation method described by Kallmeyer et al. (2004), by measuring the total pool of $^{35}S\text{-}SO_4^{2-}$ in the sample and the amount of reduced inorganic sulfur species produced.

Bioenergetic-Kinetic Model

The RTM is constructed with five dissolved (sulfate (SO_4^{2-}), methane (CH_4), hydrogen (H_2), acetate (CH_3COO^-, termed Ac here), glucose ($C_6H_{12}O_6$)) and two solid POC species (labile POC (CH_2O_{LAB}) and refractory POC (CH_2O_{REF}). SO_4^{2-} is the principle electron acceptor in the model since oxidized iron and manganese phases are absent below 10 cm depth (Canfield et al., 1993), and this layer was lost during deployment and recovery of the gravity cores. Table 1 and 2 present the reaction network and the corresponding biogeochemical parameters, respectively.

The one-dimensional mass-conservation equation (Berner, 1980; Boudreau, 1997) was used to resolve the depth profiles of solids and solutes:

Solutes: $$\varphi \frac{\partial C_i}{\partial t} = \frac{\partial}{\partial x}\left(\varphi D_S \frac{\partial C_i}{\partial x}\right) - \frac{\partial\left(\varphi v C_i\right)}{\partial t} + \varphi\alpha\left(C_0 - C_i\right) + \varphi R_i \qquad (1a)$$

Solids: $$(1-\varphi)\frac{\partial C_j}{\partial t} = \frac{\partial\left((1-\varphi)v\, C_j\right)}{\partial x}(1-\varphi)R \qquad (1b)$$

where x is the vertical axis, t is time, φ is depth-dependent porosity, C_i and C_j are the time–dependent concentrations of dissolved and solid species, respectively, C_0 is the solute concentration at the top of the core, D_S is the tortuosity-corrected molecular diffusion coefficient,

v is the burial rate, α is the bioirrigation coefficient (see Appendix) and R_i and R_j are the rate of change of solutes and solids due to biogeochemical reactions. Bioturbation was not required to simulate the field data, presumably because the bioturbated layer was within the lost surface sediment.

Rate		Type	Reaction stoichiometry	
R_1	hydr	extracellular hydrolysis of labile POC	$CH_2O_{LAB(s)} \rightarrow {}^1/_6\, C_6H_{12}O_{6(aq)}$	
R_2	hydr	extracellular hydrolysis of refractive POC	$CH_2O_{REF(s)} \rightarrow {}^1/_6\, C_6H_{12}O_{6(aq)}$	
	Key	Microbial catabolic reaction		$\Delta G^{o\prime}$
R_3	ferm	fermentation	${}^1/_{24}\, C_6H_{12}O_{6(aq)} + {}^1/_6\, H_2O_{(l)} \rightarrow {}^1/_{12}\, CH_3COO^-_{(aq)} + {}^1/_6\, H_{2(g)} + {}^1/_6\, H^+_{(aq)} + {}^1/_{12}\, HCO_3^-{}_{(aq)}$	-8.61
R_4	hySR	hydrogenotrophic sulfate reduction	${}^1/_2\, H_{2(g)} + {}^1/_8\, SO_4^{2-}{}_{(aq)} + {}^1/_8\, H^+_{(aq)} \rightarrow {}^1/_8\, HS^-_{(aq)} + {}^1/_2\, H_2O_{(l)}$	-19.04
R_5	acSR	acetotrophic sulfate reduction	${}^1/_8\, CH_3COO^-_{(aq)} + {}^1/_8\, SO_4^{2-}{}_{(aq)} \rightarrow {}^1/_8\, HS^-_{(aq)} + ¼\, HCO_3^-{}_{(aq)}$	-6.00
R_6	hyME	hydrogenotrophic methanogenesis	${}^1/_2\, H_{2(g)} + {}^1/_8\, HCO_3^-{}_{(aq)} + {}^1/_8\, H^+_{(aq)} \rightarrow {}^1/_8\, CH_{4(g)} + {}^3/_8\, H_2O_{(l)}$	-16.92
R_7	acME	acetotrophic methanogenesis	${}^1/_8\, CH_3COO^-_{(aq)} + {}^1/_8\, H_2O_{(l)} \rightarrow {}^1/_8\, CH_{4(g)} + {}^1/_8\, HCO_3^-{}_{(aq)}$	-3.88
R_8	AOM	anaerobic methane oxidation	${}^1/_8\, CH_{4(g)} + {}^3/_8\, H_2O_{(l)} \rightarrow {}^1/_2\, H_{2(g)} + {}^1/_8\, HCO_3^-{}_{(aq)} + {}^1/_8\, H^+_{(aq)}$	+16.92
R_9	acet	acetogenesis	${}^1/_2\, H_{2(g)} + {}^1/_4\, HCO_3^-{}_{(aq)} + {}^1/_8\, H^+_{(aq)} \rightarrow {}^1/_8\, CH_3COO^-_{(aq)} + {}^1/_2\, H_2O_{(l)}$	-13.05
R_{10}	actr	acetotrophy	${}^1/_8\, CH_3COO^-_{(aq)} + {}^1/_2\, H_2O_{(l)} \rightarrow {}^1/_2\, H_{2(g)} + {}^1/_4\, HCO_3^-{}_{(aq)} + {}^1/_8\, H^+_{(aq)}$	+13.05

Table 1: Reaction network implemented in the RTM. The reactions include extracellular hydrolysis (R_1,R_2) and eight microbially-mediated reactions (R_3-R_{10}). Illustrative standard Gibbs reaction energies at 298K and 1 bar are expressed per mole electrons transferred (kJ e-mol^{-1}) and corrected for neutral pH conditions with the transformation $\Delta G^{o\prime} = \Delta G^o - \mathrm{RT}\upsilon_{H+} \ln[Kw^{0.5}]$, where υ_{H+} is the stoichiometric coefficient of H^+ in the reaction (Amend and Shock, 2001) and Kw is the ion product. Reverse bicarbonate methanogenesis (hyMe) is assumed to be a feasible pathway for AOM (Krüger et al., 2003; Hallam et al., 2004). Simultaneous AOM and hyME is thus impossible, since they have equal but opposite Gibbs energy yields.

CH_2O (POC) deposited at the sediment-water interface provides the main energy source to drive the catabolic reactions. Rather than the usual approach whereby CH_2O is assumed to be directly available to the microbial community (Van Cappellen and Wang, 1996; Berg et al., 2003), a more realistic representation where CH_2O is decomposed to LMW-DOC following first-order

decay is used here. The LMW-DOC fraction is assumed to be glucose ($C_6H_{12}O_6$) (Cowie and Hedges, 1984; $R_{1,2}$; Table 1). Degradation of CH_2O to LMW-DOC simulates the extracellular hydrolysis of particulate material (Brüchert and Arnosti, 2003; Arnosti, 2004). The hydrolysis rate (mol C g^{-1} y^{-1}) of labile (R_1) and refractory (R_2) CH_2O fractions are described by:

$$R_1 = k_{hyLAB}\,[CH_2O_{LAB}] \quad (2a)$$

$$R_2 = k_{hyREF}\,[CH_2O_{REF}] \quad (2b)$$

where k_{hyLAB} and k_{hyREF} are the corresponding first-order decay constants (y^{-1}). Glucose is fermented to smaller molecules (Brüchert and Arnosti, 2003) via equation R_3 in Table 1. These reactive intermediates then serve as the electron source for reactions R_4-R_{10}.

The dynamics of the microbially-mediated reaction are based on Michaelis-Menten kinetics for enzyme-catalyzed reactions, in which the electron donor substrate is transformed into a product via an enzyme-substrate complex. Dale et al. (2006) showed that steady state biomass was a justifiable assumption for modelling microbial respiration in most marine sediments, and we therefore adopt an approach which assumes constant biomass (or enzyme concentration). Reactions R_4-R_{10} in Table 1 define the catabolism between the electron donor (E_D, mol L^{-1}) and the electron acceptor (E_A, mol L^{-1}), during transfer of 1 electron:

$$xE_D + yE_A \leftrightarrow xE_{D\text{-}ox} + yE_{A\text{-}red} \quad (3)$$

where x and y are stoichiometric coefficients. The rate of uptake of an E_D by the i-th catabolic pathway follows the reaction stoichiometries in Table 1 and is determined by the kinetic (F_K) and thermodynamic drive (F_T) for the reaction:

$$\frac{dE_D}{dt} = \sum_i f(T)\, v_{max-i}.F_{K-i}.F_{T-i} \quad (4)$$

where $$F_{K-i} = \left(\frac{[E_D]}{K_{E_D-i} + [E_D]}\right).\left(\frac{[E_A]}{K_{E_A-i} + [E_A]}\right) \quad (5)$$

$$F_{T-i} = \left(1 - \exp\left(\frac{\Delta G_{NET-i}}{\chi R T}\right)\right) \quad (6)$$

$$f(T) = Q_{10}^{\frac{T-278.15}{10}} \quad (7)$$

where v_{max-i} is the maximum rate of E_D utilization by the *i*-th catabolic pathway, K_{ED-i} and K_{EA-i} are the half-saturation constants for the E_D or E_A, respectively (SO_4^{2-} is the only E_A considered to be rate limiting), ΔG_{NET} (kJ e-mol^{-1}) is the fraction of Gibbs energy of catabolism for the *i*-th catabolic pathway which provides thermodynamic drive for reaction

(see below), χ is the average stoichiometric number (Boudart, 1976; Jin and Bethke, 2002), R is the gas constant (8.314 J K^{-1} mol^{-1}) and T is the absolute temperature (K). χ is equivalent to the number of protons translocated across the cell membrane during catabolism and is assumed to be equal to 1 per electron transferred in anaerobic metabolism (Jin and Bethke, 2002, 2005). F_K and F_T are dimensionless and vary between 0 (total limitation of E_D uptake) and 1 (no limitation). The product of F_K and F_T gives the total drive for reaction, F_{TOT}. When F_{TOT} equals 1 the rate of catabolism equals v_{max}. Note that eq (4) includes no kinetic inhibition terms, since the accumulation of reaction products limits the reaction rate via the effect of the Gibbs energy of reaction (F_T). Values for K_{S-i} are taken from Dale et al. (2006). The v_{max} values depend on the temperature according to a Q_{10} of 2.0 (eq 7).

Calculation of v_{max}

In a biomass-implicit approach, v_{max} (mol E_D L^{-1} y^{-1}) can be estimated from the growth yield (Y, mol C biomass produced per mol E_D consumed), the steady-state biomass concentration (B, mol C biomass L^{-1}), and the maximum specific growth rate (μ, y^{-1}):

$$v_{max-i}^{E_D} = \frac{\mu_i^{E_D} B}{Y_i^{E_D} \varphi} \quad (8)$$

Values for μ_i and Y_i are specific to each catabolic process and were calculated by Dale et al. (2006) from generalized principles of microbial metabolism (Rittman and McCarty, 2001) at a

reference temperature of 278.15K. The total biomass concentration at S10 and S13 is taken as 6×10^8 and 1.5×10^8 cells cm^{-3} total sediment, respectively (Knab et al., Chapter 2) or 9.5×10^{-4} and 2.4×10^{-4} mol C L^{-1} assuming a cellular carbon content of 19 fg C $cell^{-1}$ (Schippers et al, 2005). This total biomass was used in all calculations because the proportional composition of the biomass is unknown. The corresponding v_{max} values are listed in Table 2.

Parameter	Description	Baseline Value at S13/S10	Units
K_{SO4}	Half-saturation constant of SO_4^{2-}	1.0×10^{-3}	M
$K_{H2\text{-}hySR}$	Half-saturation constant of H_2 for hySR	1.0×10^{-8}	M
$K_{Ac\text{-}acSR}$	Half-saturation constant of Ac for acSR	1.0×10^{-4}	M
$K_{H2\text{-}hyME}$	Half-saturation constant of H_2 for hyME	1.0×10^{-6}	M
$K_{Ac\text{-}acME}$	Half-saturation constant of Ac for acME	5.0×10^{-3} †	M
$K_{CH4\text{-}AOM}$	Half-saturation constant of CH_4 for AOM	1.5×10^{-3}	M
$K_{H2\text{-}acet}$	Half-saturation constant of H_2 for acet	1.0×10^{-7}	M
$K_{Ac\text{-}actr}$	Half-saturation constant of Ac for actr	1.0×10^{-3}	M
$K_{glu\text{-}ferm}$	Half-saturation constant of $C_6H_{12}O_6$ for ferm	1.0×10^{-3}	M
$v_{max\text{-}hySR}$	Maximum rate of hySR	2.23 / 0.57	mol H_2 L^{-1} y^{-1}
$v_{max\text{-}acSR}$	Maximum rate of acSR	1.15 / 0.29	mol Ac L^{-1} y^{-1}
$v_{max\text{-}hyME}$	Maximum rate of hyME	2.22 / 0.57	mol H_2 L^{-1} y^{-1}
$v_{max\text{-}acME}$	Maximum rate of acME	1.12 / 0.29	mol Ac L^{-1} y^{-1}
$v_{max\text{-}AOM}$	Maximum rate of AOM	1.10 / 0.28	mol CH_4 L^{-1} y^{-1}
$v_{max\text{-}acet}$	Maximum rate of acet	2.20 / 0.57	mol H_2 L^{-1} y^{-1}
$v_{max\text{-}actr}$	Maximum rate of actr	1.10 / 0.28	mol Ac L^{-1} y^{-1}
$v_{max\text{-}ferm}$	Maximum rate of ferm	1.29 / 0.33	mol $C_6H_{12}O_6$ L^{-1} y^{-1}
χ	Average stoichiometric number	1.0	per e^{-1} transferred
$\Delta G_{BQ\text{-}hySR}$	Minimum Gibbs bioenergetic energy for hySR	3.0 †	kJ e-mol^{-1}
$\Delta G_{BQ\text{-}acSR}$	Minimum Gibbs bioenergetic energy for acSR	1.25 †	kJ e-mol^{-1}
$\Delta G_{BQ\text{-}hyME}$	Minimum Gibbs bioenergetic energy for hyME	1.25 †	kJ e-mol^{-1}
$\Delta G_{BQ\text{-}acME}$	Minimum Gibbs bioenergetic energy for acME	2.0/2.5 †	kJ e-mol^{-1}
$\Delta G_{BQ\text{-}AOM}$	Minimum Gibbs bioenergetic energy for AOM	1.42/1.3 †	kJ e-mol^{-1}
$\Delta G_{BQ\text{-}acet}$	Minimum Gibbs bioenergetic energy for acet	1.25 †	kJ e-mol^{-1}
$\Delta G_{BQ\text{-}actr}$	Minimum Gibbs bioenergetic energy for actr	0.05	kJ e-mol^{-1}
$\Delta G_{BQ\text{-}ferm}$	Minimum Gibbs bioenergetic energy for ferm	1.25 †	kJ e-mol^{-1}

†Value differs from simulations in Dale et al. (2006)

Table 2: Parameters used to describe the rate of substrate uptake (eq 4). Maximum substrate uptake rates (v_{max}) correspond to the reference temperature of 278.15 K, and differ between cores because of the different biomass concentrations at each station. Values for ΔG_{BQ} are given an en electron equivalent basis (kJ e-mol^{-1}), and ΔG_{BQ} values reported in the text as kJ mol^{-1} refer to the Gibbs energy for the catabolic reaction written with the lowest possible integer stoichiometric coefficients.

Calculation of ΔG_{NET}

ΔG_{NET} in eq (6) is the sum of two terms:

$$\Delta G_{NET} = \Delta G_{INSITU} + \Delta G_{BQ} \quad (9)$$

where ΔG_{INSITU} (kJ e-mol^{-1}) is the in situ Gibbs energy yield of the catabolic process and ΔG_{BQ} (kJ e-mol^{-1}) is the bioenergetic energy minimum. ΔG_{INSITU} is calculated from the chemical composition of the pore water which, for the catabolic reaction in eq (3), is given by:

$$\Delta G_{INSITU} = \Delta G^{o\prime} + RT\ln\left[\frac{\{E_{D-ox}\}^x.\{E_{A-red}\}^y}{\{E_D\}^x.\{E_A\}^y}\right] \quad (10)$$

where braces { } denote activity, and $\Delta G^{o\prime}$ is the standard Gibbs energy of catabolism (kJ e-mol^{-1}) at the in situ temperature and which is corrected for biologically neutral pH conditions. For a temperature of 4.5 ^{o}C (station S13) and 8.7 ^{o}C (station S10), the biologically neutral pH is equal to 7.38 and 7.30, respectively (Amend and Shock, 2001). These values are similar to measured pH values at S13 (7.26-7.43) and S10 (7.39-7.94). By assuming biologically neutral pH conditions, the proton activities for Gibbs energy calculations can be neglected if a correction to $\Delta G^{o\prime}$ is applied (see Table 1). Activity coefficients given in Dale et al. (2006) are used in the calculations.

ΔG_{BQ} is defined as the minimum bioenergetic energy that can be exploited by living cells to synthesize adenosine triphosphate (ATP) and cover cellular maintenance requirements. Accordingly, ΔG_{BQ} reflects the minimum number of moles of ATP which can be synthesized from catabolism. This quantum is widely believed to equal ~20 kJ mol^{-1} (Thauer et al., 1977; Schink, 1997), although Hoehler (2004) argues that a lower limit of 9 to 12 kJ mol^{-1} can support microbial metabolism in energy-starved communities. The values used in the model (Table 2) are comprised between 4 and 24 kJ mol^{-1} which is within the general range reported in the literature and predicted by theoretical biochemical calculations (LaRowe and Helgeson, in press).

Note that ΔG_{BQ} is defined as a positive value; it represents a fixed loss of chemical energy and thermodynamic drive. Thus, when a (negative) Gibbs energy yield of catabolism (ΔG_{INSITU}) falls

below the minimum value required for growth (ΔG_{BQ}), further catabolism between the E_D and E_A is prohibited. Substrate utilization is possible when $\Delta G_{NET} < 0$ and thus $F_T > 0$ (eq 6).

Measured ΣH_2S concentrations are below the detection limit (0.5 μM) at both stations at S13. ΣH_2S concentrations at S10 were not measurable due to the sandy sediments. Concentrations of HCO_3^- from the top of the core down to the base of the SMTZ are around 7±1 mM at S10 and S13. Thus, the concentrations of ΣH_2S and DIC are assumed to be constant at these values which considerably simplifies the model without compromising its predictive capacity. CH_4 and H_2 are modeled as dissolved species, although partial pressures are used in thermodynamic calculations. Both quantities are related by temperature- and salinity-dependent solubility constants (Crozier and Yamamoto, 1974; Yamamoto et al., 1976).

RESULTS AND DISCUSSION

Calibration of the reaction network at station S13

The calibration of the RTM is first focused at station S13 only, which provides an opportunity to verify the parameterization of the reaction network developed theoretically by Dale et al. (2006). By selecting appropriate boundary concentrations and physiological parameters (Tables 2 and A1) the profiles of the model variables (CH_2O_{LAB}, CH_2O_{REF}, SO_4^{2-}, CH_4, Ac/VFA, H_2, $C_6H_{12}O_6$) and rates (R_1 to R_{10}, Table 1) are simulated (Fig. 1a-l). Comparison with available experimental pore water data is carried out for SO_4^{2-}, CH_4 and Ac/VFA. Measured rates include hyME (R_6), acME (R_7), AOM (R_8) and sulfate reduction rate (SRR), which in our approach, is assumed to be the sum of hySR (R_4) and acSR (R_5).

The first step of the calibration is to simulate the measured sulfate concentration and SRR profiles (Fig. 1a,g). The exponential decrease in measured SRR suggests that the CH_2O profile can be represented using a single dominant fraction only (CH_2O_{LAB}). Burdige and Gardner (1998) proposed that the rate limiting step of carbon degradation in continental margin sediments is the extracellular hydrolysis of CH_2O. This implies that the decrease of SRR is controlled by the first-order decay constant of CH_2O_{LAB} to the reactive intermediates H_2 and Ac via glucose (R_1, eq 1, Table 1). From the measured SRR curve k_{hyLAB} is estimated as 0.017 y^{-1}, which results

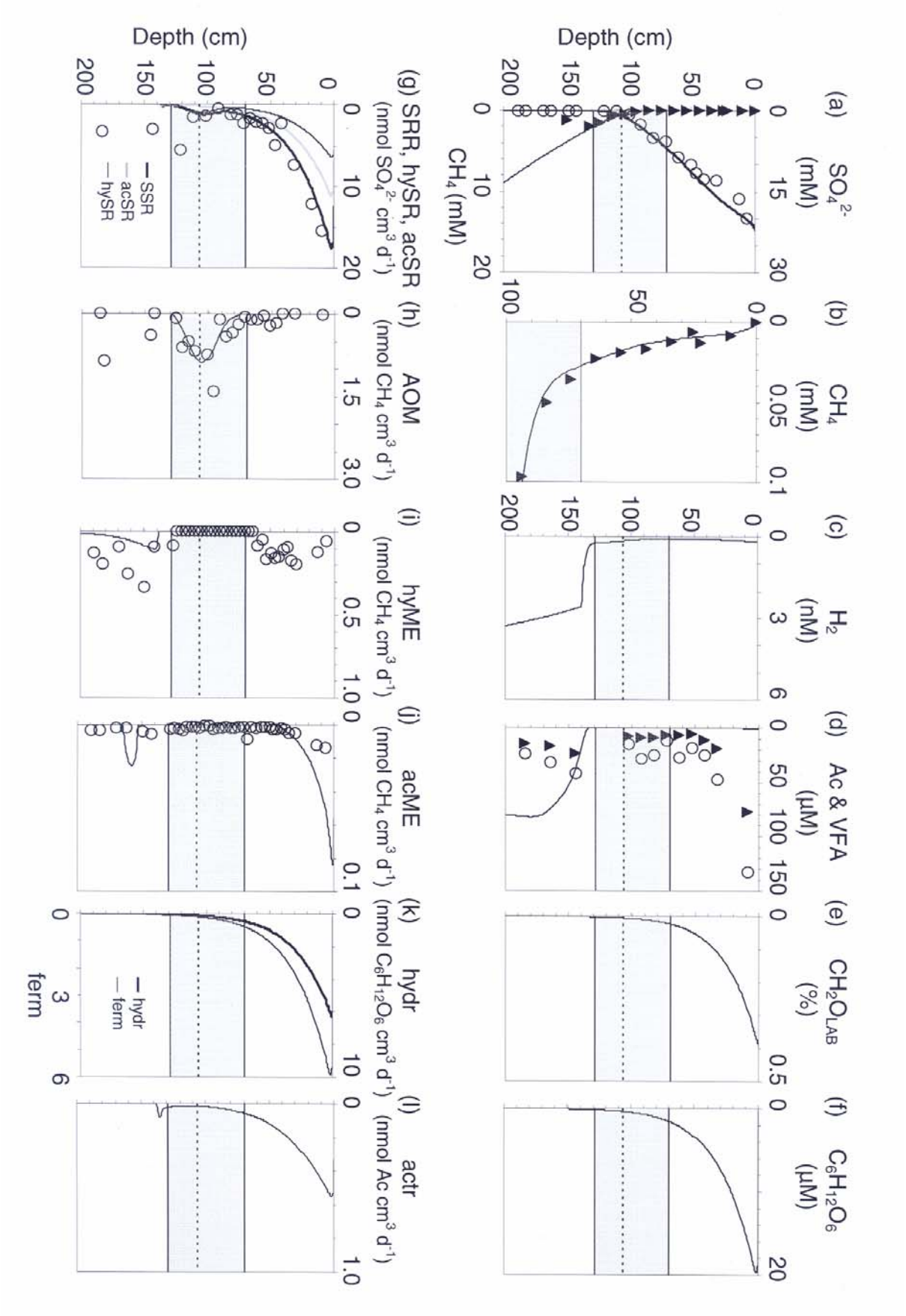
Depth (cm)
(a) SO_4^{2-} (mM)
CH_4 (mM)
(b) CH_4 (mM)
(c) H_2 (nM)
(d) Ac & VFA (µM)
(e) CH_2O_{LAB} (%)
(f) $C_6H_{12}O_6$ (µM)
(g) SRR, hySR, acSR (nmol SO_4^{2-} cm^3 d^{-1})
SSR
acSR
hySR
(h) AOM (nmol CH_4 cm^3 d^{-1})
(i) hyME (nmol CH_4 cm^3 d^{-1})
(j) acME (nmol CH_4 cm^3 d^{-1})
(k) hydr (nmol $C_6H_{12}O_6$ cm^3 d^{-1})
hydr
ferm
(l) actr (nmol Ac cm^3 d^{-1})
ferm

Figure 1.: Measured (spheres) and modeled (lines) concentrations (top row) and rates (bottom row) for station S13. Top row: sulfate (SO42-), methane (CH4), hydrogen (H2), acetate (Ac) and total volatile fatty acids (VFA), labile particulate organic carbon (CH2OLAB) and glucose (C6H12O6). Pore water and solid phase concentrations refer to the pore water volume and the weight of dry solids, respectively. Bottom row: total sulfate reduction rate (SRR), hydrogenotrophic (hySR) and acetotrophic sulfate reduction (acSR), anaerobic oxidation of methane (AOM), hydrogenotrophic (hyME), acetotrophic methanogenesis (acME), CH2O hydrolysis (hydr), fermentation of glucose (ferm), and acetotrophy (actr). All rates refer to the production or consumption of solutes and refer to the pore water volume. The shaded band indicates the SMTZ and the dashed horizontal line shows the depth of maximum AOM rate.

in the hydrolysis rate in Fig. 1k (thick line) and the CH_2O_{LAB} profile in Fig. 1e. The hydrolysis of CH_2O_{REF} (R_2) is not necessary to simulate the SRR profile. Since the CH_2O_{LAB} concentration at the top of the core is ~0.38 % and the measured CH_2O concentration is ~2.0 % (Fig. 1e), most of the CH_2O in the sediment is recalcitrant to sulfate reduction. The CH_2O is hydrolyzed to glucose ($C_6H_{12}O_6$, Fig. 1f), which is then fermented to H_2 (Fig. 1c) and Ac (Fig. 1d). Note that a non-local source of SO_4^{2-} was required to prevent its entire consumption by H_2 and Ac within the upper sediment layers. We assume that bioirrigation of surface pore water via the pumping activities of tube-dwelling animals is the active non-local transport mechanism in these sediments (Berner, 1980). The presence of bioirrigation (see Appendix for calculation) can clearly be identified from the measured linear SO_4^{2-} profile (Fig. 1a) while the SRR follows an exponential distribution. A close model fit results for the SO_4^{2-} concentration (Fig. 1a) and AOM rate (Fig. 1h).

No data are available to verify the down-core profiles of H_2 (Fig. 1c) and $C_6H_{12}O_6$ (Fig. 1f) concentration. Nonetheless, H_2 concentrations in the sulfate-reducing (~0.1 nM) and methanogenic (~3 nM) zone are in close agreement with field observations (Lovley and Goodwin, 1988; Hoehler et al., 2001). The universal constancy of H_2 concentrations in sediments results from coupling of the physiological capacity of the microorganisms to metabolize H_2 and the thermodynamic control by H_2 on H_2 uptake rates (Hoehler et al., 2001). $C_6H_{12}O_6$ concentrations decrease exponentially from 10 μM at the top following the rate of CH_2O hydrolysis and fermentation (Fig. 1k). Jensen et al. (2005) recently published dissolved free carbohydrate concentrations of 0.5-35 μM C in Skagerrak sediments, the majority of which was $C_6H_{12}O_6$. Similar measurements were made in Chesapeake Bay (Burdige et al., 2000), which suggests that the content and reactivity of organic matter is comparable in these areas. However,

the exponential decrease in $C_6H_{12}O_6$ concentration is not observed in the field. This might reflect that the close coupling between $C_6H_{12}O_6$ concentration, hydrolysis and fermentation profiles is a simplified representation of reality (Arnosti and Holmer, 1999; Burdige et al., 2000). The controls of LMW-DOC cycling in sediments are yet not well understood, and carbon-carbohydrate preservation mechanisms may be important in determining the natural distribution of DOC (Burdige and Gardner, 1998; Burdige et al., 2000).

The measured CH_4 profile displays the concave-up shape indicative of AOM (Fig. 1a). However, the expanded scale (Fig. 1b) shows that CH_4 exhibits tailing from depth into the sulfate reduction zone with concentrations of 10-30 μM. This behavior is well-captured by the model by fine-tuning of the kinetic and bioenergetic parameters of the reaction network.

Model-predicted Ac concentrations increase from ~0.7 μM at the top of the core to 50 μM at the bottom (Fig. 1d). The simulated profile shows an order-of-magnitude agreement to measured values of Ac and total VFAs below the SMTZ, while the range predicted close to the sediment-water interface is 1-2 orders of magnitude lower than measured values and observations elsewhere (Crill and Martens, 1986; Alperin et al., 1992). The reason for this difference is currently unclear. It is not possible to simulate the Ac concentrations with acetogenesis (R_9) because of competitive inhibition by hySR for H_2 (R_6). The model predicts that acetotrophy consumes 1.0 nmol Ac cm^{-3} d^{-1} at the top of the core (Fig. 1l), but turning off this pathway simply results in higher rates of acSR and acME, and not higher Ac concentrations (data not shown). Similar concentrations of Ac at the core top matching experimental evidence can be achieved by employing much higher (sub-molar) half-saturation constants for acSR (R_5) and acME (R_7). However, such values are unrealistically high compared to experimental observations (Oude Elferink et al., 1994).

Measured and modeled acME rates are very low rates throughout the sediment. The increase in acME toward the top of the core is reproduced by the model yet at higher rates (Fig. 1j). Hydrogenotrophic methanogenesis (hyME) rates are an order of magnitude higher than acME, yet hyME is only simulated where SO_4^{2-} is depleted, with maximum modeled rates of 0.5 nmol cm^{-3} d^{-1} below the SMTZ (Fig. 1i). The in situ rate of hyME actually makes very little difference to the shape of the CH_4 profile or AOM rates since the model-predicted contribution of hyME to total CH_4 input only 10-15 % of the CH_4 input by diffusion.

The methanogenic zone is also highlighted by the bicarbonate radiotracer rates, with a notable

broad peak in hyME not reproduced by the model extending over the upper 60 cm of the core. hyME is often measurable in the sulfate reducing zone (Mitterer et al., 2001; Cragg et al., 1996) even though the low H_2 concentrations (~0.1 nM) ought to be inhibiting methanogenic archaea (Lovley and Goodwin, 1988). This is probably evidence of natural sediment heterogeneity where small pockets of methanogenesis are able to exist where SO_4^{2-} is unable to penetrate. Such small-scale spatial variations in microbial community structure and enzyme activity (Brüchert and Arnosti, 2003; Arnosti, 2004) and a general lack of understanding of organic carbon dynamics in marine sediments presently limit the predictive capabilities of the model (Davis et al., 2004; Steefel et al., 2005).

Application to station S10

Calibration of the data from S10 is performed on the SRR profile following the same methodology. Here, a slightly better fit is obtained if labile (CH_2O_{LAB}) and refractory (CH_2O_{REF}) POC pools are included (Fig. 2e), with reactivities of k_{hyL} = 0.027 y^{-1} and k_{hyR} = 1.8×10^{-4} y^{-1}, respectively. The reaction network is then applied to S10 (Fig. 2) without any further adjustments to the parameterization from S13. The modeled and measured data show good agreement after slight adjustment of the parameter values for $\Delta G_{BQ\text{-}acME}$ and $\Delta G_{BQ\text{-}AOM}$ (Table 3), although the simulation of Ac/VFA concentration is again poor in the upper layers (Fig. 2d). The model is unable to simulate the increase in acME below the SMTZ (Fig. 2j), which could be evidence of different fermentation pathways than assumed in the reaction network (R_3, Table 1). Also, measured hyME in the SMTZ, as observed in a variety of environments (Hoehler et al., 1994; Orcutt et al., 2005; Seifert et al., 2006), is not reproduced in the simulations since hyME is assumed to be the reverse of AOM (Table 1) and would violate the thermodynamic rate law. In the upper layers, the absence of measurable hyME and acME could be indicative of more homogeneity of the sediment matrix compared to S13. Nonetheless, it is quite remarkable that the RTM reproduces the small-scale features of the CH_4 tailing which are a factor of 5 lower in concentration than at S13 (Fig. 2b), following only minor modifications to the parameter values. The overall parameter set seems well-suited to the available data, and demonstrates the transferability of the reaction network over the current region.

No.	Parameter	Station S13	Station S10
1.	SO_4^{2-} input by bioirrigation (nmol cm^{-2} d^{-1})	263	190
2.	SO_4^{2-} input by diffusion (nmol cm^{-2} d^{-1})	43.0	29.2
3.	SO_4^{2-} input by burial (nmol cm^{-2} d^{-1})	9.5	15.6
4.	ΣSRR_{TOT} (nmol cm^{-2} d^{-1}) (≡ total SO_4^{2-} input)	315	235
5.	Σferm (nmol cm^{-2} d^{-1}) (% in SMTZ)	95.3 (5.6 %)	66.9 (3.7 %)
6.	ΣAOM (nmol cm^{-2} d^{-1})	9.1	25.0
7.	ΣSRR_{TOT} due to AOM (%)	2.9 %	11.3 %
8.	ΣSRR_{SMTZ} (nmol cm^{-2} d^{-1})	25.3	32.8
9.	ΣSRR_{SMTZ} (%ΣSRR_{TOT})	8.0 %	14.8 %
10.	ΣSRR_{SMTZ} due to AOM (%)	36.0 %	76.1 %
11.	$C_6H_{12}O_6$ conc. at depth of max. AOM (nM)	56.9	46.2
12.	Ac conc. at depth of max. AOM rate (nM)	28.3	19.4
13.	H_2 conc. at depth of max. AOM (nM)	0.14	0.27
14.	ΣhySR (% in SMTZ)	13.2 %	28.6 %
15.	ΣacSR (% in SMTZ)	5.0 %	3.7 %

Table 3: Summary of the model-derived budget for stations S13 and S10. Vertically-integrated rates (nmol cm^{-2} d^{-1}) refer to the total sediment.

Dynamics of SO_4^{2-} and CH_4

Bioirrigation is the most important mechanism by which SO_4^{2-} enters the sediment at S13 (263 nmol cm^{-2} d^{-1}, Table 3 *(1)*; numbers in *italics* refer to the line number in Table 3). This represents 83 % of the total SO_4^{2-} input, which is equivalent to the total sulfate reduction rate (ΣSRR_{TOT}, 315 nmol cm^{-2} d^{-1} *(4)*). Diffusion (43.0 nmol cm^{-2} d^{-1} *(2)*) and burial (9.5 nmol cm^{-2} d^{-1} *(3)*) contribute 14 and 3 %, respectively. Bioirrigation at S10 is lower in absolute SO_4^{2-} flux (190 nmol cm^{-2} y^{-1} *(1)*), but supplies an equal proportion (81 %) of the total SO_4^{2-} input (235 nmol cm^{-2} d^{-1} *(4)*). The high rates of bioirrigation in Skagerrak sediments lead to the linear SO_4^{2-} profiles, as observed elsewhere (Fossing et al., 2001).

SO_4^{2-} penetrates to ~110 cm at S13 (Fig. 1a) compared to ~135 cm at S10 (Fig. 2a), even though the SO_4^{2-} input is 34 % greater at S13 *(4)*. This is because the average SRR at S13 (2.9 nmol cm^{-3} d^{-1}) is almost double than at S10 (1.6 nmol cm^{-3} d^{-1}). Additionally, CH_2O_{LAB} concentrations at

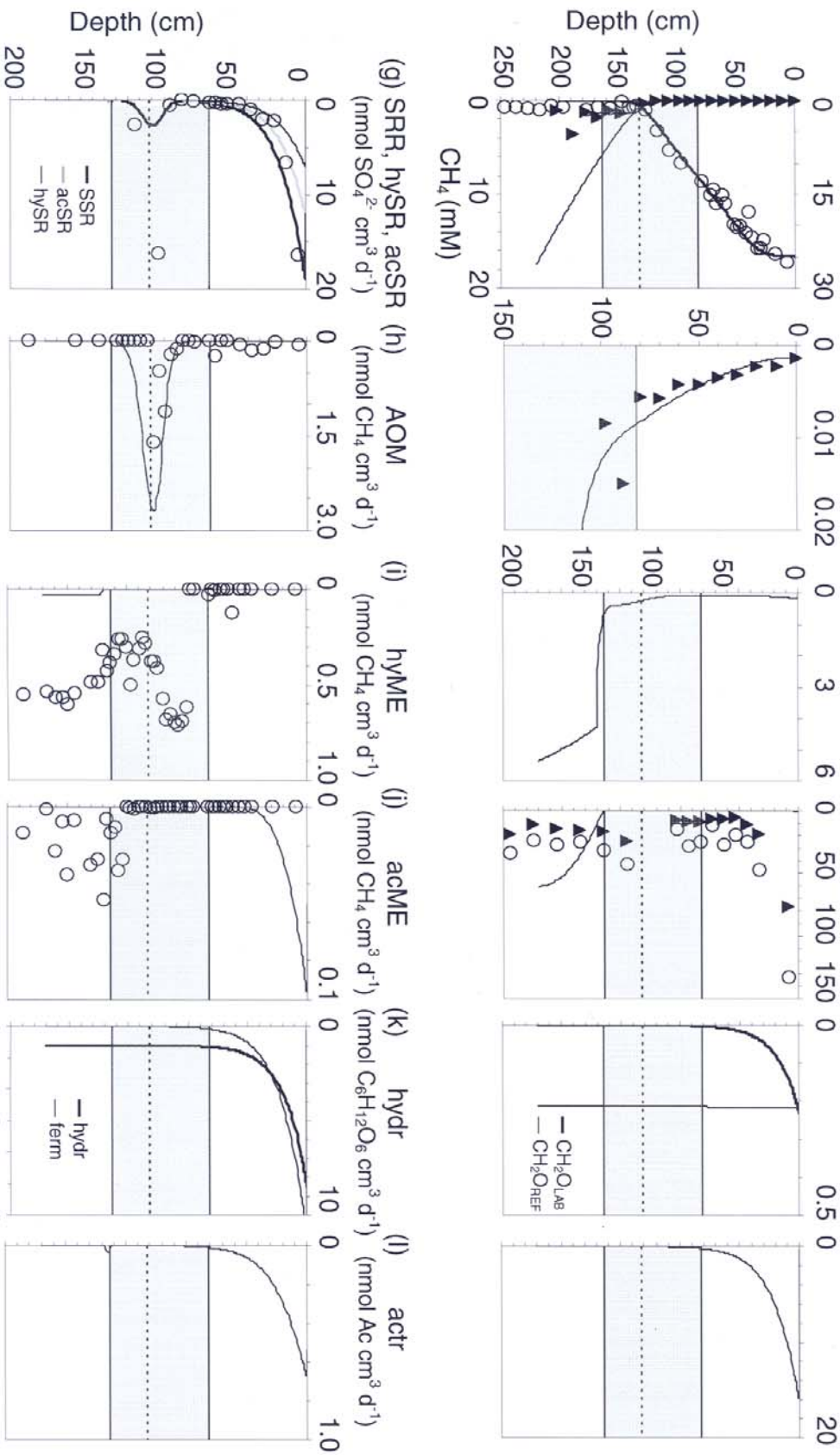
(a) SO_4^{2-} (mM)
(b) CH_4 (mM)
(c) H_2 (nM)
(d) Ac & VFA (µM)
(e) $CH_2O_{LAB/REF}$ (%)
(f) $C_6H_{12}O_6$ (µM)
Depth (cm)
CH_4 (mM)
CH_2O_{LAB}
CH_2O_{REF}
(g) SRR, hySR, acSR (nmol SO_4^{2-} cm^3 d^{-1})
(h) AOM (nmol CH_4 cm^3 d^{-1})
(i) hyME (nmol CH_4 cm^3 d^{-1})
(j) acME (nmol CH_4 cm^3 d^{-1})
(k) hydr (nmol $C_6H_{12}O_6$ cm^3 d^{-1})
(l) actr (nmol Ac cm^3 d^{-1})
SSR
acSR
hySR
hydr
ferm

Figure 2.: Measured (spheres) and modeled (lines) concentrations (top row) and rates (bottom row) for station S10. For further information see legend of Figure 1. Note that 2 fractions of CH_2O are modeled (R_1, R_2, Table1).

the top of the core are higher at S13 (0.39 %, Fig. 1e) than at S10 (0.2 %, Fig. 2e) and, given the similar burial and reaction rates, penetrate deeper into the sediment. Correspondingly, $C_6H_{12}O_6$ depth-integrated fermentation rates (Σferm, *(5)*) are 36 % higher at S13.

Additional evidence that fermentation products are more important for SRR at S13 is given by the contribution of CH_4 to total SO_4^{2-} turnover. Depth-integrated AOM rates (ΣAOM) are lower at S13 (9.1 nmol cm^{-2} d^{-1} *(6)*) than at S10 (25.0 nmol cm^{-2} d^{-1} *(6)*) despite the higher total flux of SO_4^{2-} into the sediment at S13 *(4)*. The fraction of ΣSRR_{TOT} due to AOM is therefore only 2.9 % at S13, compared to 11.3 % at S10 *(7)*.

Table 3 shows that SRR integrated over the SMTZ (ΣSRR_{SMTZ}) is similar in both cores *(8)*, and contribute a roughly equal amount to ΣSRR_{TOT} *(9)*. However, the fraction of ΣSRR_{SMTZ} due to AOM *(10)* is twice as large at S10 (76.1 %) than at S13 (36.0 %). Therefore, most sulfate reduction in the SMTZ at S10 is due to coupled hySR-AOM, but not at S13, with a SRR:AOM ratio of 1.3 (S10) and 2.8 (S13). Greater depth penetration of CH_2O_{LAB} and higher rates of fermentation at S13 give rise to greater concentrations of $C_6H_{12}O_6$ and reactive intermediates (H_2 and Ac) at the depth of maximum AOM *(11,12,13)*. This reduces the role of AOM toward sulfate reduction in the SMTZ. Similar wide ranges of ΣSRR_{SMTZ} due to AOM have also been observed in shelf sediments displaying notably different concentrations of organic carbon (Treude et al., 2005).

As a result of the lower fermentation rates in the SMTZ at S10, the SRR shows prominent peaks in the SMTZ of ~2.0 nmol cm^{-3} d^{-1} which is also reflected in the AOM peak (Fig. 2g,h). At S13, however, the SRR peak in the SMTZ (Fig. 1g,h) is obscured by the contribution of fermentative products and is barely discernable from the rate immediately above the SMTZ. Higher fermentation rates at S13 lead to 11.9 % of the depth-integrated acetotrophic sulfate reduction (ΣacSR) occurring in the SMTZ, yet only 0.3 % at station S10 *(15)*.

Kinetic and bioenergetic spatial trends of AOM

Indirect experimental evidence supports the idea that AOM depends on hySR to consume H_2 and

therefore provide the necessary thermodynamic drive for spontaneous methane oxidation (Hoehler et al., 1994). The down-core profiles of kinetic (F_K) and bioenergetic (F_T) drive calculated from eq (5) and (6) reveal interesting novel features of this dynamic interplay between AOM and hySR.

In the SMTZ at the depth of maximum AOM rate, F_K and F_T for AOM at S13 are equal to 0.18 and 0.002, respectively (Fig. 3a,b). The maximum AOM rate is thus strongly reduced by low bioenergetic drive. The product of F_K and F_T gives the total drive (F_{TOT}) for AOM and is equal to 3×10^{-4} (Fig. 3c). This means that AOM is limited to only 0.03 % of the potential maximum rate or 1.0 nmol CH_4 cm^{-3} y^{-1} (Fig. 1h). Therefore, despite microbial activity on the metabolic fringe, remarkably large quantities of methane are being oxidized. At S10, F_T is similar (0.007) and F_K equals 0.33 (Fig. 3e,f). Here, F_{TOT} is 2.2×10^{-3} (Fig. 3g) so that AOM performs at 0.22 % of v_{max} or 2.2 nmol CH_4 cm^{-3} y^{-1} (Fig. 2h). The difference in F_{TOT} is small in absolute terms, yet sufficient to cause large relative differences in the maximum AOM rate between the two sediments.

In contrast to AOM, where F_T and F_K are of similar magnitude, the bioenergetic drive is not limiting for hySR. F_T for hySR at the depth of maximum AOM rate is 2 orders of magnitude higher than for AOM (0.12 at S13 (Fig. 3b); 0.28 at S10 (Fig. 3f)), whereas F_K is 2 orders of magnitude lower (0.007 at S13 (Fig. 3a); 0.016 at S10 (Fig. 3e)). Accordingly, the bioenergetic-to-kinetic ratio (F_T:F_K) is ~20 for hySR, yet <1 for AOM at both sites. F_{TOT} shows decreasing values from the top of the core down to a pronounced SMTZ peak of 0.001 at S13 and 0.005 at S10 (Fig. 3c,g). hySR is thus restricted to 0.1 % (S13) and 0.5 % (S10) of the corresponding v_{max} value.

The spatial structure of kinetic and bioenergetic drive for AOM are analyzed with regard to the modeled SO_4^{2-}, CH_4 and H_2 profiles (Fig. 3d,h). The SMTZ indicates where AOM is both kinetically and thermodynamically viable. Above the SMTZ, F_K decreases because of lower CH_4 concentrations, and F_T is zero because of the mass-action constraints imposed by the low CH_4 concentrations. Below the SMTZ, F_K increases concomitant with CH_4, whilst F_T is again zero due to the absence of SO_4^{2-} to reduce the H_2, a reaction product of AOM (Dale et al., 2006).

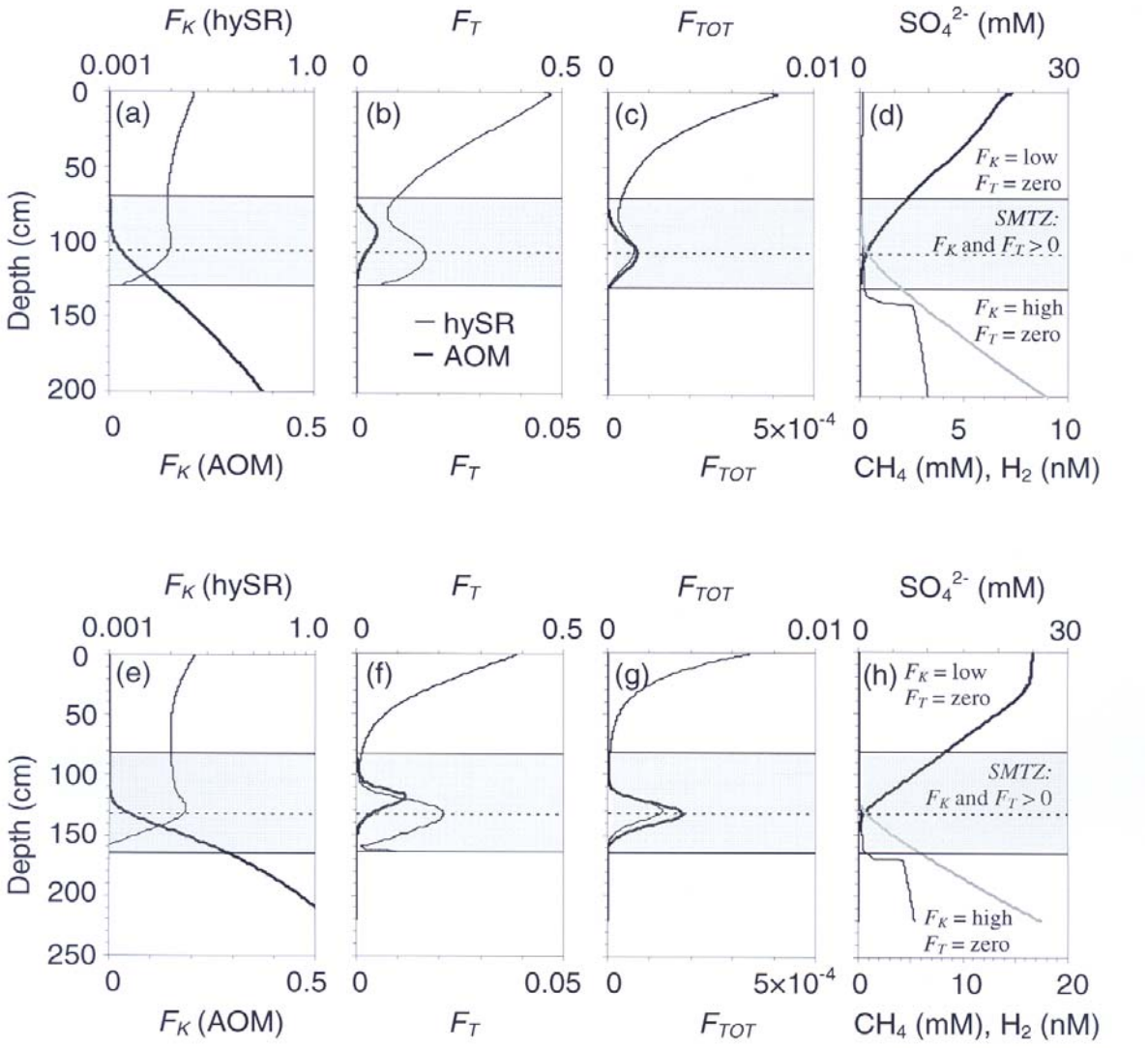

Figure 3.: Model results for kinetic driving forces (F_K, eq 5), thermodynamic driving forces (F_T, eq 6) and total driving forces ($F_{TOT} = F_K \times F_T$) for hySR and AOM at station S13 (top row) and S10 (bottom row). Panels (d) and (h) segregate AOM viability into different zones of the sediment alongside SO_4^{2-}, CH_4 and H_2 profiles reproduced from Fig. 1 and 2. The shaded band indicates the SMTZ and the dashed horizontal line shows the depth of maximum AOM rate.

CH_4 tailing into the sulfate reducing zone thus arises from bioenergetic limitation ($F_T \approx 0$) of AOM imposed by the low CH_4 concentration. For station S13, Fig. 4a shows that the tail is very sensitive to $\Delta G_{BQ\text{-}AOM}$. High values (2.0 kJ e-mol^{-1}) induce extreme tailing whereas the tail completely disappears when $\Delta G_{BQ\text{-}AOM}$ is reduced to 0.0 kJ e-mol^{-1}. In contrast, the effect of a 100-fold change in $K_{S\text{-}CH4}$ has only a minor effect on the shape of the tail (Fig. 4b), which shows

that the kinetic drive plays a secondary role in AOM above the SMTZ (Dale et al., 2006). $\Delta G_{BQ\text{-}AOM}$ is the most sensitive parameter for fitting the SO_4^{2-} and CH_4 profiles in the SMTZ, as it determines the (vertical) spatial coordinates where AOM can occur. In addition, in transient environments where the depth of AOM is seasonally variable, $\Delta G_{BQ\text{-}AOM}$ acts as a thermodynamic switch which enables AOM only when H_2 levels are maintained at low levels by the sulfate reducing bacteria (Hoehler et al., 1998; Dale et al., 2006).

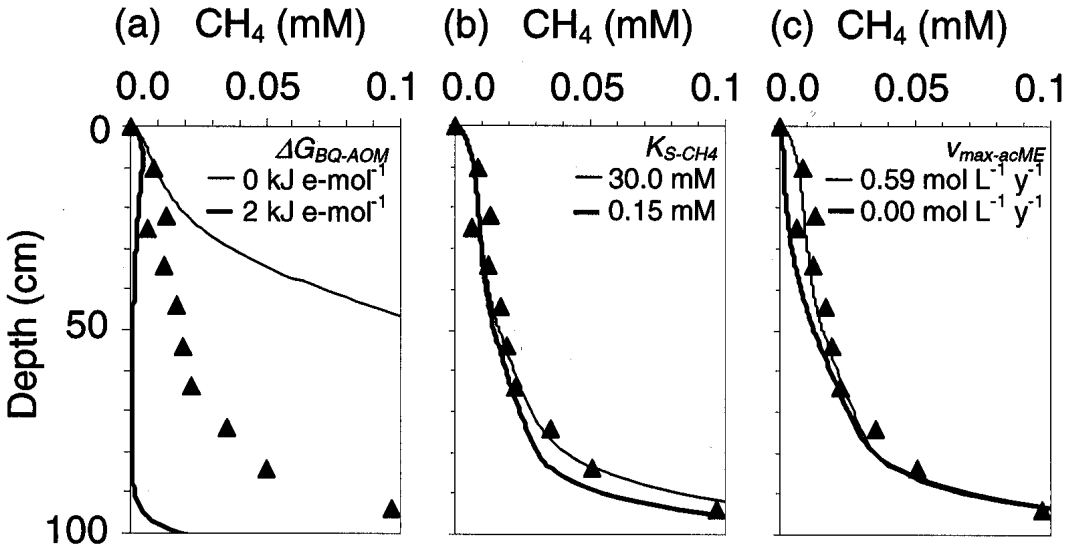

Figure 4.: The effect of changes in (a) $\Delta G_{BQ\text{-}AOM}$, (b) K_{CH4}, and (c) $v_{max\text{-}acME}$ on the CH_4 tail in the sulfate reduction zone at station S13. The measured CH_4 data are represented by the solid triangles.

The source of the CH_4 which sustains the tail above the SMTZ is either in situ production of CH_4 by acME or upwards diffusive transport from the SMTZ (the low H_2 concentrations above the SMTZ are thermodynamically inhibiting for hyME). To test this hypothesis, Fig. 4c compares the baseline simulation result for station S13 ($v_{max\text{-}acME}$ = 1.12 mol Ac L^{-1} y^{-1}, Table 2) with a simulation where $v_{max\text{-}acME}$ is set equal to zero. CH_4 concentrations are slightly reduced in the uppermost 30 cm, with tailing persisting throughout most of the sulfate-reducing zone when $v_{max\text{-}acME}$ is set to 0. Therefore, tailing mainly arises from CH_4 diffusion from the SMTZ and, to a much lesser extent, in situ acME. hyME could also contribute to the tailing in natural

heterogeneous sediments. In addition, methanogenesis from substrates which are not directly catabolizable by sulfate reducing bacteria could provide another CH_4 source (Oremland and Polcin, 1982; Ferdelman et al., 1997), and this may explain why simulated acME rates are higher than those measured experimentally (Fig. 1j). CH_4 tailing has been observed previously (Fossing et al., 2000; Treude et al., 2005) and can be exceptionally prominent (e.g. Jørgensen et al., 2001). Mostly, however, tailing is often not observable in the literature due to the concentration scale on which CH_4 data is plotted.

In situ minimum bioenergetic energies in coupled microbial reaction networks

Hoehler et al. (2001) used in situ Gibbs energies (ΔG_{INSITU}) values from Cape Lookout Bight sediments as a proxy for ΔG_{BQ}, assuming that the microbes were metabolizing at their bioenergetic limit. Down-core profiles ΔG_{INSITU} for hySR and AOM at S13 and S10 calculated from pore water measurements are shown in Fig. 5a,c. For hySR, ΔG_{INSITU} at S13 decreases from ~-35 kJ mol^{-1} at the surface down to ~-26 kJ mol^{-1} above the SMTZ. Hoehler et al. (2001) report a similar decrease of around -34.0 kJ mol^{-1} at the surface down to -20.0 kJ mol^{-1} in the SMTZ. AOM displays a constant ΔG_{INSITU} of -11.4 kJ mol^{-1} throughout the SMTZ at both stations. Such spatial difference in ΔG_{INSITU} between the various microbially-mediated redox reactions has been observed in other oligotrophic environments (Jakobsen and Potsma, 1999; Thornton et al., 2001) and reflects increasing competition for substrates by the microbial community with depth (Hoehler et al., 2001).

The net Gibbs energy yield (ΔG_{NET}) is equal to the sum of ΔG_{INSITU} and ΔG_{BQ} (eq 9). When microorganisms metabolize at the biological ATP threshold, ΔG_{BQ}, ΔG_{NET} is therefore equal, or very close, to zero. However, for hySR ΔG_{NET} is significantly negative. For instance, maximum ΔG_{NET} values for hySR in the SMTZ equal -0.3 and -0.8 kJ e-mol^{-1} for hySR at S13 and S10, respectively (Fig. 5b,d). ΔG_{NET} for AOM is only -0.004 (S13) and -0.016 kJ e-mol^{-1} (S10). The max ΔG_{NET} for hySR in the SMTZ equates to -2.4 and -6.1 kJ mol $reaction^{-1}$ at S13 and S10, respectively, which indicates that minimum Gibbs energies inferred from pore water concentrations may depart significantly from the bioenergetic threshold (Hoehler, 2004).

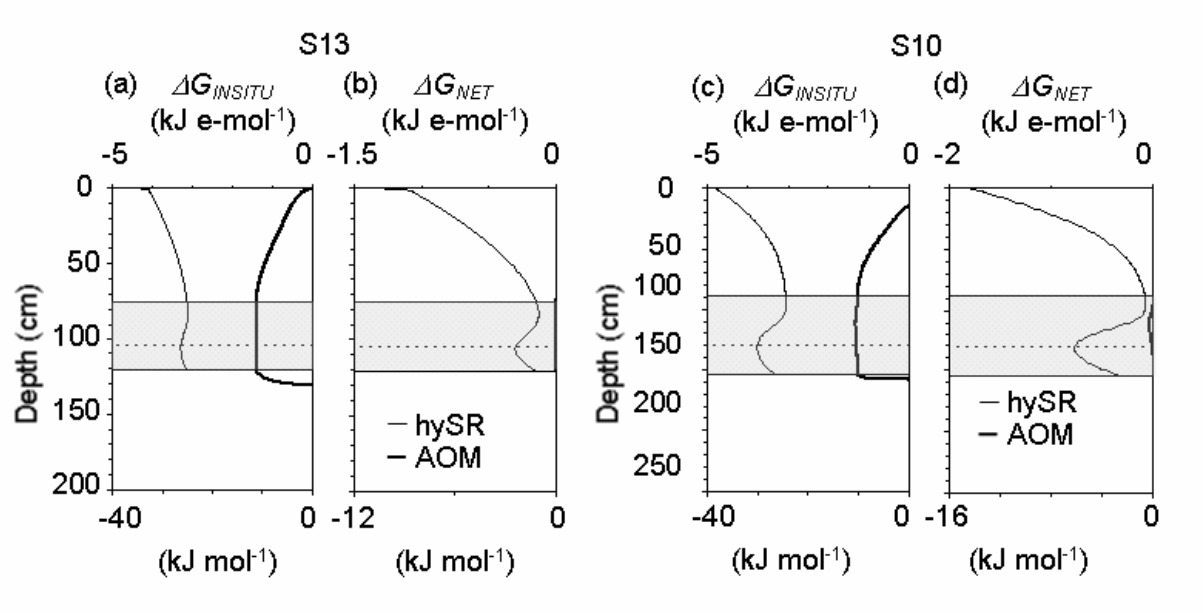

Figure 5.: Model-predicted values for the in situ Gibbs energy yield (ΔG_{INSITU}, eq 10) and the net Gibbs energy yield (ΔG_{NET}, eq 9) for hySR and AOM at station S13 (panels a and b) and S10 (c and d). Units are given in kJ e-mol^{-1} and kJ mol (reaction)$^{-1}$ (8 electron transfer). The shaded band indicates the SMTZ and the dashed horizontal line shows the depth of maximum AOM rate. Note that ΔG_{NET} for AOM is only marginally more negative than zero at S13 and S10.

The rate of a specific reaction is determined by thermodynamic mass-action constraints, via F_T, plus by microbial substrate uptake kinetics, via F_K. For kinetically-limited processes, in situ pore water concentrations are not a reliable indicator of ΔG_{BQ} because catabolism is limited by substrate uptake kinetics before the composition of pore waters becomes thermodynamically inhibiting. An example of this is hySR which is characterized by high F_T and low F_K throughout the core (Fig. 3e,f). Conversely, by definition, the pore water chemistry of a thermodynamically-limited process gives a closer estimate of ΔG_{BQ} because catabolism is restricted thermodynamically by the supply of reactants or removal of products. In our reaction network, AOM is thermodynamically inhibited above and below the SMTZ due to low CH_4 supply and low H_2 removal rates (Fig. 3b,f).

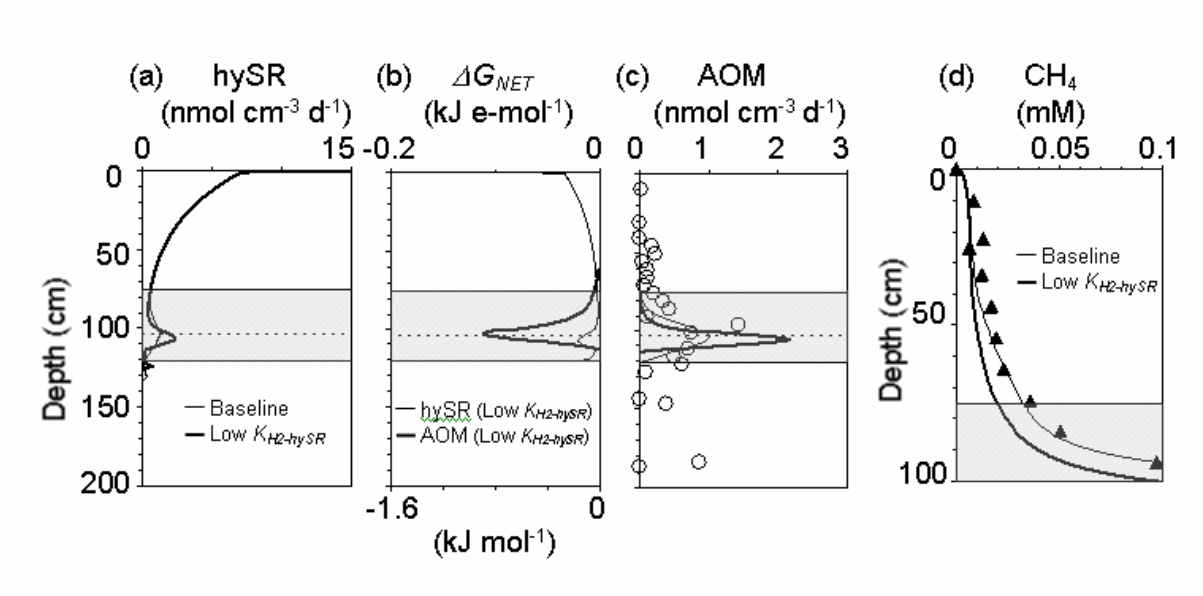

Figure 6.: Simulation results for station S13 where $K_{H2\text{-}hySR}$ for hySR is decreased by a factor of 100 from the baseline value (1×10^{-8} M, Table 2) to 1×10^{-10} M. (a) hySR, (b) net Gibbs energy yield (ΔG_{NET}, eq 9) for hySR and AOM, (c) AOM rate, and (d) CH_4 concentration. The shaded band indicates the SMTZ and the dashed horizontal line shows the depth of maximum AOM rate in the baseline simulation.

Individual reactions are typically highly coupled, as is evident for the production and consumption of reactive intermediates (H_2 and Ac) in our reaction network. F_T and F_K reflect, therefore, the synergistic and competitive behavior of the reaction network as well as rates of solute transport to and from the microorganisms. To illustrate this point further, the effect of microbial kinetic drive for hySR on the AOM rate is investigated. Fig. 6 shows the simulation result where $K_{H2\text{-}hySR}$ is decreased by a factor of 100 at station S13. Higher rates of hySR in the SMTZ are reached compared to the baseline simulation (Fig. 6a). Consequently, SO_4^{2-} and H_2 transport to the bacteria becomes a limiting factor and ΔG_{NET} for hySR is reduced from -0.3 (Fig. 5b) to -0.014 kJ e-mol^{-1} in the SMTZ (Fig. 6b). Yet, the higher hySR rates lower the H_2 concentrations in the system and, therefore, AOM becomes less thermodynamically inhibited by this reaction product. ΔG_{NET} for AOM increases from -0.004 kJ e-mol^{-1} (Fig. 5b) in the baseline simulation to -0.11 kJ e-mol^{-1} here (Fig. 6b). Consequently, the maximum AOM rate increases by a factor of 2 from 1.0 to 2.2 nmol cm^{-3} d^{-1} (Fig. 6c), and which leads to a large reduction in CH_4 tailing above the SMTZ (Fig. 6d).

The coupling of reactions should be thus considered when determination of ΔG_{BQ} energies is carried out experimentally, whether performed on sediment reactors, slurries or in situ pore water data. Our results show that pore water data only provide a realistic estimate of ΔG_{BQ} when the catabolic reaction is limited by the supply of reactants or removal of products. The wide-spread of ΔG_{BQ} values in the data synthesized in Table 1 of Hoehler (2004) may reflect the fact that this condition may not always be fulfilled where ΔG_{BQ} is estimated from whole-sediment data.

CONCLUSIONS

New insights into the role of carbon cycling and AOM in modifying the flux of methane in marine sediments from two stations in the Skagerrak (Denmark) have been gained with a reaction-transport approach. The biomass-implicit reaction network included the extracellular hydrolysis of particulate organic carbon to labile dissolved organic carbon (glucose) and subsequent fermentation to hydrogen and acetate; key reactive intermediates of anaerobic sediments. Reaction rates were determined on the basis of the pore water chemistry which defines the kinetic and bioenergetic limitations of each process. The combination of kinetic and bioenergetic drive is a more realistic approach to modelling substrate turnover, particularly when reactive intermediates are present in low concentrations and have low turnover times. The model could yet be improved by coupling the current reaction network to organic matter degradation pathways which account for the labile and refractive pools of dissolved carbohydrates (Burdige and Gardner, 1998). This calls for a fieldwork campaign which evaluates the concentrations of acetate and hydrogen in addition to carbohydrate turnover rates. Despite the extensive, the reaction network is highly transferable and successfully simulates a suite of data measured at the two stations with only minor modification to the parameter set. Applications of the model to additional data from other areas will help validate and improve the parameterizations used. However, the simulation of local sediment heterogeneities consisting of pockets of acetate production and methanogenesis in sulfate reducing sediments remains problematical, and currently limits the predictive capacity of the model.

Because of the highly-coupled nature of the reaction network, pore water concentrations are a

function of the kinetic and bioenergetic drive of all processes which produce and consume common reactive intermediates. This places a secondary constraint on substrate uptake rates because a reaction may be bioenergetically inhibited by the rate of solute production or consumption by a competitive or synergistic pathway. This combination has profound implications for coupled microbial networks and illustrates that substrate turnover rates and pore water chemistry are not uniquely driven by reaction kinetics. For instance, a lack of thermodynamic and kinetic drive allows methane to diffuse upwards from the SMTZ into the sulfate reducing zone of Skagerrak sediments producing a pronounced tailing effect. We believe that methane tailing is characteristic of passive marine sediments where methane is mostly transported upwards by diffusional processes.

The model demonstrates that estimations of the minimum catabolic threshold energies from pore water concentrations alone may be wholly inaccurate unless the microbial community is considered in its entirety. For example, in the SMTZ hydrogenotrophic sulfate reduction was functioning with an available Gibbs energy of -26.4 kJ mol^{-1} when coupled to AOM, yet -35.2 kJ mol^{-1} when uncoupled from AOM. Thermodynamic limitation for metabolism is emblematic of all the reaction pathways in the model. Given that the chemical and physical conditions of the Skagerrak sediments can be considered typical continental shelf environments, it is likely that efficient microbial metabolism and high turnover rates despite strong kinetic and/or bioenergetic limitation is a common feature of anaerobic environments.

ACKNOWLEDGMENTS

This work is financially supported by EU-project METROL (contract no. EVK3-CT-2002-00080) under the Fifth Framework Programme, and the Netherlands Organization for Scientific Research (NWO Pioneer Programme).

APPENDIX

Numerical solution of the reaction-network

The partial differential equations (eq 1) which describe the dynamics of the 7 model variables are solved with sets of coupled nonlinear process equations using the Biogeochemical Reaction Network Simulator (BRNS; Regnier et al. 2002). The BRNS consists of a Maple® interface coupled to an Automatic Code Generator and is ideal for multi-component (kinetic and equilibrium) reaction systems of varying size and complexity (e.g. Jourabchi et al., 2005; Aguilera et al., 2005). The time and space solution of the PDE is transformed into the simultaneous discretized solution within each grid space (Δx, cm) for a time interval (Δt, y) of the total simulation time.

Table A1 lists the physic-chemical parameters used to construct the RTM. The model employs an unevenly spaced grid, increasing from 0.1 cm at the surface ($x = 0$) to 1 cm at the lower model boundary ($x = L$). Molecular diffusion coefficients (D_S, $cm^2\ y^{-1}$) are calculated from the values at infinite dilution in seawater (Schulz, 2000) corrected for temperature (278K), salinity (34.5 ‰) and tortuosity, θ (Boudreau, 1997) using depth-variable porosity values.

Bioirrigation

Bioirrigation, the combined pumping action of macrofanuna plus solute diffusion through relic tubes and burrows (Berner, 1980; Boudreau, 1997), provides a transport mechanism resulting in exchange of solute species in deeper sediments with surface pore water. The rate of bioirrigation, R_b, is thus described as a non-local mixing term in the PDE (eq 1a):

$$R_b = \varphi\alpha(C_0\text{-}C) \qquad \text{(A-1)}$$

An exponential function describes the decrease in bioirrigation intensity along the depth axis:

$$\alpha = \alpha_0 e^{-k_{irr}x} \qquad \text{(A-2)}$$

where α_0 is the irrigation coefficient at the top of the core (y^{-1}), k_{irr} (cm^{-1}) is the depth attenuation coefficient, and x is the sediment depth. The down-core profile for α, and the two adjustable parameters α_0 and k_{irr} (Table A1) are estimated from the difference between the measured SRR profile and the SRR profile where sulfate is supplied by diffusion only (Fossing et al., 2000).

Parameter	Description	Baseline value for S13 / S10†	Unit
z_{H2O}	Water depth	391 / 86	m
S	Salinity	34.5	—
T	Temperature	277.5 / 281.7	K
φ_0	Porosity at $x = 0$ *	0.5 / 0.44	—
φ_x	Porosity at infinite depth	0.39 / 0.43	—
$attpor$	Depth attenuation coefficient for porosity	0.009	y^{-1}
ρ_s	Dry sediment density	2.5	g cm^{-3}
v	Sedimentation rate	0.5	cm y^{-1}
L	Length of modeled core	200 / 220	cm
α_0	Bioirrigation coefficient at $x = 0$	4.0 / 8.0	y^{-1}
k_{irr}	Attenuation coefficient for bioirrigation	0.068 / 0.09	cm^{-1}
k_{hyLAB}	Hydrolysis rate of labile CH_2O	0.017 / 0.027	y^{-1}
k_{hyREF}	Hydrolysis rate of refractive CH_2O	0.0 / 1.8×10^{-4}	y^{-1}
$D^0_{SO_4^{2-}}$	Molecular diffusion coefficient for SO_4^{2-}	180§	cm^2 y^{-1}
$D^0_{HCO_3^-}$	Molecular diffusion coefficient for HCO_3^-	192§	cm^2 y^{-1}
D^0_{DOC}	Molecular diffusion coefficient for $C_6H_{12}O_6$	30‡	cm^2 y^{-1}
D^0_{Ac}	Molecular diffusion coefficient for Ac	180§	cm^2 y^{-1}
$D^0_{CH_4}$	Molecular diffusion coefficient for CH_4	283§	cm^2 y^{-1}
$D^0_{HS^-}$	Molecular diffusion coefficient for HS^-	350§	cm^2 y^{-1}
$D^0_{H_2}$	Molecular diffusion coefficient for H_2	744§	cm^2 y^{-1}
K_{CH4}	Henry's constant for CH_4 at in situ S,T	1.764 / 1.588	mM
K_{H2}	Henry's constant for H_2 at in situ S,T	0.774 / 0.745	mM
Q_{10}	Temperature dependence of v_{max}	2.0	-
Boundary conditions:			
$C_{0\text{-}SO4}$	SO_4^{2-} concentration at $x = 0$	22 / 27	mM
$C_{0\text{-}glu}$	Glucose concentration at $x = 0$	2.3 / 0.05	µM
$C_{0\text{-}Ac}$	Ac concentration at $x = 0$	100 / 10	µM
$C_{0\text{-}CH4}$	CH_4 concentration at $x = 0$	1×10^{-9}	M
$C_{0\text{-}H2}$	H_2 concentration at $x = 0$	0.17 / 0.05	nM
$C_{0\text{-}CH2OLAB}$	CH_2O_{LAB} concentration at $x = 0$	1.39 / 1.92 ($\times10^{-4}$)	mol g^{-1}
$C_{0\text{-}CH2OREF}$	CH_2O_{REF} concentration at $x = 0$	0.0 / 1.8×10^{-5}	mol g^{-1}
$C_{L\text{-}CH4}$	CH_4 concentration at $x = L$	8.0 / 17.5	mM

Table 4: Model parameters and boundary conditions used in the baseline RTM simulations.

† A single value applies to both cores

§ Value corresponds to infinite dilution in seawater at 5 °C (Schulz, 2000). Diffusion coefficients are corrected with the dimensionless tortuosity coefficient, θ (Boudreau, 1997):

$D = D^0/\theta^2$

$\theta^2 = 1 - \ln(\varphi^2)$

‡ Value based on the diffusion coefficient for an average DOC composition used by Ståhl et al. (2004) for Skagerrak sediments. In fact, the model is insensitive to this parameter since DOC is fermented immediately after its production by hydrolysis and does not accumulate in the pore water.

* Depth dependent porosity, $\varphi_x = \varphi_L + (\varphi_0 - \varphi_L)*\exp^{(-attpor\,.\,x)}$

Boundary concentrations

The boundary conditions used to construct the reaction-transport model are listed in Table A1. Solute concentrations at the top of the gravity cores (Table A1) are determined from measured data or typical values for marine sediments. Boundary concentrations for CH_2O are adjusted until a good fit to the sulfate reduction rate is obtained. Zero concentration gradients are prescribed at the lower boundary for all species except CH_4. At both stations there is evidence of degassing upon core retrieval. Since the in situ CH_4 solubility at S13 is > 60 mM (Duan et al., 1992), the concentration at 200 cm is determined by extrapolation of the CH_4 concentration profile. At station S10 acoustic profiling revealed that the depth of free CH_4 gas lies between 2-4 m (Hübscher, unpubl. data). The in situ solubility at S10 is 17.5 mM (water depth 86 m), and a good fit to the CH_4 profile is achieved by setting this concentration at 220 cm depth; which thus defines the lower boundary depth of the model.

REFERENCES

Aguilera D. R., Jourabchi P., Spiteri C., and Regnier P. A (2005) Knowledge-based reactive transport approach for the simulation of biogeochemical dynamics in Earth systems. *Geochemistry, Geophysics, Geosystems* **6**, Q07012, doi:10.1029/2004GC000899.

Alperin M. J., Albert D. B., and Martens C. S. (1994) Seasonal variations in production and consumption rates of dissolved organic carbon in an organic-rich sediment. *Geochimica et Cosmochimica Acta* **58**, 4909-4930.

Alperin M. J., Blair N. E., Albert D. B., Hoehler T. M., and Martens C. S. (1992) Factors that control the stable carbon isotopic composition of methane produced in an anoxic marine sediment. *Global Biogeochemical Cycles* **6**, 271-291.

Alperin M. J. and Reeburgh W. S. (1985) Inhibition experiments on anaerobic methane oxidation. *Applied and Environmental Microbiology* **50**, 940-945.

Amend J. P. and Shock E. L. (2001) Energetics of overall metabolic reactions of thermophilic and hyperthermophilic archaea and bacteria. *FEMS Microbiology Reviews* **25**, 175-243.

Arnosti C. (2004) Speed bumps and barricades in the carbon cycle: Substrate structural effects on carbon cycling. *Marine Chemistry* **92**, 263-273.

Arnosti C. and Holmer M. (1999) Carbohydrate dynamics and contributions to the carbon budget of an organic-rich coastal sediment. *Geochimica et Cosmochimica Acta* **63**, 393-403.

Barnes R. O. and Goldberg, E. D. (1976) Methane production and consumption in anoxic marine sediments. *Geology* **4**, 297-300.

Berg P., Rysgaard S., and Thamdrup B. (2003) Dynamic modelling of early diagenesis and nutrient cycling. A case study in an Artic marine sediment. *American Journal of Science* **303**, 905-955.

Berner R. A. (1980) *Early Diagenesis: A Theoretical Approach*. Princeton University Press, Princeton, 241 pp.

Boetius A., Ravenschlag K., Schubert C. J., Rickert D., Widdel F., Gieseke A., Amann R., Jørgensen B. B., Witte U., and Pfannkuche O. A (2000) A marine microbial consortium

apparently mediating anaerobic oxidation of methane. *Nature* **407**, 623-626.

Boudart M. (1976) Consistency between kinetics and thermodynamics. *Journal of Physical Chemistry* **80**, 2869-2870.

Boudreau B. P. (1997) *Diagenetic Models and Their Implementation: Modelling Transport and Reactions in Aquatic Sediments*. Springer-Verlag, Berlin, 414 pp.

Boudreau B. P. and Ruddick B. R. (1991) On a reactive continuum representation of organic matter diagenesis. *American Journal of Science* **291**, 507-538.

Brüchert V. and Arnosti C. (2003) Anaerobic carbon transformation: Experimental studies with flow-through cells. *Marine Chemistry* **80**, 171-183.

Burdige D. J. (2002) Sediment pore waters. In *Biogeochemistry of marine dissolved organic matter* (ed. D. Hansell and C. Carlson). Academic Press. pp. 611-663.

Burdige D. J. and Gardner K. G. (1998) Molecular weight distribution of dissolved organic carbon in marine sediment pore waters. *Marine Chemistry* **62**, 45-64.

Burdige D. J., Skoog A., and Gardner K. (2000) Dissolved and particulate carbohydrates in contrasting marine sediments. *Geochimica et Cosmochimica Acta* **64**, 1029-1041.

Canfield D. E., Thamdrup B., and Hansen J. W. (1993) The anaerobic degradation of organic matter in Danish coastal sediments: Iron reduction, manganese reduction, and sulfate reduction. *Geochimica et Cosmochimica Acta* **57**, 3867-3883.

Cowie G. L. and Hedges J. H. (1984) Carbohydrate sources in a coastal marine environment. *Geochimica et Cosmochimica Acta* **48**, 2075-2087.

Cragg B. A., Parkes R. J., Fry J. C., Weightman A. J., Rochelle P. A., and Maxwell J. R. (1996) Bacterial populations and processes in sediments containing gas hydrates (ODP Leg 146: Cascadia Margin). *Earth and Planetary Science Letters* **139**, 497-507.

Crill P. M. and Martens C. S. (1986) Methane production from bicarbonate and acetate in an anoxic marine sediment. *Geochimica et Cosmochimica Acta* **50**, 2089-2097.

Crozier T. E. and Yamamoto S. (1974) Solubility of hydrogen in water, seawater, and NaCl solutions. *Journal of Chemical and Engineering Data*. **19**, 242-244.

Dale A. W., Regnier P., and Van Cappellen P. (2006) Bioenergetic controls on anaerobic oxidation of methane (AOM) in coastal marine sediments: A theoretical analysis. *American Journal of Science* **306**, 246-294.

Davis J. A., Yabusaki S. B., Steefel C. I., Zachara J. M., Curtis G. P., Redden G. D., Criscenti L. J., and Honeyman B. D. (2004) Assessing conceptual models for subsurface reactive transport of inorganic contaminants. *Eos Transactions*. **44**, 449-453.

Duan Z., Moller N., Greenberg J., and Weare J. H. (1992) The prediction of methane solubility in natural waters to high ionic strength from 0 degrees to 250 degrees and from 0 to 1600 bar. *Geochimica et Cosmochimica Acta* **56**, 1451-1460.

Ferdelman T. G., Fossing H., Neumann K., and Schulz H. D. (1999) Sulfate reduction in surface sediments of the southeast Atlantic continental margin between 15o38'S and 27o57'S (Angola and Namibia). *Limnology and Oceanography* **44**, 650-661.

Fossing H., Ferdelman T. G., and Berg P. (2000) Sulfate reduction and methane oxidation in continental margin sediments influenced by irrigation (South-East Atlantic off Namibia). *Geochimica et Cosmochimica Acta* **64**, 897-910.

Froelich P. N., Klinkhammer G. P., Bender M. L., Luedtke N. A., Heath G. R., Cullen D., and Dauphin P. (1979) Early oxidation of organic matter in pelagic sediments of the eastern equatorial Atlantic: Suboxic diagenesis. *Geochimica et Cosmochimica Acta* **43**, 1075-1090.

Haese R. R., Meile C., Van Cappellen P., and De Lange G. J. (2003) Carbon geochemistry of cold seeps: Methane fluxes and transformation in sediments from Kazan mud volcano, eastern Mediterranean Sea. *Earth and Planetary Science Letters* **212**, 361-375.

Hallam S. J., Putnam N., Preston C. M., Detter J. C., Rokhsar D., Richardson P. M., and DeLong E. F. (2004) Reverse methanogenesis: Testing the hypothesis with environmental genomics. *Science* **305**, 1457-1462.

Hee C. A., Pease T. K., Alperin M. J., and Martens C. S. (2001) Dissolved organic carbon production and consumption in anoxic marine sediments: A pulsed-tracer experiment. *Limnology and Oceanography* **46**, 1908-1920.

Hoehler T. M. (2004) Biological energy requirements as quantitative boundary conditions for life

in the subsurface. *Geobiology* **2**, 205-215.

Hoehler T. M., Alperin M. J., Albert D. B., and Martens C. S. (2001) Apparent minimum free energy requirements for methanogenic archaea and sulfate-reducing bacteria in an anoxic marine sediment. *FEMS Microbiology Ecology* **38**, 33-41.

Hoehler T. M., Alperin M. J., Albert D. B., and Martens C. S. (1994) Field and laboratory studies of methane oxidation in an anoxic marine sediment - evidence for a methanogen-sulfate reducer consortium. *Global Biogeochemical Cycles* **8**, 451-463.

Hoehler T. M., Alperin M. J., Albert D. B., and Martens C. S. (1998) Thermodynamic control on hydrogen concentrations in anoxic sediments. *Geochimica et Cosmochimica Acta* **62**, 1745-1756.

Jakobsen R. and Postma D. (1999) Redox zoning, rates of sulfate reduction and interactions with Fe-reduction and methanogenesis in a shallow sandy aquifer, Rømø, Denmark. *Geochimica et Cosmochimica Acta* **63**, 137-151.

Jensen M. M., Holmer M., and Thamdrup B. (2005) Composition and diagenesis of neutral carbohydrates in sediments of the Baltic-North Sea transition. *Geochimica et Cosmochimica Acta* **69**, 4085-4099. 2005.

Jin Q. and Bethke C. M. (2002) Kinetics of electron transfer through the respiratory chain. *Biophysical Journal* **83**, 1797-1808.

Jin Q. and Bethke C. M. (2005) Predicting the rate of microbial respiration in geochemical environments. *Geochimica et Cosmochimica Acta* **69**, 1133-1143.

Jørgensen B. B., Weber A., and Zopfi J. (2001) Sulfate reduction and anaerobic methane oxidation in Black Sea sediments. *Deep-Sea Research I* **48**, 2097-2120.

Jourabchi P., Van Cappellen P., and Regnier P. (2005) Quantitative interpretation of pH distributions in aquatic sediments: A reaction-transport modelling approach. *American Journal of Science* **305**, 919-956. 2005.

Kallmeyer J., Ferdelman T.G., Weber A., Fossing H., Jørgensen B.B. (2004): A cold chromium distillation procedure for radiolabelled sulfide applied to sulfate reduction measurements. *Limnology & Oceanography: Methods* **2**, 171-180.

Komada T., Reimers C. E., Luther III G. W., and Burdige D. J. (2004) Factors affecting dissolved organic matter dynamics in mixed-redox to anoxic coastal sediments. *Geochimica et Cosmochimica Acta* **68**, 4099-4111.

Krüger M., Meyerdierks A., Glöckner F. O., Amann R., Widdel F., Kube M., Reinhardt R., Kahnt J., Böcher R., Thauer R. K., and Shima S. A. (2003) A conspicuous nickel protein in microbial mats that oxidize methane anaerobically. *Nature* **426**, 878-881.

Lovley D. R. and Goodwin, S. (1988) Hydrogen concentrations as an indicator of the predominant terminal electron-accepting reactions in aquatic sediments. *Geochimica et Cosmochimica Acta* **52**, 2993-3003.

Luff R. and Wallmann K. (2003) Fluid flow, methane fluxes, carbonate precipitation and biogeochemical turnover in gas hydrate-bearing sediments at Hydrate Ridge, Cascadia Margin: Numerical modelling and mass balances. *Geochimica et Cosmochimica Acta* **67**, 3403-3421.

Middelburg J. J. (1989) A simple rate model for organic matter decomposition in marine sediments. *Geochimica et Cosmochimica Acta* **53**, 1577-1581.

Mitterer R. M., Malone M. J., Goodfriend G. A., Swart P. K., Wortmann U. G., Logan G. A., Feary D. A., and Hine A. C. (2001) Co-Generation of hydrogen sulfide and methane in marine carbonate sediments. *Geophysical Research Letters* **28**, 3931-3934.

Orcutt B., Boetius A., Elvert M., Samarkin V., and Joye S. B. (2005) Molecular biogeochemistry of sulfate reduction, methanogenesis and the anaerobic oxidation of methane at Gulf of Mexico cold seeps. *Geochimica et Cosmochimica Acta* **69**, 4297-4281.

Oremland R. S. and Polcin S. (1982) Methanogenesis and sulfate reduction: Competitive and noncompetitive substrates in estuarine sediments. *Applied and Environmental Microbiology* **44**, 1270-1276.

Oude Elferink S. J. W. H., Visser A., Hulshoff Pol L. W., and Stams, A. J. M. (1994) Sulfate reduction in methanogenic bioreactors. *FEMS Microbiology Reviews* **15**, 119-136.

Regnier P., O'Kane J. P., Steefel C. I., and Vanderborght P. A. (2002) Modelling complex multi-component reactive-transport systems: Towards a simulation environment based on the

concept of a knowledge base. *Applied Mathematical Modelling* **26**: 913-927.

Rittmann B. E. and McCarty P. L. (2001) *Environmental Biotechnology: Principles and Applications.* McGraw-Hill Book Company, New York, 768 pp.

Schink B. (1997) Energetics of syntrophic cooperation in methanogenic degradation. *Microbiology and Molecular Biology Reviews* **61**, 262-280.

Schippers A., Neretin L. N., Kallmeyer J., Ferdelman T. G., Cragg B. A., Parkes R. J., and Jørgensen B. B. (2005) Prokaryotic cells of the deep sub-seafloor biosphere identified as living bacteria. *Nature* **433**, 861-864.

Schulz H. D. (2000) Quantification of early diagenesis: Dissolved constituents in marine pore water. In *Marine Geochemistry* (ed. H. Schulz, M. Zabel), Springer-Verlag, Berlin, pp 85-128.

Seifert R., Nauhaus K., Blumenberg M., Krüger M., and Michaelis W. (2006) Methane dynamics in a microbial community of the Black Sea traced by stable carbon isotopes in vitro. *Organic Geochemistry* **37**, 1411-1419.

Shima S. and Thauer R. K. (2005) Methyl-coenzyme M reductase and the anaerobic oxidation of methane in methanotrophic archaea. *Current Opinion in Microbiology* **8**, 643-648.

Steefel C. I., DePaolo D. J., and Lichtner P. C. (2005) Reactive transport modelling: An essential tool and a new research approach for the Earth sciences. *Earth and Planetary Science Letters* **240**, 539-558.

Steefel C. I. and Van Cappellen P. (1998) Reactive transport modelling of natural systems. *Journal of Hydrology* **209**, 1-7.

Staahl H., Tengberg A., Brunnegaard J., Bjørnbom E., Forbes T. L., Josefson A. B. , Kaberi H. G., Karle Hassellöv I. M., Olsgard F., Roos P., and Hall P. O. J. (2004) Factors influencing organic carbon recycling and burial in Skagerrak sediments. *Journal of Marine Research* **62**, 867-907.

Thauer R. K., Jungermann K., and Decker K. (1977) Energy conservation in chemotrophic anaerobic bacteria. *Bacteriological Reviews* **41**, 100-180.

Thullner M., Van Cappellen P., and Regnier P. (2005) Modelling the impact of microbial activity on redox dynamics in porous media. *Geochimica et Cosmochimica Acta* **69**, 5005-5019.

Treude T., Boetius A., Knittel K., Wallmann K., Jørgensen B.B. (2003) Anaerobic oxidation of methane above gas hydrates at Hydrate Ridge, NE Pacific Ocean. *Marine Ecology Progress Series* **264**, 1-14.

Treude T., Niggemann J., Kallmeyer J., Wintersteller P., Schubert C. J., Boetius A., and Jørgensen, B. B. (2005) Anaerobic oxidation of methane and sulfate reduction along the Chilean continental margin. *Geochimica et Cosmochimica Acta* **69**, 2767-2779.

Van Cappellen P. and Wang Y. (1996) Cycling of iron and manganese in surface sediments: a general theory for the coupled transport and reaction of carbon, oxygen, nitrogen, sulfur, iron, and manganese. *American Journal of Science* **296**, 197-243.

Wallmann K., Drews M., Aloisi G., and Bohrmann G. (2006) Methane discharge into the Black Sea and the global ocean via fluid flow through submarine mud volcanoes. *Earth and Planetary Science Letters* **248**, 544-559.

Westrich J. T. and Berner R. A. (1984) The role of sedimentary organic matter in bacterial sulfate reduction: The G-model tested. *Limnology and Oceanography* **29**: 236-249.

Yamamoto S., Alcauskas J. B., and Crozier T. E. (1976) Solubility of methane in distilled water and seawater. *Journal of Chemical and Engineering Data* **21**, 78-80.

Chapter 4

Thermodynamic and kinetic control of anaerobic oxidation of methane in marine sediments

Nina J. Knab[1], Andrew W. Dale[2], Karsten Lettmann[1], Henrik Fossing[3], Bo B. Jørgensen[1]

Manuscript in preparation

[1] Max Planck Institute for Marine Microbiology, Celsiusstr. 1, 28359 Bremen, Germany

[2] Utrecht University, Department of Earth Sciences, P.O. Box 80.021, 3508 TA Utrecht, The Netherlands

[3] National Environmental Research Institute, Department of Marine Ecology, Vejlsøvej 25, P.O. Box 314, DK 8600, Silkeborg, Denmark

ABSTRACT

The free energy yield of microbial respiration reactions in anaerobic marine sediments must be sufficient to be conserved as biologically usable energy in the form of ATP. Anaerobic oxidation of methane (AOM) coupled to sulfate reduction (SRR) has a very low standard free energy yield of $\Delta G° = -33$ kJ mol^{-1}, but the *in situ* energy yield strongly depends on the concentrations of substrates and products in the pore water of the sediment. In this work ΔG for the AOM-SRR process was calculated the from the pore water concentrations of methane, sulfate, sulfide, and dissolved inorganic carbon (DIC) in sediment cores from different sites of the European continental margin in order to determine the influence of thermodynamic regulation on the activity and distribution of microorganisms mediating AOM-SRR. In the zone of methane and sulfate coexistence, the methane-sulfate transition zone (SMTZ), the energy yield was rarely less than -20 kJ mol^{-1} and was mostly rather constant throughout this zone. The kinetic drive was highest at the lower part of the SMTZ, matching the occurrence of maximum AOM rates. The results show that the location of maximum AOM rates is determined by a combination of thermodynamic and kinetic drive, whereas the rate activity mainly depends on kinetic regulation.

INTRODUCTION

Microorganisms in marine sediments use the energy they gain from the breakdown of organic matter by fermentation and redox reactions. Depending on the electron accepting process the free energy gain decreases with sediment depth, the least favorable being methanogenesis (Schink, 1997). The minimum amount of energy that microorganisms can use is estimated to be around -20 kJ mol^{-1} in growing *E. coli* cultures, which is the energy required to shuffle one proton for ATP synthesis across the cell membrane (Schink, 1997). However, it was proposed that the minimum energy requirement could be even lower in cells adapted to energy limited environments and that microorganisms can still use energy from reactions closer to thermodynamic equilibrium (Hoehler, 2004; Hoehler et al., 1994; Jackson and McInerney, 2002; Scholten and Conrad, 2000). Under such conditions populations might not be actively growing but only sustain a maintenance metabolism (Hoehler et al., 2001). Yet, they must be able to obtain enough energy from the reactions they perform for ATP synthesis. The energy required for proton translocation constitutes a minimum energy quantum that may provide the ultimate thermodynamic constraint on bacterial metabolism (Hoehler, 2004; Hoehler et al., 1998).

An example of a process in marine sediments that operates close to the thermodynamic limit is the anaerobic oxidation of methane (AOM) coupled to sulfate reduction. AOM occurs in a distinct sediment horizon, the sulfate methane transition zone (SMTZ), where sulfate and methane are present concurrently. Evidence for the coupling of AOM and sulfate reduction is provided by methane and sulfate profiles in this zone, where sulfate is the main terminal electron acceptor used. The coupling has been confirmed by radiotracer determined rate measurements with concurrent peaks of both reactions in the environment (Iversen and Jørgensen, 1985), by laboratory enrichment experiments (Nauhaus et al., 2002), by stable isotope analyses of ^{13}C-depleted carbon in sulfate reducers (Orphan et al., 2001b), and by the discovery of consortia of sulfate reducing bacteria associated with methanotrophic archaea (Boetius et al., 2000). Weather both groups are always required to perform the reaction or if the methanotrophic archaea could also mediate the entire process alone is so far unknown.

The environmental and physiological controls on AOM rates and associated sulfate reduction rates (SRR) also remain poorly understood. Various intermediates have been proposed to link AOM and SRR (Nauhaus et al., 2002; Sørensen and Finster, 2001; Zehnder A. J. B. and Brock,

1979), but none of them has been confirmed so far. Modelling of potential intermediates, such as H_2, acetate, formate, or methanol, showed that only formate could potentially function as an intermediate for a consortium of attached cells (Sørensen and Finster, 2001), Yet, formate added as intermediate to enrichment cultures had no stimulating effect on SRR or AOM rates (Nauhaus et al., 2002). In this study, the thermodynamic regulation was therefore considered for the coupled reaction of both processes:

$$CH_4 + SO_4^{2-} \rightarrow HCO_3^- + HS^- + H_2O \quad (1)$$

The location of the SMTZ is determined by methane and sulfate fluxes (Borowski and Paull, 1996; Devol and Anderson, 1984; Hensen et al., 2003; Iversen and Jørgensen, 1985), and AOM rates strongly depend on substrate concentrations (Nauhaus et al., 2002) as well as on community size (Niemann et al., 2005). A simple thermodynamic-kinetic model (TKM) has been developed to describe the regulation of the metabolic rate, R_M, of a microbial population, B, by a kinetic driving force, F_K, and a thermodynamic driving force, F_T (Dale et al., 2006; Jin and Bethke, 2003; Jin and Bethke, 2005):

$$R_M = \mu_{max} \cdot B \cdot F_K \cdot F_T \quad (2)$$

F_K is based on the Michaelis-Menten-Model (MMM) and describes the kinetic regulation for the utilization of external substrates by microorganisms (Jin and Bethke, 2002; Van Cappellen et al., 2004). F_T represents a thermodynamic constrain on the rate and varies between 0-1 (Jin and Bethke, 2003):

$$F_T = 1 - e^{\left(\frac{\Delta G - m\Delta G_{ATP}}{R \cdot T \cdot \chi}\right)} \quad (3)$$

where ΔG is the free energy of the reaction, $m\Delta G_{ATP}$ is the smallest amount of energy that can be conserved for ATP formation, χ is the stoichiometry factor, and R and T are the gas constant and the absolute temperature, respectively.

It is unknown what role thermodynamic constraints on AOM play under *in situ* conditions and how the available energy influences the microbial communities.

Sediment cores from different environments were sampled at sites with shallow and deep SMTZs, to determine the energy availability and kinetic driving force with depth at different sites and to understand the control and limitation of thermodynamics on AOM and AOM related SRR, as well as the regulation of thermodynamic versus kinetic constraints.

MATERIAL & METHODS

Sediment was sampled by gravity corer (GC), multi corer (MUC) or push cores (PC) at different sites on the European continental margins (Table 1). Gravity cores were cut into 1 m-sections after retrieval on deck, capped, and stored upright at *in situ* temperature. Samples for methane and pore water were taken every 2-5 cm within the SMTZ. When MUCs and pushcore PCs were used, all concentrations and rate measurements were performed in the same core to avoid alignment problems.

Core ID	Site	Latitude	Longitude	Water depth [m]
131GC	Aarhus Bay	56°07,08'	10°20,81'	15
789GC	Skagerrak	58°03,25'	9°36,00'	391
816GC	Skagerrak	57°57,12'	9°42,43'	147
365MUC	Western Baltic	54°54,51'	13°36,78'	45
P806GC	Black Sea	44°46,83'	31°59,30'	205
P821PC	Black Sea	44°46,41'	31°58,20'	325

Table 1: Overview of sediment cores at different locations along the European continental margins.

Temperature for ΔG calculations was measured at the top of each 1 m section right after retrieval of the core on deck.

Methane concentrations were measured in 3 cm^3 sediment samples for GC and MUC and 1 cm^3 for PC that were sealed in glass vials with 6 ml NaOH (2.5 % w/v). The headspace was analyzed with a gas chromatograph (5890A, Hewlett Packard) containing a packed stainless steel Porapak-

Q column (6 ft., 0.125 in., 80/100 mesh, Agilent Technology) and a flame ionization detector. Helium with a flow rate of 30 ml min^{-1} was used as a carrier gas.

Sulfate concentrations were measured from samples retrieved by pore water squeezing under nitrogen pressure through cellulose acetate filters (0.45 µm) and fixed in 2 % (w/v) $ZnCl_2$. Analyses were performed by non-suppressed ion-chromatography (Waters 510 HPLC Pump; Waters IC-Pak 50 x 4.6 mm anion exchange column; Waters 430 Conductivity detector) using isophtalic acid buffer (1 mM, pH 4.6) in methanol (10 %) as eluant.

For **hydrogen sulfide** determination the ZnAc-fixed pore water samples were sonicated for 5 min and diluted 1:5 to 1:100. Sulfide concentrations were analyzed by the diamine complexation method described by Cline (1969). The sulfide concentration was measured by spectrophotometry at a wavelength of 670 nm.

Dissolved inorganic carbon (DIC) concentrations were measured immediately after the cruise by flow injection (Hall and Aller, 1992) on headspace-free and sealed pore water samples, stored at 7°C. The samples were injected into a continuous flow of HCl (30 mM) and the released CO_2 was transported over a Teflon membrane where it was again dissolved in a NaOH flow (10 mM) and measured by a conductivity detector (VWR scientific, model 1054).

Porosity was determined as the difference in weight of a defined volume of sediment before and after drying at 60°C.

Diffusive fluxes of methane and sulfate into the SMTZ were calculated from the concentration gradients and from the respective diffusion coefficients according to Fick´s first law of diffusion:

$$J = -\Phi \cdot D_s \cdot \frac{dC}{dz} \qquad (4)$$

where J is the diffusive flux [mmol m^{-2} d^{-1}], Φ is the porosity [ml cm^{-3}], D_s is the diffusion coefficient in the sediment [cm^2 d^{-1}], and dC/dz is the gradient of concentration [µmol cm^{-3}]. Diffusion coefficients according to *in situ* temperature were used from Schulz and Zabel (2000),

$D(CH_4) = 0.68 \cdot 10^{-5}$ cm^2 s^{-2} and $D(SO_4^{2-}) = 1.06 \cdot 10^{-5}$ cm^2 s^{-2}, and corrected for porosity of the sediment according to Iversen and Jørgensen (1993):

$$D_s = \frac{D}{1+3(1-\Phi)} \quad (5)$$

Curve fitting of the concentration profiles was performed for the thermodynamic calculations using the transport-reaction model of Berg (Berg et al., 1998) that is based on Fick´s law of diffusion.

For the calculation of energy yields the sulfate concentrations in the deeper part of the core below the detection limit of 0.2 mM, or at a constant background concentration were considered not to be available for AOM-related sulfate reduction and have therefore been subtracted.

H_2S curves were fitted through the higher concentration values, neglecting scattered low H_2S values that might be underestimated due to reoxidation to sulfate. Values below detection limit were set to the value of the detection limit (0.001 mM).

Gibbs free energy changes (ΔG):

ΔG° under standard conditions was calculated for the combined reaction of AOM and SRR (1) from the free energy of formation, $G_f(0)$, of the different reactants, whereby $G_f(0)$ of $CH_{4\ (aq)}$= -34.4 kJ mol^{-1} was used for methane, which leads to ΔG° = -33 kJ mol^{-1}. Accordingly, to calculate the energy yield of the reaction ΔG under *in situ* conditions, methane concentrations were used in mM rather than partial pressure, as were the concentrations of SO_4^{2-}, H_2S and DIC in the Gibbs-Helmholtz equation:

$$\Delta G = \Delta G° + R \cdot T \cdot ln \frac{\gamma[H_2S] \times \gamma[HCO_3^-]}{\gamma[CH_4] \times \gamma[SO_4^{2-}]} \quad (6)$$

where R is the gas constant (0.00831441 kJ mol^{-1} K^{-1}), T is the *in situ* temperature in the SMTZ of each core, and γ are the respective activity constants. All measured concentrations were used in mM. Activity coefficients were calculated with the IUPAC Aq-solution programme, which is based on the specific ion-interaction theory (SIT) model (Grenthe et al., 1997). The activity coefficients used are $\gamma(CH_4) = 1.248$; $\gamma(SO_4^{2-}) = 0.143$; $\gamma(HS^-) = 0.745$; $\gamma(HCO_3^-) = 0.652$.

For cores where methane outgassing occurred in the SMTZ, ΔG was calculated for the estimated *in situ* concentration, determined by extrapolation of the linear methane gradient until saturation. In cores where a background of sulfate was detected the background sulfate concentration was subtracted from the measured sulfate values for the calculation of ΔG, so that sulfate concentrations were assumed to be zero at depth.

The influence of different species concentration changes on Gibbs free energy was calculated by varying each of the concentrations over the range by which it varied in the SMTZ of core 131GC from Aarhus Bay. The other concentrations contributing to the reaction were kept constant at the level observed in the SMTZ at 200 cm in this core.

Kinetic drive for AOM

The depth-dependent kinetic drive is expressed as the dependency of the AOM rate on the concentrations of methane and sulfate. If the rate of AOM is expressed as R_{AOM}:

$$R_{AOM} = k \quad \frac{[CH_4]}{K_{CH4} + [CH_4]} \quad \frac{[SO_4^{2-}]}{K_{SO42-} + [SO_4^{2-}]} \tag{7}$$

where k (time^{-1}) is a zero-order rate constant. For $K_{CH4} >> [CH_4]$ K becomes first-order and the kinetic factor is then equal to:

$$F_K = K\ [CH_4] \frac{[SO_4^{2-}]}{K_{SO42-} + [SO_4^{2-}]} \tag{8}$$

where K_{SO4} is the Michaelis-Menten half-saturation constant for sulfate uptake, equal to 1×10^{-4} M (Dale et al., 2006). In equation (8), the sulfate concentrations of cores P806GC and P821PC were corrected for the background concentration at depth. Methane concentrations in the deeper part of the core were corrected for outgassing by linear extrapolation of the methane gradient, as described for ΔG calculations.

Rates of **anaerobic methane oxidation (AOM)** were measured in three parallel samples from 5 cm intervals, except for P821PC, where 3 parallel Plexiglas sub cores were sampled from the push core and cut into 1-cm intervals. The sediment was incubated with $^{14}C\text{-}CH_4$ (1.3 kBq per sample) at *in situ* temperature between 12 and 24 h, depending on the expected turnover rate. Incubations were stopped in NaOH (2.5 % w/v) and sealed gas tight. Analyses of AOM rates were done by successive measurements of the headspace methane pool with gas chromatography (see above). The $^{14}C\text{-}CH_4$ was determined by combustion of the headspace at 800°C and detection of the produced $^{14}C\text{-}CO_2$ was by acidification of the sediment (6 ml HCl 6M) and trapping of CO_2 in 4 ml Phenylethylamine, as described by Treude et al. (2003). Rates were calculated with the equation:

$$R_{AOM} = \frac{[CH_4] \times {}^{14}CO_2}{{}^{14}CH_4 \times v \times t} \quad (9)$$

where $[CH_4]$ is the methane pool of the headspace, ${}^{14}CO_2$ is the product of tracer turnover, ${}^{14}CH_4$ is the total tracer in the sample, v is the sediment volume of the sample, and t is the incubation time.

RESULTS

The calculation of the energy yield that microbes could obtain by mediating the AOM-SRR reaction is only possible in cores with a good coverage of data in the zone of lowest concentrations. At the depths of very low concentrations even small changes in concentration profiles can change the outcome significantly. The methane and sulfate profiles from station M1 in Aarhus Bay (Figure 1) display a gradual decline at low concentrations and form a typical methane-sulfate transition zone (SMTZ), where both reactants are present simultaneously. Maximal *in situ* methane concentrations at saturation would be 2.55 mM at this site but methane was lost by outgassing in the lower part of the core, which is reflected in the scattered profile below 230 cm. The calculated methane flux of 51 µmol m^{-2} d^{-1} that diffuses into the SMTZ was exceeded by the sulfate flux of 221 µmol m^{-2} d^{-1} from above, that only very gradually decreased

in the SMTZ. The concentration of H_2S increased steadily from the top of the core and reached a maximum of 0.17 mM in the SMTZ. Below the SMTZ H_2S concentrations declined again. DIC concentrations also increased with depth from the top of the core and reached a maximum of 20 mM at a depth of 220 cm. Throughout and below the SMTZ, DIC remained constant at this level.

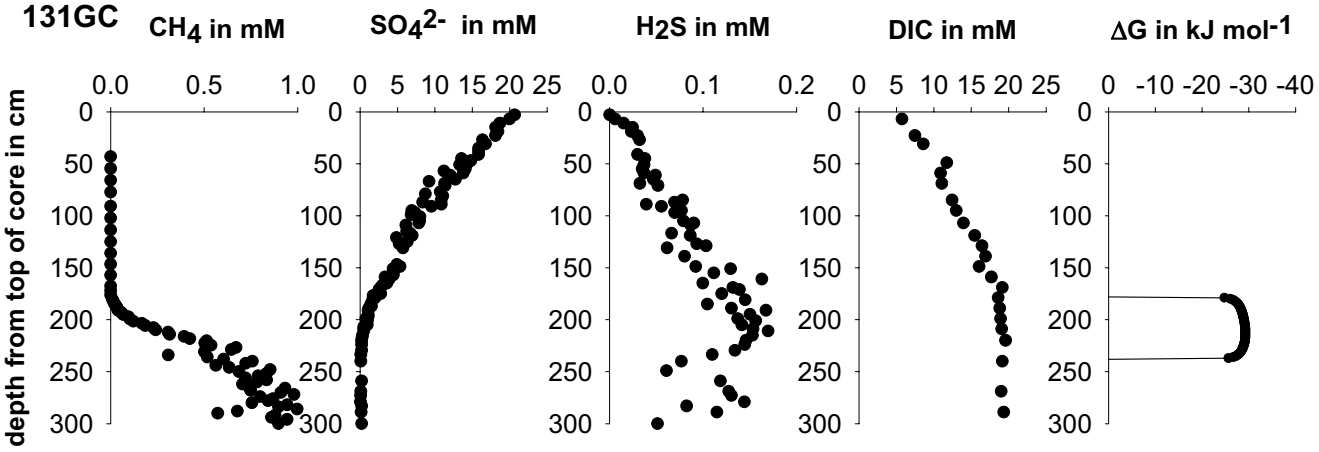

Figure 1: Pore water concentrations of core 131GC from Aarhus Bay and distribution of the energy yield for the AOM-SRR process, which show that ΔG values are almost constant throughout the SMTZ.

Using these chemical profiles to calculate ΔG of the AOM-SRR reaction shows that there was a maximum free energy yield of -29.3 kJ mol^{-1} in the SMTZ, which would be favorable to perform the reaction. The energy yield is fairly constant over the entire SMTZ, and the width of this thermodynamically favorable zone is restricted by either total sulfate below or methane depletion above ($SO_4^{2-} \approx 0$ below 230 cm, $CH_4 = 0$ above 175 cm), in which case ΔG is no longer defined any more. In the case of core 131GC, AOM rates would therefore be confined by thermodynamics to a ~ 55 cm broad sediment layer.

This favorable energy yield for AOM-SRR in the SMTZ was calculated for several sites in different continental shelf areas. The concentration profiles, AOM rates, and calculated ΔG values of the cores from the area of the North- and Baltic Sea are presented in Figure 2. Compared to the core from Aarhus Bay, methane in core 789GC from the Skagerrak (Figure 2a) was less efficiently oxidized at the methane-sulfate interface at ~ 100 cm depth. A low remaining

concentration of methane reached upwards, and was only completely depleted near the sediment surface. Because of the presence of methane in the upper 100 cm of the core

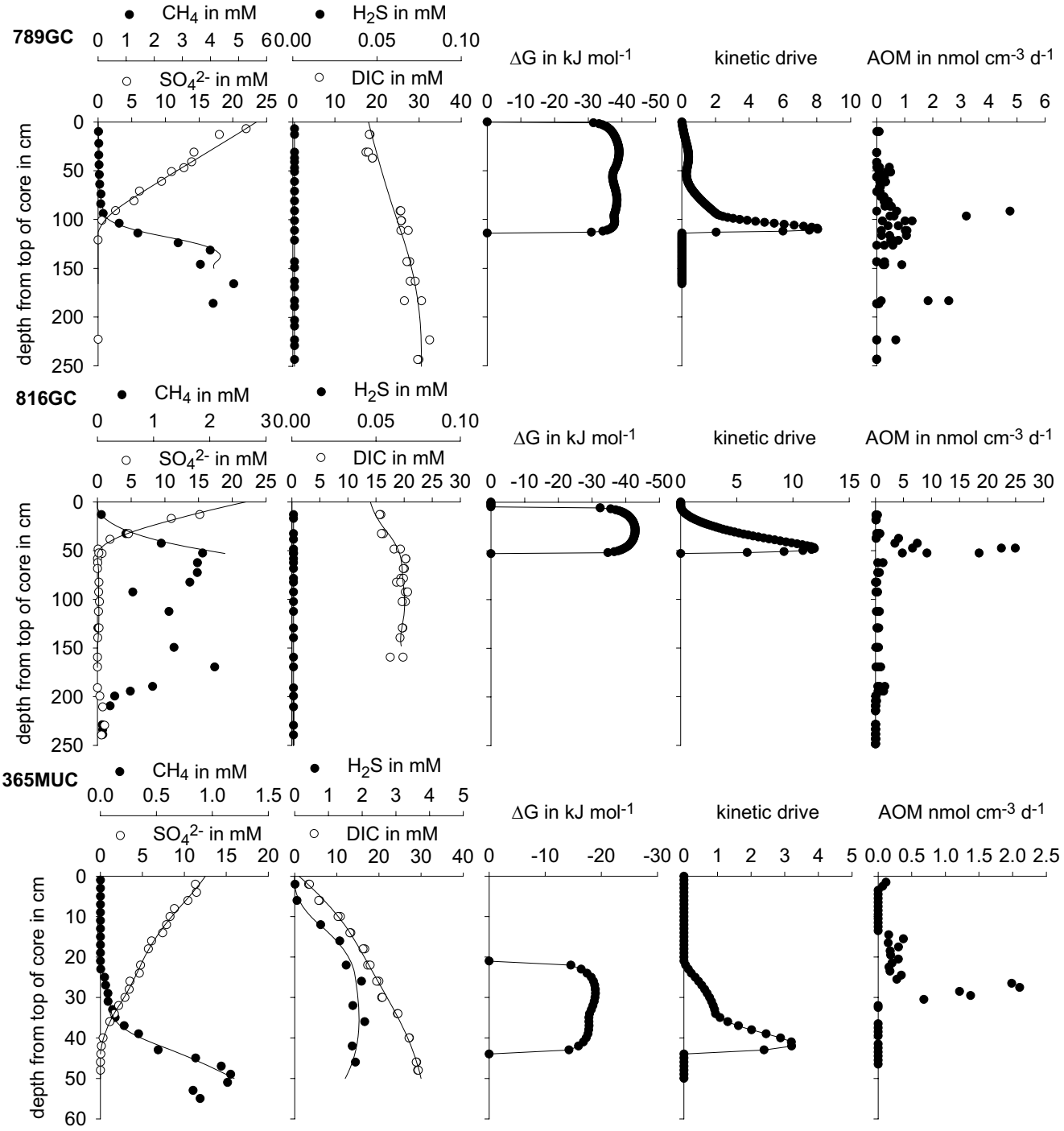

Figure 2: Depth profiles of pore water concentrations, kinetic drive, energy yield and AOM rates in sediment cores from the Skagerrak (a) and (b), and the western Baltic Sea (c).

and of high sulfate concentrations near the surface compensating for the low methane concentrations, the energy yield remained favorable and was fairly constant throughout the entire SMTZ and only decreased where sulfate disappeared below 120 cm. The maximum energy yield of -38 kJ mol^{-1} is much higher than that available in Aarhus Bay sediment.

The kinetic drive calculated from the pore water profiles of methane and sulfate increased gradually below 50 cm and reached a maximum at 110 cm, at the lower end of the thermodynamically favorable zone. The maximum rates of AOM were found at a depth of ~ 100 cm, also at the bottom of the thermodynamically favorable zone, where both the kinetic drive and the energy yield were high, though lower rates were also detected to occur between 50 cm and 130 cm depth.

A similar pattern was found also in another Skagerrak core 816GC in which the SMTZ was located much closer to the sediment surface (Figure 2b). Sulfate and methane profiles overlapped at higher concentrations in this core which, with similar concentrations of H_2S and DIC as in 789GC, lead to an even larger ΔG of -42 kJ mol^{-1}. Sulfide concentrations in both cores were below detection limit, and therefore enabled this relatively high energetic yield. The kinetic drive was again highest at the lower boundary of the thermodynamic favorable zone. As in 789GC, the tracer determined AOM rates occurred at this depth of maximum kinetic drive, but rates were five times higher in 816GC than in 789GC.

In the brackish western Baltic Sea where bottom water sulfate concentrations were only 12 mM, the shallow SMTZ from multicore 365MUC (Figure 2c) resembled the situation of the Skagerrak and Aarhus Bay in so far that the concentration clearly defined a SMTZ, where AOM coupled to SRR was thermodynamically possible. The maximum ΔG of -18 kJ mol^{-1} was much lower in 365MUC than in the Skagerrak cores, probably because of the presence of H_2S. If H_2S values of 2.0 mM were applied for the ΔG calculations at 789GC or 816GC, the energy yield would also be between -20 and -25 kJ mol^{-1}. The kinetic drive was again highest at the very bottom of the zone of favorable energy yield. Despite the lower energy yield, the AOM rates were in the same range as in core 789GC, although much lower than in 816GC, but it is not clear why AOM apparently occurred at shallower depth than the highest kinetic drive.

Pore water profiles in the Black Sea (Figure 3) differ from the Skagerrak and Baltic Sea in that the methane oxidation is less efficient, and methane and sulfate profiles exhibit an extended SMTZ over more than 250 cm in P806GC (Figure 3a).

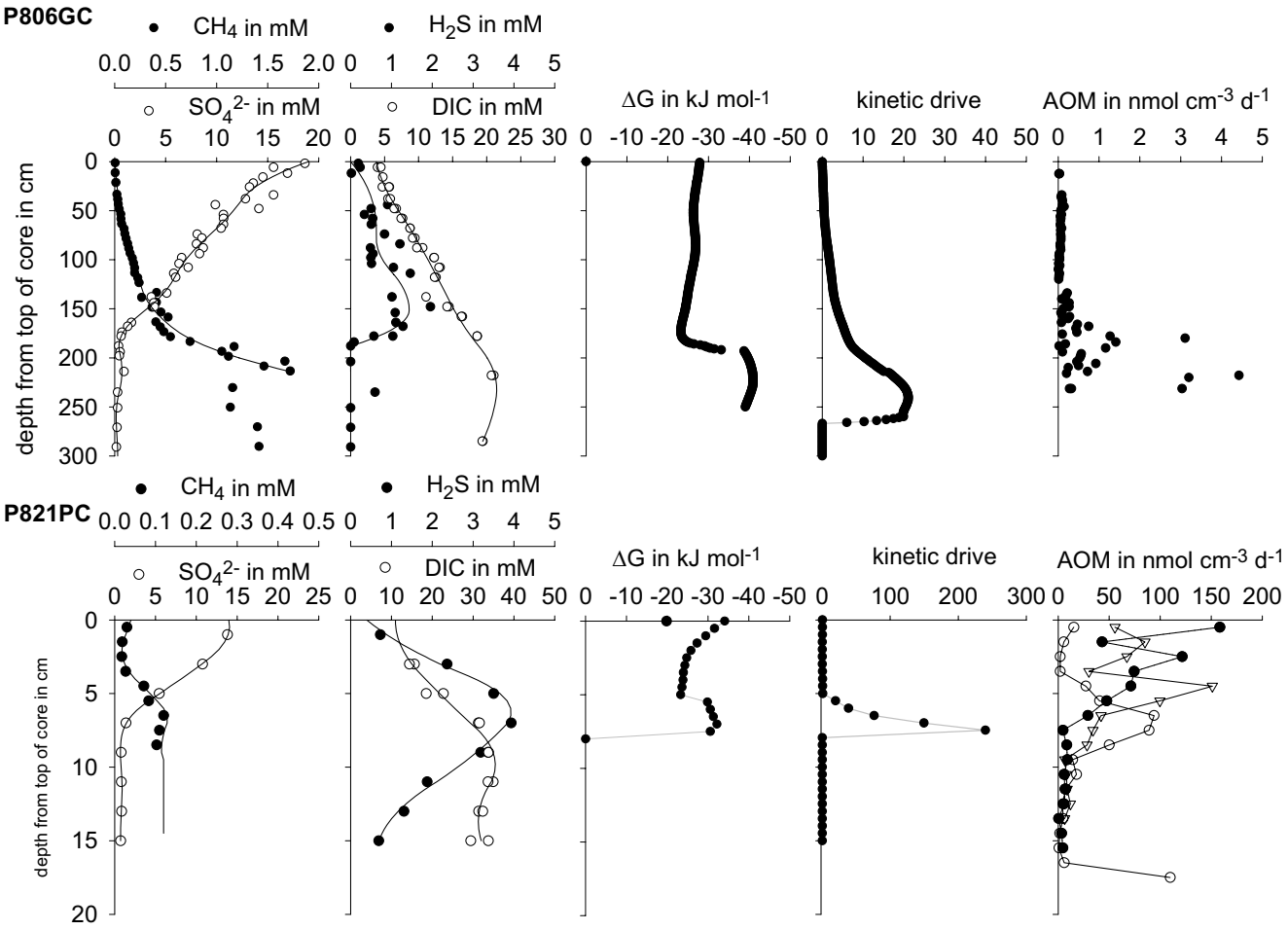

Figure 3: Depth profiles of pore water concentrations, kinetic drive, energy yield and AOM rates in a gravity core (a) and a push core (b) from the Black Sea.

This pattern, together with a steady increase in DIC and H_2S at depth leads to a very constant energy yield of ~ -28 kJ mol^{-1}, with slightly less negative values at the depth of H_2S maximum at 160 cm. At 180 cm, where methane and sulfate profiles change steeply and H_2S diminishes, the energy yield became even more favorable, with ΔG values larger than -40 kJ mol^{-1}. Like in the Skagerrak and Baltic Sea the kinetic drive had a maximum at the bottom of the SMTZ, and tailed off in the upper 200 cm of the core, despite the presence of methane and high sulfate concentrations. At ca. 200 cm depth, where thermodynamics became more favorable and the kinetic drive increased steeply, the main peak of AOM rates occurred. It was again located at the

bottom of the SMTZ, but not at the lower end of the thermodynamically favorable zone. Despite the very favorable energy yield, however, rates were not exceeding 5 nmol cm^{-3} d^{-1}. Even though a ΔG of -28 kJ mol^{-1} in the upper part of the core was more than that available in the Western Baltic, only very low AOM rates were found at 150 cm, and no activity was detected in the upper 150 cm.

The data from push core P821PC sampled in an area of methane seeps in the Black Sea is presented in Figure 3b. The SMTZ was very close to the sediment surface and both methane and sulfate were present throughout the core. Because methane gas bubbles were observed at 5 cm depth, the concentration measurements below this depth were not reliable due to outgassing and values from extrapolation of the linear methane gradient below 3.5 cm were used for the ΔG calculation. Due to the anoxic bottom water in the Black Sea, methane was not oxidized aerobically at the sediment surface. Therefore, the thermodynamically favorable zone for AOM-SRR did not have an upper limit, and the increasing methane concentrations at the top generated the highest energy yield in this core (-33.5 kJ mol^{-1}) at the surface. Also the sulfate concentration at the bottom of the SMTZ did not disappear entirely, but remained at values of ~ 0.8 mM. If these values are used for the calculation of the energy yield, ΔG would be favorable for AOM-SRR throughout the core, even getting more negative at the bottom with decreasing H_2S and increasing methane concentrations, until the depth where either H_2S or sulfate disappeared altogether, and ΔG is not defined be any more. In Figure 3b the sulfate concentration below 8 cm was considered an artifact and subtracted from the profile, in which case AOM would only be favorable down to a depth of ~ 8 cm, with a zone of most favorable energy yield between 5-8 cm. Considering the high availability and flux of methane at this site (218 μmol m^{-2} d^{-1}), with saturation so shallow underneath the surface, ΔG values are only moderate, and not higher than at some of the purely diffusive sites like 789GC. The kinetic drive also peaks in 7.5 cm when sulfate concentrations below 8 cm are considered zero and methane increasing continuously with depth, which would again match the pattern of the Skagerrak, with the highest kinetic drive at the bottom of the zone of favorable energy yield. Compared to those sites, however, the value of the kinetic drive is much higher in core P821PC. AOM rates of three parallel subcores in P821PC showed that the activity took place in the top 10 cm of the sediment, with rates up to ~ 150 nmol cm^{-3} d^{-1}, much higher than at the sites described above. But only the rates in one of the parallel

subcores matched the thermodynamic and kinetic profiles reasonably, probably due to lateral heterogeneity in the seep area.

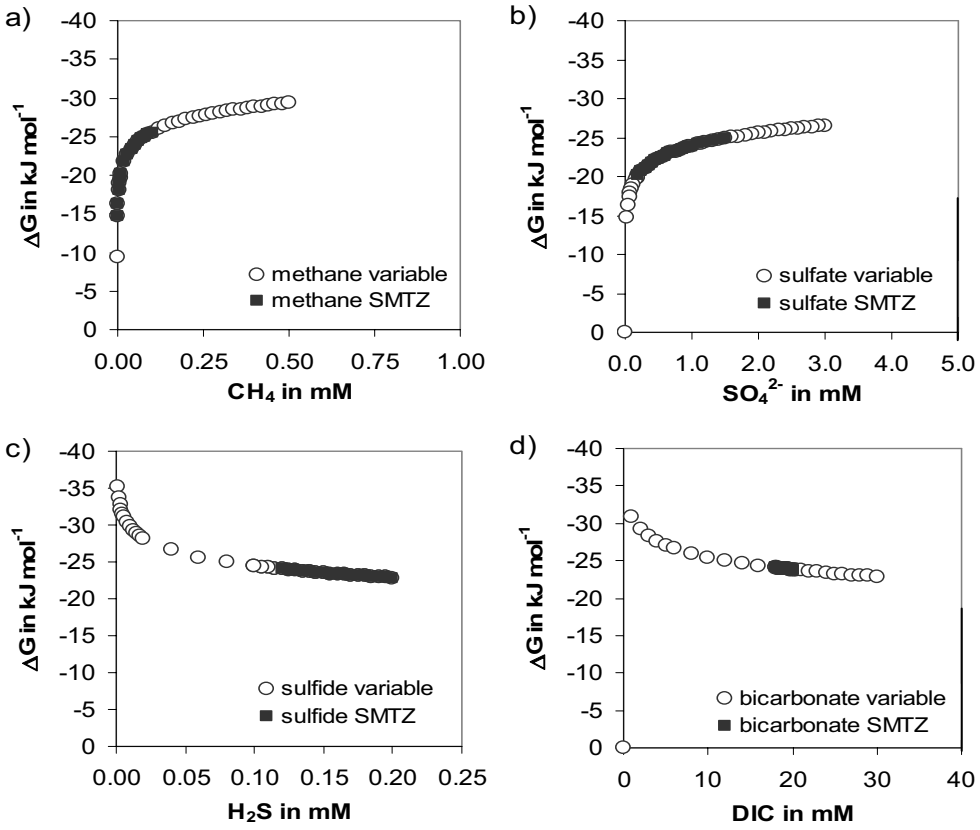

Figure 4: Influence of substrate and product concentrations on ΔG of the AOM-SRR process. The graphs reflect the change of ΔG relative to concentration changes of one of the four reactants respectively (○), under the concentration conditions in the SMTZ of 131GC. The actual range of the variable concentration in the SMTZ is marked (●).

In the Gibbs-Helmholtz equation (4), the four pore water constituents of the reaction are equally contributing to the calculated ΔG, but since the substrates and products occur in different concentrations in the SMTZ their influence in determining the energy yield of AOM-SRR differs. As an example, the consequences of concentration changes on ΔG under the measured conditions prevailing in the SMTZ of core 131GC from Aarhus Bay were calculated (Figure 4). Because low concentrations have the highest relative variation und thus influence on the energy yield, and concentrations of methane (Figure 4a) as well as sulfate (Figure 4b) approached zero

in the SMTZ, concentration changes of these substrates have a much greater influence on the ΔG values than changes of the product concentrations. The variability of methane covered the range from the detection limit (< 1 μM) to 0.1 mM and had the largest influence on the ΔG values under the concentration conditions of the SMTZ in core 131GC. Sulfate concentrations varied over a range from 0.2 mM (detection limit) up to 1.5 mM, but the relative changes of the CH_4 x SO_4^{2-} -product are smaller than these caused by methane. H_2S concentrations were also low, but the changes of H_2S (Figure 4c) were not as pronounced as with methane and sulfate and, therefore, the variation in ΔG was small. Because H_2S is multiplied with high DIC values, concentrations would need to drop below 0.02 mM in this core in order to change ΔG significantly. DIC showed very little variability (Figure 4d) and did therefore also not change the ΔG throughout the SMTZ.

The ΔG profile, thus, is mostly determined by the concentrations of methane and sulfate and a rough estimate of the thermodynamically favorable zone can in most cases be made by calculating the product of CH_4 and SO_4^{2-} concentrations, if H_2S and DIC data are not available. This does, however, not allow an estimate of the energy gain, which can be significantly altered by the abundances of the products, H_2S and DIC.

DISCUSSION

Our rate measurements show that - even though the AOM-SRR reaction is thermodynamically favorable in the entire SMTZ - the process is not distributed over this entire zone but focused towards a narrower horizon, mostly at the bottom of the thermodynamically favorable zone. The free energy of the combined reaction available for the organisms was between -20 and -40 kJ mol^{-1} at the sites investigated. This is consistent with the observations of Hoehler et al. (2001) in Cape Lookout Bight, who calculated ~ -10 kJ mol^{-1} for methanogenesis and -10 to -20 kJ mol^{-1} for SRR. These values are close to the minimum energy requirement of cells (Hoehler, 2004; Schink and Stams, 2002), but apparently are sufficient to support at least the maintenance of the microbial community mediating the process.

In contrast to the broad zone with an almost constant level of favorable energy yield, the kinetic drive, which is only determined by the substrates, methane and sulfate, showed low values throughout most of the SMTZ, and a distinct peak at the bottom of this zone. The depth where this maximum of kinetic drive occurs, together with a favorable energy yield seems to determine the location of the major AOM activity. Because this mostly occurs at the bottom of the SMTZ, Low AOM rates might occur higher up in the core, but the major AOM peak is confined by the combined drive of thermodynamics and kinetics. As an example, in P806GC from the Black Sea, AOM took place at ~ 200 cm even though methane and sulfate were concurrently available also at much shallower depths.

The importance of thermodynamic versus kinetic regulation of a process depends strongly on the $\Delta G°$ of the reaction. Processes that have energy yields with a very negative $\Delta G°$ are less influenced by the concentrations of substrates and products than reactions with a $\Delta G°$ close to equilibrium. In the case of AOM, with a $\Delta G°$ of only -33 kJ mol^{-1} the *in situ* concentrations change the energy yield significantly, and determine if the reaction is possible at all.

Influence of pore water concentrations on thermodynamics

The differences in calculated energy yield at the various sites show that the thermodynamic yield not so much depended on the individual pore water concentrations of substrates and products *in situ*, but rather on the ratio of these concentrations, and their relative changes in the SMTZ (Figure 5). The normal range of temperature changes in the SMTZ of ocean margin sediments does not seem to have a significant influence on the ΔG. When the product of methane and sulfate concentrations is higher than that of sulfide and DIC, i.e. substrates exceed the products, the ratio $x < 1$ and then ΔG is more favorable than -33 kJ mol^{-1}. In the range in which the concentrations of methane, sulfate, DIC and H_2S occur in the SMTZ, the ΔG values for the ratio of reaction products versus substrates $x > 50$ becomes less sensitive to concentration changes because of the logarithmic nature of the curve, and hardly get significantly below -20 kJ mol^{-1}. This indicates that even though the process is mostly occurring close to minimum energy requirements, it mostly does provide > 20 kJ mol^{-1} for the organisms as long as methane and sulfate are present. The energy yield seems to be not necessarily restricted by low methane or sulfate concentrations, because methane values are high in the zone of sulfate depletion and vice versa, thus compensating the low values of the other substrate. Only when one of the substrates

is not longer available the calculation of ΔG is not defined. This is problematic, however, because the concentrations might not be zero, but are eventually just too low to be detected, and therefore ΔG might still be very favorable in a much larger zone, especially below the SMTZ, where H_2S is decreasing. The effect of ΔG values only decreasing gradually with increasing x and not being defined at CH_4 or SO_4^{2-} depletion determines the shape of the ΔG profiles throughout the gravity cores lower than -25 kJ mol^{-1} (e.g. 131GC and 365MUC): a steadiness of ΔG values in the entire SMTZ with a sudden drop at the depths defined as methane or sulfate depletion.

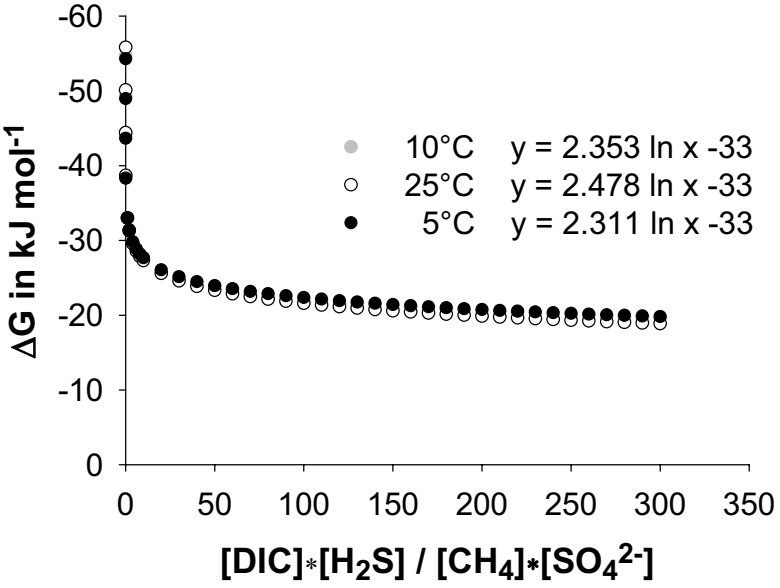

Figure 5: Dependence of ΔG on the fraction x of products and substrate concentrations in the Gibbs-Helmholtz equation for different temperatures. Even under severe substrate limitation or product accumulation ΔG does not get much lower than –20 kJ mol^{-1}. On the contrary, a surplus of substrates leads to a steep increase of ΔG.

DIC concentrations in the sediments are usually much higher than these of H_2S, CH_4 and SO_4^{2-}, yet they do not have much influence on the location of the thermodynamic peak but rather influence the absolute value of the ΔG. Because in the SMTZ the DIC concentration is not only the most constant but also highest of the four reactants, this should enhance the influence of H_2S on ΔG values (4). Similar to the ΔG calculations for the Skagerrak (789GC and 816GC) a very favorable ΔG would be expected in environments where sulfide is very low. Reactive iron that acts as a sink for H_2S can therefore become important in increasing the energy yield of AOM-SRR. On the contrary, at sites with higher amounts of AOM substrates in the SMTZ the energy yield can remain moderate because of high H_2S concentrations. In methane seep systems with high sulfate reduction rates H_2S concentrations can get very high (up to 10 mM; (Joye et al.,

2004) and the energy yield only remains at a level that can be achieved at much lower methane concentrations in less sulfidic environments.

The sensitivity analysis of the four concentrations (Figure 3) does not seem to show a strong influence of H_2S on the ΔG values, even though concentrations change over a relatively large range. But the concentration range in which H_2S influences thermodynamics varies in each core according to the concentrations of CH_4, SO_4^{2-} and DIC. In core 131GC, with $x > 38$, a rather constant ΔG is reached with H_2S concentrations as low as 0.1 mM and only lower H_2S concentrations would affect the ΔG values in this core.

Sulfate background

A problem in calculating the thermodynamic yield for the AOM-SRR reaction is to accurately determine substrate concentrations that are approaching very low values in the SMTZ and are finally lower than the detection limit. This is especially obvious at the lower boundary of the SMTZ, where sulfate concentrations diminish. It has been proposed, and also observed for Black Sea sediments that sulfate is not completely depleted to zero (Neretin et al., 2004), but apparently remains at a low level in the methanogenic zone. The sulfate profile of core 131GC from Aarhus Bay as well as 365MUC and P821PC shows that such a background sulfate concentration can also be observed at other sites, and that the amount of remaining SO_4^{2-} differs in different environments. If these low sulfate concentrations were an artifact of sulfate measurements, it would be expected that a similar background is measured at all sites, which is not the case. It is also unlikely that the deep sulfate occurrence is a remainder of diffusive sulfate from the sediment surface, because SRR in these sediments leads to an efficient sulfate turnover over a long time scale under steady state conditions. If the presence of sulfate is real and constitutes an existing sulfate pool available for SRR, it could be present as the result of a deep sulfur cycle below the SMTZ, with a steady-state between sulfate production from sulfide reoxidation and sulfate consumption by SRR. This would also explain the presence of sulfate reducing bacteria that are found below the SMTZ, e.g. in cores from the Black Sea (Leloup et al., 2006). The possibility of a deep sulfur cycle might especially apply to formerly limnic sediments like those in the Black Sea that contain a large excess of reactive iron (Neretin et al., 2004), and this might be the reason why the only cores, where a background of sulfate concentrations was detected in our study also came from the Black Sea.

The role of thermodynamic control: Threshold or direct inhibition?

The role of thermodynamic limitations on microbial rates is supposed to be particularly important in geomicrobial systems operating close to their thermodynamic limit (Jin and Bethke, 2002; Van Cappellen et al., 2004). But in which way this limitation impacts the activity of microbial rates is not known so far. In the case of AOM coupled to sulfate reduction ΔG values varied significantly between the cores, and the energy yield did not seem to be correlated to AOM rates or methane and sulfate fluxes. The energy yield of cores P806GC, 816GC and P821PC were very similar but AOM rates were as different as ~ 4 nmol cm^{-3} d^{-1} in P806GC to ~ 150 nmol cm^{-3} d^{-1} in P821PC. Therefore, the thermodynamic constraints are not supposed to directly regulate AOM rates but only limit the feasibility of the AOM-SRR process through a thermodynamic threshold. It would be conceivable that this threshold represents the amount of minimum energy, that can be biologically exploited, and rates only occur if the free energy provided by the reaction exceeds this value. Such a threshold would then be described by the minimum energy quantum as described by Hoehler (2004) and Schink and Stams, (2002).

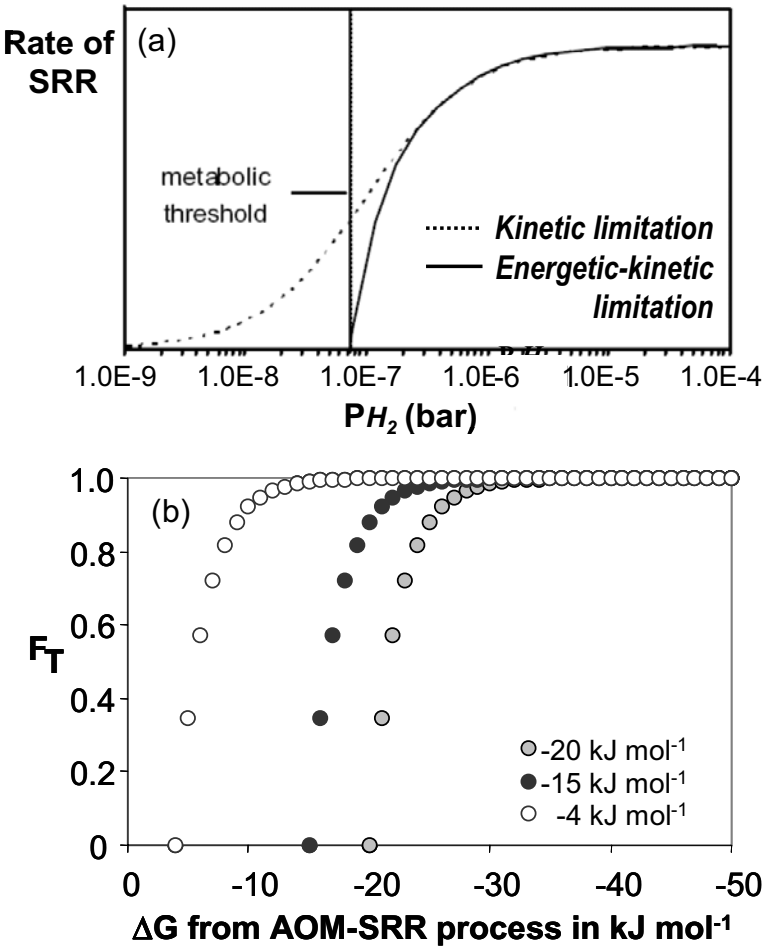

Figure 6:
(a) Regulation of microbial rates depending on substrate concentrations for the example of SRR and [H_2] (from Van Cappellen et al., 2004). The metabolic threshold marks the minimum amount of energy that can be conserved for ATP formation. Including energetic limitation in the rate model would lead to an inhibition of rates at substrate concentrations close to the threshold in addition to kinetic limitation.

(b) F_T calculated for different energy yields of the AOM-SRR process assuming a minimum energy quantum (m ΔG_{ATP}) of 4, 15, or 20 kJ mol^{-1}. If ΔG of the process is more than -20 kJ mol^{-1} F_T would already be almost 1 for m ΔG_{ATP} of -15 kJ mol^{-1}.

Alternatively, it was proposed from a mathematical model, which was developed by Jin and Bethke (2003) to describe the influence of kinetics and thermodynamics on microbial rates in geochemical environments like the AOM-SRR system (1) that low energy yields could also limit microbial respiration directly (Jin and Bethke, 2005; Van Cappellen et al., 2004) (Figure 6a). This influence is expressed by the thermodynamic factor F_T (3) included in the TKM (2). For rates that are not energetically limited F_T is 1, and such rates are only regulated by kinetics. But the rates of processes with a low energy yield would be inhibited by F_T, in addition to kinetic inhibition. The influence of this thermodynamic limitation on AOM-SRR was determined by calculation of F_T from the *in situ* pore water concentrations determined for the process, which revealed that the initial increase of F_T was very steep, so that it ultimately acts as a threshold (Figure 6b). Since the process was found to yield more than –20 kJ mol^{-1}, F_T only has an inhibiting effect on AOM-SRR rates if the minimum amount of energy that can be conserved for energy conservation by the involved organism ($m\Delta G_{ATP}$) is more than 15 kJ mol^{-1}, and this value is even higher, the more energy the process yields. The actual minimum energy requirement is not known, but literature values range from –4 kJ mol^{-1} to –20 kJ mol^{-1} (Hoehler, 2004 and references therein) and methanotrophic archaea are most likely at the lower end of this range. We therefore conclude that in practice there seems to be little difference between a thermodynamical threshold value and the TKM and AOM-SRR rates are mainly regulated kinetically, once the energy yield exceeds the thermodynamic threshold.

The kinetic drive, however, should have a more direct influence on microbial rates, increasing the microbial activity by a higher kinetic drive of the substrate concentrations. This is confirmed by the AOM measurements where, except in core P806GC, AOM rates were always higher the higher the kinetic drive was.

High turnover rates can be responsible for maintaining substrate concentrations at a low level, which also leads to a lower energy yield of the turnover, but the question is, if organisms performing high turnover rates can live on such a low energy level. This is also depending on the size of the microbial population. Variation of turnover rates can be either achieved on the cellular level, when microorganisms increase or decrease their cellular activity, or it can be altered on the population level, by increasing or decreasing the cell numbers performing the reaction. When

fluxes of substrates increase in marine sediments the first reaction would probably be a change in turnover activity per cell, and this would finally lead to higher population density, with rates per cell decreasing again to previous levels as the ratio of substrates per cell levels out.

Implications for the mechanism of AOM

It would be interesting to understand what implication the thermodynamic and kinetic control as discussed above has for the mechanism of the AOM-SRR reaction. All the presented considerations only apply to the coupled reaction of anaerobic methane oxidation and sulfate reduction. But the overall equation is only a combination of processes that either take place in two separate cells (Boetius et al., 2000; Orphan et al., 2001b) or in the same cell that can mediate both reactions. The observation that AOM rates seem to be so tightly regulated by kinetic and thermodynamic considerations of the overall AOM-SRR process might be an indication, that it is only one organism performing both reactions. If this is the case, in a zone of constant energy yield like demonstrated for the SMTZ, the process would be likely to occur in the depth with the highest kinetic drive, which is consistent with the AOM rates observed in our cores. It is not known, however, if two organisms that each mediate one of the reactions would also be as tightly controlled by the thermodynamic and kinetic constraints of the combined process as it was demonstrated. It is more likely that the rates would be more constrained by energetic limitations of the separate reactions, as was also suggested by the modelling results of AOM acting with H_2 as intermediate (Dale at al., Chapter 2).

REFERENCES

Berg P., Rysgaard-Petersen N., and Rysgaard S. (1998) Interpretation of measured pore water concentration profiles in sediment pore water. *Limnology & Oceanography* **43**(7), 1500-1510.

Boetius A., Ravenschlag K., Schubert C. J., Rickert D., Widdel F., Gieseke A., Amann R., Jørgensen B. B., Witte U., and Pfannkuche O. (2000) A marine microbial consortium apparently mediating anaerobic oxidation of methane. *Nature* **407**(6804), 623-626.

Borowski W. S. and Paull C. K. (1996) Marine pore-water sulfate profiles indicate *in situ* methane flux from underlying gas hydrates. *Geology* **24**(7), 655-658.

Cline J. D. (1969) Spectrophotometric determination of hydrogen sulfide in natural waters. *Limnology & Oceanography* **14**(3), 454-458.

Dale A. W., Regnier P., and van Cappellen P. (2006) Bioenergetic controls on anaerobic oxidation of methane (AOM) in coastal marine sediments: A theoretical analysis. *American Journal of Science* **306**(4), 246-294.

Devol A. H. and Anderson J. J. (1984) A model for coupled sulfate reduction and methane oxidation in the sediments of Saanich Inlet. *Geochimica Et Cosmochimica Acta* **48**, 993-1004.

Grenthe I., Plyasunov A. (1997) On the use of semiempirical electrolyte theories for the modelling of solution chemical data. *Pure and Applied Chemistry* **69**(5), 951-958.

Hall P. O. J. and Aller R. C. (1992) Rapid, small-volume flow-injection analysis for ΣCO_2 and NH_4^+ in marine and freshwaters. *Limnology & Oceanography* **37**, 1113-1118.

Hensen C., Zabel M., Pfeiffer K., Schwenk T., Kasten S., Riedinger N., Schulz H., and Boetius A. (2003) Control of sulfate pore-water profiles by sedimentary events and the significance of anaerobic oxidation of methane for the burial of sulfur in marine sediments. *Geochimica Et Cosmochimica Acta* **64**(14), 2631-2647.

Hoehler T. M. (2004) Biological energy requirements as quantitative boundary conditions for life in the subsurface. *Geobiology* **2**, 205-215.

Hoehler T. M., Alperin M. J., Albert D. B., and Martens C. S. (1994) Field and laboratory studies of methane oxidation in an anoxic marine sediment - evidence for a methanogen-sulfate reducer consortium. *Global Biogeochemical Cycles* **8**(4), 451-463.

Hoehler T. M., Alperin M. J., Albert D. B., and Martens C. S. (1998) Thermodynamic control on hydrogen concentrations in anoxic sediments. *Geochimica Et Cosmochimica Acta* **62**(10), 1745-1756.

Hoehler T. M., Alperin M. J., Albert D. B., and Martens C. S. (2001) Apparent minimum free energy requirements for methanogenic archaea and sulfate-reducing bacteria in an anoxic marine sediment. *Fems Microbiology Ecology* **38**(1), 33-41.

Iversen N. and Jørgensen B. B. (1985) Anaerobic methane oxidation rates at the sulfate methane transition in marine sediments from Kattegat and Skagerrak (Denmark). *Limnology and Oceanography* **30**(5), 944-955.

Iversen N. and Jørgensen B. B. (1993) Diffusion coefficients of sulfate and methane in marine sediments - influence of porosity. *Geochimica Et Cosmochimica Acta* **57**(3), 571-578.

Jackson B. E. and McInerney M. J. (2002) Anaerobic microbial metabolism can proceed close to thermodynamic limits. *Nature* **415**, 454-456.

Jin Q. and Bethke C. M. (2002) Kinetics of electron transfer through the respiratory chain. *Biophysical Journal* **83**, 1797-1808.

Jin Q. and Bethke C. M. (2003) A new rate law describing microbial respiration. *Applied and Environmental Microbiology* **69**(4), 2340-2348.

Jin Q. and Bethke C. M. (2005) Predicting the rate of microbial respiration in geochemical environments. *Geochimica Et Cosmochimica Acta* **69**(5), 1133-1143.

Joye S. B., Boetius A., Orcutt B. N., Montoya J. P., Schulz H. N., Erickson M. J., and Lugo S. K. (2004) The anaerobic oxidation of methane and sulfate reduction in sediments from Gulf of Mexico cold seeps. *Chemical Geology* **205**(3-4), 219-238.

Leloup J., Loy A., Knab N. J., Borowski C., Wagner M., and Jørgensen B. B. (2006) Diversity and abundance of sulfate-reducing microorganisms in the sulfate and methane zones of a marine sediment, Black Sea. *Environmental Microbiology* doi:10.1111/j.1462-2920.2006.01122.x.

Nauhaus K., Boetius A., Krüger M., and Widdel F. (2002) *In vitro* demonstration of anaerobic oxidation of methane coupled to sulphate reduction in sediment from a marine gas hydrate area. *Environmental Microbiology* **4**(5), 296-305.

Neretin L. N., Böttcher M. E., Jørgensen B. B., Volkov, I, Luschen H., and Hilgenfeldt K. (2004) Pyritization processes and greigite formation in the advancing sulfidization front in the

Upper Pleistocene sediments of the Black Sea. *Geochimica Et Cosmochimica Acta* **68**(9), 2081-2093.

Niemann H., Elvert M., Hovland M., Orcutt B., Judd A. G., Suck I., Gutt J., Joye S., Damm E., and Finster K. (2005) Methane emission and consumption at a North Sea gas seep (Tommeliten area). *Biogeosciences* **2**, 335-351.

Orphan V. J., House C. H., Hinrichs K. U., McKeegan K. D., and DeLong E. F. (2001) Methane-consuming archaea revealed by directly coupled isotopic and phylogenetic analysis. *Science* **293**(5529), 484-487.

Schink B. (1997) Energetics of syntropic cooperation in methanogenic degradation. *Microbiology and Molecular Biology Reviews* **61**(2), 262-280.

Schink B. and Stams A. J. M. (2002) Syntropism among prokaryotes. In *The Prokaryotes: An Evolving Electronic Resource for the Microbial Community* (ed. M. Dwokin). Springer-Verlag.

Scholten J. C. M., and Conrad R. (2000) Energetics of syntrophic propionate oxidation in defined batch and chemostat cocultures. *Applied and Environmental Microbiology* **66**(7), 2934-2942.

Schulz H. D. and Zabel M. (2000) *Marine Geochemistry*. Springer Verlag.

Sørensen K. B., Finster K., and Ramsing, N. B. (2001) Thermodynamic and kinetic requirements in anaerobic methane oxidizing consortia exclude hydrogen, acetate, and methanol as possible electron shuttles. *Microbial Ecology* **42**, 1-10.

Treude T., Boetius A., Knittel K., Wallmann K., and Jørgensen B. B. (2003) Anaerobic oxidation of methane above gas hydrates at Hydrate Ridge, NE Pacific Ocean. *Marine Ecology-Progress Series* **264**, 1-14.

Van Cappellen P., Dale A., Pallud Y., Van Lith S., Bonneville S., Hyacinthe C., Thullner M., Laverman A., and Regnier P. (2004) Incorporating geomicrobial processes in subsurface reactive transport models. *Saturated & Unsaturated Zone*, 339-348.

Zehnder A. J. B. and Brock T. D. (1979) Methane formation and methane oxidation by methanogenic bacteria. *Journal of Bacteriology* **137**(1), 420-432.

Chapter 5

Regulation of anaerobic methane oxidation in sediments of the Black Sea

Nina J. Knab[1], Barry A. Cragg[2], Ed Hornibrook[3], Lars Holmkvist[1], Christian Borowski[1], R. John Parkes[2], Bo B. Jørgensen[1]

Manuscript in preparation

[1] Max-Planck Institute for Marine Microbiology, Department of Biogeochemistry, Celsiusstr. 1, 28359 Bremen, Germany

[2] School of Earth and Oceans Sciences, Cardiff University, Main Building, Park Place, Cardiff, Wales, CF10 3YE, U.K.

[3] Department of Earth Sciences, University of Bristol, Cantocks Close, Bristol, England, BS8 1TS, U. K.

ABSTRACT

Anaerobic methane oxidation and sulfate reduction were investigated in sediments of the western Black Sea, where methane transport is controlled by diffusion. To understand the regulation and the dynamics of methane oxidation and production in the Black Sea, rates of AOM, SRR and methanogenesis were determined with radiotracers in combination with pore water chemistry and stable isotopes. In the Danube delta as well as in the Dnjepr canyon AOM did not deplete methane entirely and upwards diffusing methane created an extended sulfate-methane transition zone (SMTZ), that could spread over more than 2.5 m and was located in the formerly limnic sediment. AOM rates were not spread over the entire SMTZ, but mainly occurred in the lower part of this zone, sometimes even at depths where no sulfate seemed to be available any more. The inefficiency of methane oxidation appears to be linked to the limnic history of the sediment, but it was in all cores completely oxidized at the limnic-marine transition. The upward tailing of methane was less pronounced at the only station with a SMTZ close to the marine deposit. Sulfate reduction rates (SRR) were mostly extremely low, in the SMTZ even lower than AOM rates. Bicarbonate methanogenesis was not detectable at all in two of the cores, but the isotopic composition of methane indicated that it was of biogenic origin, and can sometimes even get lighter in the zone of AOM.

INTRODUCTION

The process of anaerobic oxidation of methane (AOM) is widespread in continental margin sediments and occurs in a variety of different environments, like gas-hydrate bearing sediments (Joye et al., 2004; Orcutt et al., 2004; Treude et al., 2003), mud volcanoes (Niemann et al., 2006), diffusive sediments (Iversen and Jørgensen, 1985), and sediments with shallow gas accumulations (Niemann et al., 2005; Treude et al., 2005a).

In the western part of the Black Sea, which is dominated by an extensive shelf in the northwest and by river deltas of the Danube and Dnjepr rivers, the sediment contains large amounts of methane, and numerous methane seeps (Popescu et al., 2001). These seeps are mainly located in the transition between the continental shelf and the upper slope, above the gas hydrate stability zone, especially in the area of the Danube canyon and the Dnjepr paleo-delta (Naudts et al., 2006). A unique feature at these methane seeps that has caught a lot of attention are carbonate chimneys that grow from the sediment into the anoxic water column and are overgrown by bacterial mats mediating AOM (Michaelis et al., 2002; Treude, 2005). The abundance of methane in the Black Sea is due to the favorable conditions for preservation of organic matter, because of slow degradation of organic matter under anoxic conditions (Arthur and Dean, 1998; Brumsack, 1989; Treude, 2005). Since electron acceptors like oxygen, nitrate, and metal-ions like Fe(III) and Mn(IV) are mostly low or absent in Black Sea sediments below the anoxic water column (Thamdrup et al., 2000), sulfate reduction and bicarbonate-methanogenesis are the dominant pathways of organic matter degradation (Jørgensen et al., 2004), enhancing the production of methane. The majority of the methane is therefore expected to be biogenic, which was confirmed by stable isotope analyses (Amouroux et al., 2002; Michaelis et al., 2002).

The stratified sediments of the Black Sea consist of limnic clays deposited before 7500 yr B.P., which are overlain by a microlaminated organic-rich sapropel, that marks the transition to marine coccolith ooze, deposited after the intrusion of sea water from the Mediterranean (Calvert et al., 1991; Ross et al., 1970). Where free gas does not reach the surface but is dissolved in the pore water at depth methane is diffusing up into the sulfate zone, where it is oxidized in combination with sulfate reduction. In most marine shelf sediments the overlapping methane and sulfate profiles form a distinct sulfate-methane transition zone (SMTZ) (Devol and Anderson, 1984; Niewöhner et al., 1998), in which AOM rates and sulfate reduction rates (SRR) occur. Earlier

studies of the SMTZ in the Black Sea revealed that the methane profile is tailing up towards the sediment surface (Jørgensen et al., 2001; Reeburgh et al., 1991) and creates an extended SMTZ, which reaches from the bottom of the sulfate zone up to the top of the methane zone. This broad zone of methane and sulfate coexistence indicates that microbial turnover rates are very sluggish (Jørgensen et al., 2001) and therefore pose an interesting opportunity to study the regulation of SRR and AOM rates and controls on AOM distribution.

In Black Sea sediments AOM provides the energy substrate for 7-18 % of the total sulfate reduction and is the main source of H_2S formation at depth (Jørgensen et al., 2004), and the occurrence of a deep sink for H_2S below the SMTZ, which is supposed to be related to a high content of reactive iron in the formerly limnic sediments might play a role in regulating SRR and AOM activity in Black Sea sediments.

The questions addressed in this study were how methane oxidation is influenced by the unique environmental characteristics of the Black Sea and what the reason for the sluggish AOM rates is which lead to methane tailing in these sediments. It is further investigated how SRR and AOM rates are distributed in the extended SMTZ, and what role methanogenesis plays in this environment.

METHODS

Sample collection

Sediment cores were samples with a gravity corer (GC) during cruise 317/3 with RV Poseidon in October 2004 at three stations in the western Black Sea (Figure 1). The 5-m long cores were cut into 1-m sections as they came on deck. At the top of each 1-m section a methane sample was immediately taken to check the loss of dissolved methane before detailed subsampling. All core sections were subsampled for concentrations and microbial process rate analyses at the latest 24 h after retrieval of the core.

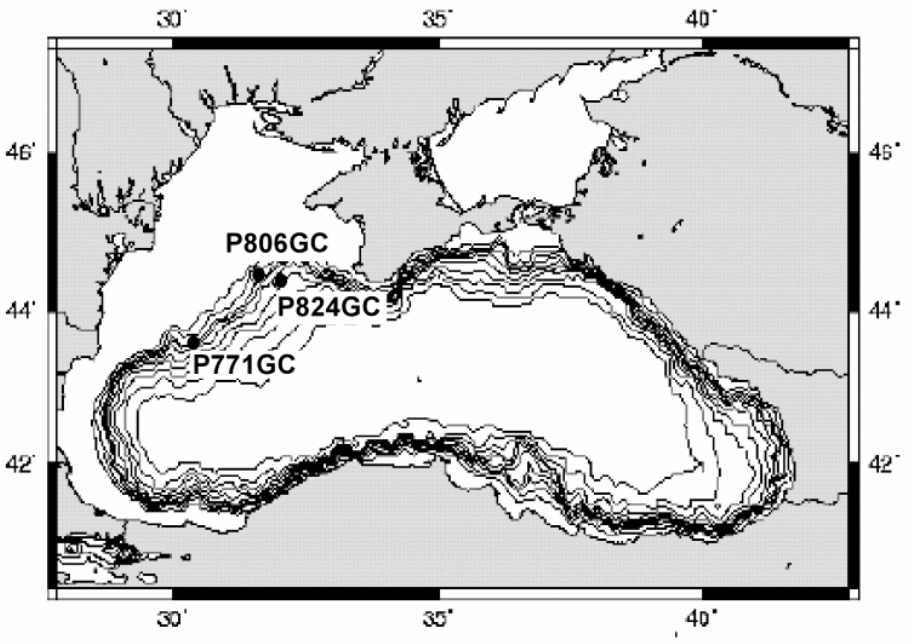

Figure 1: Map of the Black Sea with the three different sampling sites of the gravity cores.

Core ID	Location	Latitude [Deg./Min]	Longitude [Deg./Min]	Water depth [m]	Marine/limnic transition	Depth of gas front	Depth of black bands
P771GC	Palaeo-Danube	43°37.83'	30°09.69'	683	~ 70 cm	400 cm	200 cm
P806GC	Palaeo-Dnjepr	44°46.83'	31°59.30'	205	~ 10 cm	220 cm	-
P824GC	Palaeo-Dnjepr	44°39.06'	32°01.00'	1014	~ 120 cm	280 cm	390 cm

Table 1: Overview of gravity cores

Chemical analyses

Methane concentrations were measured on 3 cm^3 sediment taken with 5 ml cut-off syringes and sealed in serum vials that contained 6 ml NaOH (2.5 % w/v). The samples were shaken and stored to achieve equilibrium between the slurry and the headspace. The methane concentration in the headspace was determined by gas chromatography (5890A, Hewlett Packard) using a packed stainless steel Porapak-Q column (6 ft., 0.125 in., 80/100 mesh, Agilent Technology) and a flame ionization detector. The column temperature was 40°C, and helium was used as a carrier gas at a flow rate of 30 ml min^{-1}. The resulting profile was compared to the samples taken immediately from the 1-m sections. This confirmed that the loss of methane during storage was not significant in the SMTZ.

Sulfate concentrations were measured on pore water squeezed under nitrogen pressure in 5 cm sediment intervals. 1 ml of the pore water was directly fixed in 0.25 ml $ZnCl_2$ (2 % w/v) to trap dissolved sulfide and prevent it from oxidation. The concentration of sulfate in the pore water was analyzed by non-suppressed anion exchange chromatography (Waters 510 HPLC Pump; Waters IC-Pak 50 x 4.6 mm anion exchange column; Waters 430 Conductivity detector). Isophtalic acid (1 mM, pH 4.6) in methanol (10 % v/v) was used as eluant.

Hydrogen sulfide was determined from the pore water samples fixed in $ZnCl_2$ (2 % w/v) by the diamine complexation method described by Cline (1969). The sulfide concentration was measured by spectrophotometry at a wavelength of 670 nm.

For **dissolved inorganic carbon (DIC)** concentrations pore water was sealed headspace-free in glass vials, poisoned with $HgCl_2$ (0.25 mM), and stored at 10 °C. The samples were analyzed by flow injection (Hall and Aller, 1992), using HCl (30 mM) and NaOH (10 mM) as eluants, and a conductivity detector (VWR scientific, model 1054).

Samples for **density** and **porosity** were taken in 10 ml cut-off syringes and 8 cm^3 of sediment was weighed before and after drying at 60°C. The density was calculated as the wet weight per cm^3 and the porosity was determined from the loss of water per cm^3 after the sediment was completely dried.

Acetate concentrations were measured from undiluted squeezed pore water that was stored frozen and thawn immediately before the measurement. The samples were analyzed on a Dionex® ICS-2000 Ion Chromatography System equipped with a Dionex® AS50 autosampler at 4 °C. Determinations of VFA-species were carried out using a Dionex® Anion Self-Regenerating Suppressor (ASRS®-ULTRA II 4-mm) unit in combination with a conductivity detector.

The concentration of **dissolved iron** (Fe^{2+}) in pore water was analyzed with Ferrozine (1 g L^{-1} in 50 mM HEPES buffer, pH 7) according to Stookey (1970) using spectrophotometry at 562 nm.

Total reactive iron in the sediment was extracted with dithionite-citrate-acetic-acid (Canfield, 1989). The dithionate-extracts were analyzed for total iron (Fe^{2+} and Fe^{3+}) with Ferrozine plus 1 % (w/v) hydroxylamine hydrochloride.

Diffusional fluxes of methane, sulfate and sulfide were calculated from the slopes of the linear concentration profile into the SMTZ and the diffusion coefficients according to Fick´s first law of diffusion:

$$J = -\Phi \cdot D_s \cdot \frac{dC}{dz}$$

where J is the diffusive flux [mmol m^{-2} d^{-1}], Φ is the porosity, D_s is the diffusion coefficient in the sediment [cm^2 d^{-1}], and dC/dz is the concentration gradient [µmol cm^{-4}]. Diffusion coefficients at the respective *in situ* temperature and salinity were calculated from Schulz and Zabel (2000), corrected for porosity of the sediment, with n = 2 for $\Phi < 0.7$ and n = 3 for $\Phi > 0.7$ according to Iversen and Jørgensen (1993):

$$D_s = \frac{D}{1+n(1-\Phi)}$$

For **stable isotope analyses** gases were stripped from pore water according to McAullife (1971). The gas was stored as a headspace in inverted crimp top Wheaton® vials by displacement of a preservative solution that consisted of KCL 10 % (w/v) in de-ionized water adjusted to pH 1 using HCl. Analysis of $\delta^{13}C$-CH_4 was conducted by isotope ratio monitoring gas chromatography mass spectrometry (GC-C-IRMS) using a Varian 3400® GC coupled to a Thermoelectron XP® mass spectrometer via a Gas Bench® interface. Methane was separated on a PLOT Q capillary column (0.32 mm x 30 m) and combusted to CO_2 at 1000°C in a ceramic reactor containing Cu and Pt wires. A high purity blend of 1 % O_2 in helium was fed into the reactor at ~0.1 ml min^{-1} to ensure quantitative conversion of CH_4 to CO_2. The H_2O produced was removed using a Nafion® membrane. Accuracy and precision of $\delta^{13}C$-CH_4 analysis by this method were both better than ±0.2 ‰ based upon replicate analysis of a BOC alpha gravimetric CH_4 standard. Stable isotope ratios are reported in the standard (δ^{13}) notation in units of permil (‰) relative to Vienna Pee Dee Belemnite (VPDB).

Microbial process rates

Sediment for the measurement of **anaerobic oxidation of methane (AOM)** was a) taken for each 5 cm depth interval with glass tubes in three parallel 5 cm^3 samples and sealed headspace-free with butyl stoppers (P771GC), or b) sampled in acrylic core liners with injection holes at 2 cm depth intervals (P806GC and P824GC). ^{14}C-methane tracer (1.35 KBq) was injected into each sample and incubated for 20-24 h at the *in situ* temperature of the SMTZ. After incubation the sediment was transferred to glass vials containing 25 ml NaOH (2.5 % w/v) and suspended completely to stop microbial activity. To determine the detection limit of the rate measurement, five control samples per core were stopped immediately after tracer injection. To calculate AOM rates, the methane concentration in each sample was analyzed by gas chromatography and the pool of ^{14}C-methane was measured by combustion of the headspace and scintillation counting. The produced $^{14}C\text{-}CO_2$ in the sediment was extracted through acidic diffusion, trapped in scintillation vials with phenylethylamine and the radioactivity counted (Treude et al., 2003).

The samples for **sulfate reduction rate (SRR) measurement** were taken as described for AOM, injected with ^{35}S-sulfate tracer (500 kBq), and incubated for 20-24 h at *in situ* temperature. The microbial activity was stopped in 20 ml ZnAc (20 % w/v). Samples were analyzed by the cold distillation method described by Kallmeyer et al. (2004), where the total radiolabelled reduced inorganic sulfur (TRIS) is determined in relation to the total radioactive sulfate pool (all units in decays per minute) that remained in the sample. SRR in nmol cm^{-3} d^{-1} was calculated using the following equation (Jørgensen, 1978):

$$SRR = [SO_4^{2-}] \cdot \frac{^{35}\text{S-TRIS}}{^{35}\text{S-TRIS} + ^{35}\text{S-}SO_4^{2-}} \cdot d^{-1} \cdot 1.06$$

where $[SO_4^{2-}]$ is the sulfate concentration in mM and 1.06 is an estimated fractionation factor between ^{35}S and the normal isotope ^{32}S. Because of high variability of the remaining sulfate-tracer that was recovered in the samples for core P771GC the SRR was calculated using the injected tracer activity minus produced ^{35}S-TRIS as a $^{35}SO_4^{2-}$ pool.

Measurements of AOM and SRR were considered to be above the detection limit when the produced ^{14}C-CO_2 or ^{35}S-TRIS exceeded the mean production in the zero time controls plus 3 times their standard deviation.

Bicarbonate methanogenesis rates were measured by injecting ^{14}C-bicarbonate (activity 38 kBq) at 2-cm depth intervals into subcores taken in acrylic core liners. After incubation for 6 to 24 h at *in situ* temperature the incubations were terminated by transferring 2 cm slices of the subcores to glass vials (30 ml) containing 7 ml of NaOH (1 M). In the laboratory, the vial headspace was flushed (carrier gas 95 % N_2: 5 % O_2 at 70 ml/min for 20 min.) through a CO_2-trap (Supelco, UK) and over copper oxide at 800°C in a furnace (Carbolite, UK) to oxidize any produced $^{14}CH_4$ to $^{14}CO_2$. The $^{14}CO_2$ was trapped in Optiphase HiSafe-3 and β-phenethylamine (93:7), and measured in a scintillation counter (Perkin Elmer, UK). Activity rates were calculated from the label turnover times applied to the relevant cold-pool concentrations of DIC.

To determine **acetate methanogenesis rates** the samples were obtained as for bicarbonate methanogenesis, but were injected with ^{14}C-acetate tracer (activity 20 kBq) at 2-cm depth intervals and also incubated for 6 to 24 h at *in situ* temperature. Samples were processed the same way as described above for bicarbonate methanogenesis. Rates were calculated from the label turnover times the relevant cold-pool concentrations of acetate.

Acridine orange direct counts (AODC) were used to determine the total number of microorganisms. One cm^3 of sediment was preserved in a furnaced serum vial containing 9 ml formaldehyde (2 % v/v in artificial seawater, filter sterilized 0.2 µm). Three replicate sub-samples (5-25 µl) were stained for 3 min with 50 µl acridine orange (0.1 % w/v) in 10 ml formaldehyde (2 % v/v in artificial seawater, filter sterilized 0.1µm) and vacuum filtered through a black polycarbonate membrane filter (0.22 µm). Paraffin oil mounted membrane filters were viewed under incident UV illumination with a Zeiss Axioskop epiflourescence microscope at X1000. Both unattached cells and cells attached to particles were counted and the number of attached cells was doubled to account for cells hidden from view (Goulder, 1977). Dividing and divided cells were separately counted to provide an index of the growth potential of the populations.

RESULTS

The concentration depth profiles of methane and sulfate as the substrates of AOM mediated by sulfate reduction as well as the products sulfide and DIC from the three gravity cores are presented in Figure 2. In core P771GC the marine deposit of laminated coccolith ooze at the top was overlying a sapropel layer changing into grey limnic clay at 70 cm depth. Below 160 cm this clay was marbled with darker sediment and contained black grains as well as dark laminations at 200 cm depth.

The core was sampled in the area of the Danube Canyon at a water depth of 680 m, in between stations 6 and 7 of the transect described by Jørgensen et al. (2004). In accordance to the findings of those authors the methane profile of P771GC also showed an extended tailing up towards the sediment surface. Highest methane concentrations of ~ 1.2 mM were measured at 360 cm depth below which methane was outgassing, also indicated by cracks in the sediment observed below 400 cm. The upwards diffusive flux of methane was 19 μmol m^{-2} d^{-1} in the lower part of the SMTZ, where methane was not completely oxidized and a flux of 4 μmol m^{-2} d^{-1} remained between 70 and 232 cm. The methane concentration only approached zero at ~70 cm depth, at the boundary between the marine and limnic sediments.

Sulfate concentrations decreased nearly linearly from 25 mM at the top of the core to a depth of ~ 340 cm, with a sulfate flux into the SMTZ of 149 μmol m^{-2} d^{-1}. Yet, sulfate was not entirely depleted below this depth but a constant concentration of ~ 1 mM apparently remained below 350 cm. Sulfide concentrations in core P771GC were low for a methane rich environment and did not exceed 0.2 mM. The peak of H_2S at ~ 100 cm depth was located at the top of the limnic sediment in the upper part of the SMTZ, surprisingly shallow in comparison to the methane and sulfate profiles. H_2S diffusion occurred both up and down, with similar fluxes towards the sediment surface (0.12 nmol m^{-2} d^{-1}) and downwards (0.13 nmol m^{-2} d^{-1}). DIC concentrations were also rather low, increasing steadily from the top of the core to highest values of ~ 8 mM at 270 cm depth, coinciding with the horizon where H_2S was depleted.

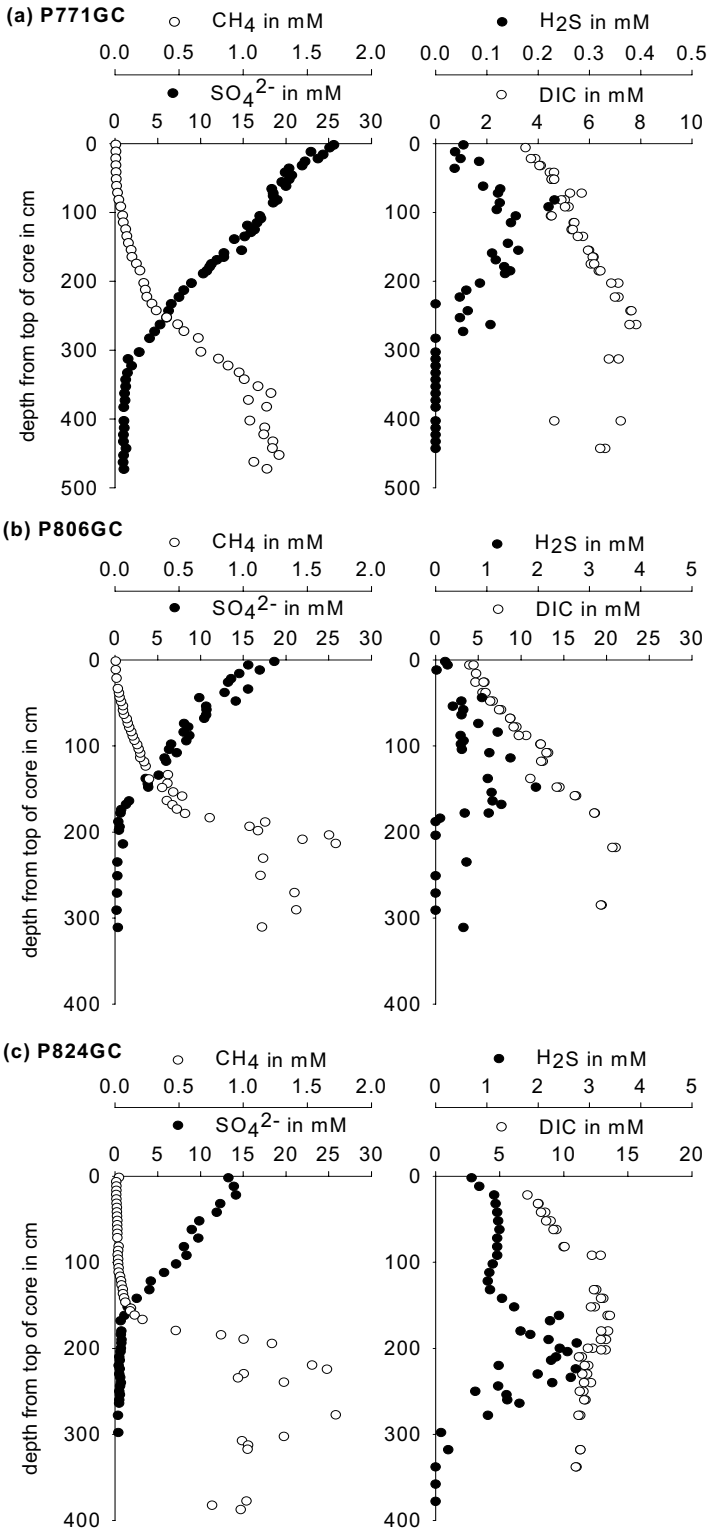

Figure 2: Pore water concentration profiles of CH_4, SO_4^{2-}, H_2S, and DIC. The top of the core is not identical with the sediment surface because some sediment might have been lost by coring.

P806GC was taken on the shelf edge of the palaeo Dnjepr delta, on the flank of a ridge that was lined with methane seeps at the top (Naudts et al., 2006). The sediment contained a dense shell layer beneath the sapropel at only 10 cm depth, and a second shell layer was observed at 80-140 cm depth. Below this layer the sediment consisted of silty fine sand that contained gas cracks from 220 cm downwards, which is consistent with the methane profile indicating outgassing below ~ 200 cm. The methane flux into the SMTZ was 98 μmol m^{-2} d^{-1}, which is much higher than in core P771GC, but the methane and sulfate profile showed a similar pattern of an extended SMTZ with methane tailing up towards the surface.

The sulfate profile was linear from the top of the core down to a depth of 180 cm, with a flux of 145 μmol m^{-2} d^{-1} into the SMTZ, 1.5 times higher than the methane flux. A remaining pool of sulfate below the SMTZ, comparable to the one in P771GC, was not detected in core P806GC, where sulfate concentrations below 200 cm were around the detection limit of 0.2 mM. The H_2S concentration at the top of the core (0.2 mM) was similar to that of core P771GC, but the sulfide flux was much higher, 1.3 mmol m^{-2} d^{-1} at the top and 1.8 mmol m^{-2} d^{-1} at the bottom, because of the higher H_2S peak of ~ 2 mM that was found in the lower part of the SMTZ. The linear increase in DIC concentrations again reached highest values in the zone of sulfide depletion at ~ 200 cm depth and, like the H_2S concentrations they were also much higher than in core 771GC.

Core P824GC sampled in the deeper part of the Black Sea on mid slope contained a thick sapropel layer with laminations that changed into uniform grey clay at 120 cm. The methane profile did not show as pronounced a tailing as at the other two sites, and resembled more the typical concave-up pattern observed in most marine environments, forming a distinct SMTZ at 110-170 cm. The methane flux into the SMTZ was 126 μmol m^{-2} d^{-1}, higher than at the other two sites. Sediment cracks indicating methane supersaturation were observed from > 280 cm depth although the methane profile would suggest outgassing from > 220 cm depth.

The sulfate profile was very similar to that at P806GC, with a concentration at the top of the core of ~ 15 mM and a sulfate flux into the SMTZ of 301 μmol m^{-2} d^{-1}. Like in P771GC sulfate did not disappear completely below 168 cm, but concentrations < 0.6 mM seemed to remain, decreasing gradually with depth.

DIC concentrations increased down through the marine deposits at the top of the core and reached a maximum of 14 mM at the bottom of the SMTZ. In the limnic part of the sediment it

decreased slightly to ~ 12 mM.

The H_2S concentration was relatively constant at ~ 1 mM in the upper 20-100 cm of the core, decreasing only at the very top of the core. In relation to the methane and sulfate profile the H_2S maximum of 3 mM at 200 cm was located deeper than in the other two cores, even below the SMTZ, and was depleted at a depth of 330 cm.

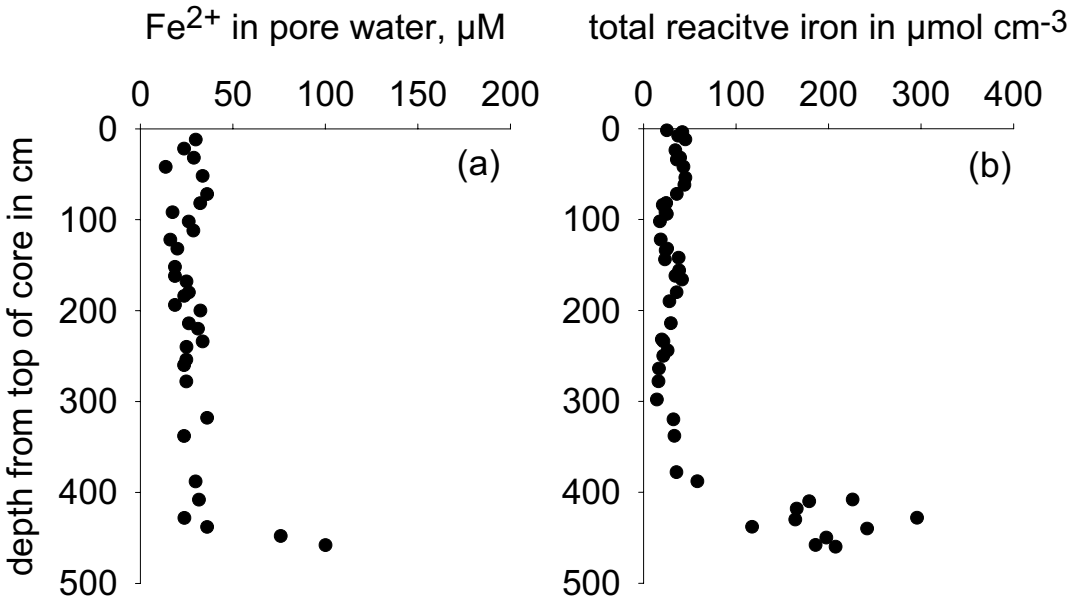

Figure 3: Iron concentrations (a) in the pore water and (b) in the solid phase of core P824GC extracted by dithionate extraction.

The concentrations of iron in the pore water and the solid phase of core P824GC are presented in Figure 3. Dissolved Fe^{2+} showed a steep increase below a depth of ~ 430 cm, forming a distinct iron diffusion front at this depth. In the solid phase, reactive iron concentrations up to 45 µmol cm^{-3} were found in the top 100 cm of the core, with a local minimum at the transition from the marine to the limnic sediment. Below the sapropel layer, reactive iron concentrations were < 40 µmol cm^{-3}, with lowest values between 200 and 300 cm. The amount of reactive iron started to increase at 300 cm, with a steep increase below 390 cm to 300 µmol cm^{-3} at 430 cm. Consistent with this peak of reactive iron black bands of FeS occurred in the sediment between 390 cm and 440 cm depth.

The rates of AOM, SRR and methanogenesis measured at station P771GC are shown in Figure 4. Low rates of AOM activity (1.2 nmol cm^{-3} d^{-1}) started to increase below 175 cm to reach a maximum of 5.6 nmol cm^{-3} d^{-1} at 253 cm depth, but they did not form a distinct AOM peak. Instead, rates of ~0.5-4 nmol cm^{-3} d^{-1} were measured throughout the entire lower part of the 500 cm long core. However, as discussed below, it is not clear if these values represent actual AOM activity.

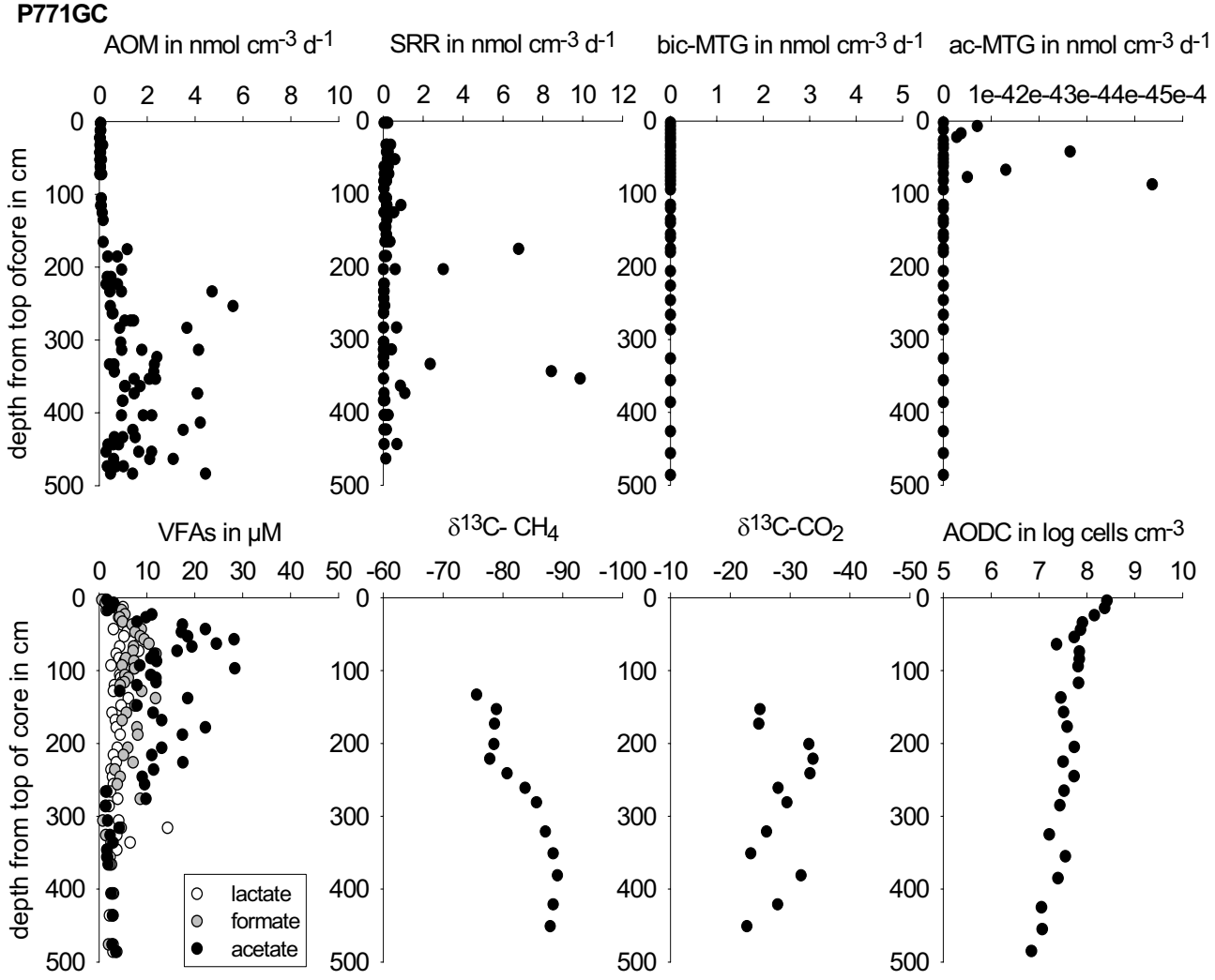

Figure 4: Depth profiles of core P771GC present the distribution of AOM, SRR, and methanogenesis rates from bicarbonate (bic-MTG) or acetate (ac-MTG). In addition, the concentrations of volatile fatty acids (VFA), δ^{13}C-stable isotope values of the methane and bicarbonate pool, as well as total cell counts are presented throughout the core.

Two peaks of sulfate reduction activity were found, one at 200 cm (3-7 nmol cm^{-3} d^{-1}) and the other at 350 cm depth (~ 9 nmol cm^{-3} d^{-1}) near the lower SO_4^{2-} boundary. Low SRR was also detected between these peaks, yet the pattern of SRR did not reflect the profile of AOM.

Bicarbonate methanogenesis was analyzed throughout the core, but rates were not detectable. Instead, acetate methanogenesis was found in the sulfate zone in the upper 100 cm of the core, but also these rates were extremely low, with a maximum of 4.3 10^{-4} nmol cm^{-3} d^{-1}. At the depth where AOM took place acetate methanogenesis rates were below detection limit. The occurrence of acetate-methanogenesis at 50-100 cm was accompanied by high acetate concentrations of up to 30 µM, whereas other VFAs, such as formate or lactate, were below 10 µM throughout the core.

Despite the lack of a clear SMTZ and a distinct zone of AOM activity, methane was enriched in the heavier isotope, ^{13}C-CH_4 at 210 cm depth, thus changing the $\delta^{13}C$ of the methane from –88 ‰ in the deep limnic sediment to –78 ‰. The $\delta^{13}C$ of methane seemed to become even lighter at the top of the AOM zone. The $\delta^{13}C$-CO_2 values, determined by AOM as well as by SRR, did not reflect this trend and varied around values of –30 ‰.

At the top of the core the total number of cells per cm^{-3} was 2.5 10^8 and decreased with depth, most steeply in the upper 70 cm.

The distribution of microbial process rates in P806GC showed distinct peaks of AOM and SRR at similar depth (Figure 5). AOM activity occurred in a ~ 70 cm wide zone with a maximum rate of ~ 2.4 nmol cm^{-3} d^{-1} at 218 cm. The peak of SRR at the bottom of the SMTZ (~ 0.8 nmol cm^{-3} d^{-1}) was much lower than the AOM rates at this depth.

Bicarbonate methanogenesis rates were highest just above the AOM zone with a maximum of 0.06 nmol cm^{-3} d^{-1}, and a rate of 0.015 nmol cm^{-3} d^{-1} at ~ 200 cm depth, in the zone of maximum AOM and sulfate reduction activities. As in P771GC, very low rates of acetate methanogenesis were detected, mostly in the top 100 cm. Additional acetate methanogenesis activity was found together with bicarbonate methanogenesis at 140 cm to 210 cm depth. Rates were not determined below 230 cm.

The concentrations of acetate, formate and lactate as substrates for SRR and methanogenesis were below 10 µM in most of the core, with some higher values up to 27 µM of lactate at 118 cm depth. Below the zone of AOM acetate concentrations increased to ~ 18 µM at 240 cm.

Stable isotope values of $\delta^{13}C$-CH_4 around -70 ‰ at 30-60 cm indicate that the methane is of biogenic origin. A shift to heavier values of the remaining pool (-67 ‰) at a depth of 180 cm was in accordance with AOM taking place in this zone. The methane turnover and production of isotopically lighter CO_2 at the depth of microbial methane turnover is, also in this core with co-occurring SRR and AOM, not reflected in the $\delta^{13}C$-CO_2 profile.

The total amount of cells was comparable to P771GC at the surface of the core and mostly changed in the top sediment. Below 36 cm cell numbers remained around ~ 3 10^7 cells cm^{-3}. Only in the zone of AOM and sulfate reduction activity a slight decrease in cell numbers was observed.

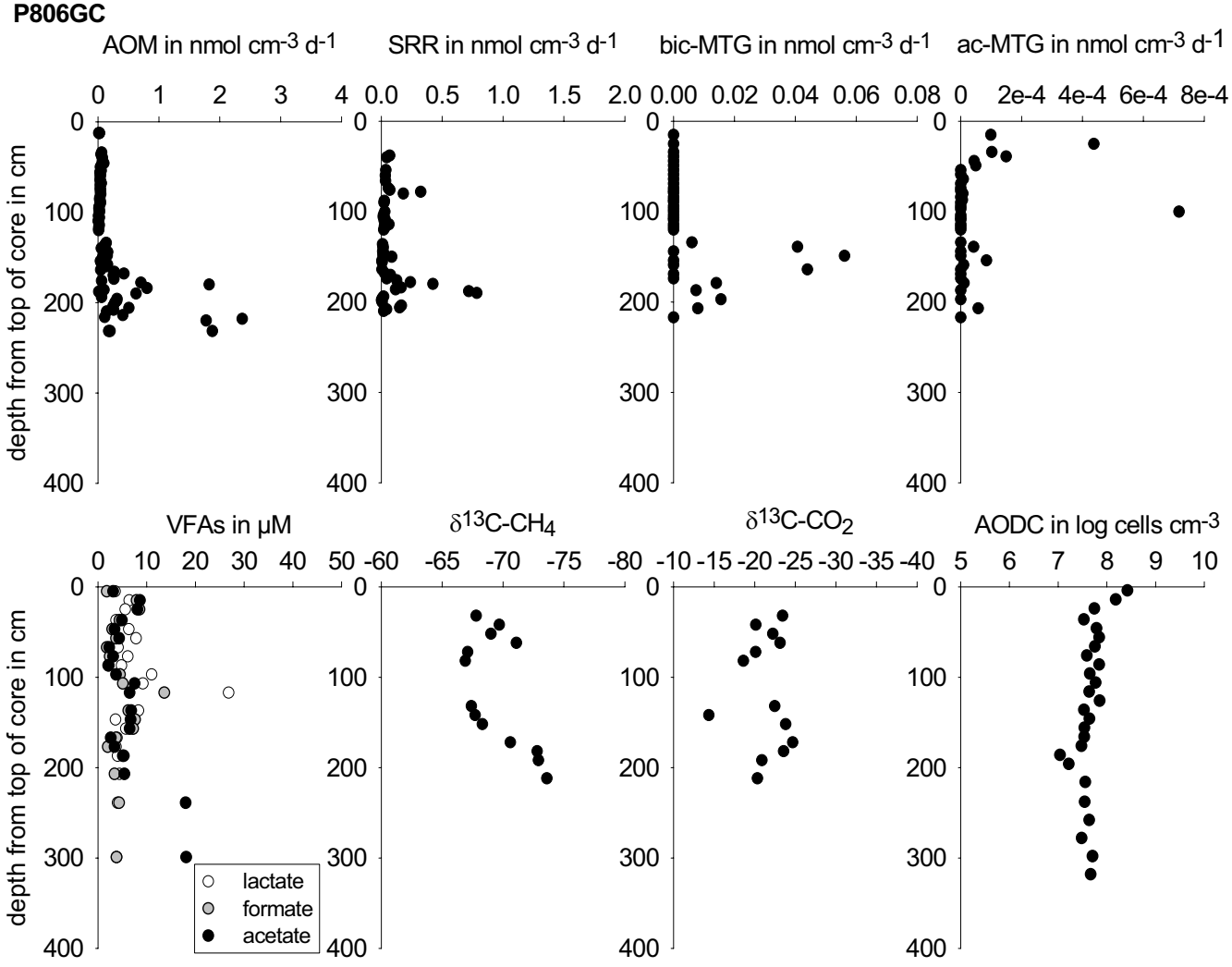

Figure 5: Depth profiles of core P806GC, as described for Figure 4.

At station P824GC (Figure 6) the profiles of methane and sulfate formed a distinct SMTZ at 130-170 cm depth and this zone also showed an increase in microbial activity. A peak of AOM rates (4.5 nmol cm^{-3} d^{-1}) occurred at 150 cm, and at almost the same depth some increased sulfate reduction rates were observed (1.2 nmol cm^{-3} d^{-1} at 162 cm depth). AOM rates seemed to continue down to 290 cm, where maximum of up to ~ 13 nmol cm^{-3} d^{-1} was measured, but like in P771GC, it is not certain if they reflect AOM activity.

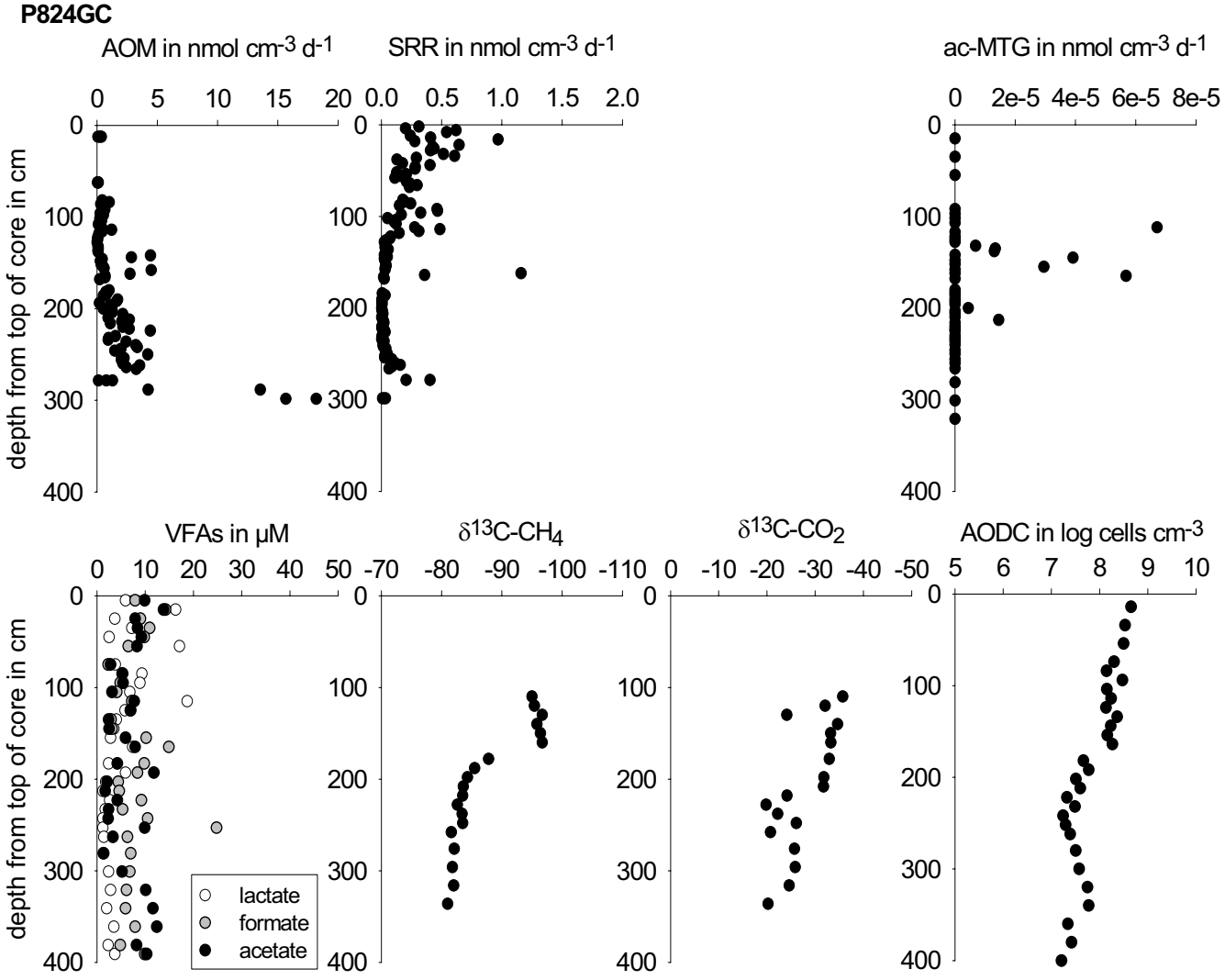

Figure 6: Depth profiles of core P824GC, as described for Figure 4.

Sulfate reduction was present in the top of the core with very low rates (< 1 nmol cm^{-3} d^{-1}), and they continued to a depth of 126 cm. In addition to the methane dependent SRR peak in the SMTZ a second increase in $^{35}S\text{-}SO_4^{2-}$ turnover to TRIS was detected at 280 cm, but because sulfate might not be present at this depth it is not clear if this represents actual sulfate reduction activity.

Bicarbonate methanogenesis rates for this core are not available, but acetate methanogenesis rates were very low (max. 6.7 10^{-5} nmol cm^{-3} d^{-1}). Detectable rates did not occur at the top of the core as in P771GC and P806GC but between 130 cm and 200 cm depth.

VFAs remained at a low level in the entire core and were evenly distributed, with concentrations mainly < 10 µM. Below the SMTZ the methane had $\delta^{13}C$ values around -83 ‰, but moving up into the SMTZ there was a sudden change to an even lighter isotopic signal reaching -97 ‰ at 160 cm. This unexpected shift in $\delta^{13}C\text{-}CH_4$ at a depth where AOM usually discriminates against the heavier isotope was more pronounced than the signal of the $\delta^{13}C\text{-}CO_2$, which shifted towards the heavier isotope at 230 cm, but also at 130 cm depth.

The total cell counts in core P824GC did not show the steep decrease of cells at the top of the core as it was observed at the other sites, and numbers decreased more steadily, with slight maxima at 164 cm and 340 cm, of which the shallower one coincided with increased AOM rates and SRR.

DISCUSSION

Anaerobic methane oxidation in connection with sulfate reduction and methanogenesis was investigated in three different diffusive sediments of the Black Sea, where the SMTZ was located in the limnic part of the sediment. Even though it spread over a broad interval, and would facilitate AOM activity and sulfate reduction also in shallower horizons, these processes were not evenly distributed over the entire SMTZ, but mainly occurred in an active zone in the lower part of the SMTZ.

AOM and SRR

The most noticeable feature of the methane profiles in the Black Sea is that AOM does not seem to turn over methane efficiently in the zone of major AOM activity. This leads to an extended zone of methane and sulfate co-occurrence, and results in tailing of the methane up towards the surface. This feature of a gradual oxidation of methane had also been observed earlier in gravity cores in the area of the western Black Sea (Jørgensen et al., 2001; Reeburgh et al., 1991) and was confirmed by the methane profile of core P771GC. It seems to be a common pattern that is also present in methane rich sediments in other parts of the Black Sea, like in P806GC from the area southwest of Crimea.

The methane tailing was described as a result of "sluggish" AOM (Jørgensen et al., 2001), and the tracer determined rates in core P806GC were indeed low, especially for SRR. But in diffusion dominated systems at other continental margins AOM rates are mostly rather low, and the peak rates from the Black Sea, especially in core P771GC with a very pronounced methane tailing, were in the same range (3-6 nmol cm^{-3} d^{-1}) as maximum AOM rates from the North Sea (Niemann et al., 2005) or Skagerrak (Knab et al., Chapter 2), where no methane tailing was observed. It is not clear why despite comparable AOM rates methane tailing occurs in the Black Sea, but not at these sites.

In contrast to the SMTZ of typical methane rich marine sediments, where SRR and AOM rates occur in a distinct zone defined by the availability of the substrates, the AOM activity in P771GC and P824GC seemed to be spread over a broad zone, and was also detected at depths where sulfate was restricted to a background value or even not measurable.

The occurrence of AOM below the major zone of activity is very unusual and questionable. In P824GC where samples were taken throughout the core the turnover of radioactive ^{14}C-CH_4 shows (Figure 7b) that the major activity took place at 140-160 cm, and the rates at depth are not based on an increased turnover, but on the increasing methane concentrations in the deeper part of the core. The detection of ^{14}C-CO_2 at ~290 cm is most likely a problem of the tracer incubation method at sites with low AOM activity. However, since in P824GC there was also a peak in SRR at the same depth as the deep AOM activity, and sulfate reducing bacteria were found to be present at this horizon (Leloup et al., 2006) it is not yet clear whether AOM values below 180 cm reflect actual activity. In P771GC the turnover in the lower part of the core did

show some data points of increased $^{14}CO_2$ production (Figure 7a). AOM rates in the deeper part of this core might be overestimated due to the higher methane concentration, but AOM might also not be strictly confined to a concise active zone.

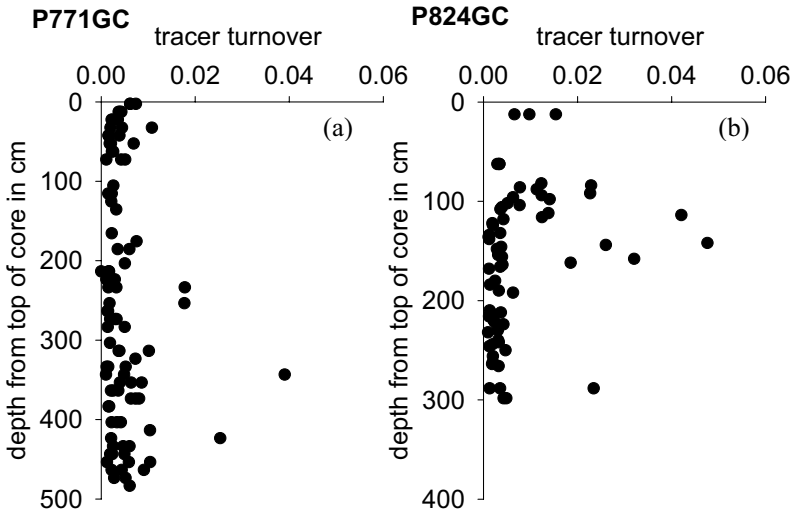

Figure 7: Tracer turnover defined as the proportion of ^{14}C-CO_2 to the total ^{14}C-pool for cores P771GC (a) and P824GC (b).

The best consilience between AOM and SRR was observed in the shallowest core P806GC, which fits to the observation of Jørgensen et al. (2001) that the coupling of both processes seems to be less tight at greater water depth. The measured rates, which could potentially take place everywhere between 10 cm and the bottom of the sulfate zone at 180 cm, were only taking place in a narrow zone. This close coupling between AOM and SRR did, however, not result in the formation of a concise SMTZ or an effective barrier for methane diffusion into the AOM zone.

The absence of sulfate reduction at the top of P771GC and P806GC is probably due to a lack of data at the sediment surface, because earlier measurements of surface SRR in the Black Sea showed that high SRR were confined to the top ~ 10 cm of the sediment (Albert et al., 1995; Dando and Niven, 1998; Weber et al., 2001). At P806GC surface SRR might have been low altogether, because the sediment could have been eroded on the flanks of the ridge, where the core was sampled, and the marine deposit on top of the limnic sediment was only very thin.

What both cores P771GC and P806GC have in common is that the AOM rates and SRR take place deep inside the limnic sediment, whereas in P824GC the SMTZ was located much closer to the marine-limnic boundary. Despite the relatively high rates of AOM and SRR in P771GC and the close coupling of these rates in P806GC, it was core P824GC that did not show the pronounced tailing of methane. It was the only station with a distinct SMTZ, similar to the typical SMTZ found in most methane bearing ocean margin sediments (Hensen et al., 2003; Niewöhner et al., 1998). The major difference between the pore water profiles of core P806GC and P824GC was the methane tailing in the upper part of the core. The sulfate profile and the lower part of the methane profile were very similar in both cores, and also rates did not differ as much as to provide an explanation why tailing occurred in one core but not in the other. Tailing might therefore not be due to low AOM rates in the major AOM zone but what was much less efficient in P806GC compared to P824GC was the methane consumption of concentrations < 0.5 mM at the upper end of the AOM zone at ~ 160 cm depth. This inefficient oxidation of the low methane concentrations at the top of the major AOM activity zone seems to be the reason for the tailing of the remaining methane and slow depletion towards the top of the SMTZ. In sediments with the typical tight overlap of methane and sulfate profiles the AOM zone reaches up as high until all the methane is oxidized. In the cores that exhibit methane tailing, this is not the case and AOM is only removing the methane very slowly. Yet, the reason why AOM is getting inefficient in oxidizing methane concentrations < 0.5 mM at P806GC and P771GC, whereas such concentrations are further depleted by methanotrophic archaea at P824G is not know. Interestingly, the tailing of methane in all cores disappeared exactly at the depth where it hit the boundary of the marine deposits.

P824GC was the only core to show sulfate reduction activity based on organic matter degradation in the top 110 cm. The drop in SRR in the top of the core coincided with the shift from sapropel to gray clay, marking the transition from marine to limnic sediment at this depth. The core was sampled in an area of mass wasting where slides from the central divide of the Dnjepr canyon have been identified (Naudts et al., 2006), and the thickness of the marine deposits at this site might be an indication that some of the sediment originated from such a submarine slide. Although the lamination that is typically observed in the marine deposits in the

Black Sea was present in the upper 10 cm of the core the sediment between 10 cm and the sapropel layer did not show lamination.

The absence of methane tailing in this core, where the zone of SRR and AOM rates at 170 cm was located very close to the marine-limnic boundary, whereas the active zone in the other two cores was much deeper in the limnic sediment, might be a hint that the location of the SMTZ in the limnic layers of the sediment is the reason for the low rates and the sluggish turnover of methane. Tailing of methane profiles is also common at other sites where buried limnic sediments are overlain by marine deposits, like the Baltic Sea (Iversen and Jørgensen, 1985; Piker et al., 1998; Treude et al., 2005a) or Saanich Inlet (Devol and Anderson, 1984), even though the tailing is not as pronounced as in the Black Sea. But at these locations AOM always takes place in the marine deposits, and the sediments of the Black Sea are so far the only sites we are aware of, where the entire SMTZ is located in the limnic sediment layers.

It is not clear what could be the reason for SRR taking place in the marine deposits of P824GC, but not, or only with low rates, in the limnic sediments. With the increase in salinity in the Black Sea sulfate became available in the formerly limnic sediments and is not limited as substrate for SRR. More important than sulfate availability might be the organic matter content. At the time it was limnic, the Black Sea did not experience a high input of organic matter from the rivers and the limnic sediment is therefore depleted in organic material, whereas the marine deposits contain large amounts of organic carbon. The flux and degradation rate constant of organic matter strongly influences the distribution of methane in sediments (Martens et al., 1998), and might play an important role for the regulation of sulfate reduction, methanogenesis and AOM in the Black Sea.

The sulfate reducing bacteria in the limnic sediment layers were phylogenetically the same as in the marine deposits (Leloup et al., 2006), and also the total abundance of cells was comparable to other diffusive systems with a more efficient AOM zone (Parkes et al., in press). Although all different kinds of organisms that are present are included in the total cell counts, there is no indication that the low rates are based on a lack of the organisms mediating the processes (Leloup et al., 2006).

Sulfate dynamics and H_2S

In core P771GC sulfate was not depleted entirely, but the influence of the methane related sulfate reduction rate was large enough to create a linear sulfate profile in the upper part of the core. Compared to the SRR and AOM rates modelled by Jørgensen et al. (2001) at the neighbouring stations the tracer determined rates were almost two orders of magnitude higher, and probably overestimate the actual activity.

AOM mediated by sulfate reduction usually takes place at the bottom of the sulfate zone, but because sulfate was not depleted at the bottom of the core it might be possible that low SRR are occurring throughout this zone, and facilitate AOM. We detected sulfate concentrations of up to 1 mM below 300 cm but it is not yet clear if the presence of this sulfate is an artifact, that originated from reoxidation of sulfide during processing of the sediment and pore water extraction, and was originally not present in the sediment, or whether it constitutes an existing sulfate pool. It is unlikely that the sulfate originated from the sediment surface because the sulfate turnover time of less than 10 years in the SMTZ would be sufficient to reduce the sulfate from above, and there was also no diffusive downward flux of sulfate below 330 cm. Therefore the only possibility for the presence of sulfate in these deep sediment layers would be a deep sulfur source, based on reoxidation of iron-sulfides to sulfate (Neretin et al., 2004), maintaining a low but steady sulfate pool at depth, but it is not clear how this could occur. The observation of these authors that H_2S is trapped by iron from the formerly limnic sediment layers, is consistent with the disappearance of H_2S at depth in all three cores of our study. Yet, the dissolved iron front usually coincides with the depletion of H_2S and this sulfidization front is marked by black bands in the sediment (Jørgensen et al., 2004). In core P824GC the concentration of dissolved iron only increased 60 cm below the depth where sulfide disappeared, and it is not known what causes this separation. The increase of the reactive iron in the solid phase started below the depth of H_2S depletion indicating that Fe^{2+} dissolved from iron sources below and diffuses upwards, where it precipitates presumably as pyrite, in addition to the pyrite formed during the sulfur-limited stage > 9800 yr ago (Jørgensen et al., 2004). Originally reduced iron had probably been present in the entire limnic sediment, but was trapped by ongoing sulfidization, as more sulfate became available with increasing salinity, and so the sulfidization front was moved downwards after the Holocene/Pleistocene transition (Neretin et al., 2004; Jørgensen et al., 2004). This

penetration of the sulfidization front was equal at all three sites, with sulfide depletion ~ 200 cm below the sapropel layer.

The consequence of the sulfide sink in deeper sediment layers, is that the thermodynamic yield that the organisms can obtain from sulfate reduction coupled to AOM is getting very favorable at this depth, and that might be the reason that these rates occur only at the bottom of the SMTZ, even though both methane and sulfate are present over a broad zone.

Methanogenesis

The presence of sulfate in the entire 500 cm of the gravity core P771GC might also be an explanation why no bicarbonate methanogenesis was detectable in this core. The methane in the Black Sea has been reported to be of biogenic origin (Amouroux et al., 2002, Michaelis et al., 2002), and this is coherent with $\delta^{13}C\text{-}CH_4$ stable isotope values of –80 ‰ to -100 ‰ in our cores. The fractionation of carbon isotopes by methanogenesis usually leads to a $\delta^{13}C\text{-}CH_4$ of around –60 ‰ to -100 ‰ (Whiticar, 1999), and the values from the cores of our study were at the lower end of this range.

A shift in isotopic composition towards the heavier isotope in the remaining methane pool due to a preference of the methanotrophic archaea to utilize $^{12}C\text{-}CH_4$, as observed in P771GC and to a lesser extent in P806GC, is characteristic for the zone of AOM activity and has been observed at several other AOM sites (Alperin et al., 1988; Whiticar and Faber, 1986). But in P824GC this shift was reversed and the $\delta^{13}C\text{-}CH_4$ values became lighter in the SMTZ. Such a pattern could perhaps be explained in case methanogenesis rates exceed AOM rates at this depth, as was proposed for microbial AOM-mediating mats from the Black Sea (Seifert et al., 2006). In our core, however, it appears unlikely that bicarbonate methanogenesis rates at 160 cm depth are higher than AOM rates of 4.5 nmol cm^{-3} d^{-1}, despite the presence of sulfate at this depth. Acetate methanogenesis was found in all three cores, with highest rates just below the transition between the marine and limnic sediment, but the rates were far lower than the AOM rates, and much too low to account for significant methane production.

The absence of measurable methanogenesis despite the evidence of biogenic origin of the methane infers that either the methanogenic zone starts below the sampling depth of these cores or rates take place at an extremely low rate. The methanogenesis rates must be lower than the

overlying SRR and high enough to sustain the methane flux into the SMTZ. It might occur at extremely low values and the methane accumulation is the result of the integrated methane production over the depth of a broad methanogenic zone, reaching far down into the sediment. A methanogenesis rate of 1.9 pmol cm^{-3} d^{-1} over a 10 m interval would be sufficient to maintain the methane flux of 19 µmol m^{-2} d^{-1} from P771GC. Integrated rates of measured AOM (45 µmol m^{-2} d^{-1}) exceed the calculated methane flux and should therefore be sufficient to oxidize methane completely. In addition, the biogenically produced methane of the Black Sea is supposed to originate from carbon degradation in old Pleistocene deposits unaffected by the shift from methanogenesis to sulfate reduction as the main mineralization process (Jørgensen et al., 2004). Therefore it is likely that methane production was not only undetectable because of low rates, but also because it was taking place below the depth of our measurements.

CONCLUSION

The incomplete oxidation of methane in the major AOM zone and resulting methane tailing is a common feature of diffusion-dominated methane rich sediments of the western Black Sea. Despite the sluggish AOM rates, all the methane is oxidized and prevented from reaching the sediment surface.

The reason for the sluggish rates seems to be related with the location of the SMTZ inside the sediment with a limnic history. Tailing of methane was less pronounced in the core, where the SMTZ was located close to the marine-limnic boundary and were the limnic sediment was covered by a thick layer of marine deposits.

The importance of the limnic-marine boundary was further indicated by the disappearance of methane at this transition in all cores, as well as the restriction of SRR to the marine deposits in P824GC.

In addition to SRR and AOM, methanogenesis rates were also extremely low, or even not detectable, although very light stable isotope values showed that methane was of biogenic origin.

In contrary to the typical increase in $\delta^{13}C\text{-}CH_4$ due to $\delta^{12}C$ CH_4 utilization in the AOM zone the stable isotopes became lighter in core P824GC, and this was not related to higher methanogenesis rates than AOM rates.

REFERENCES

Albert D. B., Taylor C., and Martens C. S. (1995) Sulfate reduction rates and low molecular weight fatty acid concentrations in the water column and surficial sediments of the Black Sea. *Deep-Sea Research I* **42**, 1239-1260.

Alperin M. J., Reeburgh W. S., and Whiticar M. J. (1988) Carbon and hydrogen isotope fractionation resulting from anaerobic methane oxidation. *Global Biogeochemical Cycles* **2**, 279-288.

Amouroux D., Roberts G., Rapsomanikis S., and Andreae M. O. (2002) Biogenic gas (CH_4, N_2O, DMS) emissions to the atmosphere from near-shore and shelf waters of the northwestern Black Sea. *Estuarine Coastal and Shelf Science* **54**, 575-587.

Arthur M. A. and Dean W. E. (1998) Organic-matter production and preservation and evolution of anoxia in the Holocene Black Sea. *Paleoceanography* **13**, 395-411.

Brumsack H. J. (1989) Geochemistry of recent TOC-rich sediments from the Gulf of California and the Black Sea. *Geochemische Rundschau* **78**, 851-882.

Calvert S. E., Karlin R. E., Toolin L. J., Donahue D. J., Southon J. R., and Vogel J. S. (1991) Low organic carbon accumulation rates in the Black Sea sediments. *Nature* **350**, 692-695.

Canfield D. E. (1989) Reactive iron in marine sediments. *Geochimica Et Cosmochimica Acta* **53**(619-632).

Cline J. D. (1969) Spectrophotometric determination of hydrogen sulfide in natural waters. *Limnology & Oceanography* **14**(3), 454-458.

Dando P. R. and Niven S. J. (1998) Sulphate reduction rates in a methane seepage area of the Black Sea. In *Berichte aus dem Zentrum für Meeres- und Klimaforschung* (ed. U. Luth, C. Luth, and H. Thiel), pp 27-35, Institut für Hydrobiologie und Fischereiwissenschaft, Universität Hamburg.

Devol A. H. and Anderson J. J. (1984) A model for coupled sulfate reduction and methane oxidation in the sediments of Saanich Inlet. *Geochimica Et Cosmochimica Acta* **48**, 993-1004.

Goulder R. (1977) Attached and free bacteria in an estuary with abundant suspended solids. *Journal of Applied Bacteriology* **43**(3), 399-405.

Egorov V. N., Luth U., Luth C., Gulin M. B. (1998) Gas seeps in the submarine Dnjepr canyon, Black Sea: Acoustic, video and trawl data. In *Berichte aus dem Zentrum für Meeres- und Klimaforschung* (ed. U. Luth, C. Luth, and H. Thiel), pp 11-21, Institut für Hydrobiologie und Fischereiwissenschaft, Universität Hamburg.

Hall P. O. J. and Aller R. C. (1992) Rapid, small-volume flow-injection analysis for ΣCO_2 and NH_4^+ in marine and freshwaters. *Limnology & Oceanography* **37**, 1113-1118.

Hensen C., Zabel M., Pfeiffer K., Schwenk T., Kasten S., Riedinger N., Schulz H., and Boetius A. (2003) Control of sulfate pore-water profiles by sedimentary events and the significance of anaerobic oxidation of methane for the burial of sulfur in marine sediments. *Geochimica Et Cosmochimica Acta* **64**(14), 2631-2647.

Iversen N. and Jørgensen B. B. (1985) Anaerobic methane oxidation rates at the sulfate methane transition in marine sediments from Kattegat and Skagerrak (Denmark). *Limnology and Oceanography* **30**(5), 944-955.

Iversen N. and Jørgensen B. B. (1993) Diffusion-coefficients of sulfate and methane in marine sediments - influence of porosity. *Geochimica Et Cosmochimica Acta* **57**(3), 571-578.

Jørgensen B. B. (1978) Comparison of methods for the quantification of bacterial sulfate reduction in coastal marine sediments 1. Measurement with radiotracer techniques. *Geomicrobiology Journal* **1**(1), 11-27.

Jørgensen B. B., Böttcher M. E., Luschen H., Neretin L. N., and Volkov, II. (2004) Anaerobic methane oxidation and a deep H_2S sink generate isotopically heavy sulfides in Black Sea sediments. *Geochimica Et Cosmochimica Acta* **68**(9), 2095-2118.

Jørgensen B. B., Weber A., and Zopfi J. (2001) Sulfate reduction and anaerobic methane oxidation in Black Sea sediments. *Deep-Sea Research I* **48**(9), 2097-2120.

Joye S. B., Boetius A., Orcutt B. N., Montoya J. P., Schulz H. N., Erickson M. J., and Lugo S. K. (2004) The anaerobic oxidation of methane and sulfate reduction in sediments from Gulf of Mexico cold seeps. *Chemical Geology* **205**(3-4), 219-238.

Kallmeyer J., Ferdelman T. G., Weber A., Fossing H., and Jørgensen B. B. (2004) A cold chromium distillation procedure for radiolabelled sulfide applied to sulfate reduction measurements. *Limnology & Oceanography: Methods* **2**, 171-180.

Leloup J., Loy A., Knab N. J., Borowski C., Wagner M., and Jørgensen B. B. (2006) Diversity and abundance of sulfate-reducing microorganisms in the sulfate and methane zones of a

marine sediment, Black Sea. *Environmental Microbiology* doi:10.1111/j.1462-2920.2006.01122.x.

Martens C. S., Albert D. B., and Alperin M. J. (1998) Biogeochemical processes controlling methane in gassy coastal sediments - Part 1. A model coupling organic matter flux to gas production, oxidation, and transport. *Continental Shelf Research* **18**(14-15), 1741-1770.

McAullife C. (1971) GC Determination of solutes by multiple phase equilibration. *Chemical Technology* **46-&**.

Michaelis W., Seifert R., Nauhaus K., Treude T., Thiel V., Blumenberg M., Knittel K., Gieseke A., Peterknecht K., Pape T., Boetius A., Amann R., Jørgensen B. B., Widdel F., Peckmann J. R., Pimenov N. V., and Gulin M. B. (2002) Microbial reefs in the Black Sea fuelled by anaerobic oxidation of methane. *Science* **297**(5583), 1013-1015.

Naudts L., Greinert J., Artemov Y., Staelens P., Poort J., Van Rensbergen P., and De Batist M. (2006) Geological and morphological setting of 2778 methane seeps in the Dnepr paleo-delta, northwestern Black Sea. *Marine Geology* **227**, 177-199.

Neretin L. N., Böttcher M. E., Jørgensen B. B., Volkov I., Luschen H., and Hilgenfeldt K. (2004) Pyritization processes and greigite formation in the advancing sulfidization front in the Upper Pleistocene sediments of the Black Sea. *Geochimica Et Cosmochimica Acta* **68**(9), 2081-2093.

Niemann H., Elvert M., Hovland M., Orcutt B., Judd A. G., Suck I., Gutt J., Joye S., Damm E., and Finster K. (2005) Methane emission and consumption at a North Sea gas seep (Tommeliten area). *Biogeosciences* **2**, 335-351.

Niemann H., Lösekann T., de Beer D., Elvert M., Nadalig T., Knittel K., Amann R., Sauter E. J., Schlüter M., Klages M., Foucher J. P., and Boetius A. (2006) Novel microbial communities of the Haakon Mosby mud volcano and their role as a methane sink. *Nature* **443**, 854-858.

Niewöhner C., Hensen C., Kasten S., Zabel M., and Schulz H. D. (1998) Deep sulfate reduction completely mediated by anaerobic methane oxidation in sediments of the upwelling area off Namibia. *Geochimica et Cosmochimica Acta* **62**(3), 455-464.

Orcutt B. N., Boetius A., Lugo S. K., MacDonald I. R., Samarkin V. A., and Joye S. B. (2004) Life at the edge of methane ice: microbial cycling of carbon and sulfur in Gulf of Mexico gas hydrates. *Chemical Geology* **205**(3-4), 239-251.

Parkes J., Banning N., Brock F., Webster G., Fry J. C., Hornibrook E., Pancost R. D., Kelly S., Knab N. J., Weightman A. J., and Cragg B. A. (in press) Biogeochemistry and biodiversity of methane cycling in subsurface marine sediments (Skagerrak, Denmark). *Environmental Microbiology*.

Piker L., Schmaljohann R., and Imhoff J. F. (1998) Dissimilatory sulfate reduction and methane production in Gotland Deep sediments (Baltic Sea) during a transition period from oxic to anoxic bottom water (1993-1996). *Aquatic Microbial Ecology* **14**, 183-193.

Popescu I., Lericolais G., Panin N., Wong H. K., and Droz L. (2001) Late Quaternary channel avulsions on the Danube deep-sea fan. *Marine Geology* **173**, 25-37.

Reeburgh W. S., Ward B. B., Whalen S. C., Sandbeck K. A., Kilpatrick K. A., and Kerkhof L. J. (1991) Black Sea methane geochemistry. *Deep-Sea Research* **38**, S1189-S1210.

Ross D. A., Degens E. T., and MacIlvaine J. (1970) Black Sea: Recent sedimentary history. *Science* **170**(3954), 163-165.

Schulz H. D. and Zabel M. (2000) *Marine Geochemistry*. Springer Verlag.

Seifert R., Nauhaus K., Blumenberg M., Krüger M., and Michaelis W. (2006) Methane dynamics in a microbial community of the Black Sea traced by stable isotopes *in vitro*. *Organic Geochemistry* **37**(10), 1411-1419.

Stookey L. L. (1970) Ferrozine - a new spectrophotometric reagent for iron. *Analytical Chemistry* **42**, 779-781.

Thamdrup B., Rossello-Mora R. A., and Amann R. (2000) Microbial manganese and sulfate reduction in Black Sea sediments. *Applied and Environmental Microbiology* **66**(7), 2888-2897.

Treude T. (2005) Subsurface microbial methanotrophic mats in the Black Sea. *Applied and Environmental Microbiology* **71**(10), 6375-6378.

Treude T., Boetius A., Knittel K., Wallmann K., and Jørgensen B. B. (2003) Anaerobic oxidation of methane above gas hydrates at Hydrate Ridge, NE Pacific Ocean. *Marine Ecology-Progress Series* **264**, 1-14.

Treude T., Krüger M., Boetius A., and Jørgensen B. B. (2005) Environmental control on anaerobic oxidation of methane in the gassy sediments of Eckernförde Bay (German Baltic). *Limnology and Oceanography* **50**(6), 1771-1786.

Weber A., Riess W., Wenzhoefer F., and Jørgensen B. B. (2001) Sulfate reduction in Black Sea sediments: *In situ* and laboratory radiotracer measurements from the shelf to 2000 m depth. *Deep-Sea Research I* **48**(9), 2073-2096.

Whiticar M. J. (1999) Carbon and hydrogen isotope systematics of bacterial formation and oxidation of methane. *Chemical Geology* **161**, 291-314.

Whiticar M. J. and Faber E. (1986) Methane oxidation in sediment and water column environments - isotope evidence. *Organic Geochemistry* **10**, 759-768.

Concluding Remarks and Perspective

In this thesis microbially mediated anaerobic oxidation of methane has been studied at different sites along the European continental margin, with the focus to investigate the magnitude and controls of this process. Detailed pore water profiles provide a contribution to the existing database, and were used in the frame of the METROL project to determine methane and sulfate fluxes in these environments and to analyse the controls on methane dynamics with reactive transport models. The combination pore water concentrations, rate measurements of sulfate reduction, AOM, and methanogenesis together with stable isotope data and biomarkers represents one of the most comprehensive datasets on methane dynamics in diffusive sediments available so far.

Pore water concentrations and microbial rates

The pore water profiles of methane and sulfate form a sulfate methane transition zone that determines the horizon, in which AOM and methane related SRR are potentially possible. Yet, AOM rates were not distributed over the entire SMTZ, but always seem to occur at the lower end of the SMTZ, which was especially obvious in the Black Sea, where the SMTZ was very broad. The vertical occurrence of AOM rates correlated with methane related SRR, although peak rates of both reactions were not always located in exactly the same depth. In most cores SRR in the SMTZ was higher than AOM, which might be attributed to additional sulfate reduction with other electron donors than methane. Rates of AOM and methane related SRR are generally highest when the SMTZ is located close to the sediment surface, but this does not apply when different environments are compared. For example in the shallow SMTZ of the Arkona Basin AOM rates were much higher than at a nearby site with a deeper SMTZ, but lower than in the deeper SMTZ of the Skagerrak.

Comparison with other AOM sites

Compared to AOM hot-spots like AOM mediating mats or cold seeps rates of AOM at our study sites were much lower, e.g. 1000 x lower than the AOM rates at Hydrate Ridge (Table 1).

Because diffusive sediments account for the vast majority of the methane bearing ocean floor the methane oxidation rates from these systems are much more representative for estimates of global marine methane budgets.

In this respect it is noticeable that the maximum rates of AOM seem to be rather similar at the different sites of our study and were generally in the range between 0.8-10 nmol cm^{-3} d^{-1}. This magnitude is also consistent with earlier tracer measurements of AOM rates that have been reported for diffusive systems, which ranged from 0.27 to 19 nmol cm^{-3} d^{-1}. However, since tracer determined rates, especially at sites with low AOM activity, tend to be higher than rates modelled from the methane profile, these AOM activities are probably overestimated.

Relation between AOM, SRR and MTG

Methane production rates were at all investigated sites much lower than AOM, and bicarbonate was preferentially utilized as substrate. In cores with a shallow SMTZ methanogenesis was restricted to the horizon below sulfate depletion, consistent with the concept of the methanogenic zone below the SMTZ. Interestingly, in two cores from the Skagerrak with a deeper SMTZ, bicarbonate methanogenesis was already detected above the zone of major AOM activity. And the same pattern was also found in one of the gravity cores from the Black Sea and at one site in the western Baltic. This indicates that methanogenesis in the sulfate zone is not only restricted to methylamines and other substrates that the sulfate reducing bacteria do not use, but can also occur with compatible substrates. The question remains why the sulfate reduction rates in this depth are so low, despite the obvious presence of substrates.

Thermodynamic and kinetic control

The kinetic and bioenergetic limitations of microbial processes in the sediment are defined by the pore water geochemistry of substrates and products, and the measured concentrations were applied to asses the control of these limitations on AOM rates. One major problem is that with the lack of information about the mechanism and intermediate this could only be determined for the overall AOM-SRR process and not for the single reactions. The calculations of the energy yield at different locations showed that in the entire SMTZ the process always provides sufficient

energy to support AOM-SRR, but rates are taking place at the bottom of the SMTZ, because this is where the kinetic drive is highest. This clearly demonstrates that the distribution of AOM rates coupled to SRR is regulated by thermodynamic and kinetic constraints, whereby the role of methane is especially important. Methane concentrations appear to have the largest influence on ΔG values and the kinetic drive is only determined by methane and sulfate as the substrates of AOM-SRR. That the kinetic drive has a maximum at the bottom of the SMTZ, where methane concentrations are highest, emphasizes the importance of methane concentrations. This explains that AOM rates strongly depend on methane fluxes and that the SMTZ in sediments with a high methane flux is still effective as a methane barrier, as long as transport is restricted to diffusion.

OUTLOOK

The results of this study confirm the importance of AOM in marine sediments, and demonstrate the need for further investigations. To understand methane dynamics and the role of AOM and methanogenesis for organic matter remineralization coordinated research is necessary in a variety of disciplines. Questions that are presently addressed in connection with AOM and SRR, reflecting this diversity, include, if these rates as well as methanogenesis are potentially possible in other sediment layers when stimulated by substrate additions, if AOM is the reversed pathway of methanogenesis, and how concentration profiles are related to seismic data. More important than measuring pore water profiles and AOM rates at new locations would be to systematically expand the already existing database, and collect complementary data at selected sites, that provide information about the organic matter abundance, composition and degradation in connection with SRR and methanogenesis, but also about other degradation pathways, and the consequences for methane fluxes and AOM.

In addition, it would be important to better understand the physiology of methanotrophic archaea and their metabolic pathways. This would not only be interesting in respect to the mechanism of AOM, but is also necessary to apply and improve mathematical models. Because the metabolic pathways might be connected with the origin of life it would be interesting to consider alternative possibilities for the mechanisms of these pathways. The methanogenic pathway is a

derivation of the acetyl-CoA pathway with a complex and irreversible last step catalyzed by MCR. The acetyl-CoA pathway is reversible, which would offer alternate possibilities to consume methane, like acetogenesis from CH_4 and CO_2.

The genomic sequences of methanotrophic archaea that are currently analyzed will provide more information to understand these pathways and their regulations, and because these organisms are not cultivated so far new molecular tools, like cloning vectors with archaeal promotors, would need to be designed for the study of archaeal gene expression. An alternate approach that might be worth pursuing would be to determine SRR or AOM rates indirectly with Real-Time PCR of *mcr* or *dsr*, which could also be applied for expression analyses of these genes under different conditions *in vitro*.

The combination of experimental work and mathematic modelling as presented in this thesis should be expanded and also used to test model predictions in *in vitro* experiments. A prerequisite to make such theoretical approaches more meaningful would be a very close cooperation of the model requirements and the data acquisition. The most severe limit to models that deal with the kinetic and thermodynamic regulation is presently the lack of physiological information of the involved organisms, which would also be essential to further interprete geochemical data.

	Location	Water depth	Sediment depth	max. AOM	integrated	Method	Source
		m	*cm*	*nmol cm^{-3} d^{-1}*	*mmol m^{-2} d^{-1}*		
Inner Shelf	Kysing Fjord	1	12	0.27	0.01	Tracer	(Iversen and Blackburn, 1981)
0-50m	Norsminde Fjord	1	40	17	2.8	Tracer	(Hansen et al., 1998)
	Cape Lookout	10	35	19	1.75	Tracer	(Hoehler et al., 1994)
	Aarhus Bay	16	300	1	0.05	Tracer	(Thomsen et al., 2001)
	Eckernförde Bay	25	50	34	0.29	Tracer	(Bussmann et al., 1999)
	Eckernförde Bay	26	20	15	1.5	Tracer	(Treude et al., 2005a)
	Aarhus Bay M1	15	321	2.3	1.47	Tracer	(Knab et al., unpubl.)
	Aarhus Bay M5	27	30	4.7	4.56	Tracer	(Knab et al., unpubl.)
	Kattegat	9.4	420	1		Tracer	(Knab et al., unpubl.)
	Arkona Basin	44	99	0.7	0.17	Tracer	(Knab et al., unpubl.)
	Arkona Basin	45	28	2	0.10	Tracer	(Knab et al., unpubl.)
Outer Shelf	Kattegat	65	170	6	0.83	Tracer	(Iversen and Jørgensen, 1985)
50-200m	Skan Bay	65	35	9	1.14	Tracer	(Reeburgh, 1980)
	Skan Bay	65	40	10	0.88	Tracer	(Alperin and Reeburgh, 1985)
	Black Sea	130	350		0.11	modelling	(Jørgensen et al., 2001)
	Black Sea	181	350		0.1	modelling	(Jørgensen et al., 2001)
	Skagerrak	86	130	4.9	0.31	Tracer	(Knab et al., unpubl.)
Upper Margin	Skagerrak	200	110	12	1.16	Tracer	(Iversen and Jørgensen, 1985)
200-1000m	Saanich Inlet	225	27	0.75	1.26	Tracer	(Devol and Anderson, 1984)
	Black Sea	396	350		0.08	modelling	(Jørgensen et al., 2001)
	Black Sea	1176	350		0.05	modelling	(Jørgensen et al., 2001)
	Gotland Deep	241		0.34	0.83	Tracer	(Piker et al., 1998)
	Chile	800	360	52	5.09	Tracer	(Treude et al., 2005b)
	Skagerrak	391	91	4.7	1.36	Tracer	(Knab et al., unpubl.)
	Black Sea	683	254	5.6		Tracer	(Knab et al., unpubl.)
	BlackSea	205	188	1.11	1.13	Tracer	(Knab et al., unpubl.)
	Bornholm Basin	336	129	1.13	1.30	Tracer	(Knab et al., unpubl.)
Lower Margin	Cariaco Trench	1300	120		0.44	modelling	(Reeburgh, 1976)
1000-4000m	Cariaco Trench		120		0.15	modelling	(Reeburgh, 1976)
	Namibia Slope	1400	70		0.08	modelling	(Niewöhner et al., 1998)
	Namibia Slope		70		0.14	modelling	(Niewöhner et al., 1998)
	Namibia Slope	1312	400		0.22	modelling	(Fossing et al., 2000)
	Namibia Slope		600		0.15	modelling	(Fossing et al., 2000)
	Amazon Fan	2060	5000	0.3		isotopes	(Burns, 1998)
	Blake Ridge	1373	2300	0.015	0.01	modelling	(Borowski et al., 2000)
	Zaire Fan	3950	1550	50	0.1	modelling	(Zabel and Schulz, 2001)
	Chile	1168	180	1.3	0.47	Tracer	(Treude et al., 2005b)
	Chile	2744	210	5	0.03	Tracer	(Treude et al., 2005b)
	Black Sea	1014	158	4.5		Tracer	(Knab et al., unpubl.)
Methane							
Seeps	Eckernförde Bay	25	50	50	5	Tracer	(Bussmann et al., 1999)
	Eel River Basin	520	10		11500	isotopes	(Hinrichs et al., 2000)
	Gulf of Mexico	590	30		1338	SRR	(Aaron & Fu, 2000)
	Hydrate Ridge	750	15	3000	16425	SRR	(Boetius et al., 2000)
	HMMV	1250	20	70	1898	Tracer	(Lein et al., 2000)
	Hydrate Ridge	787	3.5	2800	56	Tracer	(Treude et al., 2003)
	Tommeliten		170	2.2		Tracer	(Niemann et al., 2005)
	HMMV		2	500	13.7	Tracer	(Niemann et al., 2006)
	Gulf of Cadice	1315	40	26	1.05	Tracer	(Niemann, 2005)
	Gulf of Mexico	560	14	500	11.5	Tracer	(Joye et al., 2004)
	Gulf of Mexico	560	2	1	60	Tracer	(Joye et al., 2004)
	Skagerrak	86	48	25	2.81	Tracer	(Knab et al., unpubl.)
	Black Sea	190	2.5	0.67		Tracer	(Treude et al., unpubl.)
	Black Sea	332	4.5	151		Tracer	(Knab et al., unpubl.)

Table 1: Rates of AOM in marine sediments (Hinrichs and Boetius, 2002).

REFERENCES

Aharon P. and Fu B. (2000) Microbial sulfate reduction rates and sulfur oxygen isotope fractionations at oil and gas seeps in deepwater Gulf of Mexico. *Geochimica Et Cosmochimica Acta* **64**, 233-246.

Alperin M. J. and Reeburgh W. S. (1985) Inhibition experiments on anaerobic methane oxidation. *Applied and Environmental Microbiology* **50**(4), 940-945.

Boetius A., Ravenschlag K., Schubert C. J., Rickert D., Widdel F., Gieseke A., Amann R., Jørgensen B. B., Witte U., and Pfannkuche O. (2000) A marine microbial consortium apparently mediating anaerobic oxidation of methane. *Nature* **407**(6804), 623-626.

Borowski W. S., Hoehler T. M., Alperin M. J., Rodriguez N. M., and Paull C. K. (2000) Significance of anaerobic methane oxidation in methane-rich sediments overlying the Blake Ridge gas hydrates. *Proceedings of the Ocean Drilling Program, Scientific Results* **164**, 87-98.

Bussmann I., Dando P. R., Niven S. J., and Suess E. (1999) Groundwater seepage in the marine environment: role for mass flux and bacterial activity. *Marine Ecology-Progress Series* **178**, 169-177.

Devol A. H. and Anderson J. J. (1984) A model for coupled sulfate reduction and methane oxidation in the sediments of Saanich Inlet. *Geochimica Et Cosmochimica Acta* **48**, 993-1004.

Fossing H., Ferdelman T. G., and Berg P. (2000) Sulfate reduction and methane oxidation in continental margin sediments influenced by irrigation (South-East Atlantic off Namibia). *Geochimica Et Cosmochimica Acta* **64**(5), 897-910.

Hansen L. B., Finster K., Fossing H., and Iversen N. (1998) Anaerobic methane oxidation in sulfate depleted sediments: effects of sulfate and molybdate additions. *Aquatic Microbial Ecology* **14**(2), 195-204.

Hinrichs K. U. and Boetius A. (2002) The anaerobic oxidation of methane: New insights in microbial ecology and biogeochemistry. *Ocean Margin Systems (edt. G. Wefer)* Springer-Verlag Berlin Heidelberg, 457-477.

Hinrichs K. U., Summons R. E., Orphan V., Sylva S. P., and Hayes J. M. (2000) Molecular and isotopic analysis of anaerobic methane-oxidizing communities in marine sediments. *Organic Geochemistry* **31**(12), 1685-1701.

Hoehler T. M., Alperin M. J., Albert D. B., and Martens C. S. (1994) Field and Laboratory Studies of Methane Oxidation in an Anoxic Marine Sediment - Evidence for a Methanogen-Sulfate Reducer Consortium. *Global Biogeochemical Cycles* **8**(4), 451-463.

Iversen N. and Blackburn T. H. (1981) Seasonal rates of methane oxidation in anoxic marine-sediments. *Applied and Environmental Microbiology* **41**(6), 1295-1300.

Iversen N. and Jørgensen B. B. (1985) Anaerobic methane oxidation rates at the sulfate methane transition in marine-sediments from Kattegat and Skagerrak (Denmark). *Limnology and Oceanography* **30**(5), 944-955.

Jørgensen B. B., Weber A., and Zopfi J. (2001) Sulfate reduction and anaerobic methane oxidation in Black Sea sediments. *Deep-Sea Research Part I* **48**(9), 2097-2120.

Joye S. B., Boetius A., Orcutt B. N., Montoya J. P., Schulz H. N., Erickson M. J., and Lugo S. K. (2004) The anaerobic oxidation of methane and sulfate reduction in sediments from Gulf of Mexico cold seeps. *Chemical Geology* **205**(3-4), 219-238.

Niemann H. (2005) Rates and signatures of methane turnover in sediments of continental margins. PhD thesis, Max-Planck Institute for Marine Microbiology.

Niemann H., Elvert M., Hovland M., Orcutt B., Judd A. G., Suck I., Gutt J., Joye S., Damm E., and Finster K. (2005) Methane emission and consumption at a North Sea gas seep (Tommeliten area). *Biogeosciences* **2**, 335-351.

Niemann H., Lösekann T., de Beer D., Elvert M., Nadalig T., Knittel K., Amann R., Sauter E. J., Schlüter M., Klages M., Foucher J. P., and Boetius A. (2006) Novel microbial communities of the Haakon Mosby mud volcano and their role as a methane sink. *Nature* **443**, 854-858.

Niewöhner C., Hensen C., Kasten S., Zabel M., and Schulz H. D. (1998) Deep sulfate reduction completely mediated by anaerobic methane oxidation in sediments of the upwelling area off Namibia. *Geochimica et Cosmochimica Acta* **62**(3), 455-464.

Piker L., Schmaljohann R., and Imhoff J. F. (1998) Dissimilatory sulfate reduction and methane production in Gotland Deep sediments (Baltic Sea) during a transition period from oxic to anoxic bottom water (1993-1996). *Aquatic Microbial Ecology* **14**, 183-193.

Reeburgh W. S. (1976) Methane consumption in Cariaco Trench waters and sediments. *Earth and Planetary Science Letters* **28**, 337-344.

Reeburgh W. S. (1980) Anaerobic methane oxidation: Rate depth distributions in Skan Bay sediments. *Earth and Planetary Science Letters* **47**, 345-352.

Thomsen T. R., Finster K., and Ramsing N. B. (2001) Biogeochemical and molecular signatures of anaerobic methane oxidation in a marine sediment. *Applied and Environmental Microbiology* **67**(4), 1646-1656.

Treude T., Boetius A., Knittel K., Wallmann K., and Jørgensen B. B. (2003) Anaerobic oxidation of methane above gas hydrates at Hydrate Ridge, NE Pacific Ocean. *Marine Ecology-Progress Series* **264**, 1-14.

Treude T., Krüger M., Boetius A., and Jørgensen B. B. (2005a) Environmental control on anaerobic oxidation of methane in the gassy sediments of Eckernförde Bay (German Baltic). *Limnology and Oceanography* **50**(6), 1771-1786.

Treude T., Niggemann J., Kallmeyer J., Wintersteller P., Schubert C. J., Boetius A., and Jørgensen B. B. (2005b) Anaerobic oxidation of methane and sulfate reduction along the Chilean continental margin. *Geochimica Et Cosmochimica Acta* **69**(11), 2767-2779.

Zabel M. and Schulz H. (2001) Importance of submarine landslides for non-steady state conditions in pore water systems - lower Zaire (Congo) deep-sea fan. *Marine Geology* **176**(1-4), 87-99.